CANONICAL TRANSFORMATIONS AND LOOP FORMULATION OF SU(N) LATTICE GAUGE THEORY

THESIS SUBMITTED FOR THE DEGREE OF
DOCTOR OF PHILOSOPHY [SC.]
IN PHYSICS (THEORETICAL)

by
SREERAJ T P

Department of Physics
University of Calcutta

2016

Dedicated to my parents

PUBLICATIONS

The thesis is based on the following publications

1. **From Lattice Gauge Theories to Hydrogen Atoms** , M. Mathur, T.P. Sreeraj, Phys. Letts. **B** 749 (2015) 137-143, arXiv:1410.3318

2. **Canonical Transformations and Loop Formulation of SU(N) Lattice Gauge Theories**, Manu Mathur, T. P. Sreeraj , Phys. Rev **D** 92, 125018 (2015), arXiv:1509.04033.

3. **SU(N) Lattice Gauge Theory and SU(N) spin model**, Manu Mathur, T. P. Sreeraj, Under review, arXiv:1604.00315.

Other publications:

1. **Invariants, Projection Operators and $SU(N) \times SU(N)$ Irreducible Schwinger Bosons**, Manu Mathur, Indrakshi Raychowdhury, T P Sreeraj, J. Math. Phys. 52, 113505 (2011), arXiv:1108.5246.

ACKNOWLEDGEMENTS

I would like to thank my supervisor, Professor Manu Mathur, for providing me with a great and friendly work atmosphere. I would like to thank Professor Ramesh Anishetty for many useful discussions throughout this thesis work.

Thanks are also due to all the staff at S N Bose National Centre for Basic Sciences for providing me with all the facilities and a good atmosphere in which the work was completed. I would also like to acknowledge the financial support from CSIR and S N Bose National Centre for Basic Sciences.

I would like to thank all my friends at S N Bose National Centre for Basic Sciences especially Kallol, Shinde, Sandipa, Arghya, Subhashish, Sayani, Monalisa, Samiran and Aritra for making my stay a pleasureable one. Special thanks is due to Chaoba for being with me and supporting me all through my PhD.

Above all, I would like to thank my family for the faith and patience they have shown towards me without which nothing would have been possible.

CONTENTS

1 INTRODUCTION 1

1.1 Kogut Susskind approach 4

1.2 Loop approach and Mandelstam constraints 6

1.3 Canonical transformations, loops and gauge-spin duality 8

2 HAMILTONIAN FORMULATION OF SU(N) LATTICE GAUGE THEORY 12

2.1 Kogut-Susskind link formulation & Gauss law constraints 12

2.2 Wilson loop formulation & Mandelstam constraints 18

2.3 Prepotential formulation & Mandelstam constraints 20

2.4 The loop dynamics & Wigner coefficients 24

3 CANONICAL TRANSFORMATIONS, GAUSS LAW CONSTRAINTS & LOOP FORMULATION 29

3.1 Z_2 lattice gauge theory 30

3.1.1 The fundamental Z_2 canonical transformation 32

3.1.2 Z_2 Canonical transformations on a single plaquette 33

3.1.3 Z_2 canonical transformations on a finite lattice in $(2+1)$ D 39

3.2 SU(N) lattice gauge theory 43

3.2.1 Fundamental SU(N) canonical transformation 44

3.2.2 SU(N) canonical transformations on a single plaquette 45

3.2.3 SU(N) canonical transformations on a finite lattice in $2+1$ D 54

3.3 Canonical transformations in $3+1$ D 64

3.3.1 Z_2 lattice gauge theory 64

3.3.2 SU(N) lattice gauge theory 67

3.3.3 Loop Hilbert space and SU(N) loop dynamics 71

4 CANONICAL TRANSFORMATIONS, DUALITY & ORDER-DISORDER 73

4.1 Ising model & Kramers Wannier Duality 74

4.2 Z_2 lattice gauge theory & Wegner Duality 77

4.3 Duality in SU(N) lattice gauge theory 82

5 SU(2) LOOPS & HYDROGEN ATOM 88

5.1 Hydrogen atom & SO(4) symmetry 88

5.2 SU(2) Loop States & Hydrogen atom bound states 90

5.3 Loop dynamics & dynamical symmetry group SO(4,2) of Hydrogen atom 95

6 SUMMARY AND FUTURE DIRECTIONS 101

A CANONICAL TRANSFORMATIONS ON A FINITE LATTICE 105

A.1 Z_2 lattice gauge theory in $2+1$ dimensions 105

A.1.1 From links to loops & strings 105

A.1.2 From loops & strings to links (Inverse transformations) 108

A.2 SU(N) lattice gauge theory in $2+1$ dimensions 110

A.2.1 From links to loops & strings 110

A.2.2 From loops & strings to links (Inverse transformations) 115

A.3 Canonical transformations in $3+1$ dimensions 121

A.3.1 Z_2 lattice gauge theory 121

A.3.2 SU(N) lattice gauge theory. 124

B MAGNETIC BASIS OF SU(2) LATTICE GAUGE THEORY 127

C CALCULATIONAL METHODS IN THE LOOP FORMULATION 131

LIST OF FIGURES

Figure 1.1 Outline of the thesis. Canonical transformations are constructed which lead to a loop formulation of Z_2 as well as $SU(N)$ lattice gauge theory in (2+1) and (3+1) dimensions. The loop formulation also helps us in constructing an exact isomorphism between the loop Hibert space of SU(2) lattice gauge theory and the Hilbert space of Wigner coupled hydrogen atoms with no net angular momentum. 10

Figure 2.1 The location of the left and right electric fields $E_+(n;\hat{i})$ and $E_-(n+\hat{i};\hat{i})$: (a) on a link $(n;\hat{i})$, (b) around a lattice site $n = (x,y)$. The SU(N) Gauss law is also pictorially shown in (b). 16

Figure 2.2 Simplest example of Mandelstam constraints for SU(2) gauge theory on a 2 dimensional spatial lattice. 19

Figure 2.3 The left and right electric fields and the corresponding prepotentials in SU(2) lattice gauge theory. We have denoted $a^\dagger(n,\hat{i},L)$ and $a^\dagger(n,\hat{i},R)$ by $a^\dagger(L)$ and $a^\dagger(R)$ respectively. 21

Figure 2.4 $2d$ prepotential doublets $a^\dagger(n,\hat{i}); i = 1,2,\cdots 2d$ around a site n is shown for $d = 2$. 22

Figure 2.5 18j ribbon diagram representing SU(2) loop dynamics[48, 49] in d=2 in the loop basis given in (2.37). The interior (exterior) edge carries the initial(final) angular momenta and the six bridges carry the angular momenta that doesn't change under the action of TrU_p. The comparison with dynamics in the loop formulation constructed in this thesis is made in Figure. 3.15. 25

Figure 2.6 Spin network basis states on a plaquette abcd. 25

Figure 3.1 (a) represents the 4 conjugate pairs on the 4 links. (b) represents the Z_2 Gauss law operator defined at lattice site n in eqn. (3.5). ♦ represents the electric field operators σ_1. 31

Figure 3.2 The fundamental canonical transformation involving 2 neighbouring link operators. This canonical transformation is repeated to construct loop and string operators on the entire lattice. The $\sigma_1(l_1), \sigma_1(l_2)$ operators are denoted by ♦ and • respectively. 32

Figure 3.3 The four Gauss law operators $\mathcal{G}(O)$, $\mathcal{G}(A)$, $\mathcal{G}(B)$, $\mathcal{G}(C)$ at the sites O,A,B,C respectively for a single plaquette. The Gauss law constraints (3.7) imply that within the physical Hilbert space : $\mathcal{G}(O) \approx 1, \mathcal{G}(A) \approx 1, \mathcal{G}(B) \approx 1$ and $\mathcal{G}(C) \approx 1$. These four Gauss law operators are not independent and are related by (3.14). 34

Figure 3.4 The Z_2 canonical transformations (3.16), (3.18), (3.19a) and (3.19b) are pictorially illustrated in (a), (b) and (c) respectively. The ♦ and • represent the electric fields of the initial horizontal and vertical links respectively. 35

Figure 3.5 Graphical illustration of a plaquette canonical transformation defined in (3.20) and (3.21). 38

Figure 3.6 The Z_2 link operator pairs, the physical Z_2 loop conjugate pairs $\{\mu_1(\vec{n}); \mu_3(\vec{n})\}$ and the unphysical string conjugate pairs $\{\bar{\sigma}_1(\vec{n}); \bar{\sigma}_3(\vec{n})\}$ for a 2×2 lattice are shown in (a), (b) and (c) respectively. The canonical transformations convert 12 link operator pairs on a 2×2 lattice to 4 loop operator pairs and 8 string operator pairs. We label the loop operators by their top right corners and the horizontal (vertical) string operators by their right (top) endpoint. The strings decouple from the physical Hilbert space as $\bar{\sigma}_1(\vec{n}) \approx 1$ by Gauss law constraints. The corresponding dual SU(N) loop and SU(N) string operators are shown in Figure 3.11-a,b respectively. 39

Figure 3.7 The graphical illustration of the non-local relations in the net Z_2 canonical transformations: (a) we show the relations (3.26b) expressing $\mu_3(x, y)$ as the product of σ_1 operators which are denoted by ♦. In (b) and (c), we show the relations (3.28b) expressing $\bar{\sigma}_1(x, 0)$ and $\bar{\sigma}_1(x, y \neq 0)$ respectively as the product of σ_1 operators denoted by ♦. These $(\bar{\sigma}_1(x, y))$ equal the product of Gauss law operators at sites marked by x in the shaded region. For the corresponding SU(N) relations, see Figures 3.12-a,b. 40

Figure 3.8 The fundamental $SU(N)$ canonical transformation (3.34) from $\{E_+(0), U(1), E_-(1)\}; \{E_+(1), U(2), E_-(2)\}$ to $\{\mathsf{E}_-(1), \mathsf{T}(1), \mathsf{E}_+(1)\}; \{\mathsf{E}_-(1), \mathsf{T}(2), \mathsf{E}_+(2)\}$ involved in the construction of a loop formulation of $SU(N)$ gauge theory. The electric fields are denoted by •. 44

Figure 3.9 Graphical illustration of $SU(N)$ Gauss law operators $\mathcal{G}^a(O), \mathcal{G}^a(A), \mathcal{G}^a(B), \mathcal{G}^a(C)$ at O, A, B and C for a single plaquette. The Gauss law constraints are given by $\mathcal{G}^a(O) \approx 0, \mathcal{G}^a(A) \approx 0, \mathcal{G}^a(B) \approx 0, \mathcal{G}^a(C) \approx 0$. Unlike Z_2 case, they are all independent. 45

Figure 3.10 Three canonical transformations on the four link flux operators of a plaquette OABC leading to a single physical plaquette loop flux operator $\mathcal{W}_{\alpha\beta}(1,1)$ in (c). The three right electric fields $\mathsf{E}^{a}_{[xy]+}(1,0)$, $\mathsf{E}^{a}_{[xy]+}(1,1)$, $\mathsf{E}^{a}_{[xy]+}(0,1)$ of the three string flux operators ending at A, B and C respectively are the Gauss law generators $\mathcal{G}^a(A)$, $\mathcal{G}^a(B)$ and $\mathcal{G}^a(C)$ respectively. The Gauss law at the origin is: $\mathcal{G}^a(O) = E^a_+(0,0;\hat{1}) + E^a_+(0,0;\hat{2}) = \mathcal{E}^a_-(1,1) + \mathcal{E}^a_+(1,1) = 0$. 46

Figure 3.11 The plaquette loop operator $\mathcal{W}(x,y)$ and the string flux operator $\mathsf{T}(x,y)$ and their electric fields $\mathcal{E}^a_{\mp}(x,y)$ and $\mathsf{E}^a_{\mp}(x,y)$ respectively. Note that the electric fields $\mathcal{E}^a_{\mp}(x,y)$, $\mathsf{E}^a_{\mp}(x,y)$ are located at the initial and final points of the loops and strings respectively. 54

Figure 3.12 Graphical representation of the canonical relations (3.68). The Kogut-Susskind electric fields are denoted by ♦ and the plaquette loop electric fields are denoted by •. We show a) string electric field in terms of Kogut-Susskind electric fields and (b) plaquette loop electric fields $\mathcal{E}^a_+(x,y)$ in terms of the original Kogut-Susskind link electric fields. In (a) the 4 ♦ at (x,y) denotes the Gauss law operator at $\mathcal{G}^a(x,y)$. In (b) Kogut-Susskind link electric fields $E^a_-(x,y';\hat{1})$; $y' = y, y+1 \cdots \mathsf{N}_s - 1$ are parallel transported by $S(x,y,y')$ to give the loop electric field $\mathcal{E}^a_+(x,y)$. 56

Figure 3.13 Graphical representation of the inverse canonical relations (3.72): a) link electric field $E^a_+(x, y=0;\hat{1})$, (b) $E^a_+(x, y\neq 0;\hat{1})$ and (c) $E_+(x,y;\hat{2})$ in terms of plaquette loop operators and loop electric field. The • represents plaquette loop electric fields and ♦ represents Kogut-Susskind link electric fields. All loop electric fields • are parallel transported along the attached lines to give Kogut-Susskind link operator $E^a_+(x,y;\hat{i})$ or ♦ in (3.72). In (a) $\sum_p \mathsf{L}^b(p)$ gives $\Delta^b_X(x, y=0)$ in (3.72), the summations is over the plaquettes in the dotted region. In (c) we show $\Delta_Y(x,y)$ where the summation is again over the plaquettes in the dotted region. The shaded region in (c) represents $\mathcal{W}_{xy}(x,y)$ in the second equation in (3.72). 57

Figure 3.14 a) Uncoupled and b) Coupled loop (tadpole) basis diagonalizing CSCO-A and CSCO-B respectively given in (3.76) and (3.79). The global Gauss law is solved by putting the total angular momentum $L_{total} = 0$. In (a) and (b) $\bullet$ represents the j-j coupling or contraction of j flux lines within a plaquette in (3.54) and in (b) $\otimes$ represents l-l couplings or contraction of l flux lines between neighbouring plaquettes (see eqn.(3.80)). 60

Figure 3.15 SU(2) loop dynamics in (a) prepotential approach in 2+1 dimensions (b) loop formulation based on canonical transformations clearly illustrating the resulting simplifications. The matrix elements of the plaquette operators (3.85) and (2.37) are written in terms of 6j symbols for comparison purpose. 63

Figure 3.16 The final operators after Z_2 canonical transformations in a 3 dimensional spatial lattice: (a) plaquette loop operators (b) string operators. 65

Figure 3.17 (a) Graphical representation of the fundamental plaquette operators and the string operators obtained by canonical transformations in $d = 3$. The shaded horizontal plaquettes are not obtained by canonical transformations as explained in the text. They are also not independent: the shaded plaquette operator in (g) is the product of the fundamental plaquette loop operators in (b), (c), (d), (e), (f) in that order. This is just the SU(N) Bianchi identity on lattice. 70

Figure 4.1 Kramers-Wannier duality through canonical transformations. The first three steps of duality or canonical transformations (4.6) are explicitly illustrated. 75

Figure 4.2 Duality and ordered & disordered phases of $(1+1)$ dimensional Ising model. 77

Figure 4.3 Duality between Z_2 lattice gauge theory and Z_2 (Ising) spin model. The initial and the final conjugate pairs $\{\sigma_1; \sigma_3\}$ and $\{\mu_1; \mu_3\}$, are defined on the links and the plaquettes or dual sites respectively. The corresponding SU(N) duality is illustrated in Figure 4.6. 78

Figure 4.4 Duality and order, disorder in (a) $(2+1)$ dimensional Z_2 lattice gauge theory, (b) $(2+1)$ dimensional Ising model. The confining ($\lambda << 1$) and deconfining ($\lambda >> 1$) phases of Z_2 lattice gauge theory correspond to the ferromagnetic and paramagnetic phases of the Ising spin model. 80

Figure 4.5 Graphical illustration of Z_2 disorder operator creating a vortex in terms of (a) the dual operator $\mu_3(x,y)$ and (b) the original σ_1 operators which forms an infinitely long string. (c) illustrates a vortex-antivortex pair. The dark heavy horizontal links across the strings in (b) and (c) represent the flipping of the link flux operators $\sigma_3(x-1,y',\hat{1});y'>y$ by the disorder operator $\mu_3(x,y)$. Generalization of Z_2 disorder operator to SU(N) lattice gauge theory is illustrated in Figure 4.7. 82

Figure 4.6 Duality between SU(N) lattice gauge theory and an SU(N) spin model. Unlike the corresponding Z_2 duality in Figure 4.3-a,b, global SU(N) Gauss law constraints at the origin remain unsolved. The Gauss law constraints at every other point $\mathcal{G}^a(x,y)\ ;\ (x,y)\neq(0,0)$ are trivially solved in the loop/spin picture. 84

Figure 4.7 Graphical illustration of the disorder operator $\Sigma^+_\theta(x,y)$ creating a plaquette vortex (monopole) in terms of (a) the dual operators, (b) the original Kogut-Susskind link operators but now with infinitely long Dirac string, (c) a vortex-antivortex (monopole-anti-monopole) pair connected through a finite length Dirac string. The dark heavy horizontal links across the Dirac strings in (b) and (c) represent rotations of the Kogut-Susskind link flux operators $U(x-1,y';\hat{1}),\ y'\geq y$ by θ. 85

Figure 5.1 One hydrogen atom, denoted by •, is assigned to each plaquette. The Wigner coupled energy eigenstates $|n_p\ l_p\ m_p\rangle$ given in (5.19) with vanishing total angular momenta form a basis in the physical Hilbert space $\mathcal{H}^p$ of pure SU(2) lattice gauge theory. 88

Figure 5.2 A graphical tadpole representation of hydrogen atom states $|n\ l\ m\rangle$ or equivalently a SU(2) loop state over a plaquette. The dotted arch represents $j_+ = j_- = j$ in the j-j coupling (5.8) which is denoted by •. The tadpole loop represents the SU(2) flux circulating within the plaquette. The vertical leg of tadpole represents the leakage of the angular momentum flux (l,m) through the plaquette. 90

Figure 5.3 Graphical tadpole representation of [a] Uncoupled hydrogen atom basis diagonalizing CSCO-A, [b] coupled hydrogen atom basis diagonalizing CSCO-B. The dots • and • represent jj and ll couplings in (5.8) and (5.20) respectively. 93

Figure 5.4 The SU(2) ground state picture in the hydrogen atom basis (3.80). 99

Figure A.1 The 'plaquette' canonical transformations involved in the construction of the duality transformation between Z_2 lattice gauge theory and Z_2 spin model on a 2×2 lattice. The steps (a), (b), (c) and (d) are plaquette CTs on plaquettes 1, 2, 3 and 4 respectively. The electric field $\sigma_1(l)$ corresponding to the vertical and horizontal links are denoted by $\bullet$ and $\blacklozenge$ respectively. 106

Figure A.2 Graphical representation of the iterative canonical transformations (A.11). The initial $\mathsf{T}_{[x]}(x,0)$ and the final $\mathsf{T}_{[xx]}(x,0)$ string operators at $(x,0)$ are shown. The string operator $\mathsf{T}_{[x]}(x+1,0)$ in the third row replaces $\mathsf{T}_{[x]}(x,0)$ in the first row in the next iterative step. All electric fields involved in (A.11) are also shown along with their locations. 111

Figure A.3 Graphical representation of the canonical transformations: (a) vertical string constructions at $y = 0$ in (A.12) and the Gauss law (A.13) at $y = 0$, (b) iterative vertical string constructions in (A.14) and the string electric field in (A.15). 112

Figure A.4 Graphical representation of the canonical transformation in (A.16). 113

Figure A.5 Graphical representation of the canonical transformation in (A.18). 114

Figure A.6 Graphical representation of the canonical transformation in (A.20). 114

Figure A.7 (a)-(e) shows the plaquette canonical transformation steps involved in the construction of a loop formulation of Z_2 gauge theory on a cube. Just like in the 2D case, the string variables decouple. (f) shows the final plaquette loop variables that results. The plaquette loop operator corresponding to the 'roof' is missing. This solves Bianchi identity constraints automatically. 121

Figure A.8 (a) SU(N) link operators on a cube and (b) SU(N) plaquette loop operators constructed after canonical transformations. Strings to each site is not shown for clarity. 124

Figure C.1 A Wilson loop W_C can be written as the product of fundamental plaquette loop operators $\mathcal{W}(p)$. $W_C = \mathcal{W}(p_1)\,\mathcal{W}(p_2)\,\mathcal{W}(p_3)\cdots\cdots\mathcal{W}(p_{n_c})$. The tails of the fundamental plaquette loop operators connecting them to the origin (see Figure 3.11-a) are not shown for clarity. 132

LIST OF TABLES

Table 3.1 The basic conjugate operators of the original and the loop approaches in Z_2, SU(N) gauge theories in $(2+1)$ dimensions. The duality interpretation is discussed in the next chapter. 43

Table 5.1 The corresponding quantities in SU(2) lattice gauge theory and hydrogen atom 95

Table 5.2 All possible 15 SU(2) tensor operators on a plaquette which are U(1) gauge invariant. They form SO(4,2) algebra. We have defined $\mathcal{W}^{(+)}_{\alpha\beta} \equiv -\tilde{a}^{\dagger}_{\alpha} b^{\dagger}_{\beta}$ and $\mathcal{W}^{(-)}_{\alpha\beta} \equiv a_{\alpha}\tilde{b}_{\beta}$. 96

1

INTRODUCTION

Quantum Chromodynamics (QCD) was introduced in the 1970s to describe strong interactions. QCD is a non-abelian gauge field theory with quarks and gluons having color charge as the fundamental fields. But, instead of individual quarks and gluons, only colorless combinations of them like baryons and mesons are found in nature. Understanding this phenomena of color confinement has been a major puzzle in theoretical physics for more than four decades. Despite a huge amount of work [1–19], a complete analytical understanding still remains elusive. The major reasons for the difficulties in understanding the low energy features of QCD such as confinement are as follows:

- The perturbative methods which are so successful in quantum electrodynamics fail for QCD at low energies. This is because the physical coupling constant in QCD becomes large at low energies. Therefore, non-perturbative techniques are necessary to study the low energy features of QCD like color confinement and hadron spectrum.
- Gauge symmetry, unlike other physical symmetries such as Poincare symmetry etc., is not a real symmetry of nature. It represents redundancies in our description of nature. These redundancies manifest themselves in the form of spurious gauge degrees of freedom and local Gauss law constraints on the Hilbert space of the theory. Such extremely constrained systems are difficult to solve.

In order to solve the first difficulty, Wilson came up with a non-perturbative formulation of QCD on a space time lattice [5–9, 20–23] in 1974. Space time lattice acts as a regularization scheme providing a natural momentum cutoff proportional to $1/a$; where a is the lattice spacing. The idea was to gain back continuum results by taking $a \to 0$ with a simultaneous tuning of the coupling constant. Wilson's scheme was based on path integral methods and allowed for Monte Carlo simulations. In 1975, Kogut and Susskind derived a lattice Hamiltonian [6–8] in which only space is discretized while time remains continuous. Theoretically, the two formulations should be equivalent in the continuum limit. However, they both involve spurious gauge degrees of freedom. In order to deal with the second difficulty, it is desirable to reformulate gauge theories in terms of gauge invariant operators and work within the physical Hilbert space $\mathcal{H}^p$. In the context of pure gauge theory, Wilson loops provide such a set of gauge invariant variables. Moreover, even though the elementary excitations of non-abelian gauge theories at high energies are quarks and gluons [24,

25], at low energies it is expected that the elementary excitations of pure Yang Mills theory are described in terms of Wilson loops carrying non-abelian fluxes. Therefore, Wilson loops [5] and not gauge (gluon) fields provide a suitable gauge invariant set of fundamental dynamical variables to study the low energy behavior of Yang Mills theories. In fact, the importance of loop formulation in understanding long distance non-perturbative physics of non-abelian gauge theories has been amply emphasized by Mandelstam [1–3], Wilson [5] and Yang [4]. However, the early attempts [3–6, 26–46] to describe $SU(N)$ gauge theories in terms of Wilson loop operators and loop states ran into difficulties due to the fact that all loops are not mutually independent. They satisfy non-local constraints [3, 26–41, 43–51] called Mandelstam constraints. In fact, the Mandelstam constraints had been the major stumbling block in these formulations. In this thesis, we construct a Wilson loop formulation of pure $SU(N)$ gauge theory[1] by systematically reformulating Kogut-Susskind link formulation [6–8] in terms of independent loop operators by a series of canonical transformations. These canonical transformations convert the basic link operators and conjugate electric fields of the Kogut-Susskind approach to independent plaquette loop operators and string operators [52] and their corresponding conjugate electric fields. The $SU(N)$ conjugate string electric fields are the local Gauss law operators. Thus, canonical transformations enable us to isolate the spurious gauge degrees of freedom as strings which are frozen within the physical Hilbert space due to Gauss law constraints. This leads to a loop description with the plaquette loop operators and their conjugate electric fields as the fundamental operators. As these canonical transformations are $1-1$ transformations, no new degrees of freedom are generated and no new constraints are introduced. Therefore, Mandelstam constraints are trivially bypassed. The resulting loop formulation has global $SU(N)$ invariance and is dual to the link formulation. This duality [53, 54] between the link and loop degrees of freedom turns out to be a $SU(N)$ non-abelian generalization of Wegners duality[55, 56] between Z_2 lattice gauge theory and quantum Ising model. In the case of pure SU(2) lattice gauge theory, this loop formulation also allows us to construct a complete isomorphism between the physical Hilbert space of SU(2) lattice gauge theory and that of a collection of coupled hydrogen atoms with no net angular momentum [54].

As mentioned above, the main idea of the lattice approach to gauge theories [5–8, 20–23] is to incorporate a non-perturbative cut-off in the theory in the form of a finite lattice spacing a. A non zero lattice spacing implies that there is an upper momentum cutoff on the modes supported by the lattice. The quantum theory which describes the physical world is then defined as the large volume, continuum limit of a regulated theory with a short distance (ultraviolet) cut off a and a volume (infrared) cutoff L:

1 Throughout the thesis, we work with pure gauge theories without matter fields.

$$\text{Quantum Field Theory} = \lim_{a\to 0}\lim_{L\to\infty}(\text{Lattice Field Theory})_{a,L}. \tag{1.1}$$

When we take the continuum limit, all the physical quantities must approach their physical values. Usually while working on lattice, all quantities such as lattice mass (m_L) or lattice correlation lengths (ξ_L) are made dimensionless by absorbing appropriate powers[2] of the lattice spacing a.

$$m_L = m_{\text{phys}} \times a \quad \Rightarrow \quad \xi_L \approx \frac{1}{m_L} \equiv \frac{1}{m_{\text{phys}} \times a} \ , \tag{1.2}$$

where, m_{phys} is the physical mass. Since, m_{phys} is finite, the lattice correlation length must diverge when the lattice spacing a approaches zero. In a statistical mechanical theory, the divergence of correlation length happens at a critical point and is a signature of second order phase transition. In renormalization group analysis of lattice gauge theory [57], the bare coupling is a function of the lattice spacing. Hence to get a continuum limit of a field theory defined with a lattice cutoff, one needs to find the points in the coupling parameter space, where the corresponding statistical model reaches the critical point. In Yang Mills theory, the continuum limit [20] is achieved when the bare coupling $g \to g^* = 0$. A simple argument [8, 9] to show this is to observe that g^* is the bare coupling of the continuum theory. The bare coupling g is a measure of interaction strength at the cutoff scale $= (1/a)$. When lattice spacing $a \to 0$, the cutoff scale becomes large and $g \to g^*$. As Yang Mills theories are asymptotically free, at large energies the interaction strength approaches 0. Therefore, $g^* = 0$. To make this argument more quantitative, let us consider the beta function defined as,

$$\beta(g) = a\frac{d}{da}g(a). \tag{1.3}$$

The continuum limit is reached when g approaches a fixed point g^* in the coupling parameter space and g becomes independent of a. Therefore, $\beta(g^*) = 0$. In the weak coupling limit of the theory, the perturbative beta function [8] for pure $SU(N)$ gauge theory in 4-dimensions acquires the form:

$$\beta(g) = \beta_0 g^3 + \beta_1 g^5 + \mathcal{O}(g^7). \tag{1.4}$$

2 In 3+1 dimensional pure Yang Mills theory, the coupling constants are dimensionless and the only dimensionful quantity on the lattice is the lattice spacing a.

Above,

$$\beta_0 = \frac{11}{3}\left(\frac{N}{16\pi^2}\right) \qquad \beta_1 = \frac{34}{3}\left(\frac{1}{16\pi^2}\right)^2. \tag{1.5}$$

This clearly vanishes at vanishing coupling. Now, integrating the beta function, one obtains

$$a = \Lambda_{latt}^{-1}(g^2\beta_0)^{\frac{\beta_1}{2\beta_0^2}} \exp\left(-\frac{1}{2\beta_0 g^2}\right)(1+\mathcal{O}(g^2)). \tag{1.6}$$

Above, Λ_{latt} is the integration constant. It is clear from the above expression that continuum limit occurs at the weak coupling limit $g^2 \to 0$.

Consider a physical quantity X with mass dimension l. Then $X = a^{-l}X_L(g)$ where X_L is the corresponding value of X on the lattice. Since, physical quantities has to be cutoff independent near the continuum limit, we get

$$\left.\frac{dX\,(g(a))}{da}\right|_{a=0} = 0 \qquad \Longrightarrow \qquad \left.\frac{\partial X}{\partial a}\right|_g + \frac{\partial X}{\partial g}\frac{dg}{da} = 0. \tag{1.7}$$

Using the definition of beta function and the expression for X, we get, $lX - \beta(g)\frac{\partial X}{\partial g} = 0$ Solving the differential equation, $X = c\ (\Lambda_{latt})^l$ where $\Lambda_{latt} = \frac{1}{a}(\beta_0 g^2)^{\frac{\beta_1}{2\beta_0^2}} e^{\frac{-1}{2\beta_0 g^2}}$ is a cutoff independent mass parameter which sets the scale [8, 9] for QCD. Near the continuum, the g dependence of X is completely fixed by the beta function through the above relation. Therefore, in order to approach the continuum limit in 3+1 dimensions, all physical quantities must approach the above scaling behavior.

1.1 KOGUT SUSSKIND APPROACH

The Hamiltonian approach to lattice gauge theory involves formulating gauge theory on a spatial lattice while keeping the time direction continuous. This approach was pioneered by Kogut and Susskind in [6]. The Hamiltonian formulation is intuitively appealing as one directly deals with the construction and study of the physical gauge invariant Hilbert space in terms of the fundamental operators of the theory. The questions regarding the hadron spectrum [58], mass gap [59], glueball spectrum [60, 61] etc are much more directly posed in a Hamiltonian framework. Inspite of these advantages, the major trends in lattice gauge theory have mostly favored the Euclidean approach. This is because, numerical Monte Carlo simulations are easily implementable in Euclidean path-integral formalism. Such Monte-Carlo studies of lattice gauge theories yield numbers to be directly checked with particle data. But, the Monte Carlo technique is entirely numerical making analytical understanding difficult at times. On the other hand, the Hamiltonian approach, in principle, allows us to directly com-

pute the physical spectrum non-perturbatively by diagonalizing the lattice Hamiltonian. This is unlike the Euclidean path integral approach where it has to be extracted from the correlation functions. However, in practice, it is very difficult to diagonalize the Hamiltonian with sufficient accuracy. Therefore, practical calculation methods of diagonalization even for pure gauge theory on a finite lattice involve a severe truncation of the infinite dimensional Hilbert space to some finite dimension. Inappropriate truncation schemes violates continuum limit and physical quantities do not show correct scaling behavior. Truncations are done under various approximation schemes. The simplest and the oldest approximation scheme is the strong coupling expansion [6–8, 58–68] where an expansion is made around $g^2 \to \infty$. Strong coupling expansion allows us to compute the low energy spectrum by truncating the infinite dimensional physical loop Hilbert space to a finite dimensional loop Hilbert space spanned by loop states of small lengths and carrying small fluxes [see section 2.1]. However, these results are completely unphysical because, as shown by (1.6), the continuum limit of lattice gauge theory lies infinitely far away at the weak coupling ($g^2 \to 0$) end. The efforts to extrapolate the strong coupling results to the weak coupling region by Pade approximants etc did not lead to any conclusive results. The other popular variational [69–74] methods in the Hamiltonian lattice gauge theory also involve trial ground state wavefunctions and hence the success of this method strongly depends on the choice of proper variational ansatz. Moreover, they sample a very small part of the full gauge invariant Hilbert space. The Hamiltonian approach has also been exploited to develop other non-perturbative methods such as t-expansions [75, 76], plaquette expansion [77] and coupled cluster method [78–80]. Monte Carlo techniques have also been developed to study the spectrum of the lattice gauge theory Hamiltonian [81–83]. There are also renormalization group improved approaches [84] where the original Kogut-Susskind Hamiltonian is modified by including distant lattice sites/links interactions in order to minimize the discretization error and to get closer to the continuum limit. As mentioned above, all these methods, though non-perturbative, chop off the gauge invariant Hilbert space and improper truncation schemes create problems in the weak coupling limit. In order to proceed, we therefore need a complete characterization of the physical Hilbert space of SU(N) lattice gauge theory.

The redundant gauge degrees of freedom make it necessary to impose local Gauss law constraints on the solutions. Hence, it is desirable to remove these irrelevant or unphysical degrees of freedom from the theory. Within the Hamiltonian framework, where one is interested in the Hilbert space of the theory, the gauge redundancy increases its dimension considerably. For an $SU(N)$ gauge theory on lattice, each link of the lattice carries an $SU(N)$ link operator which contains $N^2 - 1$ degrees of freedom. However, there exists $SU(N)$ gauge invariance at each lattice site which corresponds to $N^2 - 1$ Gauss law constraints at each site. Hence, the actual dimension of the physical Hilbert space in $SU(N)$ lattice gauge theory, is

the dimension of the quotient space $\otimes_{links} SU(N) / \otimes_{sites} SU(N)$. On a d dimensional cubic lattice with periodic boundary condition, the number of links $\mathcal{L} = d(\mathsf{N}_s - 1)^d$ and the number of sites is $\mathcal{N} = (\mathsf{N}_s - 1)^d$, where N_s is the number of sites along any direction. Therefore, the dimension of physical Hilbert space per lattice site is exactly $(N^2 - 1)(d - 1)$. Now, there are two ways to proceed (a) one can fix the gauge to cut down the gauge degrees of freedom or (b) one can work with only gauge invariant or physical degrees of freedom. In the past few decades there have been a number of approaches proposed to reformulate $SU(N)$ Yang Mills theories [3–6, 26–51] directly in terms of loops or gauge invariant variables both in the continuum and on the lattice. All these approaches attempt to solve the non-abelian Gauss laws by first reformulating the theory in terms of operators which transform covariantly under gauge transformations and then exploiting this gauge covariance to define gauge invariant operators and gauge invariant states. In one of the earliest approaches [85], a polar decomposition of the covariant electric fields was used to solve the SU(2) Gauss law constraints. However, the resulting magnetic field term in the SU(2) gauge theory Hamiltonian is technically involved and difficult to work with. Also such a polar decomposition for SU(3) or higher $SU(N)$ gauge group is not clear. In approaches motivated by gravity [47, 86–92], a gauge invariant metric or dreilbein tensor is constructed out of the covariant SU(2) electric or magnetic field. The problem with such approaches is the exact equivalence between the initial and final (gauge invariant) coordinates is not simple. Further, the gauge group SU(2) plays a very special role and generalization of these ideas to $SU(N)$ gauge theories is not straightforward. In Nair-Karabali [93–95] approach the $SU(N)$ vector potentials enable us to define gauge covariant matrices leading to gauge invariant coordinates in $2+1$ dimensions, which are then quantized to analyze the theory directly in the physical Hilbert space $\mathcal{H}^p$. But, direct generalization to higher dimensions is difficult.

1.2 LOOP APPROACH AND MANDELSTAM CONSTRAINTS

An old and obvious choice for the gauge covariant operators [3–6, 26–41, 43–49, 51] in any dimension is the set of all possible holonomies around closed loops. These loop operators transform covariantly under gauge transformations, commute amongst themselves and their traces (Wilson loop operators) are gauge invariant. In fact, lattice formulation is tailor made for loop formulation of gauge theories. This is because in lattice formulation of gauge theories the basic variables are the link operators or equivalently holonomies and not the gluon fields like in the continuum. The loop operators are given by the product of these link operators sequentially along closed loops. In fact, the loop studies in Yang Mills theory also inspired people to utilize the loop approach to quantize gravity. This was made possible by Ashtekar's introduction of gauge theory like variables for canonical gravity, namely, a con-

nection and its canonically conjugate "electric field" with internal SU(2) degrees of freedom [96]. This approach to gauge theory eventually lead to a new non-perturbative quantization of canonical gravity [96–99] known as loop quantum gravity. This again has renewed interests in reformulating lattice gauge theories in terms of loops [33–36, 99, 100] in recent years.

The Mandelstam Constraints

In $SU(N)$ lattice gauge theories, one easily obtains a gauge invariant (Wilson) loop basis of the physical Hilbert space $\mathcal{H}^p$ by applying all possible $SU(N)$ Wilson loop operators on the gauge invariant strong coupling vacuum [3–6, 26–41, 43–49] . However, this simple construction again over describes lattice gauge theories. Now the over-description is because all possible Wilson loop operators are not mutually independent but satisfy constraints known as Mandelstam constraints [3–6, 26–41, 43–49]. They reflect the structure of the gauge group in the form of a set of relations between the loop states of the theory. More precisely, the Mandelstam constraints allow us to express products of Wilson loops in terms of the sum of the products of a number of loops implying that all loop states in the theory are not mutually independent (see section 2.2 for quantitative discussion). These identities were first introduced by Mandelstam for the gauge group O(3) [1, 3]. Extension to GL(N) was achieved by Giles [45].

The Mandelstam constraints are difficult to solve as they involve arbitrarily large number of non-local loop states of all shapes and sizes. On the other hand, the solutions of the Mandelstam constraints are of significance not only for writing non-abelian gauge theories without any spurious loop degrees of freedom but also for computing the Hamiltonian spectrum in the weak coupling limit. This is because unlike strong coupling limit ($g^2 \to \infty$), near the weak coupling or continuum ($g^2 \to 0$) limit loop states of arbitrary large sizes and fluxes become relevant [43, 48, 49]. These constraints become more and more complicated for higher N and higher dimensions. Therefore, they are the major obstacles in loop approaches to gauge theories. In fact, as also mentioned in [26], the loop approach advantages of solving the non-abelian Gauss law constraints become far less appealing due to the presence of these non-local Mandelstam constraints. In general, a common and widespread belief is that loop formulations of gauge theories, though aesthetically appealing, are seldom practically rewarding due to technical difficulties like the Mandelstam constraints. The work in this thesis directly addresses these issues (see section 1.3).

In the simplest SU(2) lattice gauge theory case the Mandelstam constraints can be exactly solved in arbitrary dimension using the prepotential approach [48–51, 101–106] (see section 2.3 for quantitative discussion) The resulting gauge invariant (loop) basis, also known as

the spin network basis, is orthonormal as well as complete. Thus, there are no redundant loop states or SU(2) Mandelstam constraints. The loop basis [48] is characterized by a set of angular momentum quantum numbers. However, the corresponding loop Schrödinger equation involves higher Wigner coefficients (eg; 18-j and 30-j Wigner symbols for 2+1 and 3+1 dimensions respectively) and is extremely complicated to solve. Further, there are numerous (angular momentum) triangular constraints at each lattice site and local abelian constraints on each link [48–51, 101–106]. All these issues make the prepotential approach less viable for any practical calculation even for the simplest SU(2) case. Also, this approach, when generalized to SU(3) or higher $SU(N)$ lattice gauge theories, further suffer from the problem of multiplicities involved with $SU(N)$ representations [101–104] for $N \geq 3$. In an alternate approach [33–36] to solve SU(2) Mandelstam constraints in 2+1 dimensions, a set of independent loops were chosen which were then used to construct arbitrary loops. But, this formalism does not describe loop-loop interactions and the dynamics cannot be studied due to the lack of a systematic transition from the links to the loops.

1.3 CANONICAL TRANSFORMATIONS, LOOPS AND GAUGE-SPIN DUALITY

Inspite of extensive research in the past [3–6, 26–41, 43–51], a systematic way of transition from the standard Kogut-Susskind link formulation of pure $SU(N)$ gauge theory to a loop formulation in terms of fundamental loop operators and loop states is still missing in the literature. In this thesis, we construct canonical transformations which allows us to systematically reformulate pure $SU(N)$ Kogut-Susskind Hamiltonian lattice gauge theories [6] in terms of a set of fundamental loop operators and loop electric fields[52–54]. We start with the standard Kogut-Susskind Hamiltonian formulation of $SU(N)$ lattice gauge theory where the fundamental operators are the link operators and its conjugate electric fields. We obtain [52] fundamental loop operators by glueing the standard Kogut-Susskind link operators along certain loops over the entire lattice through iterative canonical transformations. These loop operators are independent and any gauge invariant operator can be written in terms of them. The canonical transformations also produce a set of $SU(N)$ string flux operators and their conjugate electric fields. The relation between the initial Kogut-Susskind $SU(N)$ link operators and conjugate electric fields and the final physical $SU(N)$ loop, unphysical string operators and their corresponding conjugate electric fields are explicitly worked out in detail in a self consistent manner in this thesis. We show that as a consequence of $SU(N)$ Gauss laws, all string degrees of freedom become cyclic or unphysical and decouple, leaving only the physical and mutually independent loop degrees of freedom. As the final loop formulation and the initial Kogut-Susskind link formulation are related through a series of canonical

transformations, no extra loop degrees of freedom are generated and hence the problem of Mandelstam constraints is completely evaded for all $SU(N)$ lattice gauge theories.

The resulting loop formulation has the following features:

1. This loop formulation is free of local Gauss law, Mandelstam as well as Bianchi identity constraints.

2. The $SU(N)$ Kogut-Susskind Hamiltonian, written in terms of the fundamental loop operators and conjugate electric fields, has $SU(N)$ global gauge invariance. There are no gauge fields. Number of physical degrees of freedom exactly matches the number of loop degrees of freedom modulo a global $SU(N)$ Gauss law corresponding to global $SU(N)$ invariance. Complete and orthonormal electric as well as a dual magnetic loop bases satisfying the global $SU(N)$ gauge invariance are constructed (see chapter 3).

3. The resulting loop formulation [52, 53] is shown to be dual to the Kogut-Susskind link formulation of $SU(N)$ lattice gauge theory. This duality is the generalization of Wegners duality [7, 55, 56] between Z_2 lattice gauge theory and quantum Ising model.

4. Loop or physical Hilbert Space $\mathcal{H}^p$ of pure $SU(2)$ lattice gauge theory [54] is completely and most economically realised in terms of Hilbert space of Wigner coupled hydrogen atoms. One hydrogen atom is assigned to every plaquette of the lattice. A complete orthonormal description of the Wilson loop basis in $\mathcal{H}^p$ is obtained by all possible angular momentum Wigner couplings of hydrogen atom energy eigenstates $|n\ l\ m\rangle$ describing electric fluxes on the loops in SU(2) lattice gauge theory. SU(2) global invariance implies that the total angular momentum of all Hydrogen atoms vanish. Also, the Hamiltonian is written in terms of the generators of dynamical symmetry group of Hydrogen atom, SO(4,2) (see chapter 4).

OVERVIEW OF THE THESIS

The overview of the thesis is as follows (also see the flow chart in Figure 1.1). In chapter 2, We start with a brief review of Kogut-Susskind Hamiltonian formulation. This is done for completeness as well as fixing the notations to be used through out the thesis. We then discuss the Wilson loop formulation of gauge theories and the issue of Mandelstam constraints. As mentioned earlier, the $SU(N)$ Mandelstam constraints are the major obstacle in the loop formulation of gauge theories. This is followed by a discussion of the prepotential approach where Mandelstam constraints are made local and solved. However, new triangular (inequality) constraints involving angular momenta pop up and the loop dynamics becomes extremely complicated.

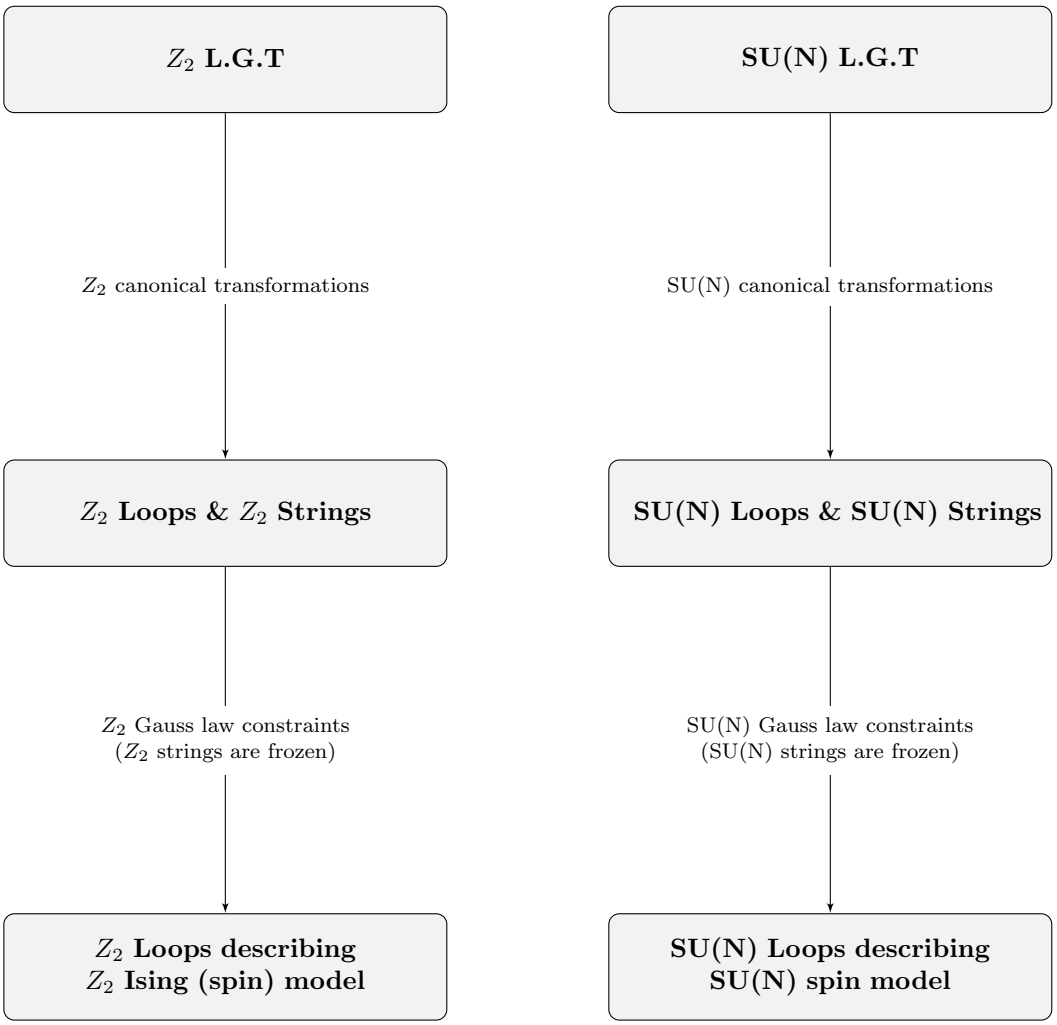

Figure 1.1: Outline of the thesis. Canonical transformations are constructed which lead to a loop formulation of Z_2 as well as $SU(N)$ lattice gauge theory in (2+1) and (3+1) dimensions. The loop formulation also helps us in constructing an exact isomorphism between the loop Hilbert space of SU(2) lattice gauge theory and the Hilbert space of Wigner coupled hydrogen atoms with no net angular momentum.

The main motivation behind the thesis is to construct a loop formulation free of Mandelstam constraints, triangular constraints which is suitable for studying $SU(N)$ loop dynamics in the weak coupling limit. Such a loop formulation is constructed in chapter 3. As illustrated in Figure 1.1, we construct canonical transformations which systematically transform the link operators of standard Kogut-Susskind formulation into loop operators and string operators. The string operators naturally decouple from the physical Hilbert space due to Gauss law constraints leaving behind a loop formulation of $SU(N)$ lattice gauge theory. These canonical transformations are first constructed for the simple case of abelian Z_2 gauge theory and then for the more involved $SU(N)$ gauge theory in 2+1 followed by 3+1 dimensional lattice.

In chapter 4, we show that in $2+1$ dimensions, the loop formulation of Z_2 gauge theory constructed through canonical transformations is exactly equivalent to a quantum Ising model within the gauge invariant Hilbert space. This is the well known Wegner's duality. We then generalize this duality to $SU(N)$ lattice gauge theory. This duality is then used to construct a disorder operator for $SU(N)$ lattice gauge theoies.

In chapter 5, we focus on the loop formulation of SU(2) lattice gauge theory and construct an exact isomorphism between the loop Hilbert space of SU(2) lattice gauge theory and that of a collection of coupled hydrogen atoms with no net angular momentum. We also discuss the connection between gauge theory dynamics and the dynamical symmetry group $SO(4,2)$ of hydrogen atom. A variational ansatz for the ground state and the first excited state motivated by this hydrogen atom correspondence is also given.

In chapter 6, We conclude by discussing possible extensions and applications of the loop formulation developed in this thesis. The basic outline of the thesis is summarized in Figure 1.1.

The technical details of the canonical transformations on a finite lattice and the construction of the magnetic basis of SU(2) lattice gauge theory are described in appendix A and appendix B respectively. Appendix C describes some calculational methods in the loop formulation.

2

HAMILTONIAN FORMULATION OF SU(N) LATTICE GAUGE THEORY

In this chapter, we will briefly review Kogut-Susskind Hamiltonian formulation [6–8] of pure SU(N) lattice gauge theory. We also briefly discuss the prepotential approach to the loop formulation [48–50] of pure SU(2) lattice gauge theory. Apart from the purpose of completeness, it will serve us in introducing the notations and conventions which will be used in the rest of the thesis. The various issues and problems involved in each of the formulations and the motivation behind the work described in chapters 3, 4 and 5 will also be discussed.

In section 2.1, we start with a brief review of the Kogut-Susskind link formulation of pure SU(N) gauge theory on a lattice. In section 2.2, we briefly discuss the issues involved in constructing a loop approach with the set of all Wilson loops. The problem of Mandelstam constraints [3–6, 26–41, 43–49]. is emphasized. In section 2.3, we discuss how SU(2) Mandelstam constraints can be solved with in the prepotential formulation. We then briefly describe the various issues involved in the loop dynamics in terms of prepotentials in section 2.4. We conclude this chapter by briefly discussing the generalization of the prepotential formulation to SU(N) gauge theory and the associated problems.

Throughout the thesis, lattice sites and links will be denoted by n and $(n,\hat{i})$ (or (n,i) where $\hat{i}$ is the unit vector along the direction of the link. We often use l and p for the link and plaquette index for convenience.

2.1 KOGUT-SUSSKIND LINK FORMULATION & GAUSS LAW CONSTRAINTS

We now briefly review the lattice formulation of the Hamiltonian pure Yang Mills theory [6, 8] due to Kogut and Susskind. The Hamiltonian formulation of SU(N) lattice gauge theory is realized on a space lattice with continuous time.

Let's start with the continuum Lagrangian formulation of $SU(N)$ gauge theory which is based on gauge field $A_\mu = A^a_\mu \lambda^a$, where $\lambda^a; a = 1, \cdots, N^2-1$ are the generators of SU(N) algebra in the fundamental representation satisfying $Tr\left(\lambda^a \lambda^b\right) = \frac{1}{2}\delta^{ab}$. The Lagrangian is given by

$$L = \frac{1}{2}\int d^3x \; Tr(F_{\mu\nu}F^{\mu\nu}). \tag{2.1}$$

Above, $F_{\mu\nu} = \partial_\mu A_\nu - \partial_\nu A_\mu + ig[A_\mu, A_\nu]$ is the field strength and g is the coupling constant. There is an internal (color) space at each space time point. Local gauge transformations are basis transformation on this internal space. One can define an operator $U(x_1, x_2)$ which 'parallel transports' a vector in the internal space at x_1 to the internal space at x_2 along a path C.

$$U_C(x_1, x_2) \equiv P_C e^{ig \int_{x_1}^{x_2} A_\mu(x) dx^\mu}. \tag{2.2}$$

Above, P_C denotes the path ordered product along curve C. This is necessary as A_μ at different points do not commute. The parallel transport operator in general depends upon the path C. $SU(N)$ gauge theory can be formulated on a space time lattice using the parallel transport operator. We consider a hyper cubical space time lattice with lattice spacing a. We define lattice gauge fields $\bar{A}_\mu(\bar{x})$ at the midpoint $\bar{x}$ of each link where $\bar{A}_\mu(\bar{x})$ is the average value of the continuum gauge field A_μ along the link in the direction μ. A link operator corresponding to a link starting at site n along the direction $\hat{i}$ is defined as

$$U(n, \hat{i}) = P e^{ig \int_{x}^{x+\hat{i}} A_\mu(x) dx^\mu} \equiv e^{iag\bar{A}_i(\bar{x})}. \tag{2.3}$$

The link operators has the following properties:

$$U(n, \hat{i})\, U^\dagger(n, \hat{i}) = \mathcal{I}, \quad U^\dagger(n, \hat{i})\, U(n, \hat{i}) = \mathcal{I}, \quad |U(n, \hat{i})| = \mathcal{I}. \tag{2.4}$$

Above, $\mathcal{I}$ is an $N \times N$ identity operator and $|U| \equiv \det U$. Consider the product of link operators along a plaquette (say, in the 12 plane) on the lattice. It is given by

$$\begin{aligned} U_{p_{12}} &= e^{iagA_1(x,y-a/2)} e^{iagA_2(x+a/2,y)} e^{-iagA_1(x,y+a/2)} e^{-iagA_2(x-a/2,y)} \\ &= e^{iag(A_1(x,y) - \nabla_2 A_1(a/2)} e^{iag(A_1(x,y) + \nabla_1 A_2(a/2)} e^{-iag(A_1(x,y) + \nabla_2 A_1(a/2)} e^{-iag(A_2(x,y) - \nabla_1 A_2(a/2)} \\ &= e^{ia^2 g F_{12} + o(a^3)}. \end{aligned} \tag{2.5}$$

Above, we have defined $\nabla_2 A_1(x,y) \equiv \frac{A_1(x,y+a/2) - A_1(x,y)}{(a/2)}$ and $\nabla_1 A_2(x,y) \equiv \frac{A_2(x+a/2,y) - A_1(x,y)}{(a/2)}$. These expression reduces to continuum partial derivatives under the limit $a \to 0$. Similarly, link operators along a general plaquette in the $\mu\nu$ plane is given by $U_P = e^{ia^2 g F_{\mu\nu} + o(a^3)}$. Now, TrU_p is given by

$$\begin{aligned} TrU_p &= Tr(1 + ia^2 g F_{\mu\nu} - \frac{a^4 g^2}{2!} F_{\mu\nu}^2 + \cdots) \\ &= Tr\big(1 - \frac{1}{2} a^4 g^2 F_{\mu\nu}^2 + \cdots\big). \end{aligned} \tag{2.6}$$

Above, we have used the fact that $TrF_{\mu\nu} = Tr(F^a_{\mu\nu}\lambda^a) = 0$. Since, TrU_P is not Hermitian, we define the lattice Lagrangian[1] as

$$L = \frac{1}{4a^4g^2}\sum_P 2N - Tr[U_P - U_P^\dagger].$$

Above, the summation is over space time plaquettes. This Lagrangian reduces to the standard continuum Lagrangian 2.1 under a naive continuum limit. Since, we are interested in the Hamiltonian formulation, temporal gauge $A_0 = 0$, is chosen so that the link operators corresponding to the links along the time direction are 1 and continuum limit is performed along the time direction. This leads to the following Lagrangian [8, 40]:

$$L = \sum_{links}\frac{a}{4g^2}Tr\left(\dot{U}^\dagger\dot{U}\right) + \sum_{plaq}\frac{1}{4ag^2}\left\{2N - (TrU_p + h.c)\right\}. \tag{2.7}$$

Above, the summation is over spatial links and spatial plaquettes. U_p is the product of link operators around a spatial plaquette. Above, we have suppressed the $(n,\hat{i})$ index for simplicity. The conjugate momentum of $U_{\alpha\beta}(n,\hat{i})$ and $U^\dagger_{\alpha\beta}(n,\hat{i})$ is given by $\Pi_{\alpha\beta}(n,\hat{i}) = \frac{a}{4g^2}(\dot{U}^\dagger_{\alpha\beta}(n,\hat{i}))$ and $\Pi^\dagger_{\alpha\beta}$ respectively. Quantization is achieved by imposing the following canonical quantization condition:

$$\left[U_{\alpha\beta}(n,\hat{i}), \Pi_{\gamma\delta}(m,\hat{j})\right] = i\delta_{\alpha\gamma}\delta_{\beta\delta}\delta_{ij}\delta_{mn}. \tag{2.8}$$

The Hamiltonian is

$$H = \sum_{links}\frac{a}{4g^2}Tr\left(\dot{U}^\dagger\dot{U}\right) - \sum_{plaq}\frac{1}{4ag^2}\left\{2N - (TrU_p + h.c)\right\}. \tag{2.9}$$

It is convenient to formulate the theory in terms of lie algebra valued conjugate fields. To this effect, conjugate electric fields are defined [8] as

$$\begin{aligned} E^a_+(n,\hat{i}) &= -i\frac{a}{4g^2}\left[Tr\left(\dot{U}^\dagger(n,\hat{i})\frac{\lambda^a}{2}U(n,\hat{i}) - h.c\right)\right]. \\ E^a_-(n+\hat{i},\hat{i}) &= -i\frac{a}{4g^2}\left[Tr\left(\dot{U}(n,\hat{i})\frac{\lambda^a}{2}U^\dagger(n,\hat{i}) - h.c\right)\right]. \end{aligned} \tag{2.10}$$

The quantization conditions (2.8) imply :

$$\begin{aligned} \left[E^a_+(n,\hat{i}), U_{\alpha\beta}(n,\hat{i})\right] &= -\left(\frac{\lambda^a}{2}U(n,\hat{i})\right)_{\alpha\beta} \Rightarrow \left[E^\alpha_+(n,\hat{i}), E^b_+(n,\hat{i})\right] = if^{abc}E^c_+(n,\hat{i}), \\ \left[E^\alpha_-(n,\hat{i}), U_{\alpha\beta}(n-\hat{i},i)\right] &= \left(U(n-\hat{i},\hat{i})\frac{\lambda^a}{2}\right)_{\alpha\beta} \Rightarrow \left[E^a_-(n,\hat{i}), E^b_-(n,\hat{i})\right] = if^{abc}E^c_-(n,\hat{i}). \end{aligned} \tag{2.11}$$

1 The higher order terms in (2.6) are irrelevant [8, 57] in the renormalization group sense.

In (2.11), f^{abc} are the SU(N) structure constants. Therefore, $E_-(n,\hat{i})$ and $E_+(n,\hat{i})$ are the generators of left and right gauge transformations. They are related to each other by the following relation

$$E_-(n+\hat{i},i) = -U^\dagger(n,\hat{i})E_+(n,\hat{i})U(n,\hat{i}). \tag{2.12}$$

In other words,

$$E^a_-(n+\hat{i},i) = -R_{ab}(U^\dagger(n,\hat{i}))E^b_+(n,\hat{i}). \tag{2.13}$$

where :

$$R_{ab}(U(n,\hat{i})) \equiv \frac{1}{2}Tr\left(\lambda^a U(n,\hat{i})\lambda^b U^\dagger(n,\hat{i})\right). \tag{2.14}$$

is a rotation matrix with $R^TR = RR^T = 1$. Note that the relation (2.12) is consistent with the commutation relations (2.11) and shows that $E_-(n,\hat{i})$ and $E_+(m,\hat{j})$ mutually commute:

$$\left[E^a_-(n,\hat{i}), E^b_+(m,\hat{j})\right] = 0.$$

From (2.12) it follows that they satisfy the kinematical constraint:

$$\sum_{a=1}^{3} E^a_+(n,\hat{i})E^a_+(n,\hat{i}) = \sum_{a=1}^{3} E^a_-(n+\hat{i},\hat{i})E^a_-(n+\hat{i},\hat{i}) \equiv E^2(n,\hat{i}), \quad \forall(n,\hat{i}). \tag{2.15}$$

ensuring that their magnitudes are equal. Using eqn. (2.10), it can be shown that $(E_\pm)^2 \equiv \sum_a E^a_\pm E^a_\pm = \frac{a^2}{g^4}Tr(\dot{U}^\dagger\dot{U})$. The Hamiltonian (2.9), when written in terms of the link operators and electric fields, become

$$\begin{aligned} H &= \sum_{links}\frac{g^2}{4a}E^2(l) - \sum_{plaq}\frac{1}{4ag^2}\left\{2N - (TrU_p + h.c)\right\} \\ &= H_E + H_B. \end{aligned} \tag{2.16}$$

In (2.16) TrU_p reduces to B^aB^a on continuum limit, where B^a is along the direction perpendicular to the plaquette p. Therefore, the above Hamiltonian (2.16) reduces to the continuum Hamiltonian under a naive continuum limit. The SU(N) gauge transformations rotates the link operator and the electric fields in the following way:

$$E_\pm(n,\hat{i}) \to \Lambda(n)E_\pm(n,\hat{i})\Lambda^\dagger(n), \quad U(n,\hat{i}) \to \Lambda(n)U(n,\hat{i})\Lambda^\dagger(n+\hat{i}). \tag{2.17}$$

The commutation relations (2.11) along with the gauge transformations (2.17) imply that

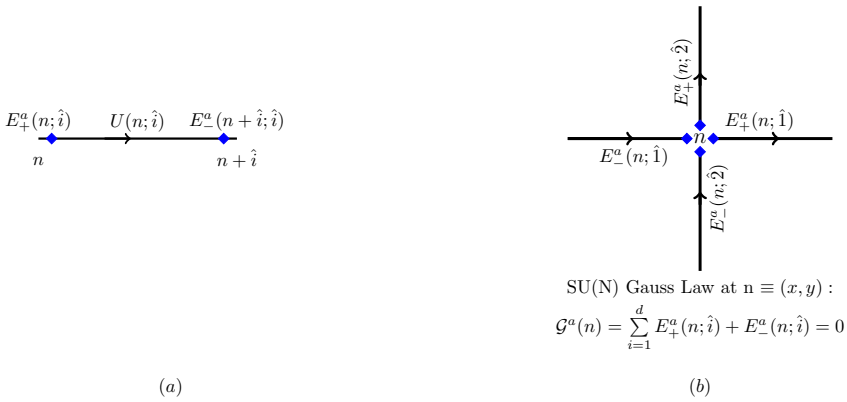

Figure 2.1: The location of the left and right electric fields $E_+(n;\hat{\imath})$ and $E_-(n+\hat{\imath};\hat{\imath})$: (a) on a link $(n;\hat{\imath})$, (b) around a lattice site $n = (x,y)$. The SU(N) Gauss law is also pictorially shown in (b).

the generators of SU(N) gauge transformations at any lattice site n are:

$$\mathcal{G}^a(n) = \sum_{i=1}^{d} \left(E^a_-(n,\hat{\imath}) + E^a_+(n,\hat{\imath})\right), \quad \forall n, a. \tag{2.18}$$

The corresponding Gauss law constraints[2] are

$$\mathcal{G}^a(n)|\psi_{phys}\rangle = 0. \tag{2.19}$$

at all lattice sites n, $|\psi_{phys}\rangle$ being any state in the physical Hilbert space $\mathcal{H}^p$ of gauge theory. Hence, the canonical variables $\left\{E_\pm(n,\hat{\imath}), U(n,\hat{\imath})\right\}$ are not free and are constrained by (2.18). The Gauss law constraints are illustrated in Figure 2.1(b).

In the strong coupling limit $g^2 \to \infty$, H_E dominates. Since, H_E is a Casimir of SU(N), the spectrum of H_E is discrete. Strong coupling vacuum state $|0\rangle$ is defined as the state which is annihilated by all the electric fields:

$$E^a_+(n,\hat{\imath})\ |0\rangle = E^a_-(n+\hat{\imath},\hat{\imath})\ |0\rangle = 0. \tag{2.20}$$

Since, $E^2_\pm|0\rangle = 0$, $|0\rangle$ is the vacuum state in the strong coupling limit. Also, $|0\rangle$ is gauge invariant as $\mathcal{G}^a(n)|0\rangle = 0$. The quantization rules (2.11) show that the link operators $U_{\alpha\beta}(n,\hat{\imath})$ acting on the strong coupling vacuum (2.20) create SU(N) fluxes on the links. As an example, using (2.11):

$$E^2(n,\hat{\imath})\Big(U_{\alpha\beta}|0\rangle\Big) \quad = \quad \frac{1}{2N}\left(N^2-1\right)\Big(U_{\alpha\beta}|0\rangle\Big). \tag{2.21}$$

Since the strong coupling Hamiltonian does not couple different links, it is clear that the eigenvectors of Hamiltonian are simply the product of U corresponding to different links

2 Hamiltonian formulation is not equivalent to the Lagrangian formulation unless the Gauss law constraints are imposed. This is because the Lagrangian formulation has Gauss law as an equation of motion while Hamiltonian formulation doesn't and therefore has to be imposed as a constraint on the states.

acting on the strong coupling vacuum $|0\rangle$. But, Gauss law constraint (2.18), implies that the lowest energy physical (gauge invariant) excitation involves the trace of the product of 4 links around the smallest loop on a lattice which is a plaquette. It has an energy given by $4\left(\frac{N^2-1}{2N}\right)$. Therefore, there is a clear mass gap in the spectrum. Consider a static quark-antiquark pair at sites x and y respectively[3]. The potential energy is defined as the energy of the lowest gauge invariant excitation. This state is obviously given by exciting the shortest path of links connecting the quark-antiquark pair. The potential energy is given by $L\left(\frac{N^2-1}{2N}\right)$, where L is the distance between the points x and y. Since, the potential energy depends linearly on the distance between the quark and antiquark, the force is independent of the distance. This leads to confinement. Therefore, strong coupling limit clearly has confinement and mass gap. However, as discussed in the previous chapter, the lattice is coarse grained when g^2 is large and therefore far away from the physical continuum limit. There have been numerous attempts in the beginning to reach the continuum limit through strong coupling expansion [6–8, 58–68] starting from the strong coupling limit $g^2 \to \infty$. In the Hamiltonian formulation, this involves solving H_E exactly and H_B in perturbation theory. For example, the first correction [6] to the strong coupling vacuum state $|0\rangle$ of H_E due to H_B is given by

$$|\psi_1\rangle = -\frac{1}{H_E} H_B |0\rangle = \frac{4}{3ag^2} \sum_p \left(Tr U_p + h.c \right) |0\rangle. \tag{2.22}$$

Above, U_p represents the product of link operators along a plaquette and the summation is over the plaquettes on the lattice. The first order correction to the vacuum energy [6] is

$$\delta E = \left\langle 0 \middle| H_B \, \frac{-1}{H_E} \, H_B \middle| 0 \right\rangle = \left(\frac{-32}{a^4 g^6} \right) V.$$

Above, V gives the volume of space. In the above two equations, we have used the expressions for the first order corrections to strong coupling vacuum state and energy in the standard Rayleigh-Schrodinger perturbation theory. We have also used the fact that the eigenvalue of H_E corresponding to the strong coupling vacuum state is 0. The higher corrections involve larger loops carrying larger fluxes suppressed by higher powers of the coupling constant g^2. A systematic expansion in $1/g^2$ can be constructed starting with the exact confining solution at $g^2 \to \infty$. It was expected that these results could be extrapolated to the continuum limit which lies at $g^2 \to 0$. The success of this method crucially depend upon the requirement of analyticity in the entire region, $g^2 \in (0, \infty)$. it runs into difficulties in the intermediate coupling region due to roughening[4] transition [107–110]. Further, when $g^2 \to 0$, large loops and loops carrying large fluxes becomes relevant. Therefore, it is desirable to reformulate the theory directly in terms of mutually independent loop operators. It is also

3 For simplicity, we consider x and y to be on the same line

4 Roughening transition does not lead to deconfinement as string tension does not vanish. However, it makes the strong coupling expansion results unreliable.

clear from eqn. (2.22) that even though the basic quantized degrees of freedom in the Kogut-Susskind formulation are defined on links, the actual gauge invariant physical excitations of a pure gauge theory are in the form of loops.

2.2 WILSON LOOP FORMULATION & MANDELSTAM CONSTRAINTS

The physical observables and physical states of a gauge theory should be gauge invariant and satisfy Gauss law constraints. Therefore, it is useful to remove the gauge redundancies by formulating the theory in terms of a set of gauge invariant Wilson loops, $W(\Gamma) = Tr(Pe^{i\int_\Gamma A_i dx^i})$, where A_i is the gauge connection and Γ is an oriented, closed loop. It was shown in [45] that the set of all Wilson loops contains all the gauge invariant information contained in a gauge theory.

In lattice gauge theory, a manifestly gauge invariant geometrical basis in the physical Hilbert space is given by the set of all possible Wilson loop states

$$|\Gamma\rangle = W(\Gamma)|0\rangle, \tag{2.23}$$

where, $W(\Gamma)$ is the product of link operators along any oriented, closed loop Γ and $|0\rangle$ is the strong coupling vacuum. The problem with the above loop basis is that it is overcomplete. The Mandelstam constraints [3–6, 26–41, 43–49] amongst the various loop states express this overcompleteness of the Wilson loop basis. The Mandelstam constraints are relations between Wilson loops which reflect the structure of the gauge group.

Mandelstam constraints on a lattice

For an $SU(N)$ gauge theory on a lattice, there are (N^2-1) degrees of freedom on each link and (N^2-1) Gauss law constraints on each site. Therefore, the number of gauge invariant degrees of freedom is given by the dimension of the quotient space $\otimes_{links} SU(N) / \otimes_{sites} SU(N)$. On a d dimensional lattice with N_s sites and $\mathsf{N}_s - 1$ links along any direction and open boundary condition, it is given by

$$\mathsf{N}_{df} = (N^2-1)\left[\mathcal{L} - \mathcal{N}\right] = (N^2-1)\left[d(\mathsf{N}_s-1)(\mathsf{N}_s)^{\mathsf{d}-1} - (\mathsf{N}_s)^{\mathsf{d}}\right].$$

Above, $\mathcal{L}$ and $\mathcal{N}$ represents the total no of links and sites on the lattice. But, there is an infinite number of Wilson loops even on a finite lattice. Therefore, the Wilson loop basis is clearly over-complete. A classical equivalence theorem [45] states that once the Mandelstam constraints are solved, the number of independent loop variables left would equal the number of physical degrees of freedom. Therefore, the extra loop degrees of freedom have to be

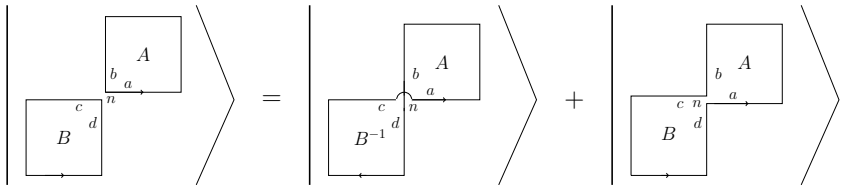

Figure 2.2: Simplest example of Mandelstam constraints for SU(2) gauge theory on a 2 dimensional spatial lattice.

removed by imposing the Mandelstam constraints. The origin of Mandelstam constraints can be traced back to the identities satisfied by the traces of $SU(N)$ matrices. For concreteness, we consider SU(2) gauge theory on a 2 dimensional lattice for illustrating the Mandelstam constraints. In order to describe a simple example of Mandelstam constraints, let's consider 2 plaquettes A and B touching each other at a common lattice site n as shown in the Figure 2.2. The corresponding Wilson loop operators satisfy [33–36]

$$(TrU_A)(TrU_B) = Tr(U_A U_B) + Tr(U_A U_B^{-1}).$$

The above relation is a trivial identity involving any two SU(2) matrices U_A and U_B. It can be easily checked by writing the SU(2) matrices in the following representation: $U_X = X_0\mathbf{1} + iX_a\sigma^a$, where σ^a are the pauli matrices, X_0, X_a are real and satisfy $X_0^2 + X_1^2 + X_2^2 + X_3^2 + X_4^2 = 1$. Therefore, $U_A = A_0\mathbf{1} + iA_a\sigma^a$, $U_B = B_0\mathbf{1} + iB_b\sigma^b$ and $Tr(U_A U_B) = 2A_0B_0 - 2A_aB_a, Tr(U_A U_B^{-1}) = 2A_0B_0 + 2A_aB_a$, $(TrU_A)(TrU_B) = 4A_0B_0$. This leads to the above identity. The above operator identity implies the following relation between the corresponding loop states:

$$\begin{aligned} &|\gamma_1\rangle = (TrU_A)(TrU_B)|0\rangle, \qquad |\gamma_2\rangle = Tr(U_A U_B)|0\rangle, \qquad |\gamma_3\rangle = Tr(U_A U_B^{-1})|0\rangle \\ &\qquad\qquad\qquad\qquad |\gamma_1\rangle = |\gamma_2\rangle + |\gamma_3\rangle. \end{aligned} \tag{2.24}$$

Thus, the loop states $|\gamma_1\rangle, |\gamma_2\rangle, |\gamma_3\rangle$ are linearly dependent. The Mandelstam constraints become more and more complicated when larger loops and loops of large fluxes are involved. To appreciate this better, let's consider most general loop states involving only these 2 plaquettes A and B [48, 49]:

$$\begin{aligned} |N_A, N_B\rangle &= (TrU_A)^{N_A}(TrU_B)^{N_B}|0\rangle \\ &= (TrU_A)^{N_A-1}(TrU_B)^{N_B-1}\left(Tr(U_A U_B) + Tr(U_A U_B^{-1})\right)|0\rangle \\ &= (TrU_A)^{N_A-2}(TrU_B)^{N_B-2}\left(Tr(U_A U_B) + Tr(U_A U_B^{-1})\right)^2|0\rangle \\ &\cdots \\ &= (TrU_A)^{N_A-N_{min}}(TrU_B)^{N_B-N_{min}}\left(Tr(U_A U_B) + Tr(U_A U_B^{-1})\right)^{N_{min}}|0\rangle, \end{aligned}$$

where N_A, N_B are two arbitrary integers giving the fluxes over the plaquettes A and B and N_{min} =Minimum(N_A, N_B). Thus, the above expression gives $2N_{min}+1$ different linearly dependent loop states. The number of loop states and the constraints between them increases with the SU(2) flux value N_{min}. Adding more plaquettes gives more complicated loop states as well as Mandelstam constraints. It is also clear that this problem becomes worse in higher dimensions and higher gauge groups. As mentioned earlier, in the strong coupling ($g^2 \to \infty$) expansion technique, in low orders of perturbation theory, one deals with only a finite number of small loops with small fluxes. Therefore, Mandelstam constraints can be easily solved using Gram-Schmidt orthogonalisation techniques. But, in going to the weak coupling continuum limit ($g^2 \to 0$), large loops with large fluxes becomes important and Mandelstam constraints becomes more and more involved. Therefore, one is confronted with the problem of finding a complete set of linearly independent loop states amongst loop states of all shapes, sizes and carrying arbitrary fluxes and touching/crossing each other at arbitrary lattice sites. One way of solving these constraints is to use prepotentials [48–51, 101–106]. The prepotential formulation and the issues involved in it are discussed in the next section.

2.3 PREPOTENTIAL FORMULATION & MANDELSTAM CONSTRAINTS

In this section, we briefly describe the prepotential formulation of SU(N) lattice gauge theory. The Mandelstam constraints can be solved in the prepotential formulation. In this formulation [48–51, 101–106], the basic link operators and conjugate electric fields are replaced by harmonic oscillator n-tuplets called prepotentials. These prepotential operators form an alternate set of variables of the theory. Both the Hamiltonian and the constraints are rewritten in terms of prepotentials. For simplicity we choose SU(2) lattice theory [48–50] for illustrations. Generalization to SU(N) prepotentials [101–106] will be briefly discussed towards the end of the chapter.

As discussed in section 2.1, two electric fields are associated with each link of the lattice which are related through a rotation. We define SU(2) prepotential operators $a^\dagger(n,\hat{i};L)$ and $a^\dagger(n,\hat{i};R)$ and associate it with left and right end of the link $(n,\hat{i})$. Using the Schwinger boson construction [111] of the angular momentum algebra, the left and the right electric fields on a link $(n,\hat{i})$ can be written as:

$$\begin{aligned} &\text{Left electric fields:} && E^a_+(n,\hat{i}) \equiv a^\dagger(n,\hat{i};L)\frac{\sigma^a}{2}a(n,\hat{i};L), \\ &\text{Right electric fields:} && E^a_-(n+\hat{i},\hat{i}) \equiv a^\dagger(n,\hat{i};R)\frac{\sigma^a}{2}a(n,\hat{i};R). \end{aligned} \tag{2.25}$$

In (2.25), $a_\alpha(n,\hat{i};l)$ and $a^\dagger_\alpha(n,\hat{i};l)$ are the doublets of harmonic oscillator creation and annihilation operators with $l = L,R, \alpha = 1,2$. Like $E^a_+(n,\hat{i})$ and $E^a_-(n+\hat{i},i)$, the locations of

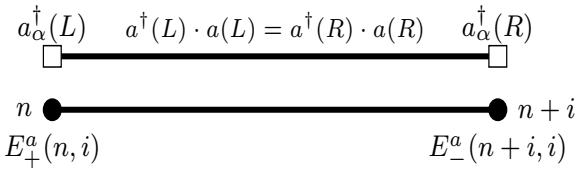

Figure 2.3: The left and right electric fields and the corresponding prepotentials in SU(2) lattice gauge theory. We have denoted $a^\dagger(n,\hat{i},L)$ and $a^\dagger(n,\hat{i},R)$ by $a^\dagger(L)$ and $a^\dagger(R)$ respectively.

$a(n,\hat{i},L), a^\dagger(n,\hat{i},L)$ and $a(n,\hat{i},R), a^\dagger(n,\hat{i},R)$ are on the left and the right of the link $(n,\hat{i})$. As we mostly work on a given link, we suppress the link indices and denote $a^\dagger(n,\hat{i},L)$ and $a^\dagger(n,\hat{i},R)$ by $a^\dagger(L)$ and $a^\dagger(R)$ respectively. This is clearly illustrated in Figure 2.3. Note that the relations (2.25) imply that the strong coupling vacuum (2.20) is also the harmonic oscillator vacuum. Under SU(2) gauge transformation, the prepotential harmonic oscillators transform as SU(2) doublets:

$$\begin{aligned} a^\dagger_\alpha(L) &\to a^\dagger_\beta(L)\ \left(\Lambda^\dagger_L\right)^\beta{}_\alpha, \qquad & a^\dagger_\alpha(R) &\to a^\dagger_\beta(R)\ \left(\Lambda^\dagger_R\right)^\beta{}_\alpha \\ a^\alpha(L) &\to \left(\Lambda_L\right)^\alpha{}_\beta\ a^\beta(L), \qquad & a^\alpha(R) &\to \left(\Lambda_R\right)^\alpha{}_\beta\ a^\beta(R). \end{aligned} \tag{2.26}$$

One can also define $\tilde{a}^{\dagger\alpha} = \epsilon^{\alpha\beta}a^\dagger_\beta$ and $\tilde{a}_\alpha = \epsilon_{\alpha\beta}a^\beta$ which under $SU(2)$ transformation transform like a^α and $a^\dagger_\alpha$ respectively. Here, $\epsilon_{\alpha\beta}$ is a completely antisymmetric Levi Cevita tensor ($\epsilon_{11} = \epsilon_{22} = 0, \epsilon_{12} = -\epsilon_{21} = 1$). The kinematical constraint (2.15), $E^a_+(n,\hat{i})E^a_+(n,\hat{i}) = E^a_-(n+\hat{i},i)E^a_-(n+\hat{i},i)$, implies that the number of harmonic oscillators at the left end of a link equals the number at the right end [48, 49]. I.e,

$$N_a = N_b; \qquad N_a \equiv a^\dagger\cdot a, \qquad N_b = b^\dagger\cdot b. \tag{2.27}$$

Above, we have defined $a(n,\hat{i},L) \equiv a$ and $a(n,\hat{i},R) \equiv b$. The equations (2.25) defines the left and right electric fields in terms of the prepotentials. To establish complete equivalence, we now write down the link operators explicitly in terms of the prepotentials. From $SU(2)$ gauge transformations of the link operator in (2.11),(2.17) and SU(2) gauge transformations (2.26) and the constraint (2.27) of the prepotentials [48–51, 101–106],

$$U_{\alpha\beta} \;=\; \frac{1}{\sqrt{(\hat{N}+1)}}\left(a_\alpha\tilde{b}_\beta - \tilde{a}^\dagger_\alpha b^\dagger_\beta\right)\frac{1}{\sqrt{(\hat{N}+1)}}. \tag{2.28}$$

Above, $\hat{N} = a^\dagger\cdot a = b^\dagger\cdot b$ is the number operator. In (2.28), we have suppressed the location of the link $(n,\hat{i})$ and defined the left and right prepotentials as a and b respectively, for ease of notation. Since prepotentials are doublets, the link operator is a 2×2 matrix and must be SU(2) valued. The prepotentials decouple the left and right part of a link which are only connected by the number operator constraint (2.27). This is clear in the explicit matrix form

[48, 49] of the link operator written as the product of the left part U_L and the right part U_R as:

$$U = \underbrace{\frac{1}{\sqrt{\hat{N}+1}} \begin{pmatrix} a_2^\dagger(L) & a_1(L) \\ -a_1^\dagger(L) & a_2(L) \end{pmatrix}}_{U_L} \underbrace{\begin{pmatrix} a_1^\dagger(R) & a_2^\dagger(R) \\ a_2(R) & -a_1(R) \end{pmatrix} \frac{1}{\sqrt{\hat{N}+1}}}_{U_R} \equiv U_L\, U_R. \tag{2.29}$$

and satisfies $U^\dagger U = UU^\dagger = 1$. Moreover using (2.29) one can show explicitly that,

$$\left[U_{\alpha\beta}, U_{\gamma\delta}\right] = \left[U_{\alpha\beta}, U^\dagger_{\gamma\delta}\right] = 0. \tag{2.30}$$

Further, in terms of prepotential operators we have an additional U(1) gauge invariance:

$$a^\dagger_\alpha(n,\hat{i}) \to e^{i\theta(n,\hat{i})} a^\dagger_\alpha(n,\hat{i}), \qquad b^\dagger_\alpha(n+\hat{i},\hat{i}) \to e^{-i\theta(n,\hat{i})} b^\dagger_\alpha(n+\hat{i},\hat{i}). \tag{2.31}$$

Therefore, we have gone from the standard SU(2) link operator, electric field description to an equivalent description in terms of harmonic oscillator prepotential operators with enlarged $SU(2) \times U(1)$ gauge invariance.

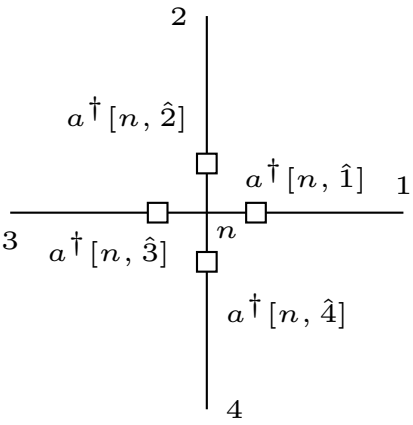

Figure 2.4: $2d$ prepotential doublets $a^\dagger(n,\hat{i}); i = 1,2,\cdots 2d$ around a site n is shown for $d = 2$.

Any site on a d dimensional lattice, has $2d$ prepotential doublets corresponding to the $2d$ links emanating from the site. The d extra Schwinger bosons are defined as $a(n, d+i) \equiv b(n-i,\hat{i})$ for simplicity. This is illustrated in Figure 2.4. SU(2) invariant operators can be constructed by anti symmetrizing pairs of different prepotential doublets.

$$L_{ij}(n) = \epsilon_{\alpha\beta} a^\dagger_\alpha(n,\hat{i}) a^\dagger_\beta(n,\hat{j}) \equiv a^\dagger(n,\hat{i}) \cdot \tilde{a}^\dagger(n,\hat{j});\ i,j = 1,2\cdots 2d,\ i<j. \tag{2.32}$$

We have ${}^{2d}C_2 = d(2d-1)$ such invariant 'intertwining' operators around any site. Thus, an SU(2) invariant basis at the site n is given by

$$|\vec{l}(n)\rangle = \prod_{\substack{i,j=1 \\ j>i}}^{2d} \left(L_{ij}(n)\right)^{l_{ij}(n)} |0\rangle; \qquad l_{ij}(n) \in \mathbb{Z}_+ \;\; ; \;\; l_{ij} = l_{ji}. \tag{2.33}$$

The constraint (2.27) implies that the number of harmonic oscillators at the left end of a link equals that at the right end. Therefore, $SU(2) \times U(1)$ invariant states are the loop states. In fact, any loop state equals $\prod_n |\vec{l}(n)\rangle$ with the corresponding $l_{ij}(n)$ given by reading off the number of flux lines going from ith direction to the jth direction. Also, given $l_{ij}(n)$ satisfying the $U(1)$ constraint (2.27), we can write down a unique loop state corresponding to it. Therefore, Wilson loops can be locally characterised by N_l =(number of intertwining operators)−(number of U(1) constraints)= $d(2d-1) - d = 2d(d-1)$ integers per site. But, number of physical degrees of freedom per site is $3(d-1)$. Therefore, the above loop basis is overcomplete. The extra redundant loop degrees of freedom is due to the Mandelstam constraints [48, 49]. The Mandelstam constraints can be cast in a local form [48, 49] using the prepotentials. For example, the simple Mandelstam constraints discussed in (2.24) and illustrated in Figure 2.2 can be written in terms of 4 prepotentials corresponding to the links meeting at the site n (see fig 2.2) a,b,c,d as follows:

$$(a^\dagger \cdot \tilde{b}^\dagger)(c^\dagger \cdot \tilde{d}^\dagger)|0\rangle = (a^\dagger \cdot \tilde{c}^\dagger)(b^\dagger \cdot \tilde{d}^\dagger)|0\rangle + (a^\dagger \cdot \tilde{d}^\dagger)(b^\dagger \cdot \tilde{c}^\dagger)|0\rangle. \tag{2.34}$$

The Mandelstam constriants can be elegantly solved in the prepotential formalism using the representation theory of angular momentum algebra. Let us denote the 2d (left or right) electric fields at site n by $J_i^a = a_\alpha^\dagger[n,\hat{i}] \left(\frac{\sigma^a}{2}\right)_{\alpha\beta} a_\beta[n,\hat{i}]$. The Gauss law operator at a site n is just the sum of all the electric fields at n :

$$\mathcal{G}^a(n) = \sum_{i=1}^{d} a_\alpha^\dagger[n,\hat{i}] \;\; \left(\frac{\sigma^a}{2}\right)_{\alpha\beta} a_\beta[n,\hat{i}] \equiv J^a_{total}.$$

Since $L_{ij}(n)$ are SU(2) invariants, they commute with the Gauss law operator. $|\vec{l}(n)\rangle$ are common eigenstates of $[J_{total}]^2$ and $[J(n,\hat{i})]^2$ with eigenvalues 0 and $j(n,\hat{i}) \cdot j(n,\hat{i})$; $j(n,\hat{i}) \equiv \frac{1}{2} \sum_{k\neq i=1}^{2d} l_{ik}(n)$. In order to solve the Mandelstam constraints, we notice that there are many different values of l_{ij} which gives the same flux $j(n,\hat{i})$. These degenerate states [48, 49] are

the states related by Mandelstam constraints. Therefore, in order to solve Mandelstam constraints, we demand that the loop basis states be eigenstates of the following operators

$$J_1^2,\ J_2^2,\ \cdots,\ J_{2d}^2\ ;$$
$$J_{12}^2 \equiv \left(\vec{J}_1+\vec{J}_2\right)^2,\ J_{123}^2 \equiv \left(\vec{J}_1+\vec{J}_2+\vec{J}_3\right)^2,\ \cdots,\ J_{12\cdots(2d-2)}^2 \equiv \left(\vec{J}_1+\vec{J}_2+\cdots\vec{J}_{2d-1}\right)^2. \tag{2.35}$$

Above, we have used the fact that $J^a_{total}=0$ by Gauss law to put $J^2_{12\cdots 2d}=0$ and $J^2_{12\cdots 2d-1}=J^2_{12\cdots 2d-2}$ with in the physical Hilbert space. The resulting 'spin network' basis $|j_1,j_2,\cdots,j_{2d};j_{12},j_{123},\ \cdots,\ j_{12\cdots(2d-1)}=j_{2d}\rangle$ which solves Mandelstam as well as Gauss law constraints are characterized by $4d-3$ quantum numbers. These basis states satisfy the triangular constraints:

$$|j_{12\cdots(k-1)}-j_k|\leq j_{12\cdots k}\leq j_{12\cdots(k-1)}+j_k\ ;\quad k=2,3,\cdots(2d-1). \tag{2.36}$$

For instance, in $2+1$ dimensions, the required gauge invariant basis states at sites n are eigenstates of $J_1^2(n)=E_-^2(n,\hat{1}), J_2^2(n)=E_-^2(n,\hat{2}), J_3^2(n)=E_+^2(n,\hat{1}), J_4^2(n)=E_+^2(n,\hat{2}), J_{12}^2(n)\equiv(J_1+J_2)^2=J_{34}^2(n)\equiv(J_3+J_4)^2$ with the eigenvalues $j_1(n)(j_1(n)+1), j_2(n)(j_2(n)+1), j_3(n)(j_3(n)+1), j_4(n)(j_4(n)+1), j_{12}(n)(j_{12}(n)+1)$ and can be written as $|j_1,j_2,j_3,j_4,j_{12}\rangle_n$. But, the $U(1)$ constraint (2.27) implies that $j_1(n)=j_3(n+\hat{1}), j_2(n)=j_4(n+\hat{2});\forall n$. Therefore, a complete basis on a finite lattice can be labelled by choosing 2 of the quantum numbers among j_1,j_2,j_3,j_4 at each site. We choose j_1,j_2 as those quantum numbers. Therefore, the resulting spin network basis is given by $|j_1,j_2,j_{12}\rangle$ at each site. j_1,j_2,j_{12} are related by the triangular constraints: $|j_1-j_2|\leq j_{12}\leq|j_1+j_2|$. But these triangular constraints are very difficult to impose on the Schrodinger[5] equation.

2.4 THE LOOP DYNAMICS & WIGNER COEFFICIENTS

To discuss dynamics of loops, we consider the Hamiltonian of pure SU(2) lattice gauge theory given by (3.59):

$$H=\sum_{n,\hat{i}}\frac{g^2}{4a}E^2(n,\hat{i})-\sum_p\frac{1}{2ag^2}\left\{2-TrU_p\right\}.$$

Above $U_p=U(n,\hat{i})U(n+\hat{i},j)U^\dagger(n+j,i)U^\dagger(n,j)$ is the plaquette operator, $\sum\limits_p$ is over all the plaquettes on the lattice. The loop (spin network) states $|j_1,j_2,j_{12}\rangle$ diagonalize the electric term $E^2(n,\hat{i})$ in the Hamiltonian with eigenvalues $j(n,\hat{i})\left(j(n,\hat{i})+1\right)$. Therefore, the electric

5 With out imposing triangular constraints on the Schrodinger equation, dynamics might take a state which satisfies triangular constraints to states which do not.

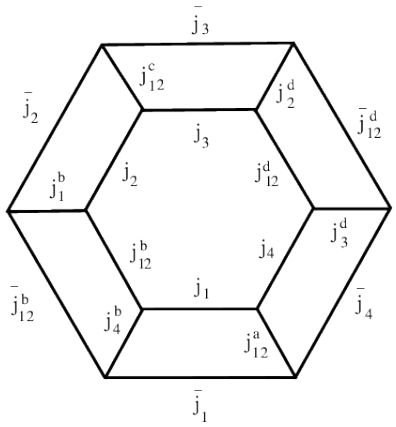

Figure 2.5: 18j ribbon diagram representing SU(2) loop dynamics[48, 49] in d=2 in the loop basis given in (2.37). The interior (exterior) edge carries the initial(final) angular momenta and the six bridges carry the angular momenta that doesn't change under the action of TrU_p. The comparison with dynamics in the loop formulation constructed in this thesis is made in Figure. 3.15.

part just counts the electric flux. The magnetic part of the Hamiltonian, TrU_p, changes the electric flux over the corresponding plaquette. TrU_p when written in terms of prepotential using (2.28) has 16 terms and its matrix element in the loop basis is given by complicated higher Wigner 3-nj coefficients. For example, in 2+1 dimensions, the matrix element [41, 48, 49, 112] of TrU_p is given by an $18j$ Wigner coefficients:

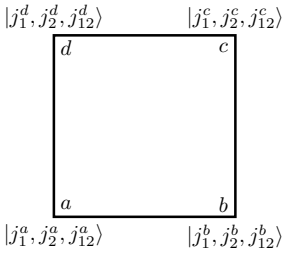

Figure 2.6: Spin network basis states on a plaquette abcd.

$$\frac{1}{g^2}\,\langle \bar{j}_{abcd}|\mathrm{Tr}U_{abcd}|j_{abcd}\rangle = \frac{N_{abcd}}{g^2}\underbrace{\begin{bmatrix} j_1 & j_4 & j^d_{12} & j_3 & j_2 & j^b_{12} \\ & j^a_{12} & j^d_3 & j^d_2 & j^c_{12} & j^b_1 & j^b_4 \\ \bar{j}_1 & \bar{j}_4 & \bar{j}^d_{12} & \bar{j}_3 & \bar{j}_2 & \bar{j}^b_{12} \end{bmatrix}}_{\text{18j coefficient of the second kind}} \prod_{i=1}^{4} \delta_{\bar{j}_i, j_i \pm \frac{1}{2}}. \tag{2.37}$$

Above, $|j_{abcd}\rangle = |j^a_1, j^a_2, j^a_{12}\rangle \otimes |j^b_1, j^b_2, j^b_{12}\rangle \otimes |j^c_1, j^c_2, j^c_{12}\rangle \otimes |j^d_1, j^d_2, j^d_{12}\rangle$ where $a \equiv n$, $b \equiv n + \hat{i}$, $c \equiv n + \hat{i} + \hat{j}$, $d \equiv n + \hat{j}$ are the 4 corners of a plaquette and U_{abcd} is the plaquette loop operator. This is illustrated in the Figure 2.6. We also define $j_1 = j^a_1$, $j_2 = j^b_2$, $j_3 = j^c_3$, $j_4 = j^d_4$ for convenience. Also, in (2.37), $N_{abcd} = \prod_{i=1}^{4} \sqrt{(2j_i+1)(2\bar{j}_i+1)(2j_{12}+1)(2\bar{j}_{12}+1)}$. In $3+1$

dimensions, the matrix elements of the plaquette operator [48, 49] is given by a 30-j Wigner coefficient. Therefore, loop dynamics is complicated in the prepotential formulation.

SU(N) prepotentials

Since, SU(N) group is of rank $(N-1)$, we require $(N-1)$ fundamental irreducible representations to construct an arbitrary representation of SU(N). Therefore, an SU(N) generalization of the prepotential formulation requires $(N-1)$ prepotential n-plets at each site of the lattice. However, a straight forward generalization of SU(N) prepotentials for $N \geq 3$ runs into problems. This is because the Hilbert space created by these prepotentials are not isomorphic to the Hilbert space of SU(N) irreps. The origin of this problem is the existence of certain SU(N) invariants which can be constructed for $N \geq 3$. Any two states which differ by the overall presence of such invariants will transform in the same way under SU(N) gauge transformation. This leads to the problem of multiplicity [102, 103, 113, 114] which in turn makes the formulation of SU(N) ($N \geq 3$) much more involved compared to SU(2). For concreteness, let us consider the Schwinger boson representation for SU(3) explicitly. Being a rank two group, two prepotential triplets, namely the $a^\dagger_\alpha \in 3$ and $b^{\dagger\alpha} \in 3^*$ are necessary at each end of a link to construct all possible irreps of SU(3). For example, the SU(3) electric fields are related to the prepotentials as:

$$\begin{aligned} \text{Left electric fields:} \quad E^{\mathrm{a}}_L(l) &= \left(a^\dagger(l,L)\frac{\lambda^{\mathrm{a}}}{2}a(l,L) + b^\dagger(l,L)\frac{\tilde{\lambda}^{\mathrm{a}}}{2}b(l,L)\right). \\ \text{Right electric fields:} \quad E^{\mathrm{a}}_R(l) &= \left(a^\dagger(l,R)\frac{\lambda^{\mathrm{a}}}{2}a(l,R) + b^\dagger(l,R)\frac{\tilde{\lambda}^{\mathrm{a}}}{2}b(l,R)\right). \end{aligned} \tag{2.38}$$

Above, λ^a are the Gellmann matrices and $\tilde{\lambda} = -\lambda^T$. But, $a^\dagger \cdot b^\dagger$ as well as $a \cdot b$ are SU(3) invariant. Hence any irrep $|R\rangle$ of SU(3) should be identified with $|R,\rho\rangle$ for any ρ, where,

$$|R,\rho\rangle \equiv \underbrace{(a^\dagger \cdot b^\dagger)^\rho}_{\text{SU(3) singlet}} |R\rangle. \tag{2.39}$$

for $\rho = 0, 1, 2, \ldots, \infty$. Note that, this degeneracy problem did not exist for SU(2) as there is only one $(2 \equiv 2^*)$ fundamental representation of SU(2). The degree of degeneracy increases with N for gauge group SU(N) leading to more and more complicated prepotential representation of SU(N).

This multiplicity problem can be solved by constructing irreducible prepotential operators for SU(N) [102, 103]. For example, in SU(3) case, the irreducible prepotentials are given by :

$$\begin{aligned} A^{\dagger}_{\alpha}(L) &= a^{\dagger}_{\alpha}(L) + F_L\, k_+(L) b_{\alpha}(L), \qquad A^{\dagger}_{\alpha}(R) = a^{\dagger}_{\alpha}(R) + F_R\, k_+(R) b_{\alpha}(R), \\ B^{\dagger\alpha}(L) &= b^{\dagger\alpha}(L) + F_L k_+(L) a^{\alpha}(L), \qquad B^{\dagger\alpha}(R) = b^{\dagger\alpha}(R) + F_L k_+(R) a^{\alpha}(R). \end{aligned} \tag{2.40}$$

In (2.40), $A^{\dagger}_{\alpha}(L/R)$ and $B^{\dagger\alpha}(L/R)$ are Irreducible $SU(3)$ triplets and anti-triplets respectively. $k_+(s) = a^{\dagger}(s)\cdot b^{\dagger}(s)$, $k_-(s) = a(s)\cdot b(s)$; $s = L, R$. The factors F_L and F_R are given by:

$$F_L = -\frac{1}{N(L) + M(L) + 1}, \qquad F_R = -\frac{1}{N(R) + M(R) + 1}. \tag{2.41}$$

In (2.41), $N(s) = a^{\dagger}(s)\cdot a(s)$, $M(s) = b^{\dagger}(s)\cdot b(s)$; $s = L, R$. Note that in terms of SU(3) irreducible prepotentials, the degenerate states (2.39) do not exist as :

$$A^{\dagger}(L)\cdot B^{\dagger}(L)|0\rangle_L \equiv 0, \qquad A^{\dagger}(R)\cdot B^{\dagger}(R)|0\rangle_R \equiv 0. \tag{2.42}$$

The link operators in terms of these irreducible Schwinger Bosons are given by:

$$U^{\alpha}_{\beta} = B^{\dagger\alpha}(L)\eta A^{\dagger}_{\beta}(R) + A^{\alpha}(L)\theta B_{\beta}(R) + \Big(B(L)\wedge A^{\dagger}(L)\Big)^{\alpha}\Big(A(R)\wedge B^{\dagger}(R)\Big)_{\beta}. \tag{2.43}$$

where, $\eta = \eta_L\eta_R$,$\theta = \theta_L\theta_R$,$\delta = \delta_L\delta_R$:

$$\begin{aligned} \eta_L &= \frac{1}{\sqrt{B(L)\cdot B^{\dagger}(L)}}, \quad \theta_L = \frac{1}{\sqrt{A^{\dagger}(L)\cdot A(L)}}, \quad \delta_L = \frac{1}{\sqrt{(A(L)\wedge B^{\dagger}(L))\cdot(B(L)\wedge A^{\dagger}(L))}}; \\ \eta_R &= \frac{1}{\sqrt{A^{\dagger}(R)\cdot A(R)}}, \theta_R = \frac{1}{\sqrt{B(R)\cdot B^{\dagger}(R)}}, \quad \delta_R = \frac{1}{\sqrt{(A(R)\wedge B^{\dagger}(R))\cdot(B(R)\wedge A^{\dagger}(R))}}. \end{aligned} \tag{2.44}$$

The SU(N) Mandelstam constraints can be cast into a local form using these irreducible SU(N) prepotentials similar to the SU(2) case discussed in the previous section. But this becomes more and more involved for higher SU(N) groups. The loop dynamics becomes more and more complicated in the prepotential formulation, when we go to higher dimensions and higher gauge groups. Therefore, even though the Mandelstam constraints are solved in the prepotential approach, the triangular constraints and the complicated loop dynamics make it difficult to make further progress. These issues are solved in this thesis by constructing a loop formulation of SU(N) lattice gauge theory through a series of canonical transformation from the Kogut-Susskind link operators and the conjugate electric fields. Canonical transformations allows us to bypass the problem of Mandelstam constraints as well as triangular constraints. Further, the new loop formulation allows us to construct a electric loop basis where the matrix elements of the plaquette operators in $2+1$ dimensions

reduce to a 6j symbol (see section 3.2.3.4) as opposed to the 18j symbol in Figure 2.5. Further, unlike the prepotential approach, it remains a 6j symbol in any dimensions in the new loop formulation.

3

CANONICAL TRANSFORMATIONS, GAUSS LAW CONSTRAINTS & LOOP FORMULATION

In this chapter, we construct a series of canonical transformations to reformulate pure SU(N) gauge theory on a lattice in terms of loops [52–54]. The canonical transformations help us in systematically isolating the local gauge degrees of freedom readily. We illustrate these ideas in the context of the simplest Z_2 lattice gauge theory before generalizing it to $SU(N)$ lattice gauge theory. As mentioned earlier, the canonical transformations acting on Kogut-Susskind link operators, produce the following two types of mutually independent operators:

- plaquette loop operators and their conjugate electric fields corresponding to $\mathcal{P}$ plaquettes on the lattice.
- string operators and their conjugate electric fields corresponding to $\mathcal{N}$ sites on the lattice.

These string operators naturally decouple from the theory due to the local Gauss law constraints leading to a loop formulation based on the mutually independent fundamental plaquette loop operators. Since canonical transformations are $1-1$ mappings, no new degrees of freedom or constraints are introduced in the process. This helps us in bypassing the difficult problem of local Mandelstam constraints discussed in section 2.2 and 2.3. The ideas are first illustrated in the case of simplest Z_2 lattice gauge theory in $(2+1)$ dimensions.

The plan of this chapter is as follows. In section 3.1, we construct the canonical transformations leading to the loop formulation of Z_2 lattice gauge theory in $2+1$ dimensions. In section 3.2, we generalize these Z_2 results to $SU(N)$ lattice gauge theory. In both the cases, we first discuss the single plaquette case and then discuss the finite lattice case. The $3+1$ dimensional case is discussed in section 3.3.

Throughout this chapter, we describe gauge theories on finite 2 and 3 dimensional spatial lattices Λ with $\mathcal{N}$ sites, $\mathcal{L}$ links and $\mathcal{P}$ plaquettes. Sites on a 2 dimensional and 3 dimensional lattice are denoted by (x,y) and (x,y,z) respectively with $x,y,z = 0,1,\cdots \mathsf{N}_s - 1$ where N_s is the number of sites in any direction. On a d dimensional lattice with open boundary conditions, $\mathcal{N} = (\mathsf{N}_s)^{\mathsf{d}}$, $\mathcal{L} = d(\mathsf{N}_s-1)(\mathsf{N}_s)^{d-1}$ and $\mathcal{P} = {}^dC_2(\mathsf{N}_s-1)^2(\mathsf{N}_s)^{d-2}$. We will often use $p = 1,2,\cdots,\mathcal{P}$ as a plaquette index without specifying their locations. We often denote a generic plaquette by p and link by l.

3.1 Z_2 LATTICE GAUGE THEORY

The dynamical variables in 3 dimensional Z_2 lattice gauge theory [7, 55, 56] are the Z_2 conjugate spin operators $\{\sigma_1(l); \sigma_3(l)\}$ on the link $l \in \Lambda$. The quantization rules amongst these conjugate pairs on every link l are

$$[\sigma_1(l), \sigma_3(l)]_+ = \sigma_1(l)\ \sigma_3(l) + \sigma_3(l)\ \sigma_1(l) = 0. \tag{3.1}$$

They further satisfy: $\sigma_3(l)^2 = \sigma_1(l)^2 = 1$. The operators on different links are mutually independent and commute among themselves. We also define electric field $E(l)$ and magnetic vector potential $A(l)$ of Z_2 lattice gauge theories as:

$$\sigma_1(l) = e^{i\pi E(l)}, \qquad \sigma_3(l) = e^{iA(l)}. \tag{3.2}$$

Above $E(l) \equiv (0, 1)$ and $A(l) \equiv (0, \pi)$. From now onwards, we will call $\sigma_1(l)$ and $\sigma_3(l)$ as the Z_2 electric field and Z_2 magnetic vector potential. This will also help us in establishing a correspondence between Z_2 lattice gauge theory and $SU(N)$ lattice gauge theory in later sections. A basis of the two dimensional Hilbert space on each link l is chosen to be the eigenstates of $\sigma_3(l) : |\pm, l\rangle$. On this basis, $\sigma_1(l)$ acts as a spin flip operator:

$$\sigma_3(l)\,|\pm, l\rangle = \pm\,|\pm, l\rangle\,, \qquad \sigma_1(l)|\pm, l\rangle = |\mp, l\rangle. \tag{3.3}$$

The Z_2 lattice gauge theory Hamiltonian [8, 56] is given by

$$H = -\sum_{l\in\Lambda} \sigma_1(l) - \lambda \sum_{p\in\Lambda} \sigma_3(l_1)\sigma_3(l_2)\sigma_3(l_3)\sigma_3(l_4) \quad \equiv H_E + \lambda H_B. \tag{3.4}$$

In (3.4), $\sigma_3(l_1)\sigma_3(l_2)\sigma_3(l_3)\sigma_3(l_4)$ represents the product of σ_3 operators along the four links of a plaquette and the sum over p in the second term in (3.4) is over all plaquettes. The parameter $\lambda > 0$ is the Z_2 lattice gauge theory coupling constant. The first term H_E and the second term H_B in (3.4) represent the Z_2 electric and magnetic field operators respectively. Note that the electric field operator $\sigma_1(l)$ is fundamental while the latter is a composite of the Z_2 magnetic vector potential operators $\sigma_3(l)$ around a plaquette. After a series of canonical transformations, the above characterization of electric, magnetic field will be reversed. More explicitly, the dynamics will be described by the Hamiltonian (3.4) rewritten in terms of the fundamental magnetic field (the second term) and the electric field operator (the first term) will be composite of the dual electric scalar potentials (see (3.31) and (3.32)). The Hamiltonian (3.4) remains invariant if all 4 spins attached to the 4 links emanating from a site n are flipped simultaneously. This symmetry operation is implemented by the Gauss law[1] operator $\mathcal{G}(n)$

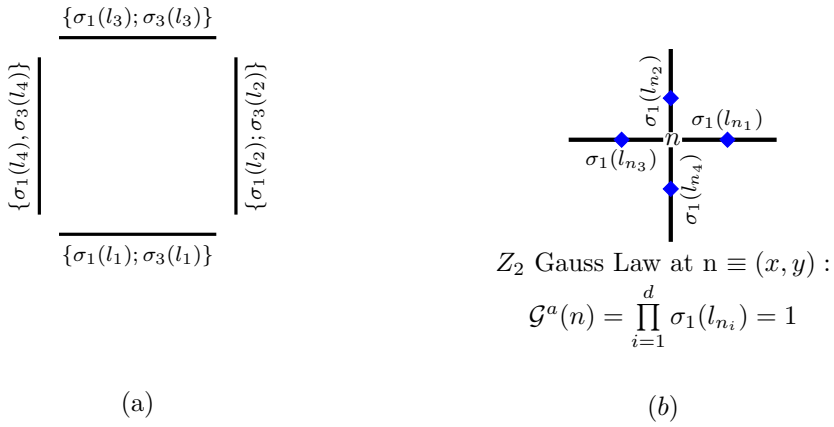

(a) (b)

Figure 3.1: (a) represents the 4 conjugate pairs on the 4 links. (b) represents the Z_2 Gauss law operator defined at lattice site n in eqn. (3.5). ♦ represents the electric field operators σ_1.

at lattice site n,

$$\mathcal{G}(n) \equiv \prod_{l_n} \sigma_1(l_n)\ ,\ n \in \Lambda. \tag{3.5}$$

In (3.5) $\prod_{l_n}$ represents the product over 4 links (denoted by l_n) which share the lattice site n in two space dimensions. More explicitly, the local Z_2 gauge transformations at site n are

$$\begin{aligned} \sigma_1(l) \to \mathcal{G}^{-1}(n)\sigma_1(l)\mathcal{G}(n) = \sigma_1(l), \qquad \forall\ l \in \Lambda, \\ \sigma_3(l_n) \to \mathcal{G}^{-1}(n)\sigma_3(l_n)\mathcal{G}(n) = -\sigma_3(l_n), \\ H \to \mathcal{G}^{-1}(n)\ H\ \mathcal{G}(n) = H. \end{aligned} \tag{3.6}$$

Thus, under a gauge transformation at site n, the 4 link flux operator $\sigma_3(l_n)$ on the 4 links l_n sharing the lattice site n change sign. All other $\sigma_3(l)$ remain invariant. Since the Hamiltonian remains invariant, this implies that total magnetization $\langle \sum_{n,i} \sigma_3(n,\hat{i}) \rangle = 0$ and there are no local order parameters. The physical Hilbert space $\mathcal{H}^p$ consists of the states $|\psi_{phys}\rangle$ satisfying the Gauss law constraints:

$$\mathcal{G}(n)\,|\psi_{phys}\rangle = |\psi_{phys}\rangle \qquad \text{or} \qquad \mathcal{G}(n) \approx 1 \qquad \forall n \in \Lambda. \tag{3.7}$$

In other words, $\mathcal{G}(n)$ are unit operators within the physical Hilbert space $\mathcal{H}^p$. Through out the thesis, all operator identities valid only when acting on states within $\mathcal{H}^p$ are expressed by $\approx$ sign.

We now define the canonical transformations involved in the construction of a loop formulation of Z_2 lattice gauge theory in $(2+1)$ dimensions. As mentioned in the beginning, the canonical transformations convert all Z_2 conjugate pair operators (Z_2 electric fields, con-

1 We call this operator 'Gauss law operator' at n instead of $\sum_{l_n} E(l_n)$ by an abuse of notation. This notation is convenient in the case of Z_2 lattice gauge theory

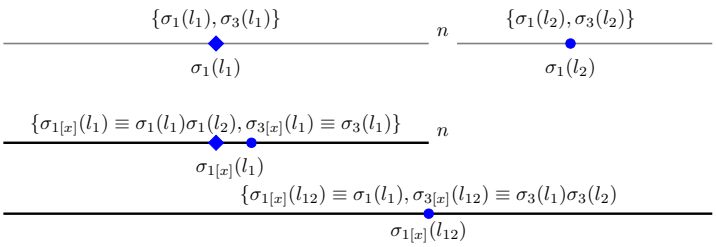

Figure 3.2: The fundamental canonical transformation involving 2 neighboring link operators. This canonical transformation is repeated to construct loop and string operators on the entire lattice. The $\sigma_1(l_1), \sigma_1(l_2)$ operators are denoted by ♦ and • respectively.

jugate magnetic vector potentials) on links (see Figure 3.6-a) into the following two distinct and mutually independent classes of operators (see Figure 3.6-a,b,c) :

1. Z_2 *plaquette loop operators*: representing the Z_2 magnetic fields and its conjugate electric scalar potentials over plaquettes (see Figure 3.6-b),

2. Z_2 *string operators*: representing the Z_2 electric fields and the Z_2 flux operators of the unphysical string degrees of freedom. These strings isolate all Z_2 gauge degrees of freedom (see Figure 3.6-c).

The first set, containing Z_2 plaquette loop operators, are all possible and mutually independent physical (gauge invariant) degrees of freedom of the Z_2 lattice gauge theory. The corresponding physical Hilbert space is denoted by $\mathcal{H}^p$. The second complimentary set, containing Z_2 string operators, represents all possible unphysical gauge degrees of freedom. As expected, all strings are frozen due to the Z_2 Gauss law constraints at lattice sites. *Note that no gauge fixing is needed at any stage*. We now work out the Z_2 canonical transformations systematically.

3.1.1 *The fundamental Z_2 canonical transformation*

We start by defining the fundamental canonical transformation on a pair of neighboring link operators. The loop formulation is then constructed by iterating this fundamental canonical transformation. Consider the operators $\{\sigma_1(l_1), \sigma_3(l_1)\}$ and $\{\sigma_1(l_2), \sigma_3(l_2)\}$ lying on 2 consecutive links $l_1,\ l_2$ as shown in Figure 3.2. We define a fundamental canonical transformation to construct the new operators $\{\sigma_{1[x]}(l_1), \sigma_{3[x]}(l_1)\}$ and $\{\sigma_{1[x]}(l_{12}), \sigma_{3[x]}(l_{12})\}$ as follows

$$\begin{aligned} \sigma_{3[x]}(l_1) &= \sigma_3(l_1), & \sigma_{3[x]}(l_{12}) &= \sigma_3(l_1)\sigma_3(l_2); \\ \sigma_{1[x]}(l_1) &= \sigma_1(l_1)\sigma_1(l_2), & \sigma_{1[x]}(l_{12}) &= \sigma_1(l_1). \end{aligned} \tag{3.8}$$

This is illustrated in Figure 3.2. The subscript $[x]$ on $\sigma_{3[x]}(l_1)$ is used to emphasize that this operator defined on the link l_1 encodes the information about the extension in x direction.

This is clear as its electric field $\sigma_{1[x]}(l_1)(\equiv \sigma_1(l_1)\sigma_1(l_2))$ includes the electric field of link l_2. The above transformation preserves canonical quantization relations.

$$\left[\hat{\sigma}_{1[x]}(l_i), \hat{\sigma}_{3[x]}(l_i)\right]_+ = 0;\ i = 1, 12. \tag{3.9}$$

Above, $[A, B]_+ \equiv AB + BA$. Further,

$$\hat{\sigma}^2_{3[x]}(l_i) = \hat{\sigma}^2_{1[x]}(l_i) = 1;\ i = 1, 12. \tag{3.10}$$

The new operators are independent as they mutually commute:

$$\begin{aligned} &\left[\sigma_{1[x]}(l_1), \sigma_{1[x]}(l_{12})\right] = 0, && \left[\sigma_{3[x]}(l_1), \sigma_{3[x]}(l_{12})\right] = 0; \\ &\left[\sigma_{3[x]}(l_1), \sigma_{1[x]}(l_{12})\right] = 0, && \left[\sigma_{1[x]}(l_1), \sigma_{3[x]}(l_{12})\right] = 0. \end{aligned} \tag{3.11}$$

The first 3 commutators in (3.11) are trivial. The fourth commutator is

$$\big(\sigma_1(l_1)\sigma_1(l_2)\big)\big(\sigma_3(l_1)\sigma_3(l_2)\big) - \big(\sigma_3(l_1)\sigma_3(l_2)\big)\big(\sigma_1(l_1)\sigma_1(l_2)\big) = 0.$$

because of the anti-commutation relation (3.1). Note that it is essential to define the conjugate operator $\sigma_{1[x]}(l_1)$ with a $\sigma_1(l_2)$ in eqn.(3.8) for the fourth commutator to be zero. This is again emphasized[2] by the subscript $[x]$. Therefore, these new link operators provides a completely equivalent description. In the above one dimensional case , the Gauss law operator (3.5) at site n becomes

$$\boxed{\mathcal{G}(n) = \sigma_1(l_1)\sigma_1(l_2) = \sigma_{1[x]}(l_1).} \tag{3.12}$$

The Gauss law (3.7) at site n implies that $\sigma_{1[x]}(l_1) = 1$ within the physical Hilbert space. Therefore, the $\{\sigma_{1[x]}(l_1), \sigma_{3[x]}(l_1)\}$ operators are frozen and decouple from the physical Hilbert space. This simple feature holds for the Z_2 and $SU(N)$ lattice gauge theories in any dimensions as discussed in the following sections.

3.1.2 *Z_2 Canonical transformations on a single plaquette*

In this section, we iterate the above fundamental canonical transformation to construct the loop formulation of Z_2 lattice gauge theory on a single plaquette. As the canonical transformations are iterative in nature, this simple example contains all essential ingredients re-

2 We emphasize this nomenclature in this simple context of Z_2 lattice gauge theory as similar subscripts will be used in the context of canonical transformations in SU(N) lattice gauge theory

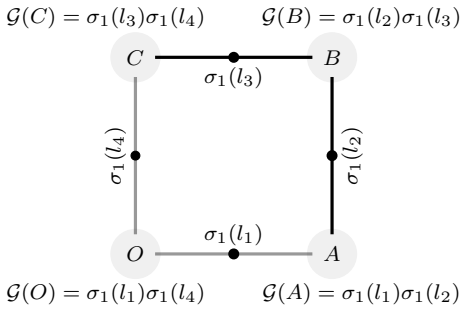

$$\mathcal{G}(O)\mathcal{G}(A)\mathcal{G}(B)\mathcal{G}(C) = 1$$

Figure 3.3: The four Gauss law operators $\mathcal{G}(O)$, $\mathcal{G}(A)$, $\mathcal{G}(B)$, $\mathcal{G}(C)$ at the sites O,A,B,C respectively for a single plaquette. The Gauss law constraints (3.7) imply that within the physical Hilbert space : $\mathcal{G}(O) \approx 1, \mathcal{G}(A) \approx 1, \mathcal{G}(B) \approx 1$ and $\mathcal{G}(C) \approx 1$. These four Gauss law operators are not independent and are related by (3.14).

quired to understand the finite lattice case. The four links OA, AB, BC, CO will be denoted by l_1, l_2, l_3, l_4 respectively. The Hamiltonian is

$$H = \sum_{l=l_1,l_2,l_3,l_4} -\sigma_1(l) - \lambda\sigma_3(l_1)\sigma_3(l_2)\sigma(l_3)\sigma(l_4).$$

In this simplest case, there are four Z_2 gauge transformation or equivalently Gauss law operators (3.5) at each of the four corners O, A, B and C:

$$\begin{aligned} &\mathcal{G}(O) = \mathcal{G}(0,0) = \sigma_1(l_4)\sigma_1(l_1) \approx 1, && \mathcal{G}(A) = \mathcal{G}(1,0) = \sigma_1(l_1)\sigma_1(l_2) \approx 1, \\ &\mathcal{G}(B) = \mathcal{G}(1,1) = \sigma_1(l_2)\sigma_1(l_3) \approx 1, && \mathcal{G}(C) = \mathcal{G}(0,1) = \sigma_1(l_3)\sigma_1(l_4) \approx 1. \end{aligned} \tag{3.13}$$

Note that these Z_2 Gauss law operators satisfy a trivial operator identity:

$$\mathcal{G}(O)\ \mathcal{G}(A)\ \mathcal{G}(B)\ \mathcal{G}(C)\ \equiv\ 1. \tag{3.14}$$

The above identity states the obvious result that a simultaneous flippings at all 4 sites has no effect. This is because of the abelian[3] nature of the gauge group. We now start with the four initial conjugate pairs on links l_1, l_2, l_3 and l_4:

$$\{\sigma_1(l_1); \sigma_3(l_1)\}, \qquad \{\sigma_1(l_2); \sigma_3(l_2)\}, \qquad \{\sigma_1(l_3); \sigma_3(l_3)\}, \qquad \{\sigma_1(l_4); \sigma_3(l_4)\}. \tag{3.15}$$

Using canonical transformations we define four new but equivalent conjugate pairs. The first three string conjugate pairs:

$$\{\bar{\sigma}_1(l_1); \bar{\sigma}_3(l_1)\}, \qquad \{\bar{\sigma}_1(l_2); \bar{\sigma}_3(l_2)\}, \qquad \{\bar{\sigma}_1(l_4); \bar{\sigma}_3(l_4)\}$$

3 The SU(N) case will be discussed in section 3.2.

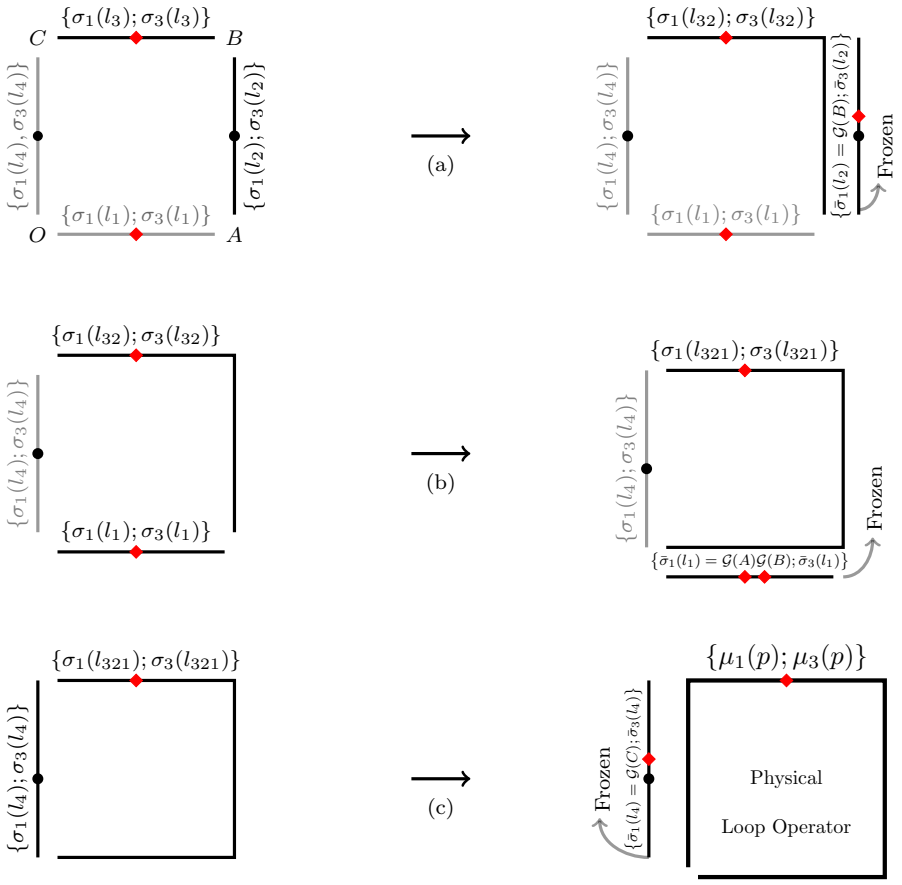

Figure 3.4: The Z_2 canonical transformations (3.16), (3.18), (3.19a) and (3.19b) are pictorially illustrated in (a), (b) and (c) respectively. The ♦ and • represent the electric fields of the initial horizontal and vertical links respectively.

describe the collective excitations on the links OA, AB, BC and shown in Figures 3.4-b,a,c respectively. The remaining collective excitations over the plaquette or the loop $p \equiv OABC$ are described by

$$\{\mu_1(p);\mu_3(p)\}$$

and shown in Figure 3.4-c.

The advantage of working with the new canonically equivalent set is that in the physical Hilbert space $\mathcal{H}^p$, the string electric fields are frozen to the value $+1$ as a consequence of the three mutually independent Gauss law constraints $\mathcal{G}(A), \mathcal{G}(B)$ and $\mathcal{G}(C)$. Therefore, there is no dynamics associated with the three strings. Also, strings appear in the Hamiltonian only through their electric fields $\sigma_1(l_1), \sigma_1(l_2)$ and $\sigma_1(l_3)$. In other words, string degrees of freedom completely decouple from $\mathcal{H}^p$. We are thus left with the final physical Z_2 loop conjugate operators $\{\mu_1(p);\mu_3(p)\}$ which are explicitly Z_2 gauge invariant.

To demonstrate the above results, we start with the initial link operators $\{\sigma_1(l_3);\sigma_3(l_3)\}$ and $\{\sigma_1(l_2);\sigma_3(l_2)\}$ as shown in Fig. (3.4)-a. We glue them canonically as follows:

$$\begin{aligned} \bar{\sigma}_3(l_2) &\equiv \quad \sigma_3(l_2), & \sigma_3(l_{32}) &\equiv \sigma_3(l_3)\sigma_3(l_2); \\ \bar{\sigma}_1(l_2) &= \sigma_1(l_3)\sigma_1(l_2), & \sigma_1(l_{32}) &= \sigma_1(l_3). \end{aligned} \tag{3.16}$$

The canonical transformations (3.16) are illustrated in Fig. 3.4-a. After the transformations, the two new but equivalent canonical sets $\{\bar{\sigma}_1(l_2) = \mathcal{G}(B);\bar{\sigma}_3(l_2)\}$, $\{\sigma_1(l_{32});\sigma_3(l_{32})\}$ are attached to the links l_2 and $l_{32} \equiv l_3 l_2$ respectively. They satisfy the same commutation relations as the original operators (3.1):

$$\begin{aligned} \bar{\sigma}_1(l_2)\bar{\sigma}_3(l_2) + \bar{\sigma}_3(l_2)\bar{\sigma}_1(l_2) = 0, \\ \sigma_1(l_{32})\sigma_3(l_{32}) + \sigma_3(l_{32})\sigma_1(l_{32}) = 0. \end{aligned} \tag{3.17}$$

One can easily check: $\bar{\sigma}_1^2(l_2) = 1$, $\bar{\sigma}_3^2(l_2) = 1, \sigma_1(l_{32})^2 = 1, \sigma_3(l_{32})^2 = 1$. Further, note that the two conjugate pairs $\{\bar{\sigma}_1(l_2);\bar{\sigma}_3(l_2)\}$ and $\{\sigma_1(l_3 l_2);\sigma_3(l_3 l_2)\}$ are also mutually independent as they commute with each other. As an example,

$$[\bar{\sigma}_1(l_2), \sigma_3(l_3 l_2)] \equiv [\sigma_1(l_3)\sigma_1(l_2), \sigma_3(l_3)\sigma_3(l_2)] = 0.$$

The new conjugate pair $\{\bar{\sigma}_1(l_2);\bar{\sigma}_3(l_2)\}$ is frozen due to the Gauss law at B:

$$\boxed{\bar{\sigma}_1(l_2) = \mathcal{G}(B) \approx 1.}$$

We now repeat (3.16) with l_2, l_3 replaced by l_1, l_{32} respectively to define new conjugate operators $\{\bar{\sigma}_1(l_1);\bar{\sigma}_3(l_1)\}$ and $\{\sigma_1(l_{321});\sigma_3(l_{321})\}$ attached to the links l_1 and $l_{321}(\equiv l_3 l_2 l_1)$ respectively:

$$\begin{aligned} \bar{\sigma}_3(l_1) &\equiv \sigma_3(l_1), & \sigma_3(l_{321}) &\equiv \sigma_3(l_{32})\sigma_3(l_1); \\ \bar{\sigma}_1(l_1) &= \sigma_1(l_{32})\sigma_1(l_1), & \sigma_1(l_{321}) &= \sigma_1(l_3). \end{aligned} \tag{3.18}$$

As before, the new conjugate pair $\{\bar{\sigma}_1(l_1);\bar{\sigma}_3(l_2)\}$ becomes unphysical as

$$\boxed{\bar{\sigma}_1(l_1) = \mathcal{G}(A)\mathcal{G}(B) \approx 1.}$$

The last canonical transformations involve gluing the conjugate pairs $\{\sigma_1(l_{321}); \sigma_3(l_{321})\}$ with $\{\sigma_1(l_4); \sigma_3(l_4)\}$ to define the dual and gauge invariant plaquette[4] to be variables $\{\mu_1(p); \mu_3(p)\}$, with $p \equiv l_1 l_2 l_3 l_4$:

$$\begin{aligned} \mu_3(p) \equiv \sigma_1(l_{321}) \ &= \sigma_1(l_3), \\ \mu_1(p) \equiv \sigma_3(l_{321})\sigma_3(l_4) &\equiv \sigma_3(l_3)\sigma_3(l_2)\sigma_3(l_1)\sigma_3(l_4). \end{aligned} \tag{3.19a}$$

$$\begin{aligned} \bar{\sigma}_3(l_4) &\equiv \sigma_3(l_4), \\ \bar{\sigma}_1(l_4) &= \sigma_1(l_{321})\sigma_1(l_4) = \sigma_1(l_3)\sigma_1(l_4). \end{aligned} \tag{3.19b}$$

The conjugate pair $\{\bar{\sigma}_1(l_4); \bar{\sigma}_3(l_4)\}$ becomes unphysical as

$$\boxed{\bar{\sigma}_1(l_4) = \mathcal{G}(C) \approx 1.}$$

Therefore, the three canonical transformations (3.16), (3.18), (3.19a) and (3.19b) transform the initial 4 conjugate sets $\{\sigma_1(l_1); \sigma_3(l_1)\}$, $\{\sigma_1(l_2); \sigma_3(l_2)\}$, $\{\sigma_1(l_3); \sigma_3(l_3)\}$, $\{\sigma_1(l_4); \sigma_3(l_4)\}$ attached to the links l_1, l_2, l_3, l_4 to 4 new and equivalent canonical sets $\{\bar{\sigma}_1(l_2); \bar{\sigma}_3(l_2)\}$, $\{\bar{\sigma}_1(l_1); \bar{\sigma}_3(l_1)\}$, $\{\bar{\sigma}_1(l_4); \bar{\sigma}_3(l_4)\}$ and $\{\mu_1(p); \mu_3(p)\}$ attached to the links l_2, l_1, l_4 and the plaquette p respectively.

From links to loops and strings

The net effect of the canonical transformation involved in the construction of the loop operators on a single plaquette can be summarized as follows:

- It replaces the top link l_3 on the plaquette by a plaquette spin operator with the same 'electric field' as the top link.

$$\mu_1(p) = \sigma_3(l_1)\sigma_3(l_2)\sigma_3(l_3)\sigma_3(l_4), \qquad \mu_3(p) = \sigma_1(l_3). \tag{3.20}$$

- The 'electric field' of the top link l_3 that vanishes gets absorbed into the electric fields of other links l_1, l_2, l_4.

$$\begin{aligned} \bar{\sigma}_3(l_1) &= \sigma_3(l_1), & \bar{\sigma}_1(l_1) &= \sigma_1(l_1)\sigma_1(l_3). \\ \bar{\sigma}_3(l_2) &= \sigma_3(l_2), & \bar{\sigma}_1(l_2) &= \sigma_1(l_2)\sigma_1(l_3). \\ \bar{\sigma}_3(l_4) &= \sigma_3(l_4), & \bar{\sigma}_1(l_4) &= \sigma_1(l_4)\sigma_1(l_3). \end{aligned} \tag{3.21}$$

4 In eqn (3.19a), we have interchanged the 3 and 1 subscript in the μ operators. This is motivated by duality which will be discussed in the next chapter.

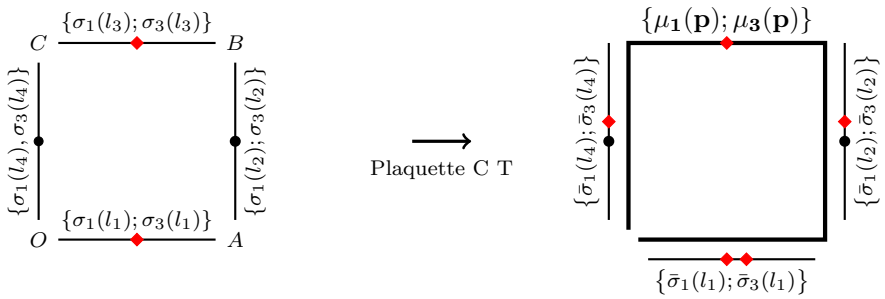

Figure 3.5: Graphical illustration of a plaquette canonical transformation defined in (3.20) and (3.21).

It is convenient to call the above net canonical transformation a 'plaquette canonical transformation'. The advantage of the new conjugate set of variables is that all the three independent Gauss law constraints at A, B and C are automatically solved. They freeze the three strings leaving us only with plaquette loop conjugate operators $\{\mu_1(p);\mu_3(p)\}$.

From loops and strings to links

The defining canonical relations (3.16), (3.18), (3.19a) and (3.19b) can also be inverted. The inverse transformations from the new loop operators to Z_2 link operators are

$$\begin{aligned} \sigma_3(l_1) &= \bar\sigma_3(l_1), & \sigma_3(l_2) &= \bar\sigma_3(l_2), \\ \sigma_3(l_3) &= \mu_1(p)\bar\sigma_3(l_4)\bar\sigma_3(l_1)\bar\sigma_3(l_2), & \sigma_3(l_4) &= \bar\sigma_3(l_4). \end{aligned} \tag{3.22}$$

Similarly, the initial conjugate Z_2 electric field operators on the links are

$$\begin{aligned} \sigma_1(l_1) = \mu_3(p)\bar\sigma_1(l_1) = \mu_3(p)\ \mathcal{G}(A)\mathcal{G}(B) \approx \mu_3(p), \\ \sigma_1(l_2) = \mu_3(p)\bar\sigma_1(l_2) = \mu_3(p)\ \mathcal{G}(B) \approx \mu_3(p), \\ \sigma_1(l_3) = \mu_3(p), \\ \sigma_1(l_4) = \mu_3(p)\bar\sigma_1(l_4) = \mu_3(p)\ \mathcal{G}(C) \approx \mu_3(p). \end{aligned} \tag{3.23}$$

Note that the Gauss law constraint at the origin does not play any role as $\mathcal{G}(O) \approx \mathcal{G}(A)\,\mathcal{G}(B)\,\mathcal{G}(C)$. The total number of degrees of freedom also match. The initial Z_2 gauge theory had 4 links with 3 Gauss law constraints. In the final picture the 3 gauge non-invariant strings take care of the 3 Gauss law constraints leaving us with the single gauge invariant loop operator pair described by $\{\mu_1(p), \mu_3(p)\}$ on the plaquette p.

The single plaquette Z_2 lattice gauge theory Hamiltonian (3.4) can now be rewritten in terms of the new gauge invariant loop operators as:

$$H \approx -4\ \mu_3(p) - \lambda\ \mu_1(p) = -\begin{pmatrix} \lambda & 4 \\ 4 & -\lambda \end{pmatrix}. \tag{3.24}$$

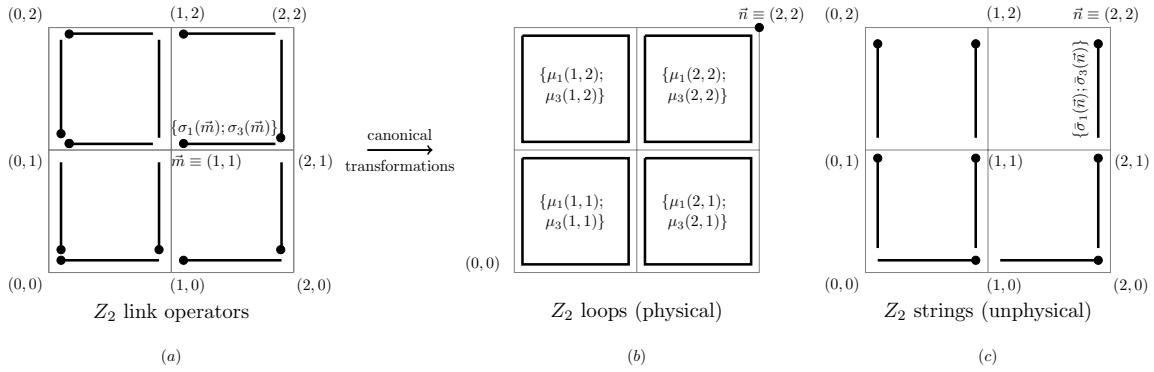

Figure 3.6: The Z_2 link operator pairs, the physical Z_2 loop conjugate pairs $\{\mu_1(\vec{n});\, \mu_3(\vec{n})\}$ and the unphysical string conjugate pairs $\{\bar{\sigma}_1(\vec{n});\bar{\sigma}_3(\vec{n})\}$ for a 2×2 lattice are shown in (a), (b) and (c) respectively. The canonical transformations convert 12 link operator pairs on a 2×2 lattice to 4 loop operator pairs and 8 string operator pairs. We label the loop operators by their top right corners and the horizontal (vertical) string operators by their right (top) endpoint. The strings decouple from the physical Hilbert space as $\bar{\sigma}_1(\vec{n}) \approx 1$ by Gauss law constraints. The corresponding dual SU(N) loop and SU(N) string operators are shown in Figure 3.11-a,b respectively.

The two energy eigenvalues of H are $\epsilon_\pm = \pm 4\sqrt{\left(1 + \left(\frac{\lambda}{4}\right)^2\right)}$.

3.1.3 Z_2 *canonical transformations on a finite lattice in* $(2+1)$ D

We now directly write down the general Z_2 canonical relations over the entire lattice. The details of these iterative canonical transformations (analogous to (3.16), (3.18), (3.19a) and (3.19b)) are given in Appendix A. Note that there are $\mathcal{L}$ initial spins (one on every link) with $\mathcal{N}$ Gauss law constraints (one at every site) satisfying the identity:

$$\prod_{(x,y)\in\Lambda} \mathcal{G}(x,y) \;\equiv\; 1. \tag{3.25}$$

The above identity again states that simultaneous flipping of all spins around every lattice site is an identity operator because each spin is flipped twice. It reduces the number of Gauss law constraints from[5] $\mathcal{N}$ to $\mathcal{N}-1$. After canonical transformations in Z_2 lattice gauge theory, there are (a) $\mathcal{P}$ physical plaquette spins (analogous to $\{\mu_1(p);\mu_3(p)\}$ in the single plaquette case) shown in Figure 3.6-b and (b) $(\mathcal{N}-1)$ stringy spins (analogous to $\{\bar{\sigma}_1(l_1);\bar{\sigma}_3(l_1)\}$; $\{\bar{\sigma}_1(l_2);\bar{\sigma}_3(l_2)\}$ and $\{\bar{\sigma}_1(l_4);\bar{\sigma}_3(l_4)\}$ in the single plaquette case) as every lattice site away from the origin can be attached to a unique string. This is shown in Figure 3.6-c. The degrees of freedom before and after the canonical transformations match as $\mathcal{L} = \mathcal{P} + (\mathcal{N}-1)$. All $(\mathcal{N}-1)$ strings decouple because of the $(\mathcal{N}-1)$ Gauss law constraints.

5 Note that the identity (3.25) is valid for all abelian lattice gauge theories. In the non-abelian SU(N) case, discussed in the next section, there is no such reduction. The global SU(N) gauge transformations, corresponding to the extra Gauss law constraints at the origin $\mathcal{G}^a(0,0) = 1$, need to be fixed by hand to get the correct number of physical degrees of freedom (see section 3.2).

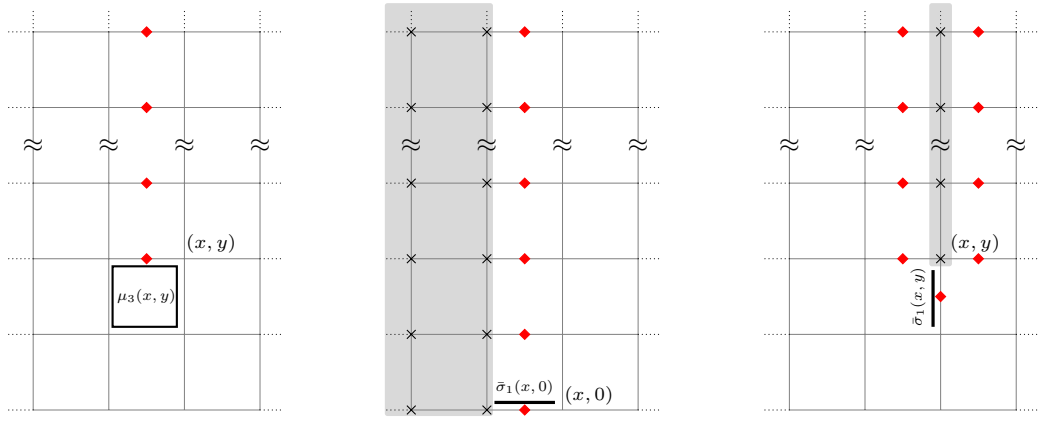

$\mu_3(x,y) = \prod_{y'=y}^{N} \sigma_1(x-1, y', \hat{1})$ (a)

$\bar{\sigma}_1(x,0) = \prod_{x'=0}^{x-1} \prod_{y'=0}^{N} \mathcal{G}(x', y') \approx 1$ (b)

$\bar{\sigma}_1(x,y) = \prod_{y'=y}^{N} \mathcal{G}(x, y') \approx 1$ (c)

Figure 3.7: The graphical illustration of the non-local relations in the net Z_2 canonical transformations: (a) we show the relations (3.26b) expressing $\mu_3(x,y)$ as the product of σ_1 operators which are denoted by ♦. In (b) and (c), we show the relations (3.28b) expressing $\bar{\sigma}_1(x,0)$ and $\bar{\sigma}_1(x, y \neq 0)$ respectively as the product of σ_1 operators denoted by ♦. These $(\bar{\sigma}_1(x,y))$ equal the product of Gauss law operators at sites marked by x in the shaded region. For the corresponding SU(N) relations, see Figures 3.12-a,b.

The algebraic details of these transformations leading to freezing of all strings are worked out in detail in Appendix A.

From now onward the $\mathcal{P}$ physical plaquette loop operators are labelled by the top right corners of the corresponding plaquettes as shown in Figure (3.6-a). The vertical (horizontal) string operators are labelled by the top (right) end points of the corresponding links as shown in Figure 3.6-b. The same notation will be used to label the dual SU(N) operators in section 3.2.

3.1.3.1 *Physical sector and Z_2 loop operators*

The final relations between the initial conjugate sets $\{\sigma_1(x,y;\hat{i}); \sigma_3(x,y;\hat{i})\}$ on every lattice link $(x,y;\hat{i})$ and the final physical conjugate loop operators $\{\mu_1(x,y);\ \mu_3(x,y)\}$ are (see Appendix A)

$$\begin{aligned}\mu_1(x,y) &= \sigma_3(x-1, y-1; \hat{1})\ \sigma_3(x-1, y-1; \hat{2})\ \sigma_3(x,y; -\hat{2})\sigma_3(x,y,-\hat{1}) \\ &\equiv \sigma_3(l_1)\sigma_3(l_2)\sigma_3(l_3)\sigma_3(l_4),\end{aligned} \tag{3.26a}$$

$$\mu_3(x,y) = \prod_{y'=y}^{N_s-1} \sigma_1(x-1, y', \hat{1}). \tag{3.26b}$$

In (3.26a) we have defined $\sigma_1(x,y;-\hat{1}) \equiv \sigma_1(x-1,y;\hat{1})$ and $\sigma_1(x,y;-\hat{2}) \equiv \sigma_1(x,y-1;\hat{2})$. The relations (3.26a) and (3.26b) are the extension of the single plaquette relations (3.19a) to the entire lattice. They are illustrated in Figure 3.7-a. The canonical commutation relations are

$$\mu_1(x,y)\mu_3(x,y) + \mu_3(x,y)\mu_1(x,y) = 0. \tag{3.27}$$

Further, $\mu_3^2(x,y) = 1, \mu_1^2(x,y) = 1$. Note that the conjugate pairs $\{\sigma_1,\sigma_3\}$ corresponding to different plaquettes commute and are independent. Therefore $\{\mu_1,\mu_3\}$ is in the same footing as $\{\sigma_1,\sigma_3\}$. *The canonical transformations (3.26a) are important as they define the magnetic field operators $\mu_1(x,y)$ as a new fundamental operator.* Note that originally the electric field $\sigma_1(x,y)$ was fundamental and the magnetic field was written in terms of its conjugate magnetic vector potentials as $\sigma_3(l_1)\sigma_3(l_2)\sigma_3(l_3)\sigma_3(l_4)$. After canonical transformations, the magnetic fields $\mu_1(x,y)$ are fundamental and their canonical conjugate, called electric scalar potential $\mu_3(x,y)$, define the electric field (see (3.31)).

3.1.3.2 *Unphysical sector and Z_2 string operators*

The unphysical string conjugate pair operators are (see Appendix A)

$$\begin{aligned} \bar{\sigma}_3(x,0) &= \sigma_3(x-1,0,\hat{1}), \\ \bar{\sigma}_3(x,y\neq 0) &= \sigma_3(x,y-1,\hat{2}). \end{aligned} \tag{3.28a}$$

$$\begin{aligned} \bar{\sigma}_1(x,0) &= \prod_{x'=0}^{x-1}\prod_{y'=0}^{N_s-1} \mathcal{G}(x',y') \approx 1, \\ \bar{\sigma}_1(x,y\neq 0) &= \prod_{y'=y}^{N_s-1} \mathcal{G}(x,y') \approx 1. \end{aligned} \tag{3.28b}$$

These Z_2 string operators are analogous to the three Z_2 string operators in (3.16), (3.18) and (3.19b) in the single plaquette case. The relations (3.28a) and (3.28b) are illustrated in Figure 3.7-b and Figure 3.7-c respectively. It is easy to see that in the full gauge theory Hilbert space all Z_2 string operators are mutually conjugate:

$$\bar{\sigma}_1(x,y)\bar{\sigma}_3(x,y) + \bar{\sigma}_3(x,y)\bar{\sigma}_1(x,y) = 0,$$

and different string operators located at different lattice sites commute with each others. As expected, their conjugate electric fields $\bar{\sigma}_1(x,y)$ are entirely in terms of the Z_2 Gauss law operators. Hence these string degrees of freedom are frozen and not dynamical. Further, one

can check that all strings and plaquette operators are mutually independent and commute with each other:

$$\begin{aligned} \left[\mu_3(x,y),\bar{\sigma}_1(x',y')\right] &= 0, \qquad & \left[\mu_3(x,y),\bar{\sigma}_3(x',y')\right] &= 0, \\ \left[\mu_1(x,y),\bar{\sigma}_1(x',y')\right] &= 0, \qquad & \left[\mu_1(x,y),\bar{\sigma}_3(x',y')\right] &= 0. \end{aligned} \tag{3.29}$$

3.1.3.3 *Inverse relations*

The inverse relations for the flux operators over the entire lattice are

$$\begin{aligned} \sigma_3(x,0;\hat{1}) &= \bar{\sigma}_3(x+1,0), \\ \sigma_3(x,y;\hat{2}) &= \bar{\sigma}_3(x,y+1), \\ \sigma_3(x,y\neq 0;\hat{1}) &= \left(\prod_{l=1}^{y}\bar{\sigma}_3(x,l)\right)\left(\prod_{q=1}^{y}\bar{\sigma}_3(x+1,y)\right)\left(\prod_{p=1}^{y}\mu_1(x+1,y)\right). \end{aligned} \tag{3.30}$$

On the other hand, the conjugate electric field operators are

$$\begin{aligned} \sigma_1(x,y;\hat{1}) &= \mu_3(x+1,y)\mu_3(x+1,y+1), \\ \sigma_1(x,y,\hat{2}) &= \mu_3(x,y+1)\mu_3(x+1,y+1). \end{aligned} \tag{3.31}$$

In the second relation in (3.31), we have used Gauss laws at (x,l) ; $l = y+1, y+2, \cdots$. The above relations are analogous to the inverse relations (3.22) and (3.23) in the single plaquette case.

3.1.3.4 *Z_2 loop dynamics*

Within $\mathcal{H}^p$ where $\mathcal{G}(x,y) \approx 1$, the Z_2 lattice gauge theory Hamiltonian (3.4) in terms of the physical loop operators takes the simple nearest neighbour interaction form:

$$\begin{aligned} H &= -\sum_{<p,p'>}\mu_3(p)\mu_3(p') - \lambda\sum_{p}\mu_1(p) \equiv H_E + \lambda H_B, \\ &= \lambda\left[-\sum_{p}\mu_1(p) - \frac{1}{\lambda}\sum_{<p,p'>}\mu_3(p)\mu_3(p')\right]. \end{aligned} \tag{3.32}$$

In (3.32) $\sum_{<p,p'>}$ denotes the sum over the nearest neighbour plaquettes. As expected, after the canonical transformations the electric and the magnetic field descriptions in terms of potentials have interchanged. The original fundamental Z_2 electric field operator is now in terms of the (dual) electric scalar potential denoted by $\mu_3(p)$ and the Z_2 magnetic field has now acquired an independent status. Thus the Z_2 gauge theory initially written in terms of electric field and magnetic vector potential operators $\{\sigma_1(l);\sigma_3(l)\}$ in (3.4) are now written in terms of the magnetic field, electric scalar potential operators $\{\mu_1(p);\mu_3(p)\}$ in (3.32).

Z_2 lattice gauge theory		SU(N) lattice gauge theory	
Gauge Operators	Dual/Spin Operators	Gauge Operators	Dual/Spin Operators
	$\{\mu_1(m,n);\mu_3(m,n)\}$ (Z_2 Loops/Z_2 Ising spins)		$\left\{\mathcal{E}^a_{\pm}(m,n);\ \mathcal{W}_{\alpha\beta}(m,n)\right\}$ (SU(N) Loops/SU(N) spins)
$\{\sigma_1(m,n;\hat{i});\sigma_3(m,n;\hat{i})\}$		$\left\{E^a_{\pm}(m,n;\hat{i});U_{\alpha\beta}(m,n;\hat{i})\right\}$	
	$\{\bar{\sigma}_1(m,n);\bar{\sigma}_3(m,n)\}$ (Frozen Z_2 Strings)		$\left\{\mathsf{E}^a_{\pm}(m,n);\ \mathsf{T}_{\alpha\beta}(m,n)\right\}$ (Frozen $SU(N)$ Strings)

Table 3.1: The basic conjugate operators of the original and the loop approaches in Z_2, SU(N) gauge theories in $(2+1)$ dimensions. The duality interpretation is discussed in the next chapter.

Further, the canonical transformations map $(2+1)$ dimensional Z_2 lattice gauge theory at coupling λ to a $(2+1)$ dimensional Z_2 spin model at coupling $(1/\lambda)$, i.e,

$$H^{Z_2}_{gauge}(\lambda) \approx \lambda\ H^{Z_2}_{spin}(1/\lambda).$$

As mentioned earlier, $\approx$ emphasizes that this equivalence is only within the physical Hilbert space $\mathcal{H}^p$. The duality aspects and their generalization to SU(N) lattice gauge theory will be discussed in detail in the next chapter.

3.2 SU(N) LATTICE GAUGE THEORY

In this section, we generalize the Z_2 canonical transformations discussed in the previous section to $SU(N)$ lattice gauge theory. The basic dynamical operators $\{E^a_{\pm}(x,y,\hat{i}),U_{\alpha\beta}(x,y,\hat{i})\}$ of $SU(N)$ lattice gauge theory are transformed into the following mutually independent classes of operators:

- SU(N) plaquette loop operators $\{\mathcal{E}^a_{\pm}(x,y),\mathcal{W}_{\alpha\beta}(x,y)\}$: representing the SU(N) electric scalar potentials and SU(N) magnetic fields (see Figure 3.11-a),
- SU(N) string operators $\{\mathsf{E}^a_{\pm}(x,y),\mathsf{T}_{\alpha\beta}(x,y)\}$: representing the SU(N) electric fields and SU(N) flux operators of the unphysical string degrees of freedom. These strings isolate the SU(N) gauge degrees of freedom (see Figure 3.11-b).

The new conjugate operator sets $\{\mathcal{E}^a_{\pm}(x,y),\mathcal{W}_{\alpha\beta}(x,y)\}$ and $\{\mathsf{E}^a_{\pm}(x,y),\mathsf{T}_{\alpha\beta}(x,y)\}$ are mutually independent. They retain the same canonical structure as specified by the commutation relation (2.11). The first set containing the SU(N) plaquette loop operators, represent all the physical degrees of freedom of SU(N) lattice gauge theory. The second set containing the string operators represents all the unphysical gauge degrees of freedom. This is analogous to the Z_2 case where the conjugate operators $\{\sigma_1(x,y,\hat{i}),\sigma_3(x,y,\hat{i})\}$ are canonically transformed

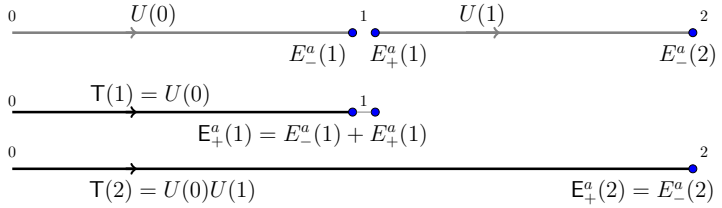

Figure 3.8: The fundamental $SU(N)$ canonical transformation (3.34) from $\{E_+(0),\ U(1), E_-(1)\}$; $\{E_+(1), U(2), E_-(2)\}$ to $\{\mathsf{E}_-(1), \mathsf{T}(1), \mathsf{E}_+(1)\}$;$\{\mathsf{E}_-(1), \mathsf{T}(2),\ \mathsf{E}_+(2)\}$ involved in the construction of a loop formulation of $SU(N)$ gauge theory. The electric fields are denoted by $\bullet$.

into the Z_2 loop operators $\{\mu_1(x,y), \mu_3(x,y)\}$ and the Z_2 string operators $\{\bar{\sigma}_1(x,y), \bar{\sigma}_3(x,y)\}$. We will see that just like in the Z_2 case, all the string degrees of freedom are frozen due to the Gauss law constraints (2.19) at the lattice sites. The correspondence between the initial and final Z_2 and $SU(N)$ conjugate operator pairs before and after canonical transformations are shown in Table 3.1.

As was done in the Z_2 case, we first discuss the fundamental SU(N) canonical transformation which fuses together 2 adjacent link operators. We then discuss the SU(N) canonical transformations on a single plaquette before dealing with SU(N) lattice gauge theory on the entire lattice.

3.2.1 *Fundamental SU(N) canonical transformation*

Consider 2 neighbouring Kogut-Susskind link conjugate operators $\{E_+(0), U(1), E_-(1)\}$ and $\{E_+(1), U(2), E_-(2)\}$ as shown in Figure (3.8). We define a fundamental canonical transformation from $\{E_+(0), U(1), E_-(1)\}$; $\{E_+(1), U(2), E_-(2)\}$ to $\{\mathsf{E}_-(1), \mathsf{T}(1), \mathsf{E}_+(1)\}$; $\{\mathsf{E}_-(1), \mathsf{T}(2), \mathsf{E}_+(2)\}$ as follows:

$$\begin{aligned} \mathsf{T}(1) &\equiv U(0), & \mathsf{T}(2) &\equiv U(0)\ U(1); \\ \mathsf{E}^a_+(1) &= E^a_-(1) + E^a_+(1), & \mathsf{E}^a_+(2) &= E^a_-(2). \end{aligned} \tag{3.33}$$

This is illustrated in Figure (3.8). The above transformation preserves commutation relations. The resulting pairs commute with each other. Therefore, the resulting conjugate pairs of operators are completely equivalent to the initial pairs. In the above 1 dimensional case, the Gauss law operator at site 1 is given by

$$\boxed{\mathcal{G}^a(1) = E^a_-(1) + E^a_+(1) = \mathsf{E}^a_+(1).} \tag{3.34}$$

Therefore, the Gauss law at 1 implies that $\mathsf{E}^a_+(1) = 0$ in the physical Hilbert space. This leads to the decoupling of the conjugate pair $\{\mathsf{E}^a_\pm(1), \mathsf{T}(1)\}$ just as in the Z_2 case.

3.2.2 *SU(N) canonical transformations on a single plaquette*

We now iterate the above fundamental canonical transformation to construct a loop formulation of SU(N) lattice gauge theory on a single plaquette. We start with a plaquette OABC with the following Kogut-Susskind SU(N) link flux operators [6–8]:

$$\begin{aligned}
&\big(E^a_+(0,0;\hat{1}),\ U(0,0;\hat{1}),\ E^a_-(1,0;\hat{1})\big) \text{ on OA}, \qquad &&\big(E^a_+(1,0;\hat{2}),\ U(1,0;\hat{2}),\ E^a_-(1,1;\hat{2})\big) \text{ on AB},\\
&\big(E^a_+(0,1;\hat{1}),\ U(0,1;\hat{1}),\ E^a_-(1,1;\hat{1})\big) \text{ on CB}, \qquad &&\big(E^a_+(0,0;\hat{2}),\ U(0,0;\hat{2}),\ E^a_-(0,1;\hat{2})\big) \text{ on OC}.
\end{aligned}$$

These link operators and their locations are clearly illustrated on the left hand side of Figure 3.10-a. As is clear from this Figure, the SU(N) Gauss laws at four corners O, A, B and C are:

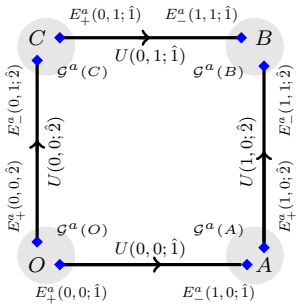

Figure 3.9: Graphical illustration of $SU(N)$ Gauss law operators $\mathcal{G}^a(O), \mathcal{G}^a(A), \mathcal{G}^a(B), \mathcal{G}^a(C)$ at O, A, B and C for a single plaquette. The Gauss law constraints are given by $\mathcal{G}^a(O) \approx 0, \mathcal{G}^a(A) \approx 0, \mathcal{G}^a(B) \approx 0, \mathcal{G}^a(C) \approx 0$. Unlike Z_2 case, they are all independent.

$$\begin{aligned}
&\mathcal{G}^a(0,0) = E^a_+(0,0;\hat{1}) + E^a_+(0,0;\hat{2}) = 0; \qquad &&\mathcal{G}^a(1,0) = E^a_-(1,0;\hat{1}) + E^a_+(1,0;\hat{2}) = 0;\\
&\mathcal{G}^a(1,1) = E^a_-(1,1;\hat{2}) + E^a_-(1,1;\hat{1}) = 0; \qquad &&\mathcal{G}^a(0,1) = E^a_+(0,1;\hat{1}) + E^a_-(0,1;\hat{2}) = 0.
\end{aligned} \tag{3.35}$$

The canonical transformations are performed in 3 sequential steps as shown in Figure (3.10-a), (3.10-b) and (3.10-c) respectively. The first canonical transformation fuses $U(0,0;\hat{1})$ with $U(1,0;\hat{2})$ to define the two new flux operators $\mathsf{T}_{[xy]}(1,0)$ and $\mathsf{T}_{[y]}(1,1)$:

$$\begin{aligned}
\mathsf{T}_{[xy]}(1,0) &\equiv U(0,0;\hat{1}), \qquad &\mathsf{T}_{[y]}(1,1) &\equiv U(0,0;\hat{1})U(1,0;\hat{2}),\\
\mathsf{E}^a_{[xy]+}(1,0) &= E^a_-(1,0;\hat{1}) + E^a_+(1,0;\hat{2}), \qquad &\mathsf{E}^a_{[y]+}(1,1) &= E^a_-(1,1;\hat{2}).
\end{aligned} \tag{3.36}$$

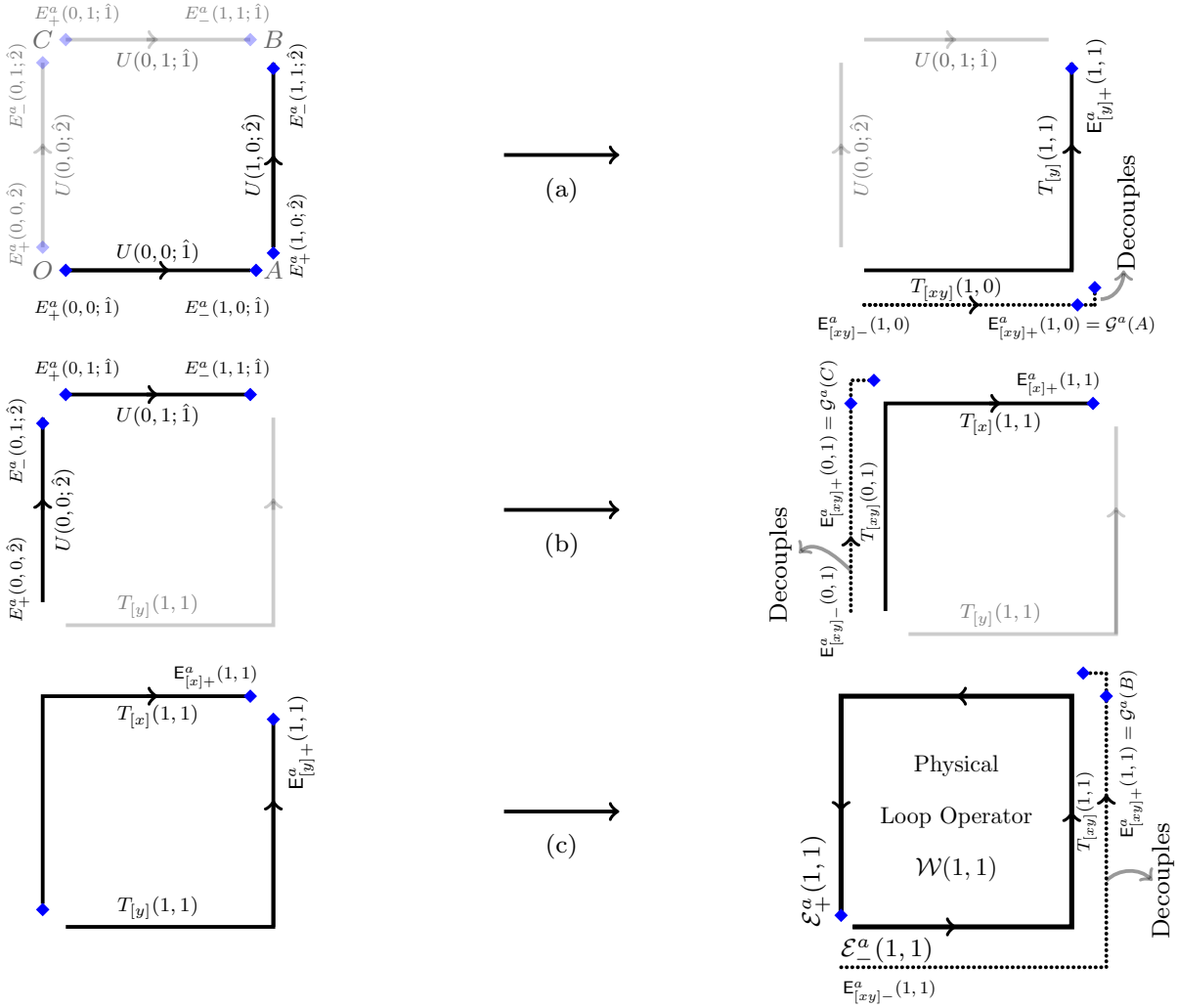

Figure 3.10: Three canonical transformations on the four link flux operators of a plaquette OABC leading to a single physical plaquette loop flux operator $\mathcal{W}_{\alpha\beta}(1,1)$ in (c). The three right electric fields $\mathsf{E}^{a}_{[xy]+}(1,0)$, $\mathsf{E}^{a}_{[xy]+}(1,1)$, $\mathsf{E}^{a}_{[xy]+}(0,1)$ of the three string flux operators ending at A, B and C respectively are the Gauss law generators $\mathcal{G}^{a}(A)$, $\mathcal{G}^{a}(B)$ and $\mathcal{G}^{a}(C)$ respectively. The Gauss law at the origin is: $\mathcal{G}^{a}(O) = E^{a}_{+}(0,0;\hat{1}) + E^{a}_{+}(0,0;\hat{2}) = \mathcal{E}^{a}_{-}(1,1) + \mathcal{E}^{a}_{+}(1,1) = 0$.

All steps in (3.36) are also illustrated in Figure 3.10-a. The notations used here are as follows. The subscripts $[xy]$ on the three unphysical flux operators $[\mathsf{T}_{[xy]}(1,0), \mathsf{T}_{[xy]}(1,1), \mathsf{T}_{[xy]}(0,1)]$ are used to encode the structure of their right electric fields in (3.36), (3.39) and (3.40). These are sums of the Kogut-Susskind electric fields in x, y directions (denoted by subscript $[x,y]$) or equivalently Gauss law operators at corners A, B and C respectively. During qualitative discussions we will often suppress these subscripts. Note that the resulting new pairs $\left(\mathsf{T}_{[xy]}(1,0),\ \mathsf{E}_{[xy]+}(1,0)\right)$ and $\left(\mathsf{T}_{[y]}(1,1), \mathsf{E}^{a}_{[y]+}(1,1)\right)$ are canonical and mutually independent exactly like the initial Kogut-Susskind pairs on links and satisfy:

$$\left[\mathsf{E}^{a}_{[xy]+}(1,0), \mathsf{T}_{[xy]}(1,0)\right] = \mathsf{T}_{[xy]}(1,0)\left(\frac{\lambda^a}{2}\right), \quad \left[\mathsf{E}^{a}_{[y]+}(1,1), T_{[y]}(1,1)\right] = \mathsf{T}_{[y]}(1,1)\left(\frac{\lambda^a}{2}\right),$$
$$\left[\mathsf{E}^{a}_{[xy]+}(1,0), \mathsf{T}_{[y]}(1,1)\right] = 0, \qquad \left[\mathsf{E}^{a}_{[y]}(1,1), \mathsf{T}_{[xy]}(1,0)\right] = 0. \tag{3.37}$$

From (3.36) the two right string electric fields $\mathsf{E}^{a}_{[xy]+}(1,0)$ and $\mathsf{E}^{a}_{[xy]+}(1,1)$ also commute with each other. The left electric fields are given by

$$\mathsf{E}^{a}_{[xy]-}(1,0) \equiv -\mathsf{R}_{ab}\left(\mathsf{T}_{[xy]}(1,0)\right)\ \mathsf{E}^{b}_{[xy]+}(1,0), \quad \mathsf{E}^{a}_{[y]-}(1,1) \equiv -\mathsf{R}_{ab}(\mathsf{T}_{[y]})\ \mathsf{E}^{b}_{[y]+}(1,1). \tag{3.38}$$

From (3.35) and the third equation in (3.36), it is clear that the string electric field $\mathsf{E}^{a}_{[xy]+}(1,0)$ satisfies

$$\boxed{\mathsf{E}^{a}_{[xy]+}(1,0) = \mathcal{G}^{a}(1,0) \approx 0.}$$

Therefore, the string flux operator $\mathsf{T}_{[xy]}(1,0)$ is unphysical as its action on any state takes that state out of $\mathcal{H}^{p}$. Therefore, we ignore it henceforth. We now iterate the above canonical transformations with $U(0,0;\hat{1}),\ U(1,0;\hat{2})$ in (3.36) replaced by $U(0,0;\hat{2}),\ U(0,1;\hat{1})$ respectively. We define:

$$\mathsf{T}_{[xy]}(0,1) \equiv U(0,1;\hat{2}), \qquad \mathsf{T}_{[x]}(1,1) \equiv U(0,0;\hat{2})\ U(0,1;\hat{1}), \tag{3.39}$$
$$\mathsf{E}^{a}_{[xy]+}(0,1) = E^{a}_{-}(0,1;\hat{2}) + E^{a}_{+}(0,1;\hat{1}), \qquad \mathsf{E}^{a}_{[x]+}(1,1) = E^{a}_{-}(1,1;\hat{1}).$$

Again, all steps in (3.39) are illustrated in Figure 3.10-b. The two new sets of string operators obtained $\left(\mathsf{T}_{[xy]}(0,1), \mathsf{E}^{a}_{[xy]+}(0,1)\right)$, $\left(\mathsf{T}_{[x]}(1,1), \mathsf{E}^{a}_{[x]+}(1,1)\right)$ are canonical and mutually independent like the previous two sets in (3.37). The left electric fields $\mathsf{E}^{a}_{[xy]-}(0,1)$, $\mathsf{E}^{a}_{[x]-}(1,1)$ are defined through parallel transports as in (2.12) or (3.38). As a consequence of Gauss law (eqn(3.35) and eqn(3.39)) at C:

$$\boxed{\mathsf{E}^{a}_{[xy]+}(0,1) = \mathcal{G}^{a}(0,1) \approx 0.}$$

Therefore, the string operator $\mathsf{T}_{[xy]}(0,1)$ (like $\mathsf{T}_{[xy]}(1,0)$) becomes unphysical. The last sets of canonical transformations fuse the remaining two strings $\mathsf{T}_{[y]}(1,1)$ and $\mathsf{T}_{[x]}(1,1)$ to define the final physical plaquette loop conjugate operators[6] $\left(\mathcal{W}(1,1), \mathcal{E}_+(1,1)\right)$:

$$\begin{aligned} \mathsf{T}_{[xy]}(1,1) &\equiv \mathsf{T}_{[y]}(1,1), & \mathcal{W}(1,1) &\equiv \mathsf{T}_{[y]}(1,1)\, \mathsf{T}^\dagger_{[x]}(1,1), \\ \mathsf{E}_{[xy]+}(1,1) &= \mathsf{E}^a_{[y]+}(1,1) + \mathsf{E}^a_{[x]+}(1,1), & \mathcal{E}^a_+(1,1) &= \mathsf{E}^a_{[x]-}(1,1). \end{aligned} \tag{3.40}$$

The above canonical transformations are illustrated in Figure 3.10-c. In the third equation in (3.40), the right electric fields $\mathsf{E}^a_{[y]+}(1,1)$ and $\mathsf{E}^a_{[x]+}(1,1)$ can be substituted in terms of the Kogut-Susskind electric fields using (3.36) and (3.39) to get

$$\boxed{\mathsf{E}_{[xy]+}(1,1) = \mathcal{G}^a(1,1) \approx 0.}$$

Therefore, $\mathsf{T}_{[xy]}(1,1)$ decouples and

$$\mathcal{W}_{\alpha\beta} \equiv \mathcal{W}_{\alpha\beta}(1,1) \equiv \left(U(0,0;\hat{1})\, U(1,0;\hat{2})\, U^\dagger(0,1;\hat{1})\, U^\dagger(0,0;\hat{2})\right)_{\alpha\beta} \tag{3.41}$$

emerges as the final physical plaquette loop flux operator. Its right electric field is

$$\begin{aligned} \mathcal{E}^a_+(1,1) = \mathsf{E}^a_{[x]-}(1,1) &\equiv -R_{ab}\left(\mathsf{T}_{[x]}(1,1)\right) \mathsf{E}^b_{[x]+}(1,1) = -R_{ab}\left(\mathsf{T}_{[x]}(1,1)\right) E^b_-(1,1;\hat{1}) \\ &= R_{ab}(U(0,0;\hat{2})E^b_+(0,1;\hat{1}) = -R_{ab}(U(0,0;\hat{2}))E^b_-(0,1;\hat{2}) = E^a_+(0,0;\hat{2}). \end{aligned} \tag{3.42}$$

In (3.42) we have used Gauss law constraint at C: $\mathsf{T}^a_+(0,1) = E^a_+(0,1;\hat{1}) + E^a_-(0,1;\hat{2}) = 0$. Similarly[7] ,

$$\mathcal{E}^a_-(1,1) = E^a_+(0,0;\hat{1}). \tag{3.43}$$

Thus we have converted all link operators into string and loop operators. Note that by construction the canonical structures are strictly maintained at all three steps ((3.36), (3.39) and (3.40)). All three $SU(N)$ string flux operators and their conjugate electric fields satisfy

$$\left[\mathsf{E}^a_{[xy]+}(x,y), \mathsf{T}(x',y')\right] = \delta_{x,x'}\delta_{y,y'}\left(\mathsf{T}(x,y)\frac{\lambda^a}{2}\right). \tag{3.44}$$

6 The plaquette loop operator $\mathcal{W}(1,1)$ is defined at $(1,1)$ (and not at $(0,0)$) because of later convenience when we deal with canonical transformations on a finite lattice.

7 Defining $U_1 = U(0,0;\hat{1})$, $U_2 = U(1,0;\hat{2}), U_3 = U(0,1;\hat{1})$, $U_4 = U(0,0;\hat{2})$, $\mathcal{W} = U_1U_2U_3^\dagger U_4^\dagger$ we get:
$\mathcal{E}^a_-(1,1) \equiv -R_{ab}(\mathcal{W})\,\mathcal{E}^b_+(1,1) = -R_{ab}(\mathcal{W})\,E^b_+(0,0;\hat{2}) = R_{ab}(\mathcal{W}U_4)\,E^b_-(0,1;\hat{2}) = -R_{ab}(\mathcal{W}U_4)E^b_+(0,1;\hat{1}) = R_{ab}(\mathcal{W}U_4U_3)E^b_-(1,1;\hat{1}) = -R_{ab}(\mathcal{W}U_4U_3)\,E^b_-(1,1;\hat{2}) = R_{ab}(\mathcal{W}U_4U_3U_2^\dagger)\,E^b_+(1,0;\hat{2}) = -R_{ab}(\mathcal{W}U_4U_3U_2^\dagger)\,E^b_-(1,0;\hat{1}) = R_{ab}(\mathcal{W}U_4U_3U_2^\dagger U_1^\dagger)\,E^b_+(0,0;\hat{1}) = E^a_+(0,0;\hat{1})$.

Above $(x,y),(x',y') = (1,0),(1,1),(0,1)$. The string electric fields $\mathsf{E}^a_{[xy]+}(x,y)$ at (x,y) satisfy SU(N) algebra and commute if they are at different lattice sites. Under SU(N) gauge transformations, these string operators transform as:

$$\begin{aligned} \mathsf{T}_{[xy]}(x,y) &\rightarrow \Lambda(0,0)\ \mathsf{T}_{[xy]}(x,y)\ \Lambda^\dagger(x,y), \\ \mathsf{E}_{[xy]+}(x,y) &\rightarrow \Lambda(x,y)\ \mathsf{E}_{[xy]+}(x,y)\ \Lambda^\dagger(x,y). \end{aligned} \tag{3.45}$$

Therefore, none of the three strings can form any gauge invariant operators at their end points $(0,1),(1,1),(0,1)$. The SU(N) Gauss laws at A, B, C state this simple fact. Having removed the three unphysical strings, we now focus on the plaquette loop operators $(\mathcal{E}^a_-(1,1),\ \mathcal{W}(1,1),\ \mathcal{E}^a_+(1,1)) \equiv (\mathcal{E}^a_-,\ \mathcal{W},\ \mathcal{E}^a_+)$. Again by construction, they satisfy the canonical quantization relations:

$$\begin{aligned} [\mathcal{E}^a_+,\mathcal{W}] &= -\left(\frac{\lambda^a}{2}\mathcal{W}\right) \quad \Rightarrow \quad \left[\mathcal{E}^a_+,\mathcal{E}^b_+\right] = if^{abc}\mathcal{E}^c_+, \\ [\mathcal{E}^a_-,\mathcal{W}] &= \left(\mathcal{W}\frac{\lambda^a}{2}\right) \quad \Rightarrow \quad \left[\mathcal{E}^a_-,\mathcal{E}^b_-\right] = if^{abc}\mathcal{E}^c_-. \end{aligned} \tag{3.46}$$

Above $\mathcal{E}^a_- \equiv -R_{ab}(\mathcal{W})\ \mathcal{E}^b_+$ implying $(\vec{\mathcal{E}}_-)^2 = (\vec{\mathcal{E}}_+)^2 \equiv (\vec{\mathcal{E}})^2$ and $[\mathcal{E}^a_-,\mathcal{E}^b_+] = 0$. They gauge transform at the origin as:

$$\mathcal{E}_\mp \rightarrow \Lambda\ \mathcal{E}_\mp\ \Lambda^\dagger, \qquad \mathcal{W} \rightarrow \Lambda\ \mathcal{W}\ \Lambda^\dagger. \tag{3.47}$$

We have defined $\mathcal{E}_\mp \equiv \sum_{a=1}^{(N^2-1)} \mathcal{E}^a_\mp\ \lambda^a$ and $\Lambda \equiv \Lambda(0,0)$ denotes the gauge rotation at the origin. The corresponding unsolved Gauss law constraints in terms of loop electric fields at the origin are:

$$\mathcal{G}^a(0,0) = \mathcal{E}^a_- + \mathcal{E}^a_+ = E^a_+(0,0;\hat{1}) + E^a_+(0,0;\hat{2}) \approx 0. \tag{3.48}$$

Only global constraints (3.48) need to be imposed to get the physical Hilbert space $\mathcal{H}^p$. Note that all gauge degrees of freedom away from the origin have been removed in the form of frozen $SU(N)$ strings: $\mathsf{E}^a_{[xy]}(x,y) = 0,\ (x,y) = (1,0),(1,1),(0,1)$.

3.2.2.1 *Inverse relations*

It is instructive and useful to invert the canonical transformations (3.36), (3.39) and (3.40) to write Kogut-Susskind link operators in terms of strings and loop variables. These relations

also enable us to write the Kogut-Susskind Hamiltonian (3.59) in terms of loop operators (see 3.83)). It is clear from Figure 3.10-a,b,c that

$$\begin{aligned} U(0,0;\hat{1}) &= \mathsf{T}_{[xy]}(1,0), & \mathsf{U}(1,0;\hat{2}) &= \mathsf{T}^{\dagger}_{[xy]}(1,0)\ \mathsf{T}_{[xy]}(1,1), \\ U(0,0;\hat{2}) &= \mathsf{T}_{[xy]}(0,1), & \mathsf{U}(0,1;\hat{1}) &= \mathsf{T}^{\dagger}_{[xy]}(0,1)\ \mathcal{W}^{\dagger}(1,1)\mathsf{T}_{[xy]}(1,1). \end{aligned} \tag{3.49}$$

Similarly, the electric field relations in (3.36), (3.39) and (3.40) can also be inverted to write :

$$\begin{aligned} E^a_+(0,0;\hat{1}) &= \mathsf{E}^a_{[xy]_-}(1,0) + \mathsf{E}^a_{[xy]_-}(1,1) + \mathcal{E}^a_-, & E^a_+(0,0;\hat{2}) &= \mathcal{E}^a_+ + \mathsf{E}^a_{[xy]_-}(0,1), \\ E^a_+(1,0;\hat{2}) &= R_{ab}\left(\mathsf{T}^{\dagger}_{[xy]}(1,0)\right)\left(\mathsf{E}^b_{[xy]_-}(1,1) + \mathcal{E}^b_-\right), & E^a_+(0,1;\hat{1}) &= R_{ab}\left(\mathsf{T}^{\dagger}_{[xy]}(0,1)\right)\mathcal{E}^b_+. \end{aligned} \tag{3.50}$$

These canonical relations between links and loops have the following interesting features:

- They are consistent with gauge transformations (2.17), (3.45) and (3.47) as well as with SU(N) algebras of link, string and loop electric fields given in (3.44) and (3.46).
- The canonical commutation relations between SU(N) link flux operators and their link electric fields also remain intact under the mappings (3.49) and (3.50) from string, loop to link operators. As an example, it is easy to see that $E^a_+(1,0;\hat{2})$ leaves $U(0,0;\hat{1})$, $U(0,0;\hat{2})$, $U(0,1;\hat{1})$ unchanged and rotates $U(1,0;\hat{2})$ from the left:

$$[E^a_+(1,0;\hat{2}), U(1,0;\hat{2})] = R_{ab}(\mathsf{T}^{\dagger}_{[xy]}(1,0))\underbrace{\mathsf{T}^{\dagger}_{[xy]}(1,0)\frac{\lambda^b}{2}\mathsf{T}_{[xy]}(1,0)}_{=R_{bc}\left(\mathsf{T}_{[xy]}(1,0)\right)\frac{\lambda^c}{2}}U(1,0;\hat{2}) = \frac{\lambda^a}{2}U(1,0;\hat{2}).$$

  All other commutation relations can be directly read off from (3.49) and (3.50).
- No string operators can appear in a gauge invariant operator[8]. As an example, the gauge invariant electric field terms in the Kogut-Susskind Hamiltonian are:

$$\left(\vec{E}_+(0,0;\hat{1})\right)^2 = \left(\vec{E}_+(1,0;\hat{2})\right)^2 = \left(\vec{E}_+(0,1;\hat{1})\right)^2 = \left(\vec{E}_+(0,0;\hat{2})\right)^2 = \left(\vec{\mathcal{E}}_-\right)^2. \tag{3.51}$$

  after putting $\mathsf{E}_{[xy]+}(x,y) = 0$ in (3.50) within $\mathcal{H}^p$. In other words, while expressing Kogut-Susskind link electric fields in terms of loop electric fields the string flux operators appear as an overall parallel transport. This is also required for the consistency of SU(N) gauge transformations.

3.2.2.2 *Loop states on a single plaquette lattice.*

After the canonical transformations and decoupling of string operators, the basic degrees of freedom of SU(N) lattice gauge theory lies on plaquettes. Therefore a loop basis can be

8 This is no longer true in the presence of matter fields. String variables no longer decouple and further canonical transformation steps are necessary to isolate the gauge variant degrees of freedom.

constructed by diagonalising a complete set of commuting operators on a plaquette. In the typical case of SU(2) lattice gauge theory, a loop basis is given by diagonalizing $\mathcal{E}_-^2 = \mathcal{E}_+^2 = \mathcal{E}^2$, $\mathcal{E}_-^{a=3}$ and $\mathcal{E}_+^{a=3}$. Such a basis state $|j, m_-, m_+\rangle$ is characterised by 3 quantum numbers j, m_-, m_+.

$$\vec{\mathcal{E}}^{\,2}\,|j,m_-,m_+\rangle = j(j+1)\;|j,m_-,m_+\rangle, \qquad \vec{\mathcal{E}}_{\mp}^{a=3}\,|j,m_-,m_+\rangle = m_{\mp}\,|j,m_-,m_+\rangle. \tag{3.52}$$

The states $|j\ m_-\ m_+\rangle$ in (3.52) describe loops carrying non-abelian quantized SU(2) loop electric fluxes. These states form a complete, orthonormal basis:

$$\sum_{j,m_-,m_+} |j\ m_-\ m_+\rangle\,\langle j\ m_-\ m_+| = \mathbf{1}\,; \qquad \langle j\ m_-\ m_+|j'\ m'_-\ m'_+\rangle = \delta_{jj'}\delta_{m_-m'_-}\delta_{m_+m'_+}.$$

Under global gauge transformation,

$$|jm_-m_+\rangle \to \sum_{m'_-,m'_+} |jm'_-m'_+\rangle D^{\,j}_{m'_-m_-}(\Lambda)\; D^{\,j}_{m'_+m_+}(\Lambda^\dagger). \tag{3.53}$$

In (3.53), $D^{\,j}_{mm'}(\Lambda)$ are the Wigner matrices, $\Lambda \equiv \Lambda(0,0)$ denotes the gauge transformation at the origin. Since, in the single plaquette case, the Gauss law operator is given by $\mathcal{G}^a = \mathsf{L}^a = \mathcal{E}_+^a + \mathcal{E}_-^a$, it is convenient to construct a coupled basis which diagonalizes $\vec{\mathsf{L}}^2, (\vec{\mathsf{L}})^{a=3}$. Therefore, we construct a coupled basis so that the following coupled and complete set of commuting operators are diagonal:

$$\left\{\vec{\mathcal{E}}_-^{\,2} = \vec{\mathcal{E}}_+^{\,2} = \vec{\mathcal{E}}^{\,2},\quad (\vec{\mathcal{E}}_- + \vec{\mathcal{E}}_+)^2,\quad (\vec{\mathcal{E}}_- + \vec{\mathcal{E}}_+)^{a=3}\right\} \equiv \left\{\vec{\mathcal{E}}^2,\ (\vec{\mathsf{L}})^2,\ (\vec{\mathsf{L}})^{a=3}\right\}.$$

The coupled basis states $|n\ l\ m\rangle$ are related to $|j\ m_-\ m_+\rangle$ by Clebsch-Gordan coefficients:

$$|\mathsf{n}\ l\ m\rangle \equiv \sum_{m_-,m_+} C^{\,l,m}_{jm_-,jm_+}\;|j\ m_-m_+\rangle. \tag{3.54}$$

Above $\mathsf{n} \equiv 2j+1 = 1,2,\cdots;\quad l = 0,1,\cdots,2j\ (\equiv \mathsf{n}-1);\quad m = -l,-(l-1),\cdots,(l-1),l.$

$$\begin{aligned} \vec{\mathcal{E}}^{\,2}\,|\mathsf{n}\ l\ m\rangle &= \frac{(\mathsf{n}^2-1)}{4}\;|\mathsf{n}\ l\ m\rangle, \\ \vec{\mathsf{L}}^{\,2}\,|\mathsf{n}\ l\ m\rangle &= l(l+1)\;|\mathsf{n}\ l\ m\rangle, \qquad \mathsf{L}^{a=3}\,|\mathsf{n}\ l\ m\rangle = m\;|\mathsf{n}\ l\ m\rangle. \end{aligned} \tag{3.55}$$

Under the global transformation Λ: $|n\ l\ m\rangle \to \sum_{\bar{m}=-l}^{l} D^l_{m\bar{m}}(\Lambda)|n\ l\ m\rangle$. The $|n\ l\ m\rangle$ states will be identified with the hydrogen atom bound states in Chapter 5 (section 5.2). The Gauss law (3.48) implies that the gauge invariant basis is given by:

$$|\mathsf{n}\rangle = |\mathsf{n} = 2j+1\ ,\ l=0\ ,\ m=0\rangle.$$

A dual magnetic (angular) basis diagonalizing all the Wilson loop operators can be constructed as follows:

$$|\Omega_W(\omega,\hat{w})\rangle = \sum_{jm_-m_+} \sqrt{\frac{2j+1}{2\pi^2}} D^j_{m_-m_+}(\omega,\hat{w})\,|j\ m_-\ m_+\rangle\,. \tag{3.56}$$

$$\Omega_W(w,\hat{w}) \equiv w\,\sigma + i\hat{w}\cdot\vec{\sigma}, \quad w^2+\hat{w}^2 = 1 : S^3.$$

Here, $(\omega,\hat{w})$ is the angle axis characterisation of a point on the SU(2) group manifold S^3. The plaquette loop operators are diagonal in this basis.

$$\mathcal{W}_{\alpha\beta}\,|\Omega_W(\omega,\hat{w})\rangle = z_{\alpha\beta}\,|\Omega_W(\omega,\hat{w})\rangle\,, \tag{3.57a}$$

where

$$z_{\alpha\beta} = \begin{bmatrix} \left(\cos\frac{\omega}{2} - i\sin\frac{\omega}{2}\cos\theta\right) & i\sin\frac{\omega}{2}\sin\theta e^{-i\phi} \\ -i\sin\frac{\omega}{2}\sin\theta e^{-i\phi} & \left(\cos\frac{\omega}{2} + i\sin\frac{\omega}{2}\cos\theta\right) \end{bmatrix}_{\alpha\beta}. \tag{3.57b}$$

Above, (θ,ϕ) are the angles characterizing the axis $\hat{w}$. The above equations (3.57a) and (3.57b) follows from the properties of Wigner matrices $D^j_{m_-m_+}$ as shown in appendix B. Therefore,

$$Tr\mathcal{W}\ \ |\Omega_W(\omega,\hat{w})\rangle = 2\cos\frac{\omega}{2}\ \ |\Omega_W(\omega,\hat{w})\rangle\,.$$

As shown in the appendix (eqn B.8), a completely gauge invariant angular basis on a single plaquette is given by:

$$|\omega\rangle \ \equiv\ \int d\Lambda |\Omega_W(\omega,\hat{w})\rangle \ =\ \sum_j \chi^j(\omega)\,|j\rangle\,. \tag{3.58}$$

Here, $|j\rangle \equiv |n\rangle_{n=2j+1}$ and $\chi^j(\omega) = \frac{\sin(2j+1)\frac{\omega}{2}}{\sin\left(\frac{\omega}{2}\right)}$ are the SU(2) characters.

3.2.2.3 *Loop dynamics on a single plaquette*

In this section, we discuss loop dynamics on a single plaquette. We consider SU(N) Kogut-Susskind Hamiltonian [6, 8] on a single plaquette lattice:

$$\begin{aligned} H \ &= \ g^2\sum_{l=1}^{4}\vec{E}^2(l) + \frac{K}{g^2}\left[2N - \mathrm{Tr}\left(U_1\,U_2\,U_3^\dagger\,U_4^\dagger\ +\ h.c\right)\right] \\ &\equiv \quad H_E\ +\ H_B. \end{aligned} \tag{3.59}$$

In (3.83), K is a constant and $U_1 \equiv U(0,0;\hat{1}), U_2 \equiv U(1,0;\hat{2}), U_3 \equiv U(0,1;\hat{1}), U_4 \equiv U(0,0;\hat{2})$. Using links to loop relations (3.41) and (3.50), the SU(N) loop Hamiltonian for the single plaquette is:

$$H = 4g^2\vec{\mathcal{E}}^2 + \frac{K}{g^2}\left[2N - \mathrm{Tr}\left(\mathcal{W} + \mathcal{W}^\dagger\right)\right]. \tag{3.60}$$

In (3.83), we have ignored all string electric fields. At this stage we specialize to SU(2) case[9]. The electric field term is:

$$H_E \;\; = g^2 \sum_{l=1}^{4} \vec{E}^2(l) = 4g^2\vec{\mathcal{E}}^2. \tag{3.61}$$

The four link magnetic field term takes its simplest possible form:

$$H_B = \frac{1}{g^2}\;\; Tr(U_1\, U_2\, U_3^\dagger\, U_4^\dagger) = \frac{1}{g^2}\;\; Tr\, \mathcal{W}. \tag{3.62}$$

The magnetic field term, important in the weak coupling continuum limit, simply creates and annihilates the fluxes on the plaquette loop:

$$H_B\;\; |\mathsf{n}\rangle \;\; = \frac{1}{g^2}\; Tr\left(U_1\, U_2\, U_3^\dagger\, U_4^\dagger\right)|\mathsf{n}\rangle \;\; = \frac{1}{g^2}\; Tr\, \mathcal{W}\; |\mathsf{n}\rangle \quad\; = \frac{1}{g^2}\left[|\mathsf{n}+1\rangle + |\mathsf{n}-1\rangle\right]. \tag{3.63}$$

We now show that the loop Schrödinger equation easily reduces to Mathieu equation in the magnetic angular basis defined in eqn. (3.58).

$$H_B\,|\omega\rangle = \;\; \frac{1}{g^2}\;\; (Tr\mathcal{W})\;\; |\omega\rangle = \;\; \frac{2}{g^2}\; cos\left(\frac{\omega}{2}\right)\;\; |\omega\rangle\,. \tag{3.64}$$

Note that, as shown in appendix B, ω is a gauge invariant angle. We now use the differential equation of the SU(2) character [115]:

$$\frac{d^2\chi_j}{d\omega^2} + cot\left(\frac{\omega}{2}\right)\frac{d\chi_j(\omega)}{d\omega} + j(j+1)\chi_j(\omega) = 0.$$

to convert H_E in (3.61) into differential operator in ω. Finally the Schrödinger equation $H\,|\psi\rangle_\epsilon = \epsilon\,|\psi\rangle_\epsilon$ in this gauge invariant loop basis is the Mathieu equation:

$$\left[\frac{d^2}{d\omega^2} + \frac{1}{4}\right]\phi_\epsilon(\omega) + \frac{\kappa}{4}\left[\epsilon - 2\kappa\left(1 - cos\left(\frac{\omega}{2}\right)\right)\right]\phi_\epsilon\,(\omega) = 0. \tag{3.65}$$

In (3.65) we have defined $\kappa \equiv \frac{1}{g^2}$ and $\phi_\epsilon(\omega) \equiv sin\frac{\omega}{2}\;\psi_\epsilon(\omega)$ where $\psi_\epsilon(\omega) \equiv \langle\omega|\psi\rangle_\epsilon$. The Mathieu equation (3.65) and its discrete solutions has been extensively discussed in the past in the context of single plaquette lattice gauge theory [41, 42, 80].

9 Similar construction is also possible for SU(N) and involves SU(N) irreducible prepotential operators discussed in the context of SU(N) lattice gauge theories in [102, 103].

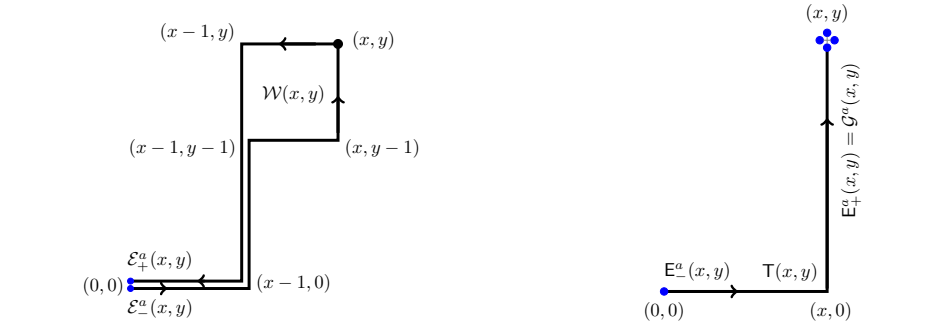

SU(N) loop operators: $\{\mathcal{E}^a_-(x,y), \mathcal{W}(x,y), \mathcal{E}^a_+(x,y)\}$ (physical) (a)

SU(N) string operators: $\{\mathsf{E}^a_-(x,y), \mathsf{T}(x,y), \mathsf{E}^a_+(x,y)\}$ (unphysical) (b)

Figure 3.11: The plaquette loop operator $\mathcal{W}(x,y)$ and the string flux operator $\mathsf{T}(x,y)$ and their electric fields $\mathcal{E}^a_\mp(x,y)$ and $\mathsf{E}^a_\mp(x,y)$ respectively. Note that the electric fields $\mathcal{E}^a_\mp(x,y)$, $\mathsf{E}^a_\mp(x,y)$ are located at the initial and final points of the loops and strings respectively.

3.2.3 *SU(N) canonical transformations on a finite lattice in* $2+1$ *D*

In this section, we directly generalize the SU(N) canonical transformations on a single plaquette described in the previous section to a finite lattice. We start with a set of $\mathcal{L}$ standard SU(N) Kogut-Susskind flux and their conjugate electric field operators: $\Big(E^a_+(n;\hat{i}), U(n;\hat{i}), E^a_-(n+\hat{i};\hat{i})\Big)$ satisfying (2.11). We construct an iterative series of canonical transformations to transform them into:

- a set of $\mathcal{P}$ "physical" SU(N) plaquette loop flux operators and their conjugate loop electric fields,

$$\Big(\mathcal{E}^a_-(n),\ \mathcal{W}(n),\ \mathcal{E}^a_+(n)\Big), \qquad a = 1,2,\cdots,N^2-1.$$

  The plaquette loop flux operator $\mathcal{W}(x,y)$ is along the path: $(0,0) \to (x-1,0) \to (x-1,y-1) \to (x,y-1) \to (x,y) \to (x-1,y) \to (x-1,0) \to (0,0)$.

- a set of independent $(\mathcal{N}-1)$ "unphysical" SU(N) string flux operators[10] and their conjugate string electric fields,

$$\Big(\mathsf{E}^a_-(n),\ \mathsf{T}(n),\ \mathsf{E}^a_+(n)\Big), \qquad a = 1,2,\cdots,N^2-1.$$

  The string $\mathsf{T}(x,y)$ start at $(0,0)$ and end at (x,y) following the path $(0,0) \to (x,0) \to (x,y)$.

10 In the appendix the string operators are denoted by $\Big[\mathsf{T}_{[xxyy]}(x,y), \mathsf{E}^a_{[xxyy]\mp}(x,y)\Big]$. The subscript $[xxyy]$ encodes the Gauss law structures of the string electric field at (x,y). In this section, for the sake of notational convenience, we have ignored the subscripts and simply denoted them by $\mathsf{T}(x,y)$ and $\mathsf{E}^a_\mp(x,y)$.

These new loop and string flux operators[11] and the location of their electric fields are shown in Figure 3.11. As is clear from this Figure, the convention chosen for loop and string electric fields is that $\mathcal{E}^a_-(n)\big(\mathcal{E}^a_+(n)\big)$, $\mathsf{E}^a_-(n)\big(\mathsf{E}^a_+(n)\big)$ are located at the initial (final) points of the loop and string flux lines. They satisfy canonical commutation relations amongst themselves. The degrees of freedom exactly match as $\mathcal{L} = \mathcal{P} + (\mathcal{N}-1)$. As shown in appendix A (see eqn (A.19)), the right electric field operators of the string attached to a site n are the Gauss law generators (2.18) at n:

$$\boxed{\mathsf{E}^a_+(n) = \mathcal{G}^a(n).} \tag{3.66}$$

Therefore, all $(\mathcal{N}-1)$ string flux operators $\mathsf{T}(n)$ create unphysical states $\notin \mathcal{H}^p$ and hence can be ignored without any loss of physics. The most general gauge invariant state can be written as:

$$|\Psi\rangle = \sum_{r_1\cdots r_{\mathcal{P}}} A_{r_1\cdots r_{\mathcal{P}}} Tr\Big((\mathcal{W}(1))^{r_1}(\mathcal{W}(2))^{r_2}\cdots(\mathcal{W}(p))^{r_{\mathcal{P}}}\Big)|0\rangle$$

Above $(r_1, r_2, \cdots, r_{\mathcal{P}})$ are sets of $\mathcal{P}$ integers, $A_{r_1\cdots r_{\mathcal{P}}}$ are complex coefficients and $|0\rangle$ is the strong coupling vacuum. The canonical transformations leading to the above new string & loop flux operators and their conjugate electric fields are explicitly constructed in the appendix A.

3.2.3.1 *Canonical relations*

The final $(\mathcal{N}-1)$ string in Figure 3.11-a and $(\mathcal{P})$ loop flux operators in Figure 3.11-b are related to the initial $(\mathcal{L})$ Kogut-Susskind link operators as (see appendix A for details):

$$\begin{aligned}\mathsf{T}(x,y) &= \prod_{x'=0}^{x} U(x',0;\hat{1}) \prod_{y'=0}^{y} U(x,y';\hat{2}),\\ \mathcal{W}(x,y) &= \mathsf{T}(x-1,y-1)\; U_p(x-1,y-1)\; \mathsf{T}^\dagger(x-1,y-1).\end{aligned} \tag{3.67}$$

In (3.67), the strings $\mathsf{T}(x,y)$ are defined at all lattice sites away from the origin and the loop operators $\mathcal{W}(x,y)$ are located at $x,y = 1,2,\cdots,\mathsf{N}_s-1$. The Kogut-Susskind plaquette operators are defined as: $U_p(x,y) = U(x,y;\hat{1})\; U(x+1,y;\hat{2})\; U^\dagger(x+1,y+1;\hat{1})\; U^\dagger(x,y+1;\hat{2})$.

11 The canonical transformations and hence the loop and string operators depend on the paths chosen for loops and strings. We have made a particular choice, shown in Figure 3.11, which lead to duality (see chapter 4)and as a consequence a simple Hamiltonian in the continuum $(g^2 \to 0)$ limit.

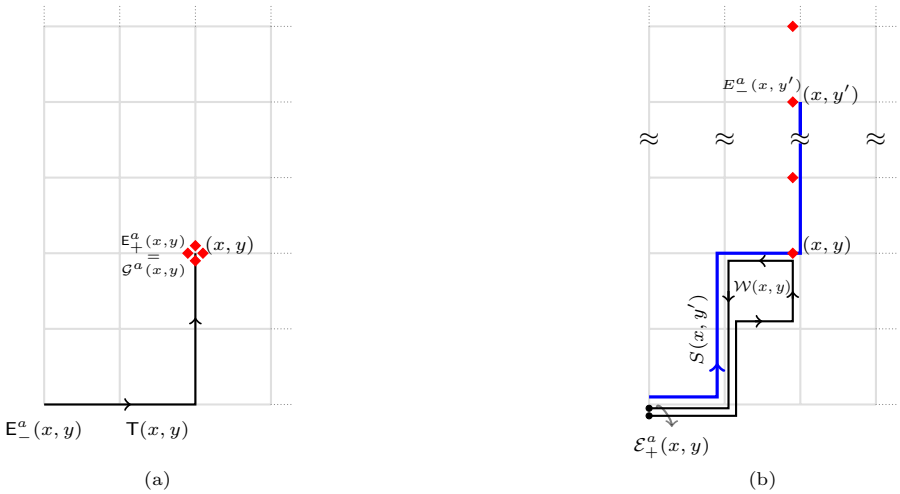

Figure 3.12: Graphical representation of the canonical relations (3.68). The Kogut-Susskind electric fields are denoted by ♦ and the plaquette loop electric fields are denoted by •. We show a) string electric field in terms of Kogut-Susskind electric fields and (b) plaquette loop electric fields $\mathcal{E}^a_+(x,y)$ in terms of the original Kogut-Susskind link electric fields. In (a) the 4 ♦ at (x,y) denotes the Gauss law operator at $\mathcal{G}^a(x,y)$. In (b) Kogut-Susskind link electric fields $E^a_-(x,y';\hat{1})$; $y' = y, y+1 \cdots \mathsf{N}_s - 1$ are parallel transported by $S(x,y,y')$ to give the loop electric field $\mathcal{E}^a_+(x,y)$.

The conjugate string and plaquette loop electric fields in terms of the initial Kogut-Susskind link electric fields are (see appendix A for details):

$$\mathsf{E}^a_+(x,y) = \sum_{i=1}^{2} \left[E^a_-(x,y;\hat{i}) + E^a_+(x,y;\hat{i})\right] = \mathcal{G}^a(x,y) = 0,$$
$$\mathcal{E}^a_+(x,y) = -\sum_{y'=y}^{\mathsf{N}_s-1} R_{ab}(S(x,y,y'))E^b_-(x,y';\hat{1}). \tag{3.68}$$

In (3.68), we have defined: $S(x,y,y') \equiv \mathsf{T}(x-1,y)\ U(x-1,y;\hat{1})\ \prod_{y''=y}^{y'} U(x,y'';\hat{2})$ and $x \neq 0; y \neq 0$. The relations (3.68) between the new string and loop electric fields and old Kogut-Susskind electric fields are derived in appendix A (see (A.19) and (A.23)) and illustrated in Figure 3.12-a and Figure 3.12-b respectively. Because of the SU(N) Gauss laws all string operators, containing gauge degrees of freedom away from the origin, naturally decouple from the theory. The remaining physical plaquette loop operators can be thought of as a set of collective coordinates which describe the theory without any redundant loop or local gauge degrees of freedom. These $\mathcal{P}$ SU(N) loop flux operators are all mutually independent (no SU(N) Mandelstam constraints) and obey the canonical quantization conditions with their loop electric fields exactly like the original Kogut-Susskind link operators in (2.11).

$$\left[\mathcal{E}^a_-(x,y), \mathcal{W}_{\alpha\beta}(x,y)\right] = -\left(\frac{\lambda^a}{2}\mathcal{W}(x,y)\right)_{\alpha\beta}, \qquad \left[\mathcal{E}^a_+(x,y), \mathcal{W}_{\alpha\beta}(x,y)\right] = \left(\mathcal{W}(x,y)\frac{\lambda^a}{2}\right)_{\alpha\beta}. \tag{3.69a}$$

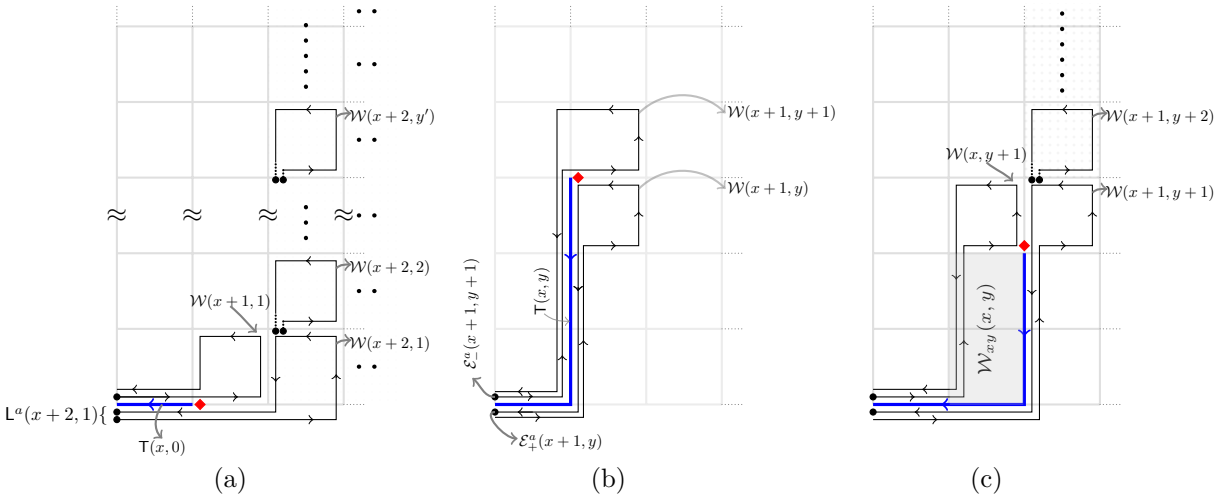

Figure 3.13: Graphical representation of the inverse canonical relations (3.72): a) link electric field $E^a_+(x, y = 0; \hat{1})$, (b) $E^a_+(x, y \neq 0; \hat{1})$ and (c) $E_+(x, y; \hat{2})$ in terms of plaquette loop operators and loop electric field. The • represents plaquette loop electric fields and ♦ represents Kogut-Susskind link electric fields. All loop electric fields • are parallel transported along the attached lines to give Kogut-Susskind link operator $E^a_+(x, y; \hat{i})$ or ♦ in (3.72). In (a) $\sum_p \mathsf{L}^b(p)$ gives $\Delta^b_X(x, y = 0)$ in (3.72), the summations is over the plaquettes in the dotted region. In (c) we show $\Delta_Y(x, y)$ where the summation is again over the plaquettes in the dotted region. The shaded region in (c) represents $\mathcal{W}_{xy}(x, y)$ in the second equation in (3.72).

$$\left[\mathcal{E}^a_-(x,y), \mathcal{E}^b_-(x,y)\right] = if^{abc}\mathcal{E}^c_-(x,y), \qquad \left[\mathcal{E}^a_+(x,y), \mathcal{E}^b_+(x,y)\right] = if^{abc}\mathcal{E}^c_+(x,y). \tag{3.69b}$$

Further, the two electric fields are related through parallel transport and commute:

$$\mathcal{E}^a_-(x,y) \equiv -R_{ab}(\mathcal{W}^\dagger(x,y))\mathcal{E}^b_+(x,y) \implies \left[\mathcal{E}^a_-(x,y), \mathcal{E}^b_+(x,y)\right] = 0. \tag{3.70}$$

The quantization relations (3.69a), (3.69b) and (3.70) are exactly similar to the original quantization rules (2.11). Thus the electric field operator $E^a(x, y; \hat{i})$ and the magnetic vector potential operator $U_{\alpha\beta}(x, y; i)$ have been replaced by their dual electric scalar potential $\mathcal{E}^a(x, y)$ and the dual magnetic field operator $\mathcal{W}_{\alpha\beta}(x, y)$. This is similar to Z_2 lattice gauge theory case where $\{\sigma_1(x, y); \sigma_3(x, y)\}$ get replaced by $\{\mu_3(x, y); \mu_1(x, y)\}$. We again emphasize that $\mathcal{E}^a(x, y)$ is the dual electric scalar potential as it is conjugate to the fundamental magnetic flux operator $\mathcal{W}_{\alpha\beta}(x, y)$. This leads to a duality between the loop formulation and the Kogut-Susskind link formulation. This duality can be used to define a disorder operator. This is discussed in detail in the next chapter.

3.2.3.2 *Inverse relations*

It is clear from Figure 3.11-a,b that the Kogut-Susskind link flux operators in terms of string & loop flux operators are:

$$U(x,y;\hat{1}) = \mathsf{T}^\dagger(x,y)\ \mathcal{W}(x+1,y)\ \mathcal{W}(x+1,y-1)\cdots\mathcal{W}(x+1,1)\ \mathsf{T}(x+1,y).$$
$$U(x,y;\hat{2}) = \mathsf{T}(x,y+1)\ \mathsf{T}^\dagger(x,y). \tag{3.71}$$

The Kogut-Susskind link electric fields in terms of the loop electric fields are (see appendix A for details):

$$E^a_+(x,y;\hat{1}) = R_{ab}(\mathsf{T}^\dagger(x,y))\Big[\mathcal{E}^b_-(x+1,y+1) + \mathcal{E}^b_+(x+1,y) + \underbrace{\delta_{y,0}\sum_{\bar{x}=x+2}^{\mathsf{N_s}-1}\sum_{\bar{y}=1}^{\mathsf{N_s}-1}\mathsf{L}^b(\bar{x},\bar{y})}_{\Delta^b_X(x,y)}\Big], \tag{3.72}$$

$$E^a_+(x,y;\hat{2}) = R_{ab}(\mathsf{T}^\dagger(x,y))\Big[\mathcal{E}^b_+(x+1,y+1) + R_{bc}(\mathcal{W}_{xy})\mathcal{E}^c_-(x,y+1) + \underbrace{\sum_{\bar{y}=y+2}^{\mathsf{N_s}-1}\mathsf{L}^b(x+1,\bar{y})}_{\Delta^b_Y(x,y)}\Big].$$

In (3.72) we have defined the parallel transport:

$$R_{bc}(\mathcal{W}_{xy}) \equiv R_{bc}\big(\mathcal{W}(x,1)\ \mathcal{W}(x,2)\ \cdots\mathcal{W}(x,y)\big). \tag{3.73}$$

and used: $\mathcal{E}^a_\pm(x,y=0)\equiv 0$, $\quad \mathsf{L}^a(x,y)\equiv[\mathcal{E}^a_-(x,y)+\mathcal{E}^a_+(x,y)]$. The inverse relations (3.72) and (3.73) are illustrated in Figure 5-a,b,c. On a single plaquette lattice (3.72) reduces to (3.50) as expected.

3.2.3.3 *Loop states on a finite lattice*

Like in the single plaquette case, the SU(N) Gauss law does not permit any string excitation and the $(\mathcal{N}-1)$ string operators become irrelevant. Therefore, all possible SU(N) gauge invariant operators are made up of the $\mathcal{P}$ fundamental plaquette loop operators and their conjugate electric fields. In other words, the non-trivial problem of SU(N) gauge invariance over the entire lattice reduces to the problem of residual SU(N) global invariance of $3\mathcal{P}$ loop operators, all starting and ending at the origin. Further, all $3\mathcal{P}$ loop operators gauge transform as adjoint matter fields at the origin:

$$\mathcal{W}(p)\to\Lambda\ \mathcal{W}(p)\ \Lambda^\dagger, \quad \mathcal{E}_\pm(p)\to\Lambda\ \mathcal{E}_\pm(p)\ \Lambda^\dagger. \tag{3.74}$$

In (3.74), $\Lambda = \Lambda(0,0)$ are the gauge transformations at the origin. This global invariance at the origin is fixed by the residual (N^2-1) SU(N) Gauss laws:

$$\mathcal{G}^a(0,0) = \sum_{p=1}^{\mathcal{P}} \left[\mathcal{E}^a_-(p) + \mathcal{E}^a_+(p)\right] \equiv \sum_{p=1}^{\mathcal{P}} \mathsf{L}^a(p) = 0. \tag{3.75}$$

We now solve the global Gauss law (3.75). We will use $SU(2)$ gauge theory for illustration. Generalization to $SU(N); N \geq 3$ will be briefly discussed at the end of this section. A basis in the full Hilbert space of SU(2) lattice gauge theory on a $\mathcal{P}$ plaquette lattice diagonalizing the following complete set of commuting operators (CSCO-A)

$$\text{Uncoupled basis :} \quad \left\{ \begin{array}{cccc} \vec{\mathcal{E}}_1^{\,2} & \vec{\mathcal{E}}_2^{\,2} & \cdots & \vec{\mathcal{E}}_{\mathcal{P}-1}^{\,2} & \vec{\mathcal{E}}_{\mathcal{P}}^{\,2} \\ \vec{\mathsf{L}}_1^2 & \vec{\mathsf{L}}_2^2 & \cdots & \vec{\mathsf{L}}_{\mathcal{P}-1}^2 & \vec{\mathsf{L}}_{\mathcal{P}}^2 \\ \vec{\mathsf{L}}_1^{a=3} & \vec{\mathsf{L}}_2^{a=3} & \cdots & \vec{\mathsf{L}}_{\mathcal{P}-1}^{a=3} & \vec{\mathsf{L}}_{\mathcal{P}}^{a=3} \end{array} \right\}. \qquad (CSCO-A) \tag{3.76}$$

is given by

$$\left| \begin{array}{cccc} \mathsf{n}_1 & \mathsf{n}_2 & \cdots & \mathsf{n}_{\mathcal{P}} \\ l_1 & l_2 & \cdots & l_{\mathcal{P}} \\ m_1 & m_2 & \cdots & m_{\mathcal{P}} \end{array} \right\rangle \equiv |\mathsf{n}_1\, l_1\, m_1\rangle \otimes |\mathsf{n}_2\, l_2\, m_2\rangle \cdots\cdots \otimes |\mathsf{n}_p\, l_p\, m_p\rangle. \tag{3.77}$$

Above basis is graphically illustrated in Figure 3.14-a. The state $|n\ l\ m\rangle$ corresponding to each plaquette was defined in (3.54). We are interested in constructing the physical Hilbert space $\mathcal{H}^p$ which is the $SU(2)$ invariant subspace of the above direct product Hilbert space. Under gauge transformation Λ at the origin, all states transform together as:

$$|\mathsf{n}_p\, l_p\, m_p\rangle \to \sum_{\bar{m}_p=-l_p}^{l_p} D^{\,l_p}_{m_p \bar{m}_p}(\Lambda)\ |\mathsf{n}_p\, l_p\, \bar{m}_p\rangle\,. \tag{3.78}$$

Therefore, all principal and angular momentum quantum numbers n_p, l_p are already gauge invariant. it is convenient to represent the states $|\mathsf{n}\, l\, m\rangle$ by tadpoles on every plaquette as shown in Figure 3.14-a. The tadpole loop at the top represents the flux flowing in a loop within the plaquette. The vertical stem represents the flux leakage (l,m) through the plaquette. In order to solve the Gauss law (3.75) we describe the states (3.77) in a coupled

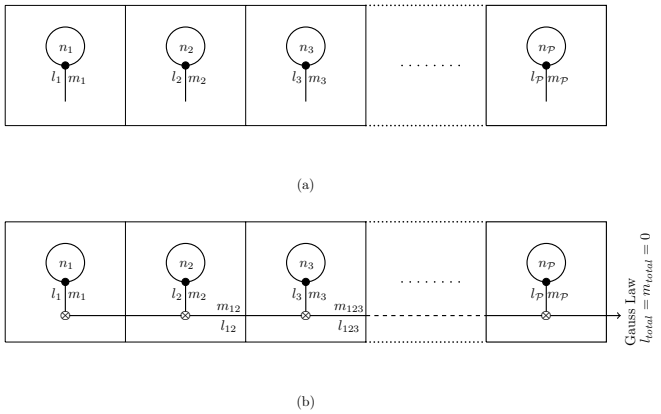

Figure 3.14: a) Uncoupled and b) Coupled loop (tadpole) basis diagonalizing CSCO-A and CSCO-B respectively given in (3.76) and (3.79). The global Gauss law is solved by putting the total angular momentum $\mathsf{L}_{total} = 0$. In (a) and (b) $\bullet$ represents the j-j coupling or contraction of j flux lines within a plaquette in (3.54) and in (b) $\otimes$ represents l-l couplings or contraction of l flux lines between neighbouring plaquettes (see eqn.(3.80)).

basis shown in Figure 3.14-b. We couple $\vec{\mathsf{L}}^a_1, \vec{\mathsf{L}}^a_2, \cdots, \vec{\mathsf{L}}^a_{\mathcal{P}}$ and go to a basis where the following complete set of commuting operators (CSCO-B) are diagonal:

$$\text{Coupled basis}: \quad \left\{ \begin{array}{cccc} \vec{\mathcal{E}}_1^{\,2} & \vec{\mathcal{E}}_2^{\,2} & \cdots \vec{\mathcal{E}}^{\,2}_{\mathcal{P}-1} & \vec{\mathcal{E}}_{\mathcal{P}}^{\,2} \\ \vec{\mathsf{L}}_1^2 & \vec{\mathsf{L}}_2^2 & \cdots \vec{\mathsf{L}}^2_{\mathcal{P}-1} & \vec{\mathsf{L}}^2_{\mathcal{P}} \\ (\vec{\mathsf{L}}_{12})^2 & (\vec{\mathsf{L}}_{123})^3 & \cdots (\vec{\mathsf{L}}_{total})^2 & \vec{\mathsf{L}}^{a=3}_{total} \end{array} \right\}. \qquad (CSCO-B) \tag{3.79}$$

Note that the total angular momentum is zero implies $(\mathsf{L}_1 + \mathsf{L}_2 + \cdots + \mathsf{L}_{\mathcal{P}-1})^2 = \mathsf{L}^2_{\mathcal{P}}$ (see Figure 3.14-b). Thus we have traded off $\mathcal{P}$ gauge non-invariant magnetic quantum numbers $(m_1, m_2, \cdots, m_{\mathcal{P}})$ in (3.77) in terms of $(\mathcal{P}-3)$ gauge invariant eigenvalues of the coupled L operators shown above. Therefore, in total there are $3(\mathcal{P}-1)$ members of the complete set of commuting operators. The resulting SU(2) gauge invariant loop basis on a lattice with $\mathcal{P}$ plaquettes is given by [12]:

$$\left| \begin{array}{cccc} \mathsf{n}_1 & \mathsf{n}_2 & \cdots & \mathsf{n}_{\mathcal{P}} \\ l_1 & l_2 & \cdots & l_{\mathcal{P}} \\ l_{12} & l_{123} & \cdots l_{total} = 0 & \end{array} \right\rangle = \left\{ |\mathsf{n}_1\ l_1\ m_1\rangle \otimes |\mathsf{n}_2\ l_2\ m_2\rangle \quad \cdots \otimes |\mathsf{n}_p\ l_p\ m_p\rangle \right\}^{l_{total}=0}_{m_{total}=0}.$$
$$= |\{\mathsf{n}\}\ \{l\}\ \{ll\}\rangle\,. \tag{3.80}$$

12 More explicitly, the states in (3.80) are:

$$|[\mathsf{n}]\ [l]\ [ll]\rangle \equiv \sum_{\{all\ m\}} \left\{ C_{l_1 m_1; l_2 m_2}^{l_{12} m_{12}}\ C_{l_{12} m_{12}; l_3 m_3}^{l_{123} m_{123}}\ C_{l_{123} m_{123}; l_4 m_4}^{l_{1234} m_{1234}} \quad \cdots C_{l_{12\cdots(p-1)} m_{12\cdots(p-1)}; l_p m_p}^{\mathbf{l_{total}=0, m_{total}=0}} \right\} \left| \begin{array}{ccc} \mathsf{n}_1 & \mathsf{n}_2 & \cdots \mathsf{n}_{\mathcal{P}} \\ l_1 & l_2 & \cdots l_{\mathcal{P}} \\ m_1 & m_2 & \cdots m_{\mathcal{P}} \end{array} \right\rangle.$$

The above loop basis will be briefly denoted by $|\{\mathsf{n}\}\ \{l\}\ \{ll\}\rangle$. The symbols $\{\mathsf{n}\}$, $\{l\}$ and $\{ll\}$ stand for the sets

- $(\mathsf{n}_1, \mathsf{n}_2, \cdots, \mathsf{n}_{\mathcal{P}})$: $\mathcal{P}$ principal quantum numbers;
- $(l_1, l_2, \cdots, l_{\mathcal{P}})$: $\mathcal{P}$ angular momentum quantum numbers and
- $(l_{12}, l_{123}, \cdots, l_{123\cdots(\mathcal{P}-1)} = l_{\mathcal{P}}, l_{123\cdots\mathcal{P}} = 0)$: $\mathcal{P}-3$ coupled angular momentum quantum numbers respectively.

These $3(\mathcal{P}-1)$ principal, angular momentum quantum numbers characterizing the loop basis are gauge invariant as is clear from the gauge transformations (3.78). As expected, this is also the number of physical degree of freedom in the original Kogut-Susskind formulation. In fact, in SU(N) Kogut-Susskind lattice gauge theory in terms of link operators, the total number of physical degrees of freedom $\mathbb{N}^d_{SU(N)}$ is given by the dimension of the quotient space $\left[\frac{\otimes_{links}\ SU(N)}{\otimes_{sites}\ SU(N)}\right]$:

$$\mathbb{N}^d_{SU(N)} = \text{Dim}\left[\frac{\otimes_{links}\ SU(N)}{\otimes_{sites}\ SU(N)}\right] = \left(N^2-1\right)\left(\mathcal{L}-\mathcal{N}\right). \tag{3.81}$$

Above, $\mathcal{L}$ and $\mathcal{N}$ are the numbers of links and sites of space lattice in d dimension.

We now discuss pure $SU(N)$, $N \geq 3$ lattice gauge theory. A $SU(N)$ tadpole state over a plaquette, analogous to the $SU(2) \otimes SU(2)$ state $|j\ m\rangle \otimes |j\ m'\rangle \sim |n\ l\ m\rangle$ in (3.54) and illustrated in Figure 3.14, is characterized by the representations of $SU(N) \otimes SU(N)$ group. These representations or equivalently orthonormal SU(N) tadpole states on each plaquette are labelled by (N^2-1) loop quantum numbers [13]. Therefore, in $d = 2$ where all $\mathcal{P}$ plaquette loops are fundamental and mutually independent, there are (N^2-1) $\mathcal{P}$ loop quantum numbers. Subtracting out global (N^2-1) degrees of freedom (or gauge transformations at the origin), we again see that there are total $(N^2-1)(\mathcal{P}-1)$ gauge invariant SU(N) loop quantum numbers. This exactly matches[14] with $\mathbb{N}^{d=2}_{SU(N)}$ in (3.81) as $(\mathcal{P}-1) = (\mathcal{L}-\mathcal{N})$ in $d = 2$.

3.2.3.4 *Loop Dynamics on finite lattice*

In this section, we discuss dynamical issues associated with the SU(N) Kogut-Susskind Hamiltonian after rewriting it in terms of the new fundamental plaquette loop operators.

13 A SU(N) irreducible representation is characterized by $(N-1)$ eigenvalues of Casimir operators and $\frac{1}{2}N(N-1)$ "SU(N) magnetic quantum numbers". As an example, the three "SU(3) magnetic quantum numbers" are the SU(2) isospin, its third component and the hypercharge. The $SU(2) \otimes SU(2)$ tadpole or hydrogen atom states $|j, m_-, m_+\rangle$ are now replaced by $|p, q, i_-, m_-, y_-, i_+, m_+, y_+\rangle$ where p, q are the common eigenvalues of the two SU(3) Casimir operators and $i_\mp, m_\mp, y_\mp$ represent their isospin, magnetic isospin and hypercharge quantum numbers respectively. These 8 quantum numbers are associated with a $SU(3) \otimes SU(3)$ tadpole diagram. Therefore, all $SU(N) \otimes SU(N)$ representations with equal Casimirs or SU(N) tadpole states are characterized by $(N-1) + N(N-1) = (N^2-1)$ quantum numbers.

14 In $d = 2$, we have $\mathcal{L} = 2(\mathsf{N}_s - 1)\mathsf{N}_s$; $\mathcal{N} = \mathsf{N}_s^2$; $\mathcal{P} = (\mathsf{N}_s - 1)^2$. Therefore, $\mathcal{L} - \mathcal{N} = \mathcal{P} - 1$.

We show that in terms of these plaquette loop operators the initial SU(N) local gauge invariance reduces to global SU(N) invariance and the loop Hamiltonian has a simple weak coupling $g^2 \to 0$ continuum limit. The Kogut-Susskind Hamiltonian [6, 8] is:

$$H = g^2 \sum_l \vec{E}_l^2 + \frac{K}{g^2} \sum_p \Big(2N - \mathrm{Tr} \Big(U_p + U_p^\dagger \Big) \Big) . \tag{3.82}$$

In (3.82) K is a constant, $l \equiv (x, y; \hat{i})$ denotes a link in $\hat{i}$ direction, p denotes a plaquette. The plaquette operator: $U_p(x,y) = U(x,y;\hat{1})\ U(x+1,y;\hat{2})\ U^\dagger(x+1,y+1;\hat{1})\ U^\dagger(x,y+1;\hat{2})$. defines the magnetic field term around a plaquette p. As mentioned earlier, we choose space dimension $d = 2$. Substituting the Kogut-Susskind electric fields in terms of the loop electric fields in (3.72), we get:

$$\begin{aligned} H = \sum_{x,y\in\Lambda} \frac{g^2}{2} \Bigg\{ & \Big[\vec{\mathcal{E}}_-(x+1,y+1) + \vec{\mathcal{E}}_+(x+1,y) + \Delta_{XY}(x,y) \Big]^2 \\ & + \Big[\vec{\mathcal{E}}_+(x+1,y+1) + R_{bc}(\mathcal{W}_{xy}) \vec{\mathcal{E}}_-^c(x,y+1) + \Delta_Y(x,y) \Big]^2 \Bigg\} \\ & + \frac{1}{2g^2} \Big(2N - (Tr\ \mathcal{W}(x,y) + h.c) \Big) \equiv g^2 \tilde{H}_E + \frac{1}{g^2} \tilde{H}_B. \end{aligned} \tag{3.83}$$

In (3.83) all operators vanish when x,y are negative or zero as plaquette loop operators are labelled by top right corner (see Figure 3.11-a). The operators $\Delta_{XY,Y}$ are defined as:

$$\Delta^a_{XY}(x,y) \equiv \delta_{y,0} \sum_{\bar{x}=x+1}^{N_s-1} \sum_{\bar{y}=1}^{N_s-1} \mathsf{L}(\bar{x},\bar{y}), \qquad \Delta^a_Y(x,y) \equiv \sum_{\bar{y}=y+1}^{N_s-1} \mathsf{L}^a(x,\bar{y}). \tag{3.84}$$

We have also used the relations: $Tr\ U_p(x,y) = Tr\ \big(\mathsf{T}^\dagger(x,y)\ \mathcal{W}(x+1,y+1)\ \mathsf{T}(x,y) \big) = Tr\ \mathcal{W}(x+1,y+1)$. The Hamiltonian (3.83) describes gauge invariant dynamics directly in terms of the bare essential, fundamental plaquette loop creation and annihilation operators without any gauge fields. As expected, the unphysical strings do not appear in the loop dynamics. There are many interesting and novel features of the Kogut-Susskind Hamiltonian (3.82) rewritten in terms of loop operators (3.83):

- There are no local SU(N) gauge degrees of freedom and at the same time there are no redundant loop operators. The (N^2-1) residual SU(N) gauge degrees of freedom in (3.74) can be removed by working in the coupled hydrogen atom basis (3.80).
- In going from links to loops ((3.82) to (3.83)), all interactions have shifted from the magnetic field part to the electric field part. Therefore, the interaction strength now is g^2 and not $\frac{1}{g^2}$.

$$H^{SU(N)}_{gauge}\big(\tfrac{1}{g^2}\big) \approx H^{SU(N)}_{spin}\big(g^2\big).$$

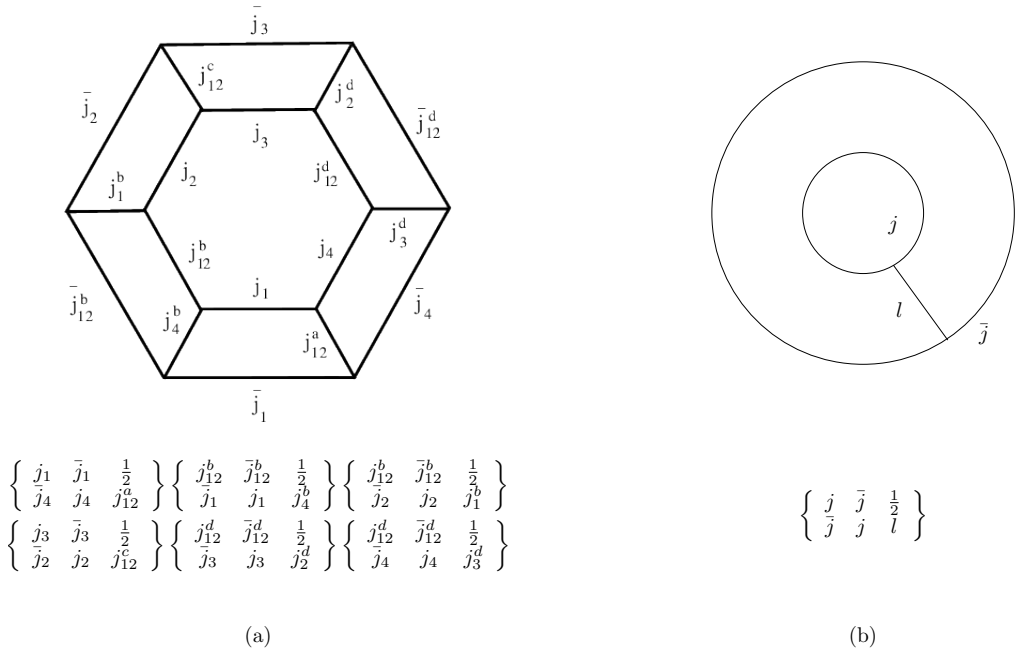

Figure 3.15: SU(2) loop dynamics in (a) prepotential approach in 2+1 dimensions (b) loop formulation based on canonical transformations clearly illustrating the resulting simplifications. The matrix elements of the plaquette operators (3.85) and (2.37) are written in terms of 6j symbols for comparison purpose.

We have used $\approx$ above to state that this equivalence is only within the physical Hilbert space $\mathcal{H}^p$. The above relation is SU(N) analogue of the Z_2 result $H^{Z_2}_{gauge}(\lambda) \approx H^{Z_2}_{spin}(\lambda^{-1})$ discussed earlier.

- The magnetic field term, dominating in the weak coupling continuum ($g^2 \to 0$) limit, acquires its simplest possible form. It creates and annihilates single electric plaquette flux loops exactly like in single plaquette case (3.63). Therefore, the loop Hamiltonian (3.83) can be used to develop a weak coupling gauge invariant loop perturbation theory near the continuum limit.

- In the tadpole basis (3.80) in SU(2) lattice gauge theory:

$$\begin{aligned} \langle \bar{\mathsf{n}}\ \bar{l}\ \bar{m}|H_B|\mathsf{n}\ l\ m\rangle &\equiv \frac{K}{g^2}\langle \bar{\mathsf{n}}\ \bar{l}\bar{m}|Tr\mathcal{W}|\mathsf{n}\ l\ m\rangle = \frac{K}{g^2}\frac{1}{\sqrt{n\ \bar{n}}}\delta_{l,\bar{l}}\delta_{m,\bar{m}}\left[\delta_{\bar{\mathsf{n}},\mathsf{n}+1}+\delta_{\bar{\mathsf{n}},\mathsf{n}-1}\right] \\ &= \frac{K'}{g^2}\left\{ \begin{matrix} j & \bar{j} & \frac{1}{2} \\ \bar{j} & j & l \end{matrix} \right\}. \end{aligned} \tag{3.85}$$

In (3.85), $\mathsf{n} = 2j+1$ and $\bar{\mathsf{n}} = 2\bar{j}+1$, $K' = K(-1)^{(2l+1-\bar{n}-n)}\sqrt{\frac{n\ \bar{n}}{(\bar{n}+n+2l+1)(\bar{n}+n-2l-1)}}$. In the second line in (3.85), we have used the explicit expression for a 6j symbol [115] with a half entry. If we put $l = 0$ in (3.85), we recover the single plaquette result (3.63). In fact, the matrix elements (3.85) in the $|n\ l\ m\rangle$ loop basis are valid in arbitrary d dimensions. This is in sharp contrast to the magnetic field term in the standard SU(2)

spin network basis[49] leading to (18-j) Wigner coefficients (2.37, Figure 2.5) in $d = 2$ and (30-j) Wigner coefficient in $d = 3$. The comparison of (3.85) and (2.37) makes it amply clear that $|n\ l\ m\rangle$ loop basis is much simpler than the spin network basis for any practical calculation especially in the weak coupling ($g^2 \to 0$) continuum limit. This is graphically depicted in Figure 3.15.

- The non local terms in the Hamiltonian, $\Delta^a_X(x,y)$, $\Delta^a_Y(x,y)$ and $R(\mathcal{W}_{xy})$ get tamed in the weak coupling limit. In weak coupling $g^2 \to 0$ limit, the relations (2.12) imply:

$$\mathsf{L}^a(x,y) = \mathcal{E}^a_-(x,y) + \mathcal{E}^a_+(x,y) \sim 0 + O(g).$$

Therefore, $\Delta^a_X(x,y) \sim 0$, $\Delta^a_Y(x,y) \sim 0$. Further, $R_{ab}(\mathcal{W}_{xy}) \sim \delta_{ab}$. This leads to a simplified local effective Hamiltonian H_{spin} which may describe pure SU(N) gauge theory at low energies, sufficiently well.

$$\begin{aligned} H_{spin} &= \frac{g^2}{2}\left[\sum_{p=1}^{\mathcal{P}} 4\vec{\mathcal{E}}^{\,2}(p) + \sum_{\langle p,p'\rangle} \vec{\mathcal{E}}_-(p)\cdot\vec{\mathcal{E}}_+(p')\right] + \frac{1}{2g^2}\left[2N - (Tr\mathcal{W}(p) + h.c)\right] + g^3\delta H \\ &\equiv \frac{g^2}{2}\tilde{H}'_E + \frac{1}{2g^2}\tilde{H}_B. \end{aligned} \tag{3.86}$$

In (3.86), $\sum_{<pp'>}$ denotes summation over nearest neighbour plaquette loop electric fields. The non-localities occur in the higher order terms in the coupling. Therefore, these terms, collectively denoted by $g^3\ \delta H$ in (3.86), can be ignored in the weak coupling limit as a first approximation. The SU(N) gauge theory Hamiltonian in the loop picture now reduces to SU(N) spin model Hamiltonian with nearest neighbour interactions. This simple spin Hamiltonian has the same global SU(N) symmetry, dynamical variables as the Hamiltonian in (3.83). Note that the elementary and important $1/g^2$ magnetic field terms (see (3.85)) are left intact and need to be treated exactly. In fact, this is an interesting model in its own right to explore confinement and the spectrum in the weak coupling continuum limit. These issues will be investigated in the future.

3.3 CANONICAL TRANSFORMATIONS IN 3 + 1 D

3.3.1 *Z_2 lattice gauge theory*

The method of constructing a loop formulation of Z_2 lattice gauge theory by a series of canonical transformations can be easily generalized to a lattice of any dimensions. To illustrate this, we will briefly describe the canonical transformations leading to a loop formulation of Z_2

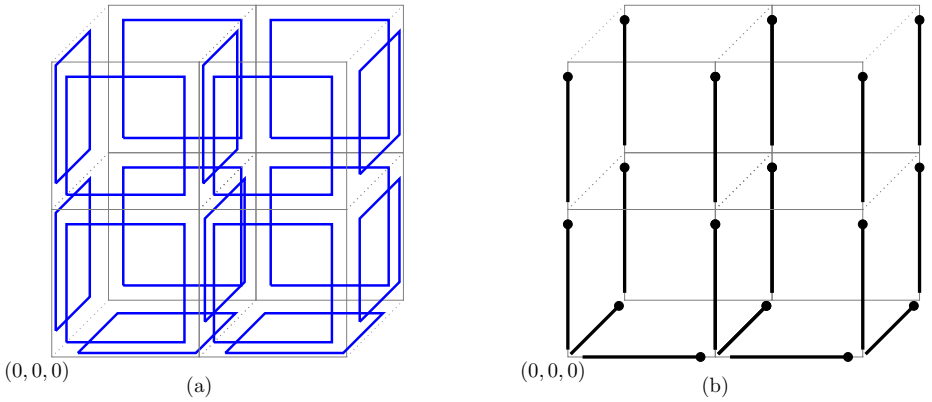

Figure 3.16: The final operators after Z_2 canonical transformations in a 3 dimensional spatial lattice: (a) plaquette loop operators (b) string operators.

gauge theory on a 3 dimensional spatial lattice. The details of the canonical transformations will be illustrated on a single cube in Appendix A.

We start with the conjugate pairs $\{\sigma_1, \sigma_3\}$ on the $\mathcal{L} = 3(N_s - 1)N_s^2$ links on a lattice with N_s sites along x,y and z direction. After a series of canonical transformations, we transform these operators to

1. a) $(N_s - 1)^2$ plaquette operator pairs $\{\mu_1(x, y, 0; \hat{3}), \mu_3(x, y, 0; \hat{3})\}$ corresponding to the plaquettes in the $z = 0$ plane.

   b) $N_s(N_s - 1)^2$ plaquette operator pairs $\{\mu_1(x, y, z; \hat{2}), \mu_3(x, y, z; \hat{2})\}$ corresponding to the plaquettes in the XZ planes.$\hat{2}$ denotes that the plaquettes are in XZ plane (i.e, perpendicular to the $\hat{2}$ direction).

   c) $N_s(N_s - 1)^2$ plaquette operator pairs $\{\mu_1(x, y, z; \hat{1}), \mu_3(x, y, z; \hat{1})\}$ corresponding to the plaquettes in the YZ planes.

2. a) $N_s - 1$ string operators $\{\bar{\sigma}_1(x, 0, 0; \hat{1}), \bar{\sigma}_3(x, 0, 0; \hat{1})\}$ corresponding to the links along the $(y = 0, z = 0)$ line.

   b) $N_s^2(N_s - 1)$ string operators $\{\bar{\sigma}_1(x, y, z; \hat{3}), \bar{\sigma}_3(x, y, z; \hat{3})\}$ corresponding to the links in the $\hat{3}$ direction.

   c) $N_s(N_s - 1)$ string operators $\{\bar{\sigma}_1(x, y, 0; \hat{2}), \bar{\sigma}_3(x, y, 0; \hat{2})\}$ corresponding to the links in the $\hat{2}$ direction in the $z = 0$ plane.

The above operators are illustrated in Figure 3.16. It can be verified that the total number of plaquette and string operators exactly equals the total number of link operators we started with.

The construction of the above string and plaquette operators is done through the following canonical transformation steps.

1. Repeat the canonical transformations corresponding to the 2 dimensional lattice on the $z = 0$ plane to get $N_s^2 - 1$ string operators and $(N_s - 1)^2$ plaquette operators.

2. Repeat the plaquette canonical transformations defined in eqn.(3.20) and eqn.(3.21) along each plaquettes on the XZ and YZ plane starting from the plaquette $(x, y, \mathsf{N}_s; \hat{1})$ to $(x, y, 1; \hat{1})$ and $(x, y, \mathsf{N}_s; \hat{2})$ to $(x, y, 1; \hat{2})$. This leads to $2\mathsf{N}_s(\mathsf{N}_s - 1)^2$ plaquette conjugate pairs corresponding to all the plaquettes in the YZ and XZ plane.

The details of the above canonical transformations are illustrated on a single plaquette which contains all the features of the finite lattice construction in appendix A.

The plaquette loop operators when written in terms of link operators are given by:

$$\begin{gathered}
\mu_3(x, y, 0; \hat{3}) = \prod_{\bar{y}=y}^{\mathsf{N}_s-1} \prod_{\bar{z}=1}^{\mathsf{N}_s-1} \sigma_1(x-1, \bar{y}, \bar{z}, \hat{1}), \\
\mu_1(x, y, 0; \hat{3}) = \sigma_3(x-1, y-1, 0, \hat{1})\sigma_3(x, y-1, 0, \hat{2})\sigma_3(x-1, y, 0, \hat{1})\sigma_3(x-1, y-1, 0, \hat{2}), \\
\mu_3(x, y, z; \hat{1}) = \prod_{\bar{z}=z}^{\mathsf{N}_s-1} \sigma_1(x, y-1, \bar{z}, \hat{2}), \\
\mu_1(x, y, z; \hat{1}) = \sigma_3(x, y-1, z-1, \hat{2})\sigma_3(x, y, z-1, \hat{3})\sigma_3(x, y-1, z, \hat{2})\sigma_3(x, y-1, z-1, \hat{3}), \\
\mu_3(x, y, z; \hat{2}) = \prod_{\bar{z}=z}^{\mathsf{N}_s-1} \sigma_1(x-1, y, \bar{z}, \hat{1}), \\
\mu_1(x, y, z; \hat{2}) = \sigma_3(x-1, y, z-1, \hat{1})\sigma_3(x, y, z-1, \hat{3})\sigma_3(x-1, y, z, \hat{1})\sigma_3(x-1, y, z-1, \hat{3}).
\end{gathered} \tag{3.87}$$

The string operators in terms of link operators are given by :

$$\begin{gathered}
\bar{\sigma}_1(x, 0, 0, \hat{1}) = \prod_{\bar{y}=0}^{\mathsf{N}_s-1} \prod_{\bar{z}=0}^{\mathsf{N}_s-1} \sigma_1(x-1, \bar{y}, \bar{z}; \hat{1})\sigma_1(x, \bar{y}, \bar{z}; \hat{2})\sigma_1(x-1, \bar{y}, \bar{z}; \hat{2}) = \prod_{\bar{x}=1}^{x-1} \prod_{\bar{y}=0}^{\mathsf{N}_s-1} \prod_{\bar{z}=0}^{\mathsf{N}_s-1} \mathcal{G}(\bar{x}, \bar{y}, \bar{z}), \\
\bar{\sigma}_3(x, y, 0, \hat{2}) = \sigma_3(x-1, y, 0, \hat{2}),
\end{gathered}$$

$$\bar{\sigma}_1(x, y, 0, \hat{2}) = \prod_{\bar{y}=y}^{\mathsf{N}_s-1} \prod_{\bar{z}=0}^{\mathsf{N}_s-1} \sigma_1(x, y-1, \bar{z}; \hat{2})\sigma_1(x, \bar{y}, \bar{z}; \hat{1}) = \prod_{\bar{y}=y}^{\mathsf{N}_s-1} \prod_{\bar{z}=0}^{\mathsf{N}_s-1} \mathcal{G}(x, \bar{y}, \bar{z}), \tag{3.88}$$

$$\bar{\sigma}_3(x, y, z, \hat{3}) = \sigma_3(x, y, z-1, \hat{3}),$$

$$\bar{\sigma}_1(x, y, z, \hat{3}) = \prod_{\bar{z}=z}^{\mathsf{N}_s-1} \sigma_1(x, y, \bar{z}; \hat{1})\sigma_1(x, y, \bar{z}; \hat{2})\sigma_1(x-1, y, \bar{z}; \hat{1})\sigma_1(x, y-1, \bar{z}; \hat{2}) = \prod_{\bar{z}=z}^{\mathsf{N}_s-1} \mathcal{G}(x, y, \bar{z}). \tag{3.89}$$

As is clear from the eqn. (3.89), the string electric field $\bar{\sigma}_1$ operators gets frozen to 1 in the physical Hilbert space H^p due to local Gauss laws. Therefore, string operators decouple just like in $2+1$ dimensions. However, in $3+1$ dimensions unlike $2+1$ dimensions, not all plaquette loops are independent. Canonical transformations automatically lead to all mutually independent and complete set of loop operators. Therefore, canonical transformations does not lead to plaquette operators on $z = 1, 2 \cdots (\mathsf{N}_s - 1)$ planes.

3.3.2 *SU(N) lattice gauge theory*

We now briefly discuss canonical transformations leading to a loop formulation of SU(N) lattice gauge theory in $3+1$ dimensions. It can be easily generalized to a lattice of any dimensionality. The series of canonical transformations bypasses the issues of Mandelstam as well as Bianchi identity constraints[116, 117]. This is not surprising as the number of degrees of freedom after the canonical transformations equals the number of physical degrees of freedom modulo a global Gauss law constraints at the origin. This is discussed in section (3.3.2.3).

We repeat $d = 2$ canonical transformations on the $z = 0$ plane and then extent the string operators $\mathsf{T}(x, y, z = 0)$ in the z directions to construct plaquette loops in xz and yz planes as shown in Figure 3.17. Thus the canonical transformations already convert all horizontal links on (xy) planes at $z \neq 0$ in forming plaquette loops in the perpendicular (xz) and (yz) planes. Therefore, there are no fundamental xy plaquette loops on $z = 1, 2, \cdots (\mathsf{N}_s - 1)$ surfaces. These surfaces are shown as shaded planes in Figure 3.17. Therefore, canonical transformations transform the link operators on a 3 dimensional lattice to the following operators:

1. $(\mathsf{N}_s)^3 - 1$ string operators $\mathsf{T}(x, y, z)$ starting from $(0, 0, 0)$ and ending at $(x, y, z) \neq (0, 0, 0)$. These operators takes the path[15] $(0, 0, 0) \to (x, 0, 0) \to (x, y, 0) \to (x, y, z)$. This is illustrated in Figure 3.17. Their conjugate left(right) electric fields are denoted as $\mathsf{E}^a_-(x, y, z)\big(\mathsf{E}^a_+(x, y, z)\big)$.

2. $2(\mathsf{N}_s + 1)(\mathsf{N}_s - 1)^2$ independent plaquette loop operators $\mathcal{W}(x, y, z, \hat{1})$, $\mathcal{W}(x, y, z, \hat{2})$, $\mathcal{W}(x, y, 0)$; $x, y, z = 1, 2, \cdots (\mathsf{N}_s - 1)$. Here, $\mathcal{W}(x, y, z, \hat{i})$ denotes a plaquette loop operator on a plane perpendicular to $\hat{i}$ with (x, y, z) being the top right corner[16] of the plaquette. Their conjugate left(right) electric fields are denoted as $\mathcal{E}^a_-(x, y, z, \hat{i})\big(\mathcal{E}^a_+(x, y, z, \hat{i})\big)$.

3.3.2.1 *Canonical relations*

The final string and plaquette loop operators mentioned above is related to the initial Kogut-Susskind link operators as follows:

$$\mathsf{T}(x, y, z) = \prod_{\bar{x}=0}^{x} U(\bar{x}, 0, 0) \prod_{\bar{y}=0}^{y} U(x, \bar{y}, 0) \prod_{\bar{z}=0}^{z} U(x, y, \bar{z}). \tag{3.90}$$

15 This is a matter of convention. There exist other series of canonical transformations which leads to string operators to sites $(x, y, z) \neq (0, 0, 0)$ which follows a different path.

16 The top right corner of a plaquette is defined as the point (x', y', z') on the plaquette with the largest $(x' + y' + z')$.

$$\mathcal{W}(x,y,z,\hat{1}) = \mathsf{T}(x,y,z)U(x,y,z,\hat{2})U(x,y+1,z,\hat{3})U^\dagger(x,y,z+1,\hat{2})U^\dagger(x,y,z,\hat{3}),$$
$$\mathcal{W}(x,y,z,\hat{2}) = \mathsf{T}(x,y,z)U(x,y,z,\hat{1})U(x+1,y,z,\hat{3})U^\dagger(x,y,z+1,\hat{1})U^\dagger(x,y,z,\hat{3}),$$
$$\mathcal{W}(x,y,0,\hat{3}) = \mathsf{T}(x,y,0)U(x,y,0,\hat{1})U(x+1,y,0,\hat{2})U^\dagger(x,y+1,0,\hat{1})U^\dagger(x,y,0,\hat{2}). \tag{3.91}$$

The conjugate string and plaquette loop right electric fields in terms of Kogut-Susskind electric fields are :

$$\begin{aligned}
\mathsf{E}^a_+(x,y,z) &= \mathcal{G}^a(x,y,z),\\
\mathcal{E}^a_+(x,y,z,\hat{1}) &= -\sum_{z'=z}^{\mathsf{N}_s-1} R_{ab}(S_x(x,y,z,z'))E^b_-(x,y,z',\hat{1}),\\
\mathcal{E}^a_+(x,y,z,\hat{2}) &= -\sum_{z'=z}^{\mathsf{N}_s-1} R_{ab}(S_y(x,y,z,z'))E^b_-(x,y,z',\hat{2}),\\
\mathcal{E}^a_+(x,y,0,\hat{3}) &= -\sum_{z'=z}^{\mathsf{N}_s-1} R_{ab}(S_x(x,y,z,z'))E^b_-(x,y,z',\hat{1}) - \sum_{y'=y}^{\mathsf{N}_s-1} R_{ab}(S(x,y,y'))E^b_-(x,y',0,\hat{1}).
\end{aligned} \tag{3.92}$$

Above,

$$S_x(x,y,z,z') \equiv \mathsf{T}(x-1,y,z)U(x-1,y,z,\hat{1})\prod_{\bar{z}=z}^{z'} U(x,y,\bar{z},\hat{3}),$$

$$S_y(x,y,z,z') \equiv \mathsf{T}(x,y-1,z)U(x,y-1,z,\hat{2})\prod_{\bar{z}=z}^{z'} U(x,y,\bar{z},\hat{3}),$$

$$S_x(x,y,y') \equiv \mathsf{T}(x-1,y,0)U(x-1,y,0,\hat{1})\prod_{\bar{y}=y}^{y'} U(x,\bar{y},0,\hat{2}).$$

String electric fields vanishes due to Gauss laws leading to the decoupling of string operators from the physical Hilbert space. The only xy plaquette created are those on the $z = 0$ plane.

3.3.2.2 *Inverse relations*

The link operators in terms of plaquette and string operators are given as follows:

$$\begin{aligned}
U(x,y,z;\hat{1}) &= \mathsf{T}^\dagger(x,y,z)\left[\prod_{\bar{z}=1}^{z}\mathcal{W}^\dagger(x+1,y,\bar{z},\hat{2})\right]\mathsf{T}(x+1,y,z),\\
U(x,y,z;\hat{2}) &= \mathsf{T}^\dagger(x,y,z)\left[\prod_{\bar{z}=1}^{z}\mathcal{W}^\dagger(x,y+1,\bar{z},\hat{1})\right]\mathsf{T}(x,y+1,z),\\
U(x,y,z;\hat{3}) &= \mathsf{T}(x,y,z+1)\mathsf{T}^\dagger(x,y,z).
\end{aligned} \tag{3.93}$$

The corresponding conjugate link electric field in terms of plaquette electric field:

$$E^a_+(x,y,z;\hat{1}) = R_{ab}(\mathsf{T}(x,y,z))\Bigg(\mathcal{E}^b_-(x+1,y,z+1,\hat{2}) + \mathcal{E}^b_+(x+1,y,z,\hat{2}) + \delta_{z0}\Big[\mathcal{E}^b_-(x+1,y+1,0,\hat{3}) + \mathcal{E}^b_+(x+1,y,0,\hat{3})\Big] + \delta_{z0}\delta_{y0}\Big[\sum_{\bar{z}=1}^{\mathsf{N}_s-1}\sum_{\bar{y}=1}^{\mathsf{N}_s-1}\sum_{\bar{x}=x+2}^{\mathsf{N}_s-1}\{\mathsf{L}^b(\bar{x},\bar{y},\bar{z},\hat{1}) + \mathsf{L}^b(\bar{x},\bar{y},\bar{z},\hat{2})\} + \sum_{\bar{y}=1}^{\mathsf{N}_s-1}\sum_{\bar{x}=x+2}^{\mathsf{N}_s-1}\mathsf{L}^b(\bar{x},\bar{y},0,\hat{3})\Big]\Bigg). \tag{3.94}$$

$$E^a_+(x,y,z;\hat{2}) = R_{ab}(\mathsf{T}(x,y,z))\Bigg(\mathcal{E}^b_-(x,y+1,z+1,\hat{1}) + \mathcal{E}_+(x,y+1,z,\hat{1}) + \delta_{z0}\Big[\sum_{\bar{y}=y+2}^{\mathsf{N}_s-1}\mathsf{L}^b(x+1,\bar{y},0,\hat{3}) + \sum_{\bar{y}=y+2}^{\mathsf{N}_s-1}\sum_{\bar{z}=1}^{\mathsf{N}_s-1}\{\mathsf{L}^b(x,\bar{y},\bar{z},\hat{1}) + \mathsf{L}^b(x+1,\bar{y},\bar{z},\hat{2})\} + \mathcal{E}^b_+(x+1,y+1,0,\hat{3}) + R_{ab}\Big(\prod_{\bar{y}=1}^{y}\mathcal{W}(x,\bar{y},0,\hat{3})\Big)\mathcal{E}^b_-(x,y+1,0,\hat{3})\Big]\Bigg). \tag{3.95}$$

$$E^a_+(x,y,z;\hat{3}) = R_{ab}(\mathsf{T}(x,y,z))\Bigg[\sum_{\bar{z}=z+2}^{\mathsf{N}_s-1}\Big\{\mathsf{L}^b(x,y+1,\bar{z},\hat{1}) + \mathsf{L}^b(x+1,y,\bar{z},\hat{2})\Big\} + \mathcal{E}^b_+(x,y+1,z+1,\hat{1}) + \mathcal{E}^b_+(x+1,y,z+1,\hat{2}) + R_{ab}\Big(\prod_{z'=1}^{z}\mathcal{W}(x-1,y,z',\hat{2})\Big)\mathcal{E}^b_-(x,y,z+1,\hat{2}) + R_{ab}\Big(\prod_{z'=1}^{z}\mathcal{W}(x,y-1,z',\hat{1})\Big)\mathcal{E}^b_-(x,y,z+1,\hat{1})\Bigg]. \tag{3.96}$$

The xy plaquettes $\mathcal{W}(x,y,z,\hat{3}); z \neq 0$ are not created. This is because they are not independent and can be written in terms of the other plaquette variables as follows:

$$\mathcal{W}(x,y,z,\hat{3}) = \prod_{\bar{z}=0}^{z}\mathcal{W}(x,y-1,\bar{z},\hat{2})\prod_{\bar{z}=0}^{z}\mathcal{W}(x,y,\bar{z},\hat{1})\prod_{\bar{z}=0}^{z}\mathcal{W}(x,y,\bar{z},\hat{2})\prod_{\bar{z}=0}^{z}\mathcal{W}(x-1,y,\bar{z},\hat{1}). \tag{3.97}$$

3.3.2.3 *Bianchi identity on a 3D lattice*

The SU(N) Bianchi identity on a lattice [116, 117] is given by

$$\mathcal{W}(b)\mathcal{W}(c)\mathcal{W}(d)\mathcal{W}(e)\mathcal{W}(f)\mathcal{W}^\dagger(g) = 1. \tag{3.98}$$

Above, $\mathcal{W}(b), \mathcal{W}(c), \mathcal{W}(d), \mathcal{W}(e), \mathcal{W}(f), \mathcal{W}^\dagger(g)$ are the plaquette loop operators along the faces of a cube, as shown in Figure 3.17.

As explained earlier, the canonical transformation steps do not create the loop operators corresponding to (xy) plaquette loops at $z \neq 0$. In fact, these plaquette loops can be written in terms of the fundamental plaquette loops in (xz) and (yz) planes as shown in eqn.(3.97)

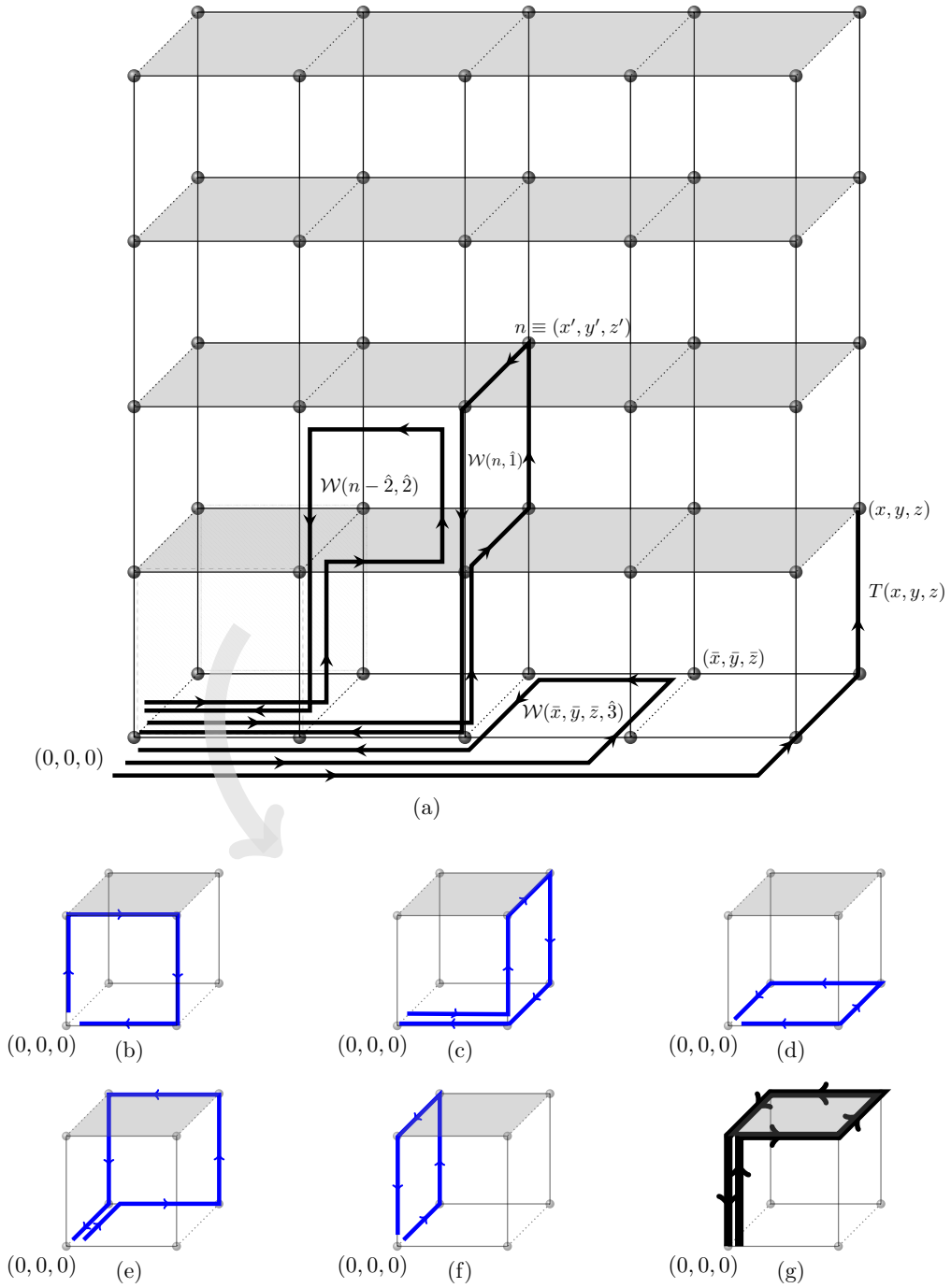

Figure 3.17: (a) Graphical representation of the fundamental plaquette operators and the string operators obtained by canonical transformations in $d = 3$. The shaded horizontal plaquettes are not obtained by canonical transformations as explained in the text. They are also not independent: the shaded plaquette operator in (g) is the product of the fundamental plaquette loop operators in (b), (c), (d), (e), (f) in that order. This is just the SU(N) Bianchi identity on lattice.

and illustrated in Figure 3.17-b,c,d,e,f,g. Therefore, the loop operators automatically satisfy Bianchi identity constraints (3.98). This way the canonical transformations also bypass the problem of SU(N) Bianchi identity constraints confronted in the loop formulation of SU(N) lattice gauge theories [116, 117] in any dimension $d \geq 3$. In $d = 3$, we have the number of sites $\mathcal{N} = (\mathsf{N}_s)^3$, number of links $\mathcal{L} = 3(\mathsf{N}_s - 1)\mathsf{N}_s^2$ and number of plaquettes $\mathcal{P} = 3(\mathsf{N}_s - 1)^2\mathsf{N}_s$. The total number of (xy) plaquettes is $\mathcal{P}_{xy} \equiv \frac{\mathcal{P}}{3} = (\mathsf{N}_s - 1)^2\mathsf{N}_s$. The number of (xy) plaquette at $z = 0$ plane is $\mathcal{P}_{xy}(z = 0) = \frac{\mathcal{P}_{xy}}{\mathsf{N}_s} = (\mathsf{N}_s - 1)^2$. Therefore, the number of dependent (xy) plaquettes $\mathcal{P}_{xy}(z \neq 0) = \mathcal{P}_{xy} - \mathcal{P}_{(xy)}(z = 0) = (\mathsf{N}_s - 1)^3 \equiv$ the number of Bianchi identities. Hence the number of independent SU(N) loop quantum numbers after subtracting $(N^2 - 1)$ gauge degrees of freedom at the origin $= \left(N^2 - 1\right)\ \left(\mathcal{P} - \mathcal{P}_{xy}(z \neq 0) - 1\right) = \left(N^2 - 1\right)\ (\mathcal{L} - \mathcal{N}) = \mathbb{N}^{d=3}_{SU(N)}$. This is again an expected result because the canonical transformations used for converting links into (physical) loops & (unphysical) strings can not introduce any spurious degrees of freedom in any dimension. Therefore, the SU(N) plaquette loop operators are mutually independent and contain complete physical information.

3.3.3 *Loop Hilbert space and SU(N) loop dynamics*

The construction of a basis of the physical Hilbert space $\mathcal{H}^p$ is done essentially as in $2 + 1$ dimensions by constructing tadpole states corresponding to the plaquette loop operators constructed by canonical transformations and coupling them together to find states satisfying $\sum_p \mathsf{L}^a(p) = 0$. The only difference stems from the fact that since canonical transformations do not create the plaquette operators $\mathcal{W}(x, y, z, \hat{3}); z \neq 0$, there are no tadpole states corresponding to these plaquettes. The corresponding SU(N) coupled tadpole basis is orthonormal as well as complete in $\mathcal{H}^p$ bypassing all non-trivial and notorious SU(N) Mandelstam or Bianchi identity constraints.

The Hamiltonian of pure SU(N) gauge theory in terms of independent plaquette loop operators and conjugate electric fields in $3 + 1$ dimensions is given by :

$$H = \frac{g^2}{2}\Big[E^a_+(x, y, z, \hat{1})E^a_+(x, y, z, \hat{1}) + E^a_+(x, y, z, \hat{2})E^a_+(x, y, z, \hat{2}) + E^a_+(x, y, z, \hat{3})E^a_+(x, y, z, \hat{3})\Big] + \frac{1}{2g^2}\Big[2N - Tr\Big\{\mathcal{W}(x, y, z, \hat{1}) + \mathcal{W}(x, y, z, \hat{2}) + \mathcal{W}(x, y, z, \hat{3}) + \ h.c\Big\}\Big]. \tag{3.99}$$

Above, $E^a_+(x, y, z, \hat{1})$, $E^a_+(x, y, z, \hat{2})$, $E^a_+(x, y, z, \hat{3})$ and $\mathcal{W}(x, y, z, \hat{3}); z \neq 0$ is given by equations (3.94), (3.95), (3.96) and (3.97) respectively. These 4 terms are non local. The essential difference from the $2 + 1$ dimensional case is that here both the electric and magnetic part, H_B and H_E, are non-local. However, the magnetic part can be made local by introducing the $\mathcal{W}(x, y, z, \hat{3}); z \neq 0$ operators as fundamental operators satisfying the Bianchi identity con-

straints. As $g^2 \to 0$, $\mathsf{L}^a \approxeq 0 + O(g)$. Therefore, a useful local, effective Hamiltonian that may describe SU(N) lattice gauge theory at low energies is given by

$$H = \frac{g^2}{2}\Big[\sum_p \mathcal{E}^2(p) + \sum_{\langle p,p'\rangle} \mathcal{E}^a_-(p)\mathcal{E}^a_-(p')\Big] + \frac{1}{2g^2}\Big[2N - Tr\Big\{\sum_{i=1}^{3} \mathcal{W}(x,y,z,\hat{i}) + \ h.c\Big\}\Big]. \tag{3.100}$$

Above, $\langle p, p'\rangle$ denotes that p and p' are nearest neighboring plaquettes.

4

CANONICAL TRANSFORMATIONS, DUALITY & ORDER-DISORDER

In this chapter we show that the canonical transformations leading to the loop formulation of SU(N) lattice gauge theory in $(2+1)$ dimensions in the previous chapter can also be interpreted as SU(N) duality transformation. We note that the original Kogut-Susskind Hamiltonian (3.82) is in terms of SU(N) electric vector fields and their conjugate holonomies $\{E^a(l); U_{\alpha\beta}(l)\}$ on each link l. The electric fields satisfy local Gauss law constraints. We now show that the equivalent SU(N) loop Hamiltonian (3.83) is in terms of the SU(N) magnetic fields and their conjugate scalar electric potentials. The local Gauss law constraints are trivially solved in the dual representation. All dual (loop) fields are defined on plaquettes and are scalars in $(2+1)$ dimensions. The same interpretation also holds for the much simpler Z_2 lattice gauge theory in $(2+1)$ dimensions. The canonical transformations in Z_2 lattice gauge theory solve the Z_2 Gauss law constraints leading to loop formulation described by the Ising model Hamiltonian (3.32). This Ising model is in terms of Z_2 magnetic fields and their conjugate electric scalar potentials. In fact, this is the well known Z_2 gauge-spin duality found by Franz Wegner in 1971 [55]. Wegner was strongly influenced and motivated by the self duality of Ising model in lower $(1+1)$ dimensions found by Kramers and Wannier [118] in 1941. We show that the SU(N) canonical transformations discussed in the last chapter can also be used to obtain Kramers-Wannier duality.

In general, a duality transformation relates model at a strong coupling or high temperature to another model at weak coupling or low temperature. Therefore, they are useful to understand theories and their phases better using alternative dual descriptions. They often expose the hidden topological degrees of freedom relevant for determining the properties of the system [7, 119]. The classic examples are the two dimensional x-y model and compact abelian lattice gauge theories [119]. Another general and important feature of these dualities is that the dual theory is expressed in terms of 'disorder variables' which are given by a non-local combination of the original variables. These dual variables have small fluctuations at regions where the original variables have large fluctuations [120]. Therefore, dual models are useful in studying the large fluctuation region of the original theory which is usually inaccessible by other methods [120]. In gauge theories, phase transitions cannot be characterized by local order parameters [121]. But, often the dual theories can have local order parameters which acts as a non-local disorder parameter [56, 122] for the original theories. In fact, such alternative dual descriptions have been extensively discussed in the past in the context of abelian [7, 55, 56, 118–137] and non-abelian gauge theories [3, 14, 120, 138–145].

In this chapter, using canonical transformations discussed in the last chapter, we systematically obtain Kramers-Wannier as well as Wegner duality in $(1+1)$ dimensional Ising model and $(2+1)$ dimensional Ising gauge theory respectively. These Z_2 duality transformations are used to define disorder operators in the corresponding models. These dual descriptions and results are well known and have been extensively discussed in the review papers [7, 120, 122]. We then generalize these Z_2 results to SU(N) lattice gauge theory in $(2+1)$ dimensions.

The organization of this chapter is as follows. In section 4.1, working within the Hamiltonian formulation, we show that the canonical transformations, discussed in the last chapter, also provide a systematic way to obtain the old and well known Kramers-Wannier duality [118] in $(1+1)$ dimensional Ising model. We end the section with a discussion on order-disorder operators. In section 4.2, we then interpret the loop formulations of $(2+1)$ dimensional Z_2 lattice gauge theory obtained in the last chapter as the dual formulation in terms of Z_2 magnetic fields and their conjugate Z_2 electric scalar potential. This is the famous Wegner gauge-spin duality with electric scalar potentials playing the role of Ising spins. Again order and disorder operators are discussed in this simplest Z_2 lattice gauge theory. In section 4.3, we then show that the loop formulation of SU(N) lattice gauge theories is dual to the Kogut- Susskind formulation of SU(N) lattice gauge theory. *This is a non-abelian generalization of Z_2 Wegner's duality*. Further, the SU(N) duality enables us to define a new SU(N) disorder operator in section 4.3. As expected, it's construction is a nonabelian generalization of the disorder operator in Z_2 lattice gauge theory.

4.1 ISING MODEL & KRAMERS WANNIER DUALITY

In this section, we construct the canonical transformations leading to the famous Kramers-Wannier self duality of quantum Ising model in $1+1$ dimensions. The kinematical variables of the $1+1$ dimensional quantum Ising model [56] are $\{\sigma_1(x), \sigma_3(x)\}$. In Figure 4.1, these operators are represented over links of the lattice for visual convenience[1]. The σ operators satisfy the following relations:

$$\sigma_1^2(x) = 1\ ;\ \sigma_3^2(x) = 1; \quad \sigma_1(x)\sigma_3(x) = -\sigma_3(x)\sigma_1(x) \ \text{ or } \ [\sigma_1(x), \sigma_3(x)]_+ = 0. \tag{4.1}$$

The $(1+1)$-D Ising model [56] Hamiltonian is

$$H \ = \ \sum_{x=0}^{\infty} \Big[-\sigma_1(x) - \lambda\ \sigma_3(x)\sigma_3(x+1) \Big]. \tag{4.2}$$

We now start the link operator pairs $\{\sigma_1(x), \sigma_3(x)\}$ on a 1 dimensional lattice and convert them iteratively into a new (dual) set $\{\mu_1(x), \mu_3(x)\}$ using canonical transformations. This is

1 Each link should be thought of as representing the starting lattice site of the link.

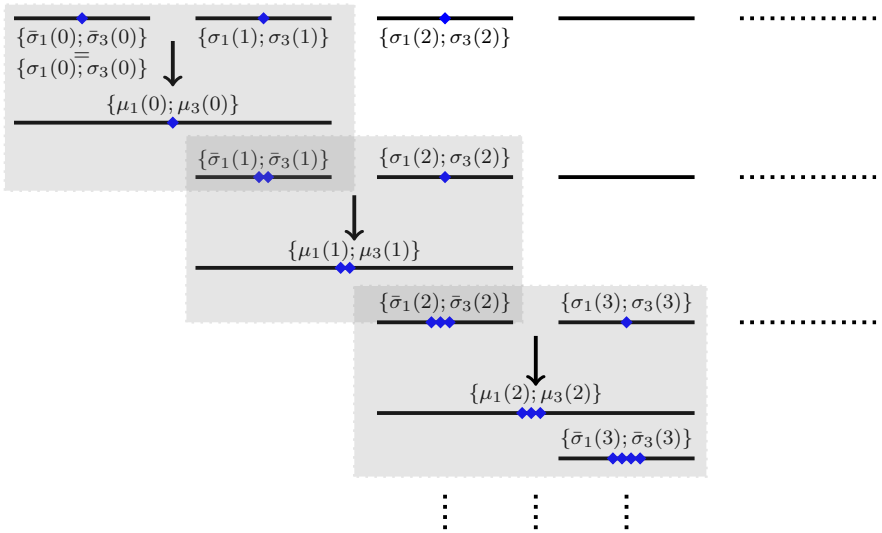

Figure 4.1: Kramers-Wannier duality through canonical transformations. The first three steps of duality or canonical transformations (4.6) are explicitly illustrated.

shown in Figure 4.1. We first perform canonical transformations from the first two conjugate pairs $\{\sigma_1(0),\sigma_3(0)\}$, $\{\sigma_1(1),\sigma_3(1)\}$ attached to the first two links to a new set of conjugate pairs $\{\mu_1(0),\mu_3(0)\}$ and $\{\bar{\sigma}_1(1),\bar{\sigma}_3(1)\}$:

$$\begin{aligned} \mu_1(0) &\equiv \sigma_3(0)\sigma_3(1); & \bar{\sigma}_3(1) &\equiv \sigma_3(1); \\ \mu_3(0) &= \sigma_1(0); & \bar{\sigma}_1(1) &= \sigma_1(0)\sigma_1(1). \end{aligned} \tag{4.3}$$

The canonical transformation (4.3) is illustrated in the first shaded box on the left in Figure 4.1. Note that the two new canonical sets are conjugate and mutually independent.

$$\begin{aligned} [\mu_1(0),\mu_3(0)]_+ &= 0, & [\bar{\sigma}_1(1),\bar{\sigma}_3(1)]_+ &= 0, \\ [\mu_a(0),\bar{\sigma}_b(1)] &= 0; \quad a,b = 1,3. \end{aligned} \tag{4.4}$$

Further,

$$\mu_1(0)^2 = 1, \quad \mu_3(0)^2 = 1, \quad \bar{\sigma}_1(1)^2 = 1, \quad \bar{\sigma}_3(1)^2 = 1.$$

The conjugate pair $\{\bar{\sigma}_1(1),\bar{\sigma}_3(1)\}$ are the intermediate operators to be traded off with $\{\mu_1(1),\mu_3(1)\}$ at the next step.

We now repeat the canonical transformation with $\{\sigma_1(0),\sigma_3(0)\}$, $\{\sigma_1(1),\sigma_3(1)\}$ replaced by $\{\bar{\sigma}_1(1),\bar{\sigma}_3(1)\}$ and $\{\sigma_1(2),\sigma_3(2)\}$ to give the conjugate pairs $\{\mu_1(1),\mu_3(1)\}$ and $\{\bar{\sigma}_1(2),\bar{\sigma}_3(2)\}$:

$$\begin{aligned} \mu_1(1) &= \bar{\sigma}_3(1)\sigma_3(2); & \bar{\sigma}_1(2) &= \bar{\sigma}(1)\sigma_1(2); \\ \mu_3(1) &= \bar{\sigma}_1(1); & \bar{\sigma}_3(2) &= \sigma_3(2). \end{aligned} \tag{4.5}$$

This canonical transformation is then iterated all along the 1 dimensional lattice. If we define, $\bar{\sigma}_1(0) \equiv \sigma_1(0)$ and $\bar{\sigma}_3(0) \equiv \sigma_3(0)$, then the general relations take the form:

$$\begin{aligned} \mu_1(x) &\equiv \bar{\sigma}_3(x)\sigma_3(x+1); & \bar{\sigma}_1(x+1) &= \bar{\sigma}_1(x)\sigma_1(x+1) = \mu_3(x)\sigma_1(x+1); \\ \mu_3(x) &= \bar{\sigma}_1(x); & \bar{\sigma}_3(x+1) &= \sigma_3(x+1). \end{aligned} \tag{4.6}$$

The above canonical transformations iteratively replace the conjugate pair $\{\sigma_1(x); \sigma_3(x)\}$ or equivalently $\{\bar{\sigma}_1(x); \bar{\sigma}_3(x)\}$ by a new conjugate pair $\{\mu_1(x); \mu_3(x)\}$. This process is graphically illustrated in Figure 4.1. The above relations lead to

$$\mu_3(x) = \prod_{s=0}^{x} \sigma_1(s); \qquad \mu_1(x) = \sigma_3(x+1)\sigma_3(x). \tag{4.7}$$

Therefore, $\mu_3(x)\mu_3(x-1) = \sigma_1(x)$ with the convention $\mu_3(x=-1) \equiv 1$. It can easily be checked that the μ variables also satisfy the relations (4.1).

$$\mu_1^2(x) = 1 \; ; \; \mu_3^2(x) = 1; \qquad \mu_1(x)\mu_3(x) = -\mu_3(x)\mu_1(x). \tag{4.8}$$

The Ising model Hamiltonian can now be rewritten in its self-dual form in terms of the dual conjugate pairs $\{\mu_1(x); \mu_3(x)\}$:

$$H \; = \; \sum_{x=0}^{\infty} \Big[-\mu_3(x)\mu_3(x+1) - \lambda \; \mu_1(x) \Big] = \lambda \sum_{x=0}^{\infty} \Big[-\; \mu_1(x) - \frac{1}{\lambda}\mu_3(x)\mu_3(x+1) \Big]. \tag{4.9}$$

Therefore,

$$H(\sigma; \lambda) = \lambda^{-1} H(\mu; \lambda^{-1}).$$

This is the famous Kramers-Wannier self duality.

Since, σ variables and μ variables satisfy the same algebra, the above expression shows that the high λ behavior of the system is the same as the low λ behavior. In particular, the energy eigenvalues at different values of coupling are related by $E(\lambda) = \lambda^{-1} E(\lambda^{-1})$. So, if we assume that there is a critical value λ_c of λ where there is a phase transition, the mass gap $G(\lambda)$ vanishes at λ_c. The above expression says that if the mass gap $G(\lambda)$ vanishes at λ_c it should also vanish at λ_c^{-1}. Therefore, if there is a single critical point then, $\lambda_c = 1$. This is a simple illustration of the usefulness of such dualities in the study of the phase structure of various systems. Another interesting and important feature of duality is that it has interchanged the interacting and non interacting parts of the Hamiltonian on going from the $\{\sigma_1, \sigma_3\}$ to the dual $\{\mu_1, \mu_3\}$ variables. In other words, duality maps strong coupling region to the weak coupling region and vice versa.

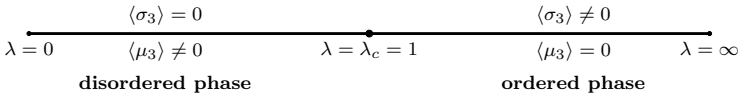

Figure 4.2: Duality and ordered & disordered phases of $(1+1)$ dimensional Ising model.

Duality also helps us define the disorder operators. In this simple Ising model case, the magnetization operator, $\sigma_3(x)$ is the order operator as it's expectation value measures the degree of order of the σ_3 variables. It is zero for $\lambda < \lambda_c$ and non-zero for $\lambda > \lambda_c$. This implies that the $\lambda > \lambda_c$ phase spontaneously breaks the global Z_2 symmetry, $\sigma_3 \to -\sigma_3$. On the other hand, exploiting duality, it is natural to define $\mu_3(x)$ as a disorder operator [7, 56, 124]. The vacuum expectation value ${}_\lambda\langle 0|\mu_3(x)|0\rangle_\lambda$ is the disorder parameter. We also note that the disorder operator $\mu_3(\bar{x}) \equiv \prod_{x<\bar{x}} \sigma_1(x)$ acting on a completely ordered state (all $\sigma_3(x) = +1$ or -1), flips all σ_3 spins at $x < \bar{x}$ and creates a kink. Therefore, the resulting kink state is orthogonal to the original ordered state and the expectation value of the disorder operator μ_3 in an ordered state vanishes:

$$ {}_{\lambda=\infty}\langle 0|\mu_3(x)|0\rangle_{\lambda=\infty} = 0, \qquad {}_{\lambda=\infty}\langle 0|\sigma_3(x)|0\rangle_{\lambda=\infty} = 1. \tag{4.10} $$

On the other hand, at the other end at $\lambda = 0$, the dual description of Ising model in (4.9) implies that it is in ordered state with respect to μ_3 spins. All μ_3 point in the same direction. As a consequence, the disorder parameter does not vanish and order parameter vanishes:

$$ {}_{\lambda=0}\langle 0|\mu_3(x)|0\rangle_{\lambda=0} = 1, \qquad {}_{\lambda=0}\langle 0|\sigma_3(x)|0\rangle_{\lambda=0} = 0. \tag{4.11} $$

The duality relations (4.10), (4.11) are illustrated in Figure 4.2.

4.2 Z_2 LATTICE GAUGE THEORY & WEGNER DUALITY

As mentioned earlier, Franz Wegner generalized Kramers Wannier duality to higher dimensional Ising models in 1971. In particular, he showed that in two space dimensions Z_2 lattice gauge theory can be exactly mapped into a Z_2 Ising model describing spin half magnets [55]. This is the earliest and the simplest example of the intriguing gauge-spin duality.

The two essential features of the Wegner duality [55] are

- It eliminates all unphysical gauge degrees of freedom in Z_2 lattice gauge theory mapping it into Z_2 spin model with a Z_2 global symmetry. There are no Z_2 Gauss law constraints in the dual Z_2 spin model.

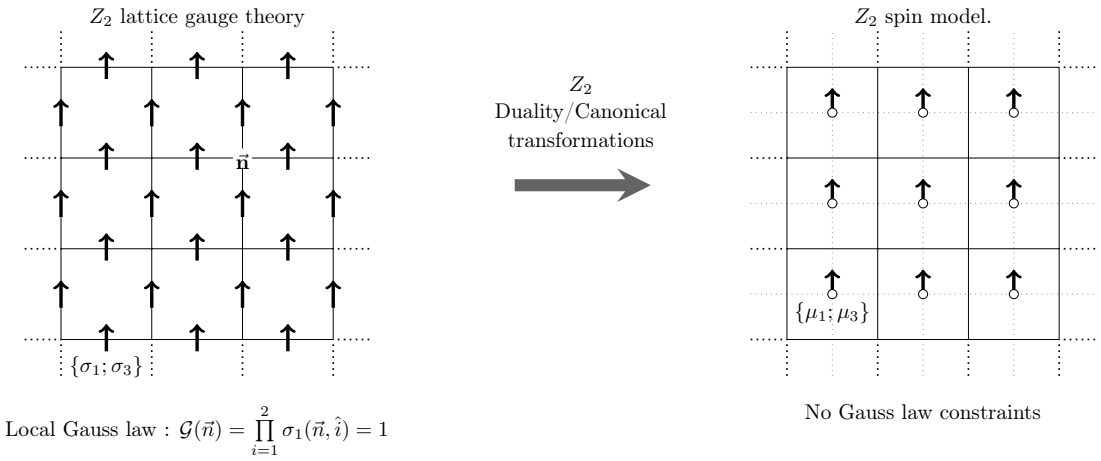

Figure 4.3: Duality between Z_2 lattice gauge theory and Z_2 (Ising) spin model. The initial and the final conjugate pairs $\{\sigma_1;\sigma_3\}$ and $\{\mu_1;\mu_3\}$, are defined on the links and the plaquettes or dual sites respectively. The corresponding SU(N) duality is illustrated in Figure 4.6.

- It maps the interacting (non-interacting) terms in the Z_2 lattice gauge theory Hamiltonian into non-interacting (interacting) terms in the Z_2 spin model Hamiltonian resulting in the inversion of the coupling constant.

This gauge-spin duality is through the loop description of Z_2 lattice gauge theory. In fact, the dual Z_2 spin degrees of freedom are the original Z_2 plaquette-loop degrees of freedom which are gauge invariant, mutually independent as well as complete. As a consequence, the redundant or unphysical gauge degrees of freedom do not appear in the dual spin model. The dual spin model, in turn, has a global Z_2 symmetry which is physical and completely independent of the initial Z_2 gauge group. This discrete symmetry is spontaneously broken leading to a phase transition separating ferromagnetic or ordered phase from the paramagnetic or disordered phase. In fact, the initial motivation to study Z_2 gauge-spin duality was to get better understanding of the phase transition in Z_2 lattice gauge theory in terms of the order-disorder phase transitions in the dual spin model [7, 55, 56, 122]. The Z_2 duality transformations show that the confinement and free phases of Z_2 lattice gauge theory correspond to the ordered and disordered phases of the spin model. As in the Ising model case in the previous section, the dual formulation also leads to construction of a (non-local) disorder operator for Z_2 lattice gauge theory.

We now revisit the Z_2 gauge - Z_2 spin results obtained in the last chapter (section 3.1) from a duality perspective. For the sake of convenience, we rewrite some of the equations derived in the last chapter. The Z_2 lattice gauge theory Hamiltonian (3.4) is

$$H = -\sum_{l\in\Lambda} \sigma_1(l) - \lambda \sum_{p\in\Lambda} \sigma_3(l_1)\sigma_3(l_2)\sigma_3(l_3)\sigma_3(l_4) \quad \equiv H_E - \lambda H_B. \tag{4.12}$$

The Z_2 Gauss law constraint at every lattice site is

$$\mathcal{G}(n) \equiv \prod_{l_n} \sigma_1(l_n) = 1,\ n \in \Lambda. \tag{4.13}$$

In (3.5), $\prod_{l_n}$ represents the product over 4 links (denoted by l_n) which share the lattice site n in two space dimensions. After canonical transformations, the Hamiltonian takes the simple nearest neighbour interaction form in terms of the physical loop operators (3.32):

$$\begin{aligned} H &= -\sum_{<p,p'>} \mu_3(p)\mu_3(p') - \lambda \sum_p \mu_1(p) \equiv H_E + \lambda H_B, \\ &= \lambda \Big[-\sum_p \mu_1(p) - \frac{1}{\lambda} \sum_{<p,p'>} \mu_3(p)\mu_3(p') \Big]. \end{aligned} \tag{4.14}$$

We note that after all the iterative canonical transformations over the entire lattice, the electric and the magnetic field descriptions in terms of potentials have interchanged. The final canonical relations are

$$\underbrace{\sigma_1(l)}_{Z_2 \text{ electric field}} \equiv \underbrace{\mu_3(p)\mu_3(p')}_{Z_2 \text{ electric scalar potentials}} \quad ; \quad \underbrace{\sigma_3(l_1)\sigma_3(l_2)\sigma_3(l_3)\sigma_3(l_4)}_{Z_2 \text{ Magnetic vector potentials}} \equiv \underbrace{\mu_1(p)}_{Z_2 \text{ Magnetic field}} . \tag{4.15}$$

In the first relation above, p and p' denote the two plaquettes sharing the link l. In the second relation, p denotes the plaquette enclosed by the links l_1, l_2, l_3, l_4 in two space dimensions. We immediately see that the new μ_3 operators in (4.15) trivially solve the Z_2 Gauss law constraints 4.13:

$$\mathcal{G}(n) \equiv \prod_{l_n} \sigma_1(l_n) = (\mu_3(p_1))^2\,(\mu_3(p_2))^2(\mu_3(p_3))^2(\mu_1(p_4))^2 \equiv 1. \tag{4.16}$$

Above, p_1, p_2, p_3, p_4 denote the 4 plaquettes surrounding the lattice site n. Note that after all the canonical transformations over the entire lattice,

- the description in terms of $\{\mu_1(p); \mu_3(p)\}$ has no constraints,
- instead of the fundamental magnetic vector potential $\sigma_3(l)$, the Z_2 magnetic field $\mu_1(p)$ now acquires an independent status,
- instead of the fundamental Z_2 electric field $\sigma_1(l)$ the (dual) Z_2 electric scalar potential $\mu_3(p)$ solve the Gauss law constraints (4.16) and acquire the independent status,
- the magnetic field and the dual electric scalar potentials $\{\mu_1(p), \mu_3(p)\}$ form a mutually conjugate pair on each plaquette.

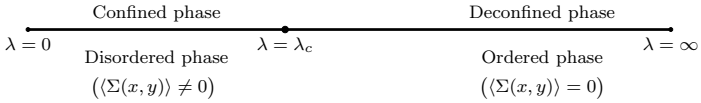

(a) Z_2 lattice gauge theory

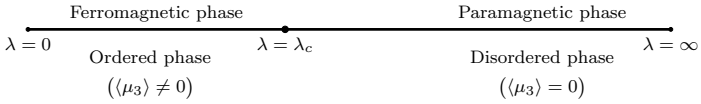

(b) Z_2 spin model

Figure 4.4: Duality and order, disorder in (a) $(2+1)$ dimensional Z_2 lattice gauge theory, (b) $(2+1)$ dimensional Ising model. The confining ($\lambda << 1$) and deconfining ($\lambda >> 1$) phases of Z_2 lattice gauge theory correspond to the ferromagnetic and paramagnetic phases of the Ising spin model.

Thus the Z_2 gauge theory initially written in terms of electric field and magnetic vector potential operators $\{\sigma_1(l); \sigma_3(l)\}$ in (4.12) is now written in terms of the magnetic field, electric scalar potential operators $\{\mu_1(p); \mu_3(p)\}$ in (4.14). Therefore, the net effect of canonical transformations on the entire lattice is to produce Wegner duality transformations in $(2+1)$ dimensional Z_2 lattice gauge theory. As expected, under duality transformations, the initial gauge coupling λ goes to spin model coupling $(1/\lambda)$, i.e,

$$H^{Z_2}_{gauge}(\lambda) \approx \lambda \; H^{Z_2}_{spin}(1/\lambda).$$

We have used $\approx$ above to emphasizes that this equivalence is only within the physical Hilbert space $\mathcal{H}^p$. The resulting Z_2 spin model (4.14) on an infinite lattice is invariant under the global Z_2 transformation:

$$\mu_1(p) \to \mu_1(p), \qquad \mu_3(p) \to -\mu_3(p), \qquad \forall p \in \Lambda. \tag{4.17}$$

Its generator $G_\Lambda \equiv \prod_{p \in \Lambda} \mu_1(p)$ leaves the Hamiltonian (4.14) invariant: $G_\Lambda H G_\Lambda^{-1} = H$. Unlike the initial Z_2 gauge symmetry of Z_2 gauge theory, the global Z_2 symmetry of the dual spin model (4.14) is the symmetry of the spectrum. Being independent of gauge invariance, it allows the Ising spin model (4.14) to be magnetized through spontaneous symmetry breaking for $\lambda << 1$. As a consequence of canonical transformations or duality:

$$\begin{aligned} \Big\langle \mu_1(p) \Big\rangle_{H^{z_2}_{spin}(1/\lambda)} &= \Big\langle \sigma_3(l_1)\sigma_3(l_2)\sigma_3(l_3)\sigma_3(l_4) \Big\rangle_{H^{z_2}_{gauge}(\lambda)} \\ \Big\langle \mu_3(x,y) \Big\rangle_{H^{z_2}_{spin}(1/\lambda)} &= \left\langle \prod_{y'=y}^{N} \sigma_1(x,y',\hat{1}) \right\rangle_{H^{z_2}_{gauge}(\lambda)} \end{aligned} \tag{4.18}$$

The above equations describe the dual relationship between order and disorder in the gauge and spin systems at different couplings. The first relation above states that at large coupling

(low temperature) $\lambda >> 1$ when the gauge system is in ordered phase,

$$< \mu_1(p) >_{H^{z_2}_{spin}(1/\lambda<<1)} = < \sigma_3(l_1)\sigma_3(l_2)\sigma_3(l_3)\sigma_3(l_4) >_{H^{z_2}_{gauge}(\lambda>>1)} \approx 1,$$

the dual spin system is at high temperature and in the disordered phase. In other words, the dual electric scalar potential or the spin values $\mu_3(p) = \pm 1$ are equally probable in the ground state. This is deconfined phase with Wilson loop following perimeter law [7, 56, 122, 125–129, 144]:

$$\langle W_{[\mathcal{C}]} \rangle \equiv \langle \prod_{l \in \mathcal{C}} \sigma_3(l) \rangle = exp\Big(- \lambda^{-2} \, Perimeter(\mathcal{C}) \Big), \qquad \lambda >> 1. \tag{4.19}$$

On the other hand, at small coupling ($\lambda << 1$), the spin system is in ordered phase,

$$< \mu_3(x,y) >_{H^{z_2}_{spin}(1/\lambda>>1)} = \left\langle \prod_{y'=y}^{N} \sigma_1(x,y',\hat{1}) \right\rangle_{H^{z_2}_{gauge}(\lambda<<1)} \approx 1,$$

with all electric scalar potentials $\mu_3(p)$ aligned. The gauge system is now disordered as the two values of the magnetic vector potentials $\sigma_3(l) = \pm 1$ are equally probable in the ground state. This is the confining phase with the Z_2 Wilson loop $W_{[\mathcal{C}]}$ around a closed curve $\mathcal{C}$ following the area law [7, 56, 122, 125–129, 144]:

$$\langle W_{[\mathcal{C}]} \rangle \equiv \langle \prod_{l \in \mathcal{C}} \sigma_3(l) \rangle \sim (\lambda)^{Area(\mathcal{C})} = exp\Big(- |ln\lambda| \; Area(\mathcal{C}) \Big), \qquad \lambda << 1. \tag{4.20}$$

The Z_2 gauge and Z_2 spin model phase mapping is illustrated in Figure 4.4.

The second non-local relation in (4.18) is of particular interest as we generalize it to define a disorder operator for SU(N) lattice gauge theories in the next section. As $\mu_3(x,y)$ is an order parameter for the Ising model and the duality mapping interchanges high and low temperatures, we define a nonlocal disorder operator $\Sigma(x,y)$ for Z_2 lattice gauge theory as

$$\Sigma(x,y) = \prod_{y'=y}^{N} \sigma_1(x,y',\hat{1}) \equiv \mu_3(x,y). \tag{4.21}$$

Just like in the case of Kramers-Wannier duality [7, 56, 118, 123], the disorder operator $\Sigma(x,y)$ in Z_2 gauge theory acting on an ordered state creates an infinitely long kink state [7, 56] which is orthogonal to the original ordered state. Therefore, the expectation value of the disorder operator in an ordered state is 0. Below the critical point λ_c, its expectation value is non-zero. This is the disordered phase and can be understood as because of kink condensation [7, 124]. We therefore obtain:

$$\langle \Sigma(x,y) \rangle \neq 0 \quad \lambda << 1, \qquad\qquad \langle \Sigma(x,y) \rangle = 0 \quad \lambda >> 1. \tag{4.22}$$

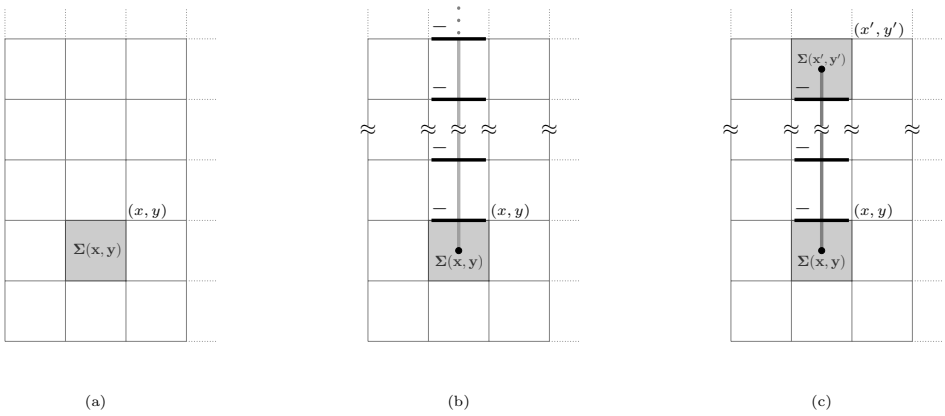

Figure 4.5: Graphical illustration of Z_2 disorder operator creating a vortex in terms of (a) the dual operator $\mu_3(x,y)$ and (b) the original σ_1 operators which forms an infinitely long string. (c) illustrates a vortex-antivortex pair. The dark heavy horizontal links across the strings in (b) and (c) represent the flipping of the link flux operators $\sigma_3(x-1,y',\hat{1});y'>y$ by the disorder operator $\mu_3(x,y)$. Generalization of Z_2 disorder operator to SU(N) lattice gauge theory is illustrated in Figure 4.7.

The duality between Z_2 gauge theory and Ising model and the corresponding phase diagrams are shown in Figure 4.4. Note that the disorder operator $\Sigma(x,y)$ is gauge invariant as it commutes with the local Gauss law operators $\mathcal{G}(n)=\prod_{l_n}\sigma_1(l_n)$ given in (3.5). In order to generalize (4.21) to SU(N) disorder operators (discussed in the next section), it is convenient to define Z_2 loop electric field $\mathcal{E}(x,y)$ as $\mu_3(x,y)\equiv e^{i\pi\mathcal{E}(x,y)}$. Using the Z_2 electric field and vector potential representation (3.2), we write (4.21) as

$$\Sigma(x,y)=\exp\ i\Big(\pi\sum_{y'=y}^{N}E(x,y';\hat{1})\Big)\equiv\ \exp\ i\Big(\pi\,\mathcal{E}(x,y)\Big). \tag{4.23}$$

Using the anticommutation relation between $\sigma_1(l)$ and $\sigma_3(l)$ with the defining relation (4.21):

$$W_{[\mathcal{C}]}\ \Sigma(x,y)=\Big(e^{im\pi}\Big)\ \Sigma(x,y)\ W_{[\mathcal{C}]}. \tag{4.24}$$

As $\mathcal{C}$ is a closed loop: $m=1$ if the point (x,y) is inside $\mathcal{C}$ and $m=0$ if (x,y) is outside $\mathcal{C}$. This can be generalized to more complicated curves where m equals the winding number which is number of times the curve $\mathcal{C}$ winds around the plaquette p. The algebra (4.24) is the standard Wilson-t'Hooft loop algebra for the simplest Z_2 lattice gauge theory in $(2+1)$dimensions. We will generalize the Z_2 disorder operator (4.21) or equivalently (4.23) to SU(N) lattice gauge theory in section 4.3 after discussing SU(N) duality in the next section.

4.3 DUALITY IN SU(N) LATTICE GAUGE THEORY

Just like in Z_2 lattice gauge theory, we now show that the canonical transformations leading to loop formulation of SU(N) lattice gauge theory in section 3.2 are SU(N) duality trans-

formations. To keep the discussion simple, we will systematically generalize the Z_2 lattice gauge theory results of the last section to SU(N) lattice gauge theory in this section.

In the Kogut-Susskind formulation, (chromo) electric field operators $(\vec{E}(l))$ were fundamental whereas magnetic field operators were composite of the fundamental link operators $(U_{\alpha\beta}(l))$. Further, $\{E^a(l), U_{\alpha\beta}(l)\}$ form conjugate pairs (2.11) on every link l and the Hamiltonian (3.59) is

$$\begin{aligned} H &= g^2 \sum_{l=1}^{4} \vec{E}^2(l) + \frac{K}{g^2}\left[2N - Tr\left(U_1\, U_2\, U_3^\dagger\, U_4^\dagger \;+\; h.c\right)\right] \\ &\equiv \quad H_E \;+\; H_B. \end{aligned} \tag{4.25}$$

The SU(N) Gauss law constraints (2.18) are

$$\mathcal{G}^a(n) = \sum_{i=1}^{2} \left(E_-^a(n,\hat{i}) + E_+^a(n,\hat{i})\right) = 0, \quad \forall n, a. \tag{4.26}$$

On the other hand, in the loop description the Kogut-Susskind Hamiltonian (3.83)

$$\begin{aligned} H = \sum_{x,y\in\Lambda} \frac{g^2}{2} \Bigg\{ &\left[\vec{\mathcal{E}}_-(x+1,y+1) + \vec{\mathcal{E}}_+(x+1,y) + \Delta_{XY}(x,y)\right]^2 \\ &+ \left[\vec{\mathcal{E}}_+(x+1,y+1) + R_{bc}(W(x,y))\vec{\mathcal{E}}_-^c(x,y+1) + \Delta_Y(x,y)\right]^2 \Bigg\} \\ &+ \frac{1}{2g^2}\Big(2N - (Tr\ \mathcal{W}(x,y) + h.c)\Big) \equiv g^2 \tilde{H}_E + \frac{1}{g^2}\tilde{H}_B. \end{aligned} \tag{4.27}$$

The above expressions (4.25), (4.26) and (4.27) are the SU(N) lattice gauge theory analogs of the corresponding Z_2 expressions (4.12), (4.13) and (4.14) respectively.

We further note that after all SU(N) canonical transformations over the entire lattice, the original link operators in (4.25) and the loop operators in (4.27) are related as (3.72):

$$\begin{aligned} E_+^a(x,y;\hat{1}) &= R_{ab}(\mathsf{T}^\dagger(x,y))\left[\mathcal{E}_-^b(x+1,y+1) + \mathcal{E}_+^b(x+1,y) + \Delta_X^b(x,y)\right] \\ E_+^a(x,y;\hat{2}) &= R_{ab}(\mathsf{T}^\dagger(x,y))\left[\mathcal{E}_+^b(x+1,y+1) + R_{bc}(\mathcal{W}_{xy})\mathcal{E}_-^c(x,y+1) + \Delta_Y^b(x,y)\right]. \\ U_1\, U_2\, U_3^\dagger\, U_4^\dagger &= \mathcal{W}(x,y). \end{aligned} \tag{4.28}$$

The left and right electric fields $E_+^a(\vec{n},\hat{i}), E_-^a(\vec{n}+\hat{i},\hat{i})$ on a link $(\vec{n},\hat{i})$ are related through parallel transport (2.13):

$$\begin{aligned} E_-^a(x,y;\hat{1}) &\equiv R_{ab}\left(U^\dagger(x-1,y,\hat{1})\right) E_+^b(x-1,y;\hat{1}), \\ E_-^a(x,y;\hat{2}) &\equiv R_{ab}\left(U^\dagger(x,y-1,\hat{2})\right) E_+^a\,(x,y-1;\hat{2})\,. \end{aligned} \tag{4.29}$$

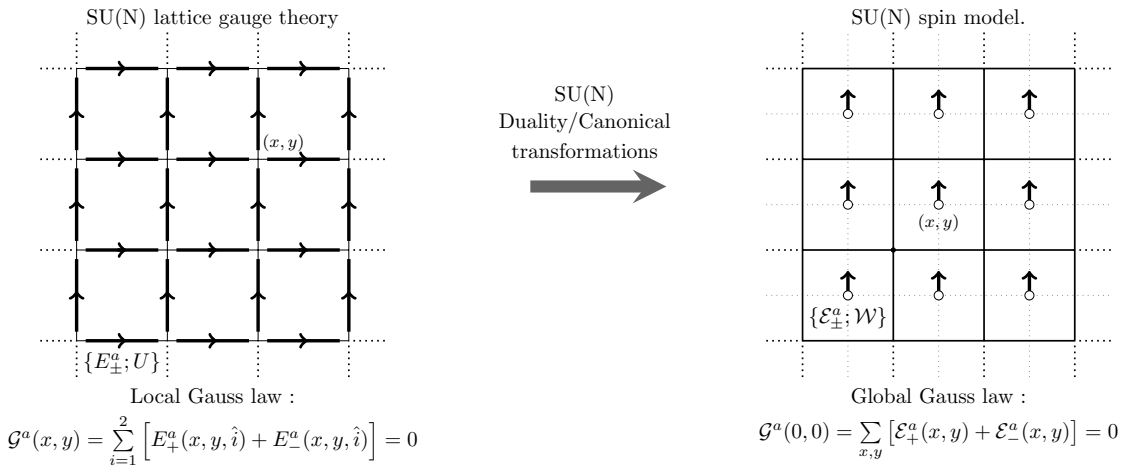

Figure 4.6: Duality between SU(N) lattice gauge theory and an SU(N) spin model. Unlike the corresponding Z_2 duality in Figure 4.3-a,b, global SU(N) Gauss law constraints at the origin remain unsolved. The Gauss law constraints at every other point $\mathcal{G}^a(x,y)$; $(x,y) \neq (0,0)$ are trivially solved in the loop/spin picture.

Like in Z_2 lattice gauge theory (4.16), in terms of the loop electric fields the SU(N) Gauss law constraints, away from the origin, become identities. In other words;

$$E^a_+(x,y;\hat{1}) + E^a_+(x,y;\hat{2}) + E^a_-(x,y;\hat{1}) + E^a_-(x,y;\hat{2}) \equiv 0. \qquad (x,y) \in \Lambda, \;\; (x,y) \neq (0,0). \tag{4.30}$$

The identities (4.30) are shown in Appendix A (see equation (A.44)). In Appendix A, we also show (see equation A.46) that in terms of loop electric fields, the Gauss law constraints at the origin $(0,0)$ are

$$\mathcal{G}^a(0,0) \equiv E^a_+(0,0;\hat{1}) + E^a_+(0,0;\hat{2}) = \sum_{x,y=1}^{N_s-1} \Big(\mathcal{E}^a_+(x,y) + \mathcal{E}^a_-(x,y)\Big). \tag{4.31}$$

Thus, unlike Wegner's Z_2 gauge theory duality where the dual variables were gauge invariant[2], in SU(N) lattice gauge theory, all dual operators transform under the gauge transformations at the origin (3.74). This is the global gauge invariance. The Gauss law constraints (4.31) reflects this gauge invariance. More explicitly, in abelian gauge theories the left electric field $(\mathcal{E}_-(x,y))$ and the right electric field $(\mathcal{E}_+(x,y))$ of a loop operator differ by sign $(\mathcal{E}_-(x,y) + \mathcal{E}_+(x,y) \equiv 0)$ and (4.31) identically vanishes for each plaquette. The duality from links to loops or spins in SU(N) lattice gauge theory and the special role of the Gauss law at the origin are illustrated in Figure 4.6. Note that the conjugate loop operators $\{\mathcal{W}_{\alpha\beta}(x,y); \mathcal{E}^a_\pm(x,y)\}$ have the interpretation of dual operators. They are the SU(N) analogues of the dual pairs $\{\mu_1(x,y); \mu_3(x,y)\}$ in the Z_2 lattice gauge theory case. All other general features of duality extensively discussed in the context of the simplest Z_2 lattice gauge theory are also valid.

2 The global Z_2 invariance of the dual Ising model is a real symmetry of the spectrum.

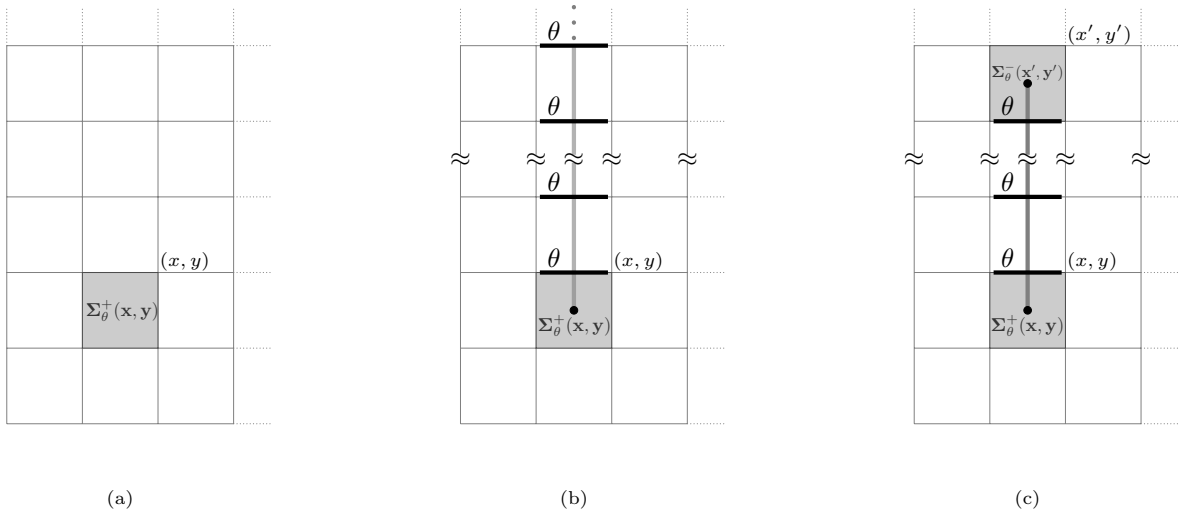

(a) (b) (c)

Figure 4.7: Graphical illustration of the disorder operator $\Sigma_\theta^+(x,y)$ creating a plaquette vortex (monopole) in terms of (a) the dual operators, (b) the original Kogut-Susskind link operators but now with infinitely long Dirac string, (c) a vortex-antivortex (monopole-antimonopole) pair connected through a finite length Dirac string. The dark heavy horizontal links across the Dirac strings in (b) and (c) represent rotations of the Kogut-Susskind link flux operators $U(x-1,y';\hat{1})$, $y' \geq y$ by θ.

SU(N) Disorder Operator

Exploiting duality transformations, we now construct a SU(N) gauge invariant disorder operator which measure the magnetic disorder in the gauge system [14, 64, 128, 144, 146, 147]. This is analogous to the disorder operator in Z_2 lattice gauge theory discussed in the last section. we will focus on a single plaquette $p = (x,y)$ in this section. To keep the arguments simple, we consider SU(2) lattice gauge theory. The magnetic plaquette flux operator in the magnetic basis can be written as:

$$\mathcal{W}(x,y) \equiv cos\left(\frac{\omega_{(x,y)}}{2}\right)\sigma_0 + i\left(\hat{w}_{(x,y)}\cdot\vec{\sigma}\right)\sin\left(\frac{\omega_{(x,y)}}{2}\right); \quad \hat{w}_{(x,y)}\cdot\hat{w}_{(x,y)} = 1, \quad \forall\ (x,y). \tag{4.32}$$

In (4.32), $\omega(x,y)$ are gauge invariant angles, $\hat{w}(x,y)$ are the unit vectors in the group manifold S^3 and $\sigma_0, \vec{\sigma}(\equiv \sigma_1,\sigma_2,\sigma_3)$ are the unit, Pauli matrices. Under global gauge transformation $\Lambda \equiv \Lambda(0,0)$ in (3.74), $(\omega,\hat{w})$ transform as:

$$\omega(x,y) \to \omega(x,y), \qquad \hat{w}^a(x,y) \to R_{ab}(\Lambda)\ \hat{w}^b(x,y). \tag{4.33}$$

Above, $R_{ab}(\Lambda)$ are defined in (2.13). We define two unitary operators:

$$\Sigma_\theta^\pm(x,y) \equiv exp\ i\Big(\hat{w}(x,y)\cdot\mathcal{E}_\pm(x,y)\ \frac{\theta}{2}\Big) \ = \ exp\ i\Big(Tr\left(\sigma^a\mathcal{W}(x,y)\right)\mathcal{E}^a_\pm(x,y)\ \frac{\theta}{2}\Big), \tag{4.34}$$

which are located on a plaquette $p \equiv (x,y)$ as shown in the Figure 4.7-a. They both are gauge invariant because $\mathcal{E}^a_{\pm}(x,y)$ and $\hat{w}(x,y)$ gauge transform like vectors as shown in (3.74) and (4.33). In other words, $\left[\mathcal{G}^a, \Sigma^{\pm}_{\theta}(x,y)\right] = 0$, where $\mathcal{G}^a$ is defined in (3.75). As the left and right electric scalar potentials are related through (3.70), $\Sigma^{\pm}_{\theta}(x,y)$ are not independent and satisfy:

$$\Sigma^{+}_{\theta}(x,y)\ \Sigma^{-}_{\theta}(x,y) = \Sigma^{-}_{\theta}(x,y)\ \Sigma^{+}_{\theta}(x,y) = I. \tag{4.35}$$

Above I denotes the unit operator in the physical Hilbert space $\mathcal{H}^p$ and $\Sigma^{-}_{\theta} = \Sigma^{+}_{-\theta}$. The physical meaning of the operators $\Sigma^{\pm}_{\theta}(x,y)$ is simple. The non-abelian electric scalar potentials $\mathcal{E}^a_{\pm}(x,y)$ are conjugate to the magnetic flux operators $\mathcal{W}_{\alpha\beta}(x,y)$. They satisfy the canonical commutation relations (3.69a). Therefore, the gauge invariant operator $\Sigma^{\pm}_{\theta}(x,y)$ locally and continuously changes the magnetic flux on the plaquette $p = (x,y)$ as a function of θ. To see this explicitly, we consider common eigenstates $|\omega(x,y), \hat{w}(x,y)\rangle$ of $\mathcal{W}_{\alpha\beta}(x,y)$ on a single plaquette. These states are explicitly constructed in appendix B. They satisfy:

$$Tr\mathcal{W}\ \ |\omega,\hat{w}\rangle = 2\cos\left(\frac{\omega}{2}\right)\ |\omega,\hat{w}\rangle\,. \tag{4.36}$$

We have ignored the irrelevant plaquette index $p \equiv (x,y)$ in (4.36) as we are dealing with a single plaquette. It is easy to check:

$$|\omega,\hat{w}\rangle_{\pm\theta} \equiv \Sigma^{\pm}_{\theta}\,|\omega,\hat{w}\rangle = |\omega \pm \theta, \hat{w}\rangle\,, \tag{4.37}$$

implying,

$$Tr\ \mathcal{W}\ |\omega,\hat{w}\rangle_{\pm\theta} = 2\ cos\left(\frac{\omega \pm \theta}{2}\right)\ |\omega,\hat{w}\rangle_{\pm\theta}. \tag{4.38}$$

We further define:

$$\Sigma_{2\pi} \equiv \Sigma^{+}_{\theta=2\pi} = \Sigma^{-}_{\theta=2\pi}\ ; \qquad (\Sigma_{2\pi})^2 = I. \tag{4.39}$$

The equations (4.36) and (4.39) state:

$$\Sigma_{2\pi}\,(Tr\mathcal{W}) = -\ (Tr\mathcal{W})\ \Sigma_{2\pi}. \tag{4.40}$$

We thus recover the standard Wilson-'t Hooft loop Z_2 algebra [14, 64, 128, 144, 146, 147] for SU(2) at $\theta = 2\pi$. The operator $\Sigma_{2\pi}$ is the SU(2) 't Hooft operator. The plaquette magnetic flux operators $\Sigma^{\pm}_{\theta}(x,y)$ in (4.34) can also be written as a non-local sum of Kogut-Susskind link electric fields along a line and the corresponding parallel transports using (3.68). The magnetic flux on the plaquette $p = (x,y)$ thus develops an infinite kink or Dirac string in the original (standard) $\{E^a(l); U(l)\}$ description. This is similar to the discrete Z_2 disorder

operator $\Sigma(x,y)$ written in terms of the original electric field operators $\sigma_1(x,y')$; $y' = y, y+1, \cdots N_s - 1$ in (4.21) and (4.23). The singular Dirac string is shown in Figure 4.7-b. Note that the disorder operator in the strong coupling ($g^2 \to 0$) vacuum $|0\rangle$ satisfies:

$$\langle 0|\Sigma_\theta^\pm(x,y)|0\rangle = 1, \qquad \langle 0|Tr\mathcal{W}_C(U)|0\rangle = 0,$$

showing that the strong coupling ground state $|0\rangle$ is maximally disordered with respect to the original magnetic vector potentials. The expectation values of Wilson loops, on the other hand, are zero. The study of $\Sigma^\pm(\theta)$ across deconfinement transition in SU(2) lattice gauge theory along with the vacuum correlation functions of $\langle \Sigma_\theta^\pm(p)\Sigma_\theta^\mp(p')\rangle$, as $|p-p'| \to \infty$ are some of the issues yet to be explored. The SU(N) generalization of of the construction (4.34) using SU(N) group manifolds is also under investigation.

5

SU(2) LOOPS & HYDROGEN ATOM

In this chapter, we show that the gauge invariant physical or loop Hilbert space $\mathcal{H}^p$ of pure SU(2) lattice gauge theory can be completely and most economically realized in terms of the Wigner coupled bound energy eigenstates $|n\ l\ m\rangle$ of hydrogen atoms [54]. One hydrogen atom is assigned to every plaquette of the lattice. The SU(2) global invariance (3.75) implies that the total angular momenta of all hydrogen atoms vanish. This Wigner coupled hydrogen atoms basis describe quantized SU(2) loop electric fluxes in terms of (n, l, m) and is orthonormal as well as complete in $\mathcal{H}^p$. Following Fock [148–150], we describe $\mathcal{P}$ hydrogen atoms on their momentum hypersphere S^3 (see section 5.2) so that their hidden $SU(2) \times SU(2)$ symmetries become manifest. We show that the equivalence of the gauge theory and hydrogen atom Hilbert spaces has its origin in the identification of SU(2) group manifold S^3 associated with each plaquette loop holonomy with the S^3 of the corresponding hydrogen atom (see discussion towards the end of section 5.2).

5.1 HYDROGEN ATOM & SO(4) SYMMETRY

The hydrogen atom can be elegantly solved using group theory[148–153] which exploits manifest rotational and hidden Runge Lenz symmetries generated by angular momentum

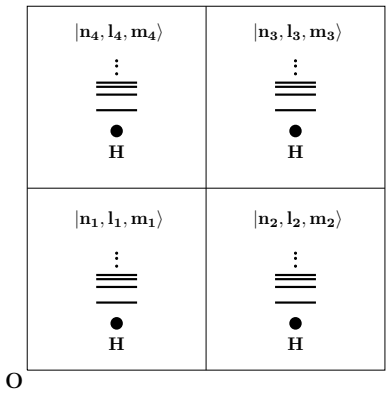

Figure 5.1: One hydrogen atom, denoted by •, is assigned to each plaquette. The Wigner coupled energy eigenstates $|n_p\ l_p\ m_p\rangle$ given in (5.19) with vanishing total angular momenta form a basis in the physical Hilbert space $\mathcal{H}^p$ of pure SU(2) lattice gauge theory.

($\vec{L}$) and Laplace Runge Lenz ($\vec{A}$) operators[1] respectively. These generators commute with the hydrogen atom Hamiltonian and satisfy $\vec{L}\cdot\vec{A}=0$. This leads to $SU(2)\otimes SU(2)$ symmetry algebra generated by

$$\vec{J}_{\pm}\equiv\frac{1}{2}(\vec{L}\pm\vec{A}), \tag{5.1}$$

on the bound states of hydrogen atom ($E<0$) [151, 152]. Further, the two angular momentum operators satisfy

$$\left[J_{+}^{a},J_{-}^{b}\right]=0, \qquad \vec{J}_{+}^{\,2}=\vec{J}_{-}^{\,2}\equiv\vec{J}^{\,2}. \tag{5.2}$$

As a consequence, the two equivalent complete set of commuting operators (CSCO) are

$$\text{Uncoupled basis}: \quad [(\vec{J}_{+})^{\,2},\ J_{+}^{z};\ \ (\vec{J}_{-})^{2},\ J_{-}^{z}]\equiv[(\vec{J})^{\,2},\ J_{+}^{z},\ J_{-}^{z}]: \quad (CSCO-I), \tag{5.3}$$

$$\text{Coupled basis}: \quad [(\vec{J})^{\,2},\ (\vec{J}_{+}+\vec{J}_{-})^{2},\ (\vec{J}_{+}^{z}+\vec{J}_{-}^{z})]\equiv[\vec{J}^{\,2},\ \vec{L}^{2},\ \vec{L}^{z}]: \quad (CSCO-II) \tag{5.4}$$

Following Wybourne [151, 152], we define :

$$J_{-}^{a}\equiv a^{\dagger}\left(\frac{\sigma^{a}}{2}\right)a; \qquad J_{+}^{a}\equiv b^{\dagger}\left(\frac{\sigma^{a}}{2}\right)b. \tag{5.5}$$

In (5.5) $(a_1^{\dagger},a_2^{\dagger})$ and $(b_1^{\dagger},b_2^{\dagger})$ represent SU(2) doublets of Schwinger boson (prepotential) creation operators, σ^{a} (a=1,2,3) are the Pauli matrices. The condition $\vec{J}_{-}^{\,2}=\vec{J}_{+}^{\,2}$ implies $N_a=N_b$ where $N_a=a^{\dagger}\cdot a$ and $N_b=b^{\dagger}\cdot b$ are the total number operators. The orthonormal and complete basis diagonalizing CSCO-I is given by [151, 152]:

$$|j=j_{-}=j_{+},m_{-},m_{+}\rangle=|j,m_{-}\rangle\otimes|j,m_{+}\rangle; \tag{5.6}$$

$$|j_{-}=j,m_{-}\rangle\equiv\frac{(a_1^{\dagger})^{(j+m_{-})}(a_2^{\dagger})^{(j-m_{-})}}{(j+m_{-})!(j-m_{-})!}|0\rangle, \qquad |j_{+}=j,m_{+}\rangle\equiv\frac{(c_1^{\dagger})^{(j+m_{+})}(c_2^{\dagger})^{(j-m_{+})}}{(j+m_{+})!(j-m_{+})!}|0\rangle. \tag{5.7}$$

Above[2], $c_{\alpha}\equiv\epsilon_{\alpha\beta}b_{\beta}$.

1 We follow Wybourne [151] for hydrogen atom discussions. The Runge Lenz vector has been scaled by $\frac{1}{\sqrt{-2E}}$ i.e, $\vec{A}=\frac{1}{2m\sqrt{-2E}}\left[\vec{p}\times\vec{\mathrm{L}}-\vec{\mathrm{L}}\times\vec{p}-\frac{k}{r}\vec{r}\right]$. Here E and m are the energy and the reduced mass. The operators $\vec{p}$, $\vec{L}$, $\vec{r}$ are the momentum, angular momentum and the position operators respectively[151].

2 Under an SU(2) transformation $\Lambda_{\alpha\beta}$, $c_{\alpha}^{\dagger}$ transform from the right i.e, $c_{\alpha}^{\dagger}\to c_{\beta}^{\dagger}\Lambda_{\beta\alpha}$, unlike $b_{\alpha}^{\dagger}$ which transforms from the left, $b_{\alpha}^{\dagger}\to\Lambda_{\alpha\beta}b_{\beta}^{\dagger}$. This is important in the construction of the magnetic basis which diagonalizes Wilson loops.

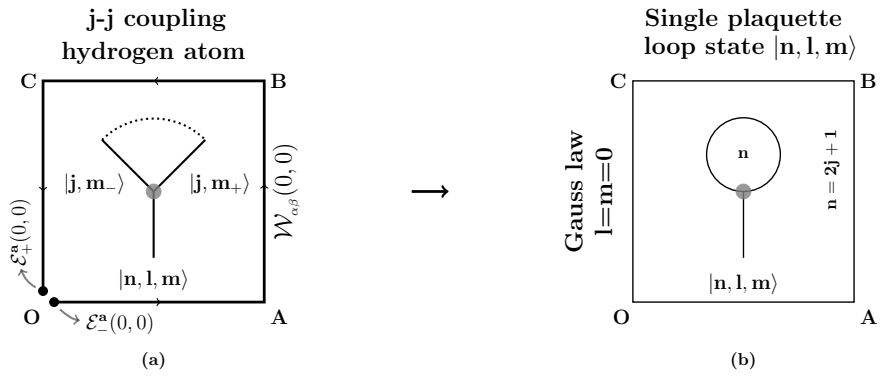

Figure 5.2: A graphical tadpole representation of hydrogen atom states $|n\ l\ m\rangle$ or equivalently a SU(2) loop state over a plaquette. The dotted arch represents $j_+ = j_- = j$ in the j-j coupling (5.8) which is denoted by •. The tadpole loop represents the SU(2) flux circulating within the plaquette. The vertical leg of tadpole represents the leakage of the angular momentum flux (l, m) through the plaquette.

The other equivalent coupled hydrogen atom basis diagonalizing the CSCO-II is given by:

$$|n\ l\ m\rangle \equiv \sum_{m_-,m_+} C^{l,m}_{jm_-,jm_+}\ |j,m_-\rangle \otimes |j,m_+\rangle. \tag{5.8}$$

In (5.8), $n \equiv (2j+1) = 1, 2\cdots; l = 0, 1, 2, \cdots, 2j \equiv (n-1); m = -l, \cdots, +l$; $C^{l,m}_{jm',j\tilde{m}}$ are the Clebsch-Gordan coefficients. The states $|j,m_-\rangle$ and $|j,m_+\rangle$ are coupled together using Clebsch-Gordon coefficients to give the coupled hydrogen atom states $|n\ l\ m\rangle$. • in Figure 5.2 and Figure 5.3 a,b represents the j-j coupling in eqn.(5.8) . These $|n\ l\ m\rangle$ states are eigenstates of J^2, L^2, L^z with eigenvalues $j(j+1)\big(\equiv \frac{1}{4}(n^2-1)\big)$, $l(l+1)$, m respectively. They are also the eigenstates of the hydrogen atom Hamiltonian with energy [151, 152] $E_n \sim -1/n^2$. The states $|n,\ l\ ,m\rangle$ are graphically represented by tadpoles as shown in Figure 5.2-b.

5.2 SU(2) LOOP STATES & HYDROGEN ATOM BOUND STATES

a. Single plaquette case

We first start with the simple single plaquette case to illustrate the correspondence between hydrogen bound states and SU(2) loop states. We identify the hydrogen atom angular momentum $\vec{L}$, Lenz vector operators $\vec{A}$ (combinations of $\vec{L}$ and $\vec{A}$ to be precise) with the SU(2) loop electric field operators $\vec{\mathcal{E}}_\pm$ of the gauge theory:

$$J^a_\mp \leftrightarrow \mathcal{E}^a_\mp. \tag{5.9}$$

Above, $J^a_{\mp} = \frac{1}{2}(L^a \pm A^a)$. This identification further implies:

$$L^a \ (\equiv J^a_+ + J^a_-) \quad \leftrightarrow \quad \mathsf{L}^a \ (\equiv \mathcal{E}^a_+ + \mathcal{E}^a_-). \tag{5.10}$$

where L^a are the angular momentum operators of a hydrogen atom and $\mathsf{L}^a = \mathcal{E}^a_+ + \mathcal{E}^a_-$ are the generators of Gauss law (3.48) in a single plaquette case. The $SU(2)$ Gauss law constraint on a single plaquette and its hydrogen atom analogue is :

$$\mathcal{G}^a(0,0) \ = \ \mathsf{L}^a \ = \ \mathcal{E}^a_- + \mathcal{E}^a_+ = 0 \quad \leftrightarrow \quad L^a \ (\equiv J^a_+ + J^a_-) = 0. \tag{5.11}$$

This immediately implies that CSCO-I (see (5.3)) $\left[J^2, J^z_+, J^z_-\right]$ and CSCO-II(see (5.4)) $\left[J^2, L^2, L^z\right]$ of hydrogen atom also characterize lattice gauge theory Hilbert space. CSCO-II is more natural for gauge theory as the SU(2) Gauss law constraints (5.11) are trivially solved in the coupled $|n,\ l,\ m\rangle$ basis diagonalizing CSCO-II by demanding $l = m = 0$. Therefore, the spherically symmetric energy eigenstates $|n,\ l = 0,\ m = 0\rangle$ of hydrogen atom also form a complete, orthonormal loop basis of SU(2) lattice gauge theory on a single plaquette. In order to construct these states, it is convenient to use Schwinger boson (prepotential) representation of SU(2) loop electric field and flux operators [48, 49]:

$$\begin{aligned} \mathcal{E}^a_- &= \ a^\dagger \left(\frac{\sigma^a}{2}\right) a; \qquad\qquad \mathcal{E}^a_+ = \ b^\dagger \left(\frac{\sigma^a}{2}\right) b; \\ \mathcal{W}_{\alpha\beta} &= \frac{1}{\sqrt{(N+1)}} \Big(\tilde{a}^\dagger_\alpha \, b^\dagger_\beta \ - \ a_\alpha \, \tilde{b}_\beta \Big) \frac{1}{\sqrt{(N+1)}}. \end{aligned} \tag{5.12}$$

Above $\tilde{a}_\alpha \equiv \epsilon_{\alpha\gamma} a_\gamma$. Like link electric fields, loop electric fields satisfy $(\vec{\mathcal{E}}_-)^2 = (\vec{\mathcal{E}}_+)^2$ (see eqn (2.14)) implying $N_a = N_b \equiv N$. Above loop basis states $|n,\ l = 0,\ m = 0\rangle$ can be constructed in terms of loop prepotentials as follows:

$$\begin{aligned} |n\rangle \equiv |n, l = 0, m = 0\rangle &= \frac{(k_+)^n}{\sqrt{n!(n+1)!}} \, |0\rangle. \\ \sum_{n=1}^{\infty} \ |n\rangle\langle n| = \mathcal{I}, \qquad \langle m|n\rangle &= \delta_{nm}. \end{aligned} \tag{5.13}$$

In (5.13) $\mathcal{I}$ is the identity operator in $\mathcal{H}^p$. The loop creation-annihilation and number operators are defined as:

$$k_+ \equiv a^\dagger \cdot \tilde{b}^\dagger, \quad k_- \equiv a \cdot \tilde{b}; \quad k_0 \equiv 1/2(N_a + N_b + 2).$$

These operators form $SU(1,1)$ algebra which is discussed in section 5.3 in the context of the dynamical symmetry group $SO(4,2)$ of hydrogen atom .

b. Finite lattice case

We now generalize the above results to a finite lattice. Some equations from the last chapter are repeated here for ease of presentation. One hydrogen atom is associated with each plaquette of the lattice. Just like in the single plaquette case, we identify $J^a_{\mp}(p)$ of the hydrogen atom associated with each plaquette p with the $SU(2)$ loop electric field $\mathcal{E}^a_{\mp}(p)$.

$$J^a_{\mp}(p) \;\leftrightarrow\; \mathcal{E}^a_{\mp}(p); \qquad p = 1, \cdots \mathcal{P}. \tag{5.14}$$

Above, $\mathcal{P}$ is the total number of plaquettes on the lattice. As before, this identification implies

$$L^a(p)\ (\equiv J^a_+(p) + J^a_-(p)) \quad \leftrightarrow \quad \mathsf{L}^a(p)\ (\equiv \mathcal{E}^a_+(p) + \mathcal{E}^a_-(p)); \qquad p = 1, \cdots \mathcal{P}. \tag{5.15}$$

The global SU(2) Gauss law constraints on a finite lattice implies that the total angular momentum of all the hydrogen atoms is 0 :

$$\mathcal{G}^a(0,0) \;=\; \sum_p \mathsf{L}^a(p) \;=\; 0 \quad \leftrightarrow \quad \sum_p L^a(p) \;=\; 0. \tag{5.16}$$

Above, the p summation is over all the plaquettes. The above correspondence implies that $SU(2)$ lattice gauge theory Hilbert space on a lattice with $\mathcal{P}$ plaquettes are characterized by the following Complete Set of Commuting Operators (CSCO):

$$\text{Uncoupled basis :} \quad \left\{ \begin{array}{cccc} \vec{J}_1^{\,2} & \vec{J}_2^{\,2} & \cdots & \vec{J}_{\mathcal{P}-1}^{\,2} & \vec{J}_{\mathcal{P}}^{\,2} \\ \vec{L}_1^2 & \vec{L}_2^2 & \cdots & \vec{L}_{\mathcal{P}-1}^2 & \vec{L}_{\mathcal{P}}^2 \\ \vec{L}_1^z & \vec{L}_2^z & \cdots & \vec{L}_{\mathcal{P}-1}^z & \vec{L}_{\mathcal{P}}^z \end{array} \right\} \quad (CSCO - A) \tag{5.17}$$

$$\text{Coupled basis :} \quad \left\{ \begin{array}{cccc} \vec{J}_1^{\,2} & \vec{J}_2^{\,2} & \cdots \vec{J}_{\mathcal{P}-1}^{\,2} & \vec{J}_{\mathcal{P}}^{\,2} \\ \vec{L}_1^2 & \vec{L}_2^2 & \cdots \vec{L}_{\mathcal{P}-1}^2 & \vec{L}_{\mathcal{P}}^2 \\ (\vec{L}_{12})^2 & (\vec{L}_{123})^3 & \cdots (\vec{L}_{total})^2 & \vec{L}^z_{total} \end{array} \right\}. \quad (CSCO - B) \tag{5.18}$$

Above, $(\vec{L}_{1,2,\cdots q})^2 \equiv (\vec{L}_1 + \vec{L}_2 + \cdots \vec{L}_q)^2$ with eigenvalue $l_{1,2\cdots q}(l_{1,2\cdots q}+1)$ and $q = 2, 3, \cdots, \mathcal{P}$ and $(\vec{L}_{total})^2 \equiv (\vec{L}_{1,2,\cdots \mathcal{P}})^2$. For the special case of $\mathcal{P} = 4$, the uncoupled basis diagonalizing CSCO-A and the coupled basis diagonalizing CSCO-B are graphically illustrated in Figure 5.3 (a) and (b) respectively. These CSCOs were discussed in the context of SU(2) lattice gauge theory in eqns (3.76) and (3.79). CSCO-B is more suitable for SU(2) gauge theory as the SU(2) Gauss law can be trivially solved by demanding that $(L_{total})^2 = L^z_{total} = 0$. Such a gauge invariant loop basis diagonalizing CSCO-B (see equation (3.79) was already described in

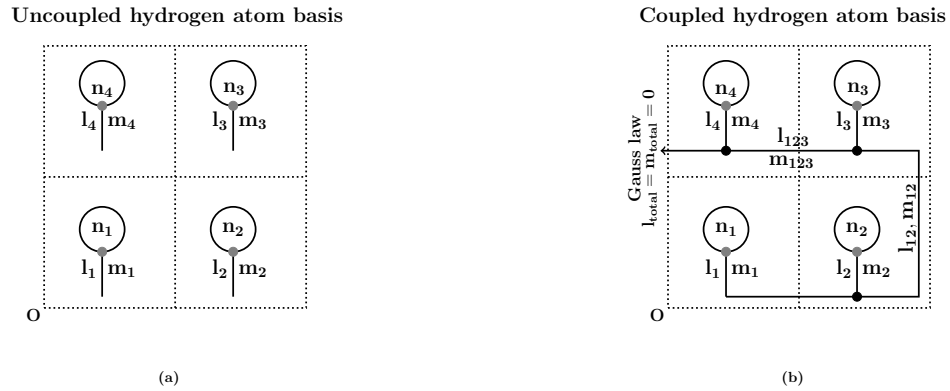

Figure 5.3: Graphical tadpole representation of [a] Uncoupled hydrogen atom basis diagonalizing CSCO-A, [b] coupled hydrogen atom basis diagonalizing CSCO-B. The dots • and • represent *jj* and *ll* couplings in (5.8) and (5.20) respectively.

section 3.2.3.3. We now interpret those results in terms of hydrogen atoms. Some of the equations are repeated for convenience. We draw tadpoles over each of the $\mathcal{P}$ plaquettes and then couple their emerging angular momentum fluxes (l_p, m_p) with $p = 1, \cdots, \mathcal{P}$ in a sequential manner as in Figure (5.3-b). It corresponds to going from decoupled tadpole basis diagonalizing CSCO-A to the coupled basis diagonalizing CSCO-B. The resulting orthonormal and complete coupled hydrogen basis describing SU(2) lattice gauge theory is given by:

$$\left| \begin{array}{cccc} n_1 & n_2 & \cdots & n_P \\ l_1 & l_2 & \cdots & l_P \\ l_{12} & l_{123} & \cdots & l_{12\cdots\mathcal{P}-2} \end{array} \right\rangle \equiv \Big\{ \underbrace{|n_1\ l_1\ m_1\rangle \otimes |n_2\ l_2\ m_2\rangle \cdots \otimes |n_P\ l_P\ m_P\rangle}_{\textbf{Wigner coupled states of hydrogen atoms}} \Big\}^{l_{total}=0}_{m_{total}=0} \tag{5.19}$$

Above, we have used the fact that $l_{12\cdots\mathcal{P}} = 0$ and therefore, $l_{12\cdots\mathcal{P}-1} = l_{12\cdots\mathcal{P}-2}$. This follows from the Gauss law (5.16). As an example the loop states over 4 plaquettes in Figure (5.3-b) are constructed as:

$$\left| \begin{array}{cccc} n_1 & n_2 & n_3 & n_4 \\ l_1 & l_2 & l_3 & l_4 \\ & l_{12} & & \end{array} \right\rangle = \sum_{\substack{m_1 m_2 m_3 m_4 \\ m_{12} m_{123}}} C^{l_{12} m_{12}}_{l_1 m_1, l_2 m_2} C^{l_{123} m_{123}}_{l_{12} m_{12}, l_3 m_3} C^{0\ 0}_{l_{123} m_{123}, l_4 m_4} \quad |n_1\ l_1\ m_1\rangle |n_2\ l_2\ m_2\rangle\ |n_3\ l_3\ m_3\rangle\ |n_4\ l_4\ m_4\rangle. \tag{5.20}$$

Above, the $|n_p\ l_p\ m_p\rangle\ ;\ p = 1,2,3,4$ states are coupled through Clebsch-Gordon coefficients. This is the *ll* coupling. The • in Figure 5.3-b shows the *ll* coupling in eqn.(5.20). The above loop basis (3.80) will be briefly denoted by $|[n]\ [l]\ [ll]\rangle$. As discussed in section 3.2.3.3, the symbols $[n]; [l]$ and $[ll]$ stand for the sets $(n_1 \cdots n_{\mathcal{P}})$: $\mathcal{P}$ principle quantum numbers; $[l_1 \cdots l_{\mathcal{P}}]$: $\mathcal{P}$ angular momentum quantum numbers and $(l_{12}, l_{123}, \cdots, l_{123\cdots(\mathcal{P}-2)})$: $(\mathcal{P}-3)$ coupled angular momentum quantum numbers respectively. Thus the hydrogen

atom loop basis (5.19) in $\mathcal{H}^p$ is labelled by $\mathbb{N}^{d=2}_{SU(2)} = 3(\mathcal{P}-1)$ gauge invariant quantum numbers. As expected, this is also the dimension of quotient space $\mathbb{N}^{d=2}_{SU(2)} = \dim\left[\frac{\otimes_{links} SU(2)}{\otimes_{sites} SU(2)}\right]$

Hydrogen atom hypersphere S^3:

As shown by Fock [148–150], the $SU(2) \otimes SU(2)$ symmetry for hydrogen bound states ($p_0^2 \equiv -2E > 0$) becomes manifest if we transcribe the hydrogen atom dynamics on a hypersphere $S^3 : (q_0,\ \vec{q};\ q_0^2 + \vec{q}^{\,2} = 1)$ embedded in $R^4 : (p_0, p_1, p_2, p_3)$ through a stereographic projection:

$$\begin{aligned} q_0 &\equiv \frac{(p_0^2 - \vec{p}^{\,2})}{(p_0^2 + \vec{p}^{\,2})}, & \vec{q} &\equiv \frac{2p_0\vec{p}}{(p_0^2 + \vec{p}^{\,2})}, \\ \Omega_H(q_0, \vec{q}) &\equiv q_0\sigma_0 + i\vec{q}\cdot\vec{\sigma}, & q_0^2 + \vec{q}^{\,2} &= 1. \end{aligned} \tag{5.21}$$

Above $\sigma_0, \vec{\sigma}$ are the identity, Pauli matrices respectively. The mapping (5.21) enables us to transform [148–150] momentum space hydrogen atom Schrodinger equation into the integral equation of the 4-dimensional spherical harmonics $Y_{n,l,m}(\Omega_H)$ representing a free particle on S^3. It was later shown by Bargmann [154] that (L_1, L_2, L_3) and (A_1, A_2, A_3) correspond to rotations in $(q_2q_3), (q_1q_3), (q_1q_2)$ and $(q_0q_1), (q_0q_2), (q_0q_3)$ planes respectively making $SU(2) \otimes SU(2)$ symmetry of hydrogen atom manifest. We will identify hydrogen atom S^3 on a plaquette p with the SU(2) group manifold S^3 associated with the plaquette loop flux operator $\mathcal{W}_{\alpha\beta}(p)$.

Wilson loop hypersphere S^3:

We now analyze the equivalence between the Hilbert space of hydrogen atom and SU(2) lattice gauge theory in the dual magnetic description. We again start with single plaquette basis $|j\ m_-\ m_+\rangle$ in (5.6) and define states on SU(2) group manifold S^3 as:

$$|\Omega_W\rangle = \sum_{j=0}^{\infty} \sum_{m_\mp = -j}^{+j} \{j\}\ D^j_{m_-m_+}(\Omega_W)\ |j, m_-, m_+\rangle. \tag{5.22}$$

In (5.22) $\{j\} \equiv \sqrt{\frac{(2j+1)}{2\pi^2}}$, $D^j_{m_-m_+}(\Omega_W)$ are the Wigner matrices characterized by SU(2) group manifold S^3:

$$\Omega_W\,(w_0, \vec{w}) \equiv w_0\ \sigma_0 + i\vec{w}\cdot\vec{\sigma}, \quad w_0^2 + \vec{w}^2 = 1 : S^3.$$

SU(2) lattice gauge theory	**hydrogen atom**
SU(2) group manifold S^3	Momentum space S^3
$\Omega_W(\omega, \hat{w})$	$\Omega_H(\omega, \hat{w})$
$\mathcal{E}^a_\pm$	$J^a_\pm$
$\mathsf{L}^a = \mathcal{E}^a_+ + \mathcal{E}^a_-$	$L^a = J^a_+ + J^a_-$
$\mathsf{A}^a = \mathcal{E}^a_+ - \mathcal{E}^a_-$	$A^a = J^a_- - J^a_-$

Table 5.1: The corresponding quantities in SU(2) lattice gauge theory and hydrogen atom

As shown in appendix B, the recursion relations of Wigner matrices show that the orthonormal and complete angular states (5.22) also diagonalize the plaquette loop operators $\mathcal{W}_{\alpha\beta}$.

$$\mathcal{W}_{\alpha\beta}\,|\Omega_W\rangle = \big(\Omega_W\,(\omega_0, \vec{w})\,\big)_{\alpha\beta}\,|\Omega_W\rangle. \tag{5.23}$$

Thus the $SU(2)$ matrix $\Omega_W(\omega_0, \hat{w})$ on S^3 describes the $SU(2)$ magnetic fluxes on a plaquette. Under global SU(2) transformation:

$$|\Omega_W\rangle \to |\Lambda_o\;\Omega_W\;\Lambda_o^\dagger\rangle. \tag{5.24}$$

The gauge generators L^1, L^2, L^3 in (3.47) rotate (w_2w_3), (w_3w_1), (w_1w_2) planes respectively leaving w_0 (gauge) invariant. Defining "Lenz operators" in lattice gauge theory as $\mathsf{A}^a \equiv \mathcal{E}^a_+ - \mathcal{E}^a_-$, we see that $(\mathsf{A}^1, \mathsf{A}^2, \mathsf{A}^3)$ generate rotations in (w_0w_1), (w_0w_2), (w_0w_3) planes respectively. Therefore, the actions of $(\mathsf{L}^a, \mathsf{A}^a)$ on Ω_W in gauge theory is exactly same as the actions of (L^a, A^a) on Ω_H in hydrogen atom. Therefore, we further identify:

$$\Omega_H \sim \Omega_W \equiv \Omega.$$

The correspondence between quantities in SU(2) lattice gauge theory and hydrogen atom are shown in table 5.1.

5.3 LOOP DYNAMICS & DYNAMICAL SYMMETRY GROUP SO(4,2) OF HYDROGEN ATOM

It is well known in hydrogen atom literature [151, 152] that the operators which takes $|n\;l\;m\rangle$ to $|n'\;l'\;m'\rangle$ form an SO(4,2) algebra on closure. This is called the dynamical symmetry group of hydrogen atom. In this section, we will see how this dynamical symmetry group naturally emerges in SU(2) lattice gauge theory. We will also study its role in describing $SU(2)$ loop dynamics through the loop Hamiltonian (5.34).

$\mathsf{L}_{ab} = \epsilon_{abc}\left(\mathcal{E}^c_- + \mathcal{E}^c_+\right)$	$\mathsf{L}_{45} = -\frac{i}{2}\left(k_+ - k_-\right)$	$\mathsf{L}_{a5} = \frac{1}{2} Tr\sigma_a \left(\mathcal{W}^{(+)} - \mathcal{W}^{(-)}\right)$	$\mathsf{L}_{56} = k_0$
$\mathsf{L}_{a4} = \left(\mathcal{E}^a_- - \mathcal{E}^a_+\right)$	$\mathsf{L}_{46} = \frac{1}{2}\left(k_+ + k_-\right)$	$\mathsf{L}_{a6} = \frac{i}{2} Tr\sigma_a \left(\mathcal{W}^{(+)} + \mathcal{W}^{(-)}\right)$	

Table 5.2: All possible 15 SU(2) tensor operators on a plaquette which are U(1) gauge invariant. They form SO(4,2) algebra. We have defined $\mathcal{W}^{(+)}_{\alpha\beta} \equiv -\tilde{a}^\dagger_\alpha b^\dagger_\beta$ and $\mathcal{W}^{(-)}_{\alpha\beta} \equiv a_\alpha \tilde{b}_\beta$.

We now discuss the structure of a general gauge invariant operator in $\mathcal{H}^p$. We first consider the single plaquette case. Any gauge invariant operator on a single plaquette can be created out of the loop creation, annihilation (k_+, k_-) and number operators (k_0). They

1. are invariant under U(1) gauge transformations (2.31) :

$$a_\alpha \to e^{i\theta} a_\alpha,$$

2. form $SU(1,1) \subset SO(4,2)$ algebra

$$[k_-, k_+] = 2k_0, \qquad [k_0, k_\pm] = \pm k_\pm \qquad \text{and}$$

3. generate transitions $|\mathsf{n}\rangle \to |\bar{\mathsf{n}}\rangle$ within the single plaquette hydrogen atom basis in $\mathcal{H}^p$.

Therefore, the dynamical symmetry group of SU(2) lattice gauge theory on a single plaquette is given by SU(1,1).

We now generalize the above three results to the entire lattice by constructing an algebra of U(1) invariant and $SU(2)$ gauge covariant operators. We will then see the action of these operators on $|n,l,m\rangle$ and show that they generate transitions $|n,l,m\rangle \to |\bar{n},\bar{l},\bar{m}\rangle$. We then show that this algebra is an SO(4,2) algebra as is expected from the corresponding result in hydrogen atom.

We note that all $4\mathcal{P}$ loop prepotential operators $\left(a^\dagger_\alpha(p),\ a_\beta(p)\right)$ and $\left(b^\dagger_\alpha(p),\ b_\beta(p)\right)$ of the theory transform as matter doublets under the global SU(2) gauge transformations. Therefore, the basic SU(2) tensor operators which are also invariant under U(1) gauge transformations of prepotentials can be classified[3] into the following four classes:

$$\Big[\ a^\dagger_\alpha(p) b^\dagger_\beta(p);\ \ a_\alpha(p)\ b_\beta(p);\ \ a^\dagger_\alpha(p) a_\beta(p);\ \ b^\dagger_\alpha(p) b_\beta(p)\ \Big] \quad p = 1, 2, \cdots, \mathcal{P}. \tag{5.25}$$

These are 16 SU(2) gauge covariant and U(1) gauge invariant operators on every plaquette of the lattice. The magnitude of the left and the right electric fields on every plaquette being equal, the number operators on each plaquette satisfy $a^\dagger(p)\cdot a(p) = b^\dagger(p)\cdot b(p) = \hat{N}(p)$.

3 Like single plaquette case, the remaining quadratic operators: $[a^\dagger_\alpha(p) a^\dagger_\beta(p), b^\dagger_\alpha(p) b^\dagger_\beta(p),\ a^\dagger_\alpha(p) b_\beta(p)]$ and their hermitian conjugates are not invariant under U(1) gauge transformations and therefore ignored.

Thus their number reduces to 15. These 15 operators on every plaquette, arranged as in Table 5.2, form SO(4,2) algebra[151] :

$$[\mathsf{L}_{AB}, \mathsf{L}_{CD}] = -i\ (g_{AC}\ \mathsf{L}_{BD}\ +\ g_{AD}\ \mathsf{L}_{CB}\ +\ g_{BC}\ \mathsf{L}_{DA}\ +\ g_{BD}\ \mathsf{L}_{AC}\ ). \tag{5.26}$$

Above, $A, B = 1, \cdots, 6$ and g_{AB} is the metric $(- - - - - + +)$. The algebra (5.26) can be explicitly checked using the prepotential representations of $\mathcal{E}^a_{\mp}$ and $\mathcal{W}_{\mp}$. Note that the fundamental loop quantization relations (3.46) are also contained in (5.26).

It is expected that since any gauge invariant operators can be constructed out of the above SO(4,2) generators, it forms the dynamical symmetry group of SU(2) lattice gauge theory. This can be seen as follows. Let $|\psi\rangle$ be a physical state and $\hat{\mathcal{O}}$ be any gauge invariant operator. Then the state $|\psi'\rangle \equiv \hat{\mathcal{O}}\,|\psi\rangle$ is also a physical state. As $|\psi\rangle\,, |\psi'\rangle \in \mathcal{H}^p$, both can be expanded in the "hydrogen atom loop basis". We, therefore, conclude that any gauge invariant operator $\hat{\mathcal{O}}$ will generate a transition:

$$|\mathsf{n}\ l\ m\rangle \ \xrightarrow{\hat{\mathcal{O}}}\ \sum_{\bar{\mathsf{n}},\bar{l},\bar{m}} O^{\bar{\mathsf{n}}\ \bar{l}\ \bar{m}}_{\mathsf{n}\ l\ m}\ |\bar{\mathsf{n}}\ \bar{l}\ \bar{m}\rangle\,.$$

Above, $O^{\bar{\mathsf{n}}\ \bar{l}\ m}_{\mathsf{n}\ l\ m}$ are some coefficients depending on the operator $\hat{\mathcal{O}}$.

We now show that any transition from $|n, l, m\rangle \to |\bar{n}, \bar{l}, \bar{m}\rangle$ can be achieved by the $SO(4,2)$ generators[151]. The operator L_{56} acts as a number operator which counts the n value ,

$$\mathsf{L}_{56}|nlm\rangle = n|nlm\rangle. \tag{5.27}$$

From the SO(4,2) algebra (table 5.2) , $[\mathsf{L}_{45}, \mathsf{L}_{46}] = i\mathsf{L}_{56}$. Therefore, $k_{\pm} = \mathsf{L}_{45} \mp i\mathsf{L}_{46}$ acts as ladder operators on n since $[\mathsf{L}_{56}, k_{\pm}] = \pm k_{\pm}$. Similarly, we define $\mathsf{L}_{\pm} = \mathsf{L}^{(1)} \pm \mathsf{L}^{(2)}$ and $\mathsf{A}_{\pm} = \mathsf{A}^{(1)} \pm \mathsf{A}^{(2)}$.

$$\begin{aligned}
k_+\ |n\ l\ m\rangle &= \sqrt{(n+1)(n+2)}\ |n+1\ l\ m\rangle,\\
k_-\ |n\ l\ m\rangle &= \sqrt{(n+1)(n-1)}\ |n-1\ l\ m\rangle,\\
\mathsf{L}^{(3)}\ |n\ l\ m\rangle &= m\ |n\ l\ m\rangle,\\
\mathsf{L}_{\pm}\ |n\ l\ m\rangle &= \mp\frac{1}{\sqrt{2}}\sqrt{(l \mp m)(l \pm m + 1)}\ |n\ l\ m \pm 1\rangle, \qquad (5.28)\\
\mathsf{A}^{(3)}\ |n\ l\ m\rangle &= c_1\ |n\ l+1\ m\rangle - c_2\ |n\ l-1\ m\rangle, \qquad (5.29)\\
\mathsf{A}_{\pm}\ |n\ l\ m\rangle &= d_1\ |n\ l\ m \pm 1\rangle + d_2\ |n\ l+1\ m \pm 1\rangle + d_3\ |n\ l-1\ m \pm 1\rangle. \qquad (5.30)
\end{aligned}$$

where

$$c_1 = \sqrt{\frac{(l-m+1)(l+m+1)}{(l+1)(2l+1)(2l+3)}}\langle n\ l+1||\mathsf{A}||n\ l\rangle; \qquad c_2 = -\sqrt{\frac{l^2-m^2}{l(2l-1)(2l+1)}}\langle n\ l-1||\mathsf{A}||n\ l\rangle;$$
$$d_1 = \mp\sqrt{\frac{(l\mp m)(l\pm m+1)}{2l(l+1)(2l+1)}}\langle n\ l||\mathsf{A}||n\ l\rangle; \qquad d_2 = \sqrt{\frac{(l\pm m+1)(l\mp m+2)}{2(l+1)(2l+1)(2l+3)}}\langle n\ l+1||\mathsf{A}||n\ l\rangle;$$
$$d_3 = \sqrt{\frac{(l\mp m)(l\mp m-1)}{2l(2l-1)(2l+1)}}\langle n\ l-1||\mathsf{A}||n\ l\rangle. \tag{5.31}$$

Since $\mathsf{L}^a = \frac{1}{2}\epsilon^{abc}\mathsf{L}_{bc}$ and $\mathsf{A}^a = \mathsf{L}_{a4}$, the above equations implies that the operators $\mathsf{L}_{ab}, \mathsf{L}_{a4}, \mathsf{L}_{45}$ and L_{46} allows us to pass from any loop basis state $|n_p, l_p, m_p\rangle$ to any other basis state $|n'_p, l'_p, m'_p\rangle$. But, these operators do not close under commutation. Therefore, introducing L_{a5} and L_{a6} for closure, we get the SO(4,2) algebra in table (5.2). Appropriate combination of the generators L_{a5} and L_{a6} can be used to construct flux creation and annihilation operators corresponding to bigger Wilson loops. These operators acting on separable states creates entangled states on the lattice. As an example, a flux creation operator for a 2 plaquette loop $Tr\{\mathcal{W}^+(p_1)\mathcal{W}^+(p_2)\}$ is given by

$$\frac{1}{2}\Big[\big(\mathsf{L}_{a5}(p_1) - i\mathsf{L}_{a6}(p_1)\big)\big(\mathsf{L}_{a5}(p_2) - i\mathsf{L}_{a6}(p_2)\big) - \big(\mathsf{L}_{45}(p_1) - i\mathsf{L}_{46}(p_1)\big)\big(\mathsf{L}_{45}(p_2) - i\mathsf{L}_{46}(p_2)\big)\Big].$$

The plaquette loop operator and the corresponding electric fields can be written in terms of $SO(4,2)$ generators.

$$\mathcal{W}_{\alpha\beta} = \frac{1}{2}(Tr\mathcal{W})\delta_{\alpha\beta} + Tr(\sigma^k\mathcal{W})\left(\frac{\sigma^k}{2}\right)_{\alpha\beta} = \left(\frac{-1}{\sqrt{\mathsf{L}_{56}}}\mathsf{L}_{46}\frac{1}{\sqrt{\mathsf{L}_{56}}}\right)\delta_{\alpha\beta} + \left(\frac{2i}{\sqrt{\mathsf{L}_{56}}}\mathsf{L}_{k6}\frac{1}{\sqrt{\mathsf{L}_{56}}}\right)\left(\frac{\sigma^k}{2}\right)_{\alpha\beta}; \tag{5.32}$$

$$\mathcal{E}^j_{\pm} = \frac{1}{2}\left(\frac{1}{2}\epsilon_{cab}L_{ab} \mp L_{c4}\right). \tag{5.33}$$

In the above, $a, b, c = 1, 2, 3$. Since any gauge invariant flux state on the lattice can be created using the generators of SO(4,2) algebra, the Hamiltonian can be written in terms of these operators. This is also clear from eqns. (5.32) and (5.33). for eg: The Hamiltonian for the single plaquette case is given by

$$H = 4g^2\mathcal{E}^2 - \frac{K}{g^2}Tr\mathcal{W} = g^2\left(L_{56}\right)^2 - \frac{K}{g^2}\frac{1}{\sqrt{L_{56}}}\mathsf{L}_{46}\frac{1}{\sqrt{L_{56}}}. \tag{5.34}$$

The finite plaquette Hamiltonian can also be written in terms of SU(2) invariant combinations of these SU(2) covariant and U(1) invariant SO(4,2) generators using equations (5.32) and (5.33). Therefore, SU(2) loop dynamics is governed by the generators of SO(4,2). These results

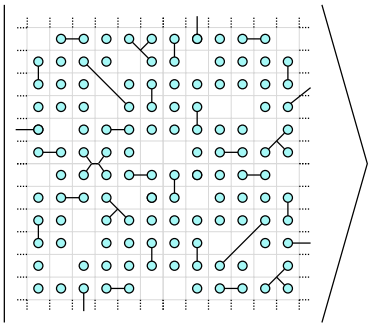

Figure 5.4: The SU(2) ground state picture in the hydrogen atom basis (3.80).

can also be appropriately generalized to higher SU(N) group by replacing SU(2) prepotential operators by SU(N) irreducible prepotential operators discussed in [102, 103].

5.3.0.1 *A variational ansatz*

The above correspondence between hydrogen atom and SU(2) gauge theory inspires the following simple variational ansatzes for the ground state $|\Psi_0\rangle$ and the first excited state $|\Psi_1\rangle$ of SU(2) lattice gauge theory:

$$\begin{aligned} |\Psi_0\rangle &= e^{\Gamma}\,|0\rangle\,, \qquad \langle\Psi_0|\,\Psi_0\rangle = 1, \\ |\Psi_1\rangle &= \Sigma^{+}\;|\Psi_0\rangle\,, \quad \langle\Psi_0|\,\Psi_1\rangle = 0. \end{aligned} \tag{5.35}$$

In (5.35) Γ and Σ are the $SU(2)\otimes U(1)$ gauge invariant operators constructed out of SO(4,2) generators in the Table 1. It is convenient to write $\Gamma = \Gamma^{+} - \Gamma^{-}$ where $\Gamma^{-} \equiv (\Gamma^{+})^{\dagger}$ and Γ^{+}, Σ^{+} have the structures:

$$\begin{aligned} \Gamma^{+} &\equiv G_1 \sum_{p=1}^{\mathcal{P}} k_{+}(p) + \sum_{p_1,p_2=1}^{\mathcal{P}} G_2(|p_1-p_2|)\,\vec{k}_{+}(p_1)\cdot\vec{k}_{+}(p_2) + \cdots, \\ \Sigma^{+} &\equiv F_1 \sum_{p=1}^{\mathcal{P}} k_{+}(p) + \sum_{p_1,p_2=1}^{\mathcal{P}} F_2(|p_1-p_2|)\,\vec{k}_{+}(p_1)\cdot\vec{k}_{+}(p_2) + \cdots. \end{aligned} \tag{5.36}$$

In the first term above $k_{+}(p)$ is the gauge invariant $SU(1,1) \in SO(4,2)$ plaquette loop creation operator. In the second term, we have defined SU(2) adjoint loop flux creation operator $\vec{k}_{+}(p)$ on every plaquette p using SO(4,2) generators in Table 1:

$$k^{a}_{+}(p) \equiv L_{a5}(p) - iL_{a6}(p) \;=\; Tr(\sigma^{a}\,W^{(+)}),\;\; a = 1,2,3.$$

Note that the expansion (5.36) is in terms of number of fundamental loops and not in terms of coupling constant. In fact, g^2 dependence of the structure functions $G_1,\ G_2, \cdots$ and $F_1,\ F_2, \cdots$ have been completely suppressed. The physical interpretations of (5.35) and (5.36) are extremely simple. The operator e^{Γ} acting on the strong coupling vacuum in (5.35)

creates loops of all shapes and sizes in terms of the fundamental loop operators to produce the ground state $|\Psi_0\rangle$. The first term $k_+(p)$ in (5.36) creates hydrogen atom s-states on plaquette p or simple one plaquette loops. These are shown as small circles (tadpoles without legs) in Figure 5.4. The second term describes doublets of hydrogen atoms with vanishing total angular momentum. These are shown as two tadpoles joined together in Figure 5.4. The three hydrogen atom or three tadpole states over three plaquettes (p_1, p_2, p_3) can be created by including a term of the form $\left(\vec{k}_+(p_1) \times \vec{k}_+(p_2)\right) \cdot \vec{k}_+(p_3)$ in Γ^+ and so on and so forth. As shown in Figure 5.4, the ground state is a soup of all such coupled tadpoles or coupled hydrogen atom clusters, each with vanishing angular momentum. The first excited state in (5.36) is obtained by exciting loops in this ground state by a creation operator Σ^+. The sizes of the "hydrogen atom clusters" and their importance depend on the structure functions G and F which in turn are fixed by the loop Schrödinger equation with Hamiltonian (3.86). These qualitative features can be made more precise by putting the ansatz (5.35) in (3.86). The resulting Schrödinger equation can be analyzed for the structure constants[4] $(G_1,\ G_2, \cdots)$ and $(F_1,\ F_2, \cdots)$ in the complete, orthonormal hydrogen atom loop basis (3.80) using its dynamical symmetry group SO(4,2) algebra in (5.26).

4 A reasonable assumption is $G_1 >> G_2 >> \cdots$, $F_1 >> F_2 >> \cdots$ in (5.36). In this case the matrix elements of δH in (3.86) are small in the states in (5.35): $\langle\Psi_0|\,\delta H\,|\Psi_0\rangle \approx 0$ and $\langle\Psi_1|\,\delta H\,|\Psi_1\rangle \approx 0$ as $[\mathsf{L}^a(p), k_\mp(p)] = 0$ and $\mathsf{L}^a\,|0\rangle = 0$.

6

SUMMARY AND FUTURE DIRECTIONS

SU(N) Mandelstam constraints were the major stumbling block in the conventional loop formulation of lattice gauge theories near the weak coupling (continuum) limit. In SU(2) lattice gauge theory, all Mandelstam constraints could be solved by constructing a spin network basis. As discussed in chapter 2, this introduces new triangular constraints and the dynamics becomes very complicated. All these issues of over-completeness of loop basis stems from the fact that there is no systematic method to go from the standard link formulation of Kogut and Susskind to a loop formulation. In this thesis, we have constructed a series of canonical transformations from the standard link variables to fundamental plaquette loop variables and string variables. String variables naturally decouple due to the Gauss law constraints, leaving behind a loop formulation which is free of local constraints. Since the transformation is one-one, no new constraints are introduced. This canonical transformation method of constructing a loop formulation was developed for SU(N) lattice gauge theory in 2+1 and 3+1 dimensions. Also, in the resulting loop basis, the magnetic part of the Hamiltonian, which is important in the weak coupling limit, takes the simplest possible form. It is a single plaquette loop holonomy instead of product of 4 link holonomies in the Kogut-Susskind formulation. In the angular momentum description of SU(2) lattice gauge theory, for instance, the matrix element of TrU_p becomes a 6j symbol instead of a 18j symbol. We showed that the canonical transformation techniques developed in this thesis can also be applied to Z_2 Ising model and Z_2 lattice gauge theory to obtain old and well known Kramers-Wannier and Wegner gauge-spin dualities respectively. We further showed that the resulting SU(N) loop formulation is dual to the link formulation of SU(N) lattice gauge theory due to Kogut and Susskind. In fact, as discussed in chapter 4, $SU(N)$ duality is a generalization of Wegners duality between Z_2 lattice gauge theory and quantum Ising model in 2+1 dimensions. The non-local part of the loop/spin Hamiltonian is proportional to atleast g^3. Therefore, in the weak coupling continuum limit, $g^2 \to 0$, the non-local terms may be ignored to compute low energy spectrum. These issues are under investigation.

A gauge invariant loop basis was constructed for SU(2) lattice gauge theory by coupling together electric fields conjugate to the fundamental plaquette loop operators and diagonalizing them. The global gauge invariance is imposed by requiring that the total loop electric field is 0. This lead to an exact isomorphism between the physical Hilbert space of SU(2) lattice gauge theory and that of a collection of hydrogen atoms (one for each plaquette) with no net angular momentum. We also constructed an angular basis which diagonalizes all

Wilson loops. In the above angular basis, the Schrodinger equation for the free part of the Hamiltonian leads to a Mathieus equation for the single plaquette case.

We now briefly discuss some new future directions. Having reformulated pure SU(N) gauge theory in terms of loop variables without any local Gauss law, Mandelstam or other constraints, the natural next step is to solve the Hamiltonian to get the spectrum. We note that the magnetic part of the loop Hamiltonian does not contain any interactions. This is unlike the Kogut-Susskind picture where all the interactions are contained in this term. This makes the loop picture suitable for a weak coupling loop expansion. Many of the the standard methods of solution like variational method, coupled cluster method etc becomes much more simpler in the loop formulation. The $SU(N)$ gauge-spin duality should also allow us to compute the gauge theory spectrum using techniques like tensor networks, Matrix product states etc which have been extensively used in the context of spin models [155–159]

It is well known [56, 122] that Z_2 lattice gauge theory is self dual in $3+1$ dimensions. The Hamiltonian of Z_2 lattice gauge theory in $3+1$ dimensions is given by

$$H = -\sum_{links} \sigma_1 - \lambda \sum_{plaquettes} \sigma_3\sigma_3\sigma_3\sigma_3.$$

Just like in the $2+1$ case, there is a local Gauss law constraint at each lattice site n. But, unlike $2+1$ dimensions, in $3+1$ dimensions there are Bianchi identities which state that the product of σ_3 operators along the plaquettes which form the faces of a basic cube $= 1$. A dual lattice can be defined as follows : The sites of the dual lattice are given by the centre of each basic cube of the original lattice. Links of dual lattice passes through the plaquettes of the original lattice. The dual operators $\{\mu_1, \mu_3\}$ lying on the dual lattice can be defined through the following relations[56, 122]:

$$\mu_1 = \sigma_3\sigma_3\sigma_3\sigma_3; \qquad\qquad \sigma_1 = \mu_3\mu_3\mu_3\mu_3.$$

The second equation above can be inverted [56, 122] within the axial gauge to give a non-local duality relation. The resulting dual Hamiltonian in terms of the μ variable is :

$$H = \lambda \left(-\sum_{dual\ links} \mu_1 - \frac{1}{\lambda} \sum_{dual\ plaq} \mu_3\mu_3\mu_3\mu_3 \right).$$

Therefore, the dual theory is also a Z_2 lattice gauge theory in terms of the μ variables with an inverted coupling constant $\frac{1}{\lambda}$. The above self duality can be obtained systematically by a series of canonical transformations. The fundamental link operators in terms of which Z_2 lattice gauge theory is described get transformed into fundamental plaquette loop operators over each plaquette on the lattice. This leads to a dual theory with the fundamental degrees of freedom lying on plaquettes (or dual links piercing the plaquettes). Such canonical

transformations will transform Gauss law constraints on the original lattice in terms of σ operators to Bianchi identities on the dual lattice in terms of μ operators and vice versa. It will be interesting to generalize Z_2 duality/canonical transformations to SU(N) lattice gauge theory in $(3+1)$ dimensions. It is expected that the roles of SU(N) Gauss law and SU(N) Bianchi identity constraints will get interchanged under such canonical/duality transformations. Construction of such a duality should proceed similar to the canonical transformations described in the thesis. The essential difference being that there would not be any string operators which decouple due to local Gauss laws. These canonical transformations are under investigation.

The loop formulation also provides a natural framework to study the entanglement entropy in gauge theories. The absence of local SU(N) Gauss laws should help us in defining entanglement entropy in lattice gauge theories. The entanglement entropy of two complimentary regions in a gauge invariant state suffers from serious obstacles [160, 161] created by SU(N) Gauss laws at the boundary. In the present formulation the two regions can have mutually independent hydrogen atom/tadpole basis which are coupled together across the boundary through a single flux line at the end. The present loop approach may also be interesting in the context of cold atom experiments [162–165]. The hydrogen atom interpretation of $\mathcal{H}^P$ and absence of local gauge invariance should bypass the challenging task of imposing non-trivial and exotic non-abelian Gauss law constraints at every lattice site in the laboratory. Quantum simulations of $SU(2)$ lattice gauge theory can be realized by trapping hydrogen like atoms on an optical lattice.

In this thesis, we constructed the loop formulation of pure SU(N) lattice gauge theory without matter fields. Next step would be to study the inclusion of matter fields into the loop picture. Again, we start with the Kogut-Susskind picture where matter fields are introduced on the sites of the lattice. This modifies the Gauss law at each site of the lattice to :

$$\left[\sum_{i=1}^{d} E^a_-(n,i) + E^a_+(n,i) + \rho^a(n)\right] |\psi_{phys}\rangle = 0.$$

Above, d is the dimensionality of space and $\rho^a(n)$ is the color density of matter field at the site n. This implies that, after the canonical transformations described in the thesis, the string degrees of freedom no longer decouple. Therefore, further canonical transformations are needed to isolate the redundant degrees of freedom which decouples from the physical Hilbert space to solve the local Gauss law constraints. This will be pursued in a future work.

Appendices

A

CANONICAL TRANSFORMATIONS ON A FINITE LATTICE

In this appendix, We give the details of canonical transformations and their inverse transformations in $2+1$D on a finite lattice for Z_2 (section A.1) and $SU(N)$ (section A.2) lattice gauge theory. Canonical transformations in $3+1$D is illustrated on a single cube in section A.3 for both Z_2 as well as $SU(N)$ lattice gauge theory.

A.1 Z_2 LATTICE GAUGE THEORY IN $2+1$ DIMENSIONS

A.1.1 *From links to loops & strings*

In this section, we describe the canonical transformation involved in the construction of the loop/spin formulation of Z_2 lattice gauge theory on a finite lattice. The net canonical transformation leads to the duality relation between the basic operators of Z_2 gauge theory and Ising model in $2+1$ dimensions. Construction of this duality relation on a single plaquette was described in section 3.1.2. We now generalize the duality transformation relation to a finite lattice by iterating the plaquette canonical transformation (C.T) ((3.20),(3.21)) all over the two dimensional lattice starting from the top left plaquette of the lattice and systematically repeating it from top to bottom and left to right. We will illustrate this procedure on a 2×2 lattice which contains all the essential features of the construction on any finite lattice. The sites of the lattice are labelled as $O\equiv(0,0), A\equiv(0,1), B\equiv(0,2), C\equiv(1,0), D\equiv(1,1), E\equiv(1,2), F\equiv(2,0), G\equiv(2,1), H\equiv(2,2)$ and the plaquettes are numbered from top to bottom and left to right (see Figure A.1) for convenience. The dual spin operators are constructed on a 2×2 lattice in 4 steps.

1. We begin by performing the plaquette canonical transformation (3.20),(3.21) on plaquette 1. The spin conjugate operators $\{\mu_1(1);\mu_3(1)\}$ on plaquette 1 are

$$\begin{aligned}\mu_1(1)\equiv\mu_1(E)&=\sigma_3(A,\hat{1})\sigma_3(D,\hat{2})\sigma_3(B,\hat{1})\sigma_3(A,\hat{2}),\\ \mu_3(1)\equiv\mu_3(E)&=\sigma_1(B,\hat{1}).\end{aligned}\tag{A.1}$$

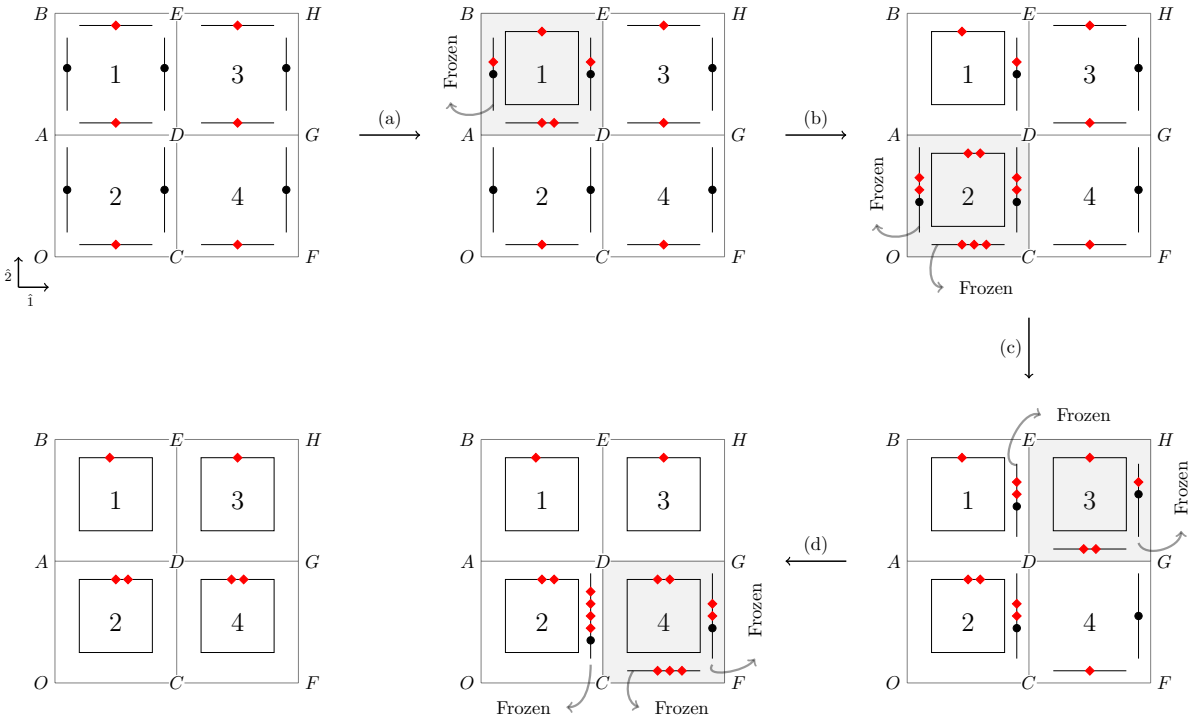

Figure A.1: The 'plaquette' canonical transformations involved in the construction of the duality transformation between Z_2 lattice gauge theory and Z_2 spin model on a 2×2 lattice. The steps (a), (b), (c) and (d) are plaquette CTs on plaquettes 1, 2, 3 and 4 respectively. The electric field $\sigma_1(l)$ corresponding to the vertical and horizontal links are denoted by • and ♦ respectively.

The redefined link and string operators around plaquette 1 are

$$\sigma_{3[x]}(D,\hat{2}) = \sigma_3(D,\hat{2}), \qquad \sigma_{1[x]}(D,\hat{2}) = \sigma_1(D,\hat{2})\sigma_1(B,\hat{1})$$
$$\sigma_{3[x]}(A,\hat{2}) = \sigma_3(A,\hat{2}), \qquad \sigma_{1[x]}(A,\hat{2}) = \sigma_1(A,\hat{2})\sigma_1(B,\hat{1})$$
$$\sigma_{3[x]}(A,\hat{1}) = \sigma_3(A,\hat{1}), \qquad \sigma_{1[x]}(A,\hat{1}) = \sigma_1(A,\hat{1})\sigma_1(B,\hat{1}).$$

Our notation is such that $\sigma_3(A,\hat{1})$ denotes the σ_3 operator corresponding to the link which starts at site A and is in the $\hat{1}$ direction. The subscript $[x]$ on $\sigma_{3[x]}(A,\hat{1})$ indicates that the electric field $\sigma_1(A,\hat{1})$ absorbs the electric field of the vanishing horizontal link $(B,\hat{1})$ to become $\sigma_{1[x]}(A,\hat{1})$ during the plaquette canonical transformation. Note that by our convention, the plaquette or spin operators are labelled by the top right corner of the plaquette. This plaquette canonical transformation is illustrated in Figure A.1 (a). As a result of Gauss law at B:

$$\sigma_{1[x]}(A,\hat{2}) \equiv \mathcal{G}(B) \approx 1.$$

Therefore, $\left\{\sigma_{1[x]}(A,\hat{2}); \sigma_{3[x]}(A,\hat{2})\right\} \equiv \{\bar{\sigma}_1(B); \bar{\sigma}_3(B)\}$ are frozen and hence decouple from the physical Hilbert space. Again, as in the main text, the string operators are labelled by their right/top endpoints. We are now left with the conjugate spin opera-

tors $\{\mu_1(1);\mu_3(1)\}$ and the two link conjugate pair operators $\{\sigma_{1[x]}(D,\hat{2});\ \sigma_{3[x]}(D,\hat{2})\}$, $\{\sigma_{1[x]}(A,\hat{1});\ \sigma_{3[x]}(A,\hat{1})\}$. These link operators undergo further canonical transformations.

2. We now iterate the plaquette canonical transformation. on plaquette 2 to construct the spin or plaquette conjugate operators $\{\mu_1(2);\mu_3(2)\}$ and the link conjugate operators $\left\{\sigma_{1[x]}(C,\hat{2});\sigma_{3[x]}(C,\hat{2})\right\}$, $\left\{\sigma_{1[x]}(O,\hat{1});\sigma_{3[x]}(O,\hat{1})\right\}$, $\left\{\sigma_{1[x]}(O,\hat{2});\sigma_{3[x]}(O,\hat{2})\right\}$ as illustrated in Figure A.1-b. The spin operators are

$$\begin{aligned}\mu_1(2) \equiv \mu_1(D) &= \sigma_3(A,\hat{1})\sigma_3(O,\hat{2})\sigma_3(O,\hat{1})\sigma_3(C,\hat{2}),\\ \mu_3(2) \equiv \mu_3(D) &= \sigma_{1[x]}(A,\hat{1}) = \sigma_1(A,\hat{1})\sigma_1(B,\hat{1})\end{aligned} \tag{A.2}$$

The redefined link and new string operators around plaquette 2 are

$$\begin{aligned}\sigma_{3[x]}(C,\hat{2}) &= \sigma_3(C,\hat{2}), & \sigma_{1[x]}(C,\hat{2}) &= \sigma_1(C,\hat{2})\sigma_{1[x]}(A,\hat{1}) = \sigma_1(C,\hat{2})\sigma_1(A,\hat{1})\sigma_1(B,\hat{1})\\ \sigma_{3[x]}(O,\hat{1}) &= \sigma_3(O,\hat{1}), & \sigma_{1[x]}(O,\hat{1}) &= \sigma_1(O,\hat{1})\sigma_{1[x]}(A,\hat{1}) = \mathcal{G}(O)\mathcal{G}(A)\mathcal{G}(B) \approx 1\\ \sigma_{3[x]}(O,\hat{2}) &= \sigma_3(O,\hat{2}), & \sigma_{1[x]}(O,\hat{2}) &= \sigma_1(O,\hat{2})\sigma_{1[x]}(A,\hat{1}) = \mathcal{G}(A)\mathcal{G}(B) \approx 1.\end{aligned}$$

Thus the string conjugate pairs $\left\{\sigma_{1[x]}(O,\hat{1});\sigma_{3[x]}(O,\hat{1})\right\} \equiv \left\{\bar{\sigma}_1(C);\bar{\sigma}_3(C)\right\}$ and $\left\{\sigma_{1[x]}(O,\hat{2});\right.$ $\left.\sigma_{3[x]}(O,\hat{2})\right\} \equiv \left\{\bar{\sigma}_1(A);\bar{\sigma}_3(A)\right\}$ are frozen due to Gauss law at O, A and B.

3. The third step involves iterating the plaquette canonical transformation. on plaquette 3 as shown in Figure A.1(c). This leads to decoupling of $\left\{\sigma_{1[x]}(G,\hat{2});\ \sigma_{3[x]}(G,\hat{2})\right\} \equiv$ $\left\{\bar{\sigma}_1(H);\bar{\sigma}_3(H)\right\}$, $\left\{\sigma_{1[xx]}(D,\hat{2});\ \sigma_{3[xx]}(D,\hat{2})\right\} \equiv \left\{\bar{\sigma}_1(E);\bar{\sigma}_3(E)\right\}$ due to the Z_2 Gauss laws at E and H. The canonical transformations on plaquette 3 defining the spins are

$$\begin{aligned}\mu_1(3) \equiv \mu_1(H) &= \sigma_3(E,\hat{1})\sigma_3(G,\hat{2})\sigma_3(D,\hat{1})\sigma_3(D,\hat{2}),\\ \mu_3(3) \equiv \mu_3(H) &= \sigma_3(E,\hat{1}).\end{aligned} \tag{A.3}$$

The redefined links and strings around plaquette 3 are

$$\begin{aligned}\sigma_{3[xx]}(D,\hat{2}) = \sigma_{3[x]}(D,\hat{2}) &= \sigma_3(D,\hat{2}), & \sigma_{1[xx]}(D,\hat{2}) &= \sigma_{1[x]}(D,\hat{2})\sigma_1(E,\hat{1}) = \mathcal{G}(E) \approx 1\\ \sigma_{3[x]}(G,\hat{2}) &= \sigma_3(G,\hat{2}), & \sigma_{1[x]}(G,\hat{2}) &= \sigma_1(G,\hat{2})\sigma_1(E,\hat{1}) = \mathcal{G}(H) \approx 1\\ \sigma_{3[x]}(D,\hat{1}) &= \sigma_3(D,\hat{1}), & \sigma_{1[x]}(D,\hat{1}) &= \sigma_1(D,\hat{1})\sigma_1(E,\hat{1})\end{aligned} \tag{A.4}$$

4. Finally, we iterate the plaquette canonical transformation. on plaquette 4 which are shown in Figure A.1(d). The conjugate spin operators $\{\mu_1(4);\mu_3(4)\}$ on plaquette 4 are

$$\begin{aligned}\mu_1(4) \equiv \mu_1(G) &= \sigma_3(D,\hat{1})\sigma_3(F,\hat{2})\sigma_3(C,\hat{1})\sigma_3(C,\hat{2}),\\ \mu_3(4) \equiv \mu_3(G) &= \sigma_{1[x]}(D,\hat{1}) = \sigma_1(D,\hat{1})\sigma_1(E,\hat{1})\end{aligned} \tag{A.5}$$

The remaining string operators are

$$\begin{gathered}\sigma_{3[xx]}(C,\hat{2}) = \sigma_{3[x]}(C,\hat{2}) = \sigma_3(C,\hat{2}),\\ \sigma_{1[xx]}(C,\hat{2}) = \sigma_{1[x]}(C,\hat{2})\sigma_{1[x]}(D,\hat{1}) = \mathcal{G}(D)\mathcal{G}(E) \approx 1\\ \sigma_{3[x]}(C,\hat{1}) = \sigma_3(C,\hat{1})\\ \sigma_{1[x]}(C,\hat{1}) = \sigma_1(C,\hat{1})\sigma_{1[x]}(D,\hat{1}) = \mathcal{G}(C)\mathcal{G}(O)\mathcal{G}(A)\mathcal{G}(D)\mathcal{G}(B)\mathcal{G}(E) \approx 1\\ \sigma_{3[x]}(F,\hat{2}) = \sigma_3(F,\hat{2}),\\ \sigma_{1[x]}(F,\hat{2}) = \sigma_1(F,\hat{2})\sigma_{1[x]}(D,\hat{1}) = \mathcal{G}(G)\mathcal{G}(H) \approx 1.\end{gathered} \tag{A.6}$$

Gauss laws at O, A, B, C, D, E, G and H implies that the remaining string operators $\left\{\sigma_{1[xx]}(C,\hat{2});\sigma_{3[xx]}(C,\hat{2})\right\} \equiv \{\bar{\sigma}_1(D);\bar{\sigma}_3(D)\}$, $\left\{\sigma_{1[x]}(C,\hat{1});\sigma_{3[x]}(C,\hat{1})\right\} \equiv \{\bar{\sigma}_1(F);\bar{\sigma}_3(F)\}$ and $\left\{\sigma_{1[x]}(F,\hat{2});\sigma_{3[x]}(F,\hat{2})\right\} \equiv \{\bar{\sigma}_1(G);\bar{\sigma}_3(G)\}$ are frozen. As a result, after the series of 4 plaquette canonical transformation.s, all the Gauss law constraints are solved. Only the plaquette/spin variables $\{\mu_1(1);\mu_3(1)\}, \{\mu_1(2);\mu_3(2)\}, \{\mu_1(3);\mu_3(3)\}$ and $\{\mu_1(4);\mu_3(4)\}$ remains in the physical Hilbert space. This leads to a dual Z_2 spin model. These results can be directly generalized to any finite lattice without any new issues, to give the duality relations (3.26a),(3.26b), (3.28a)-(3.28b).

A.1.2 *From loops & strings to links (Inverse transformations)*

In this section we will Invert the above transformations to write down the link operators $\{\sigma_1(n,\hat{i}), \sigma_2(n,\hat{i}\}$ in terms of the plaquette and string variables,$\{\mu_1(p),\mu_3(p)\}$ and $\{\bar{\sigma}_1(n,\hat{i}), \bar{\sigma}_3(n,\hat{i})\}$ respectively. We will consider a 2×2 lattice and explicitly construct these inverse relations by inverting the steps 4-1 involved in the construction of the loop formulation described in the previous section.

1. We start by inverting step (4) in section A.1.1 by the inverse transformation:
$\Big[\mu(4), \sigma_{[x]}(F,\hat{2}), \sigma_{[x]}(C,\hat{1}), \sigma_{[xx]}(C,\hat{2})\Big] \to \Big[\sigma(F,\hat{2}), \sigma(C,\hat{1}), \sigma_{[x]}(C,\hat{2}), \sigma_{[x]}(D,\hat{1})\Big]$.

$$\sigma_{3[x]}(D,\hat{1}) = \mu_1(4)\sigma_{3[x]}(F,\hat{2})\sigma_{3[x]}(C,\hat{1})\sigma_{3[xx]}(C,\hat{2}) = \mu_1(4)\bar{\sigma}_3(G)\bar{\sigma}_3(F)\bar{\sigma}_3(D);$$
$$\sigma_{1[x]}(D,\hat{1}) = \mu_3(4) \tag{A.7}$$
$$\sigma_3(F,\hat{2}) = \sigma_{3[x]}(F,\hat{2}) = \bar{\sigma}_3(G); \qquad \sigma_1(F,\hat{2}) = \sigma_{1[x]}(F,\hat{2})\mu_3(4) = \bar{\sigma}_1(G)\mu_3(4)$$
$$\sigma_3(C,\hat{1}) = \sigma_{3[x]}(C,\hat{1}) = \bar{\sigma}_3(F); \qquad \sigma_1(C,\hat{1}) = \sigma_{1[x]}(C,\hat{1})\mu_3(4) = \bar{\sigma}_1(F)\mu_3(4)$$
$$\sigma_{3[x]}(C,\hat{2}) = \sigma_{3[xx]}(C,\hat{2}) = \bar{\sigma}_3(D); \qquad \sigma_{1[x]}(C,\hat{2}) = \sigma_{1[xx]}(C,\hat{2})\mu_3(4) = \bar{\sigma}_1(D)\mu_3(4)$$

In the above, the σ without a subscript 1 or 3 denotes the conjugate pair $\{\sigma_1, \sigma_3\}$. Same is true for μ also.

2. Inverting step (3) in section A.1.1 by the inverse transformation :
$\Big[\mu(3), \sigma_{[x]}(D,\hat{1}), \sigma_{[x]}(G,\hat{2}), \sigma_{[xx]}(D,\hat{2})\Big] \to \Big[\sigma(D,\hat{1}), \sigma(G,\hat{2}), \sigma(E,\hat{1}), \sigma_{[x]}(D,\hat{2})\Big]$.

$$\sigma_3(D,\hat{1}) = \sigma_{3[x]}(D,\hat{1}) = \mu_1(4)\bar{\sigma}_3(G)\bar{\sigma}_3(F)\bar{\sigma}_3(D);$$
$$\sigma_1(D,\hat{1}) = \sigma_{1[x]}(D,\hat{1})\mu_3(3) = \mu_3(4)\mu_3(4). \tag{A.8}$$
$$\sigma_3(G,\hat{2}) = \sigma_{3[x]}(G,\hat{2}) = \bar{\sigma}_3(H); \qquad \sigma_1(G,\hat{2}) = \sigma_{1[x]}(G,\hat{2})\mu_3(3) = \bar{\sigma}_1(H)\mu_3(3).$$
$$\sigma_{3[x]}(D,\hat{2}) = \sigma_{3[xx]}(D,\hat{2}) = \bar{\sigma}_3(E); \qquad \sigma_{1[x]}(D,\hat{2}) = \sigma_{1[xx]}(D,\hat{2})\mu_3(3) = \bar{\sigma}_1(E)\mu_3(4).$$
$$\sigma_3(E,\hat{1}) = \mu_{1[3]}\sigma_{3[x]}(G,\hat{2})\sigma_{3[x]}(D,\hat{1})\sigma_{3[x]}(D,\hat{2}) = \mu_1(3)\bar{\sigma}_3(H)\mu_1(4)\bar{\sigma}_3(G)\bar{\sigma}_3(F)\bar{\sigma}_3(D)\bar{\sigma}_3(E);$$
$$\sigma_1(E,\hat{1}) = \mu_3(3).$$

3. Inverting step (2) in section A.1.1 by the inverse transformation :
$\Big[\mu(2), \sigma_{[x]}(C,\hat{2}), \sigma_{[x]}(O,\hat{1}), \sigma_{[x]}(O,\hat{2})\Big] \to \Big[\sigma(O,\hat{1}), \sigma(O,\hat{2}), \sigma(C,\hat{2}), \sigma(A,\hat{1})\Big]$.

$$\sigma_3(O,\hat{1}) = \sigma_{3[x]}(O,\hat{1}) = \bar{\sigma}_3(C); \qquad \sigma_1(O,\hat{1}) = \sigma_{1[x]}(O,\hat{1})\mu_3(2) = \bar{\sigma}_1(C)\mu_3(2).$$
$$\sigma_3(O,\hat{2}) = \sigma_{3[x]}(O,\hat{2}) = \bar{\sigma}_3(A); \qquad \sigma_1(O,\hat{2}) = \sigma_{1[x]}(O,\hat{2})\mu_3(2) = \bar{\sigma}_1(A)\mu_3(2).$$
$$\sigma_3(C,\hat{2}) = \sigma_{3[x]}(C,\hat{2}) = \bar{\sigma}_3(D); \qquad \sigma_1(C,\hat{2}) = \sigma_{1[x]}(C,\hat{2})\mu_3(2) = \bar{\sigma}_1(D)\mu_3(2).$$
$$\sigma_{3[x]}(A,\hat{1}) = \mu_1(2)\sigma_{3[x]}(C,\hat{2})\sigma_{3[x]}(O,\hat{2})\sigma_{3[x]}(O,\hat{1}) = \mu_1(2)\bar{\sigma}_3(D)\bar{\sigma}_3(C)\bar{\sigma}_3(A);$$
$$\sigma_{1[x]}(A,\hat{1}) = \mu_3(2). \tag{A.9}$$

4. Inverting step (1) in section A.1.1 by the inverse transformation :
$\Big[\mu(1), \sigma_{[x]}(D,\hat{2}), \sigma_{[x]}(A,\hat{1}), \sigma_{[x]}(A,\hat{2})\Big] \rightarrow \Big[\sigma(A,\hat{1}), \sigma(D,\hat{2}), \sigma(B,\hat{1}), \sigma(A,\hat{2})\Big]$.

$$\begin{gathered}
\sigma_3(A,\hat{1}) = \sigma_{3[x]}(A,\hat{1}) = \mu_1(2)\bar{\sigma}_3(D)\bar{\sigma}_3(C)\bar{\sigma}_3(A); \\
\sigma_1(A,\hat{1}) = \sigma_{1[x]}(A,\hat{1})\mu_3(1) = \mu_3(4)\mu_3(1). \\
\sigma_3(O,\hat{2}) = \sigma_{3[x]}(O,\hat{2}) = \bar{\sigma}_3(C); \qquad \sigma_1(O,\hat{2}) = \sigma_{1[x]}(O,\hat{2})\mu_3(1) = \bar{\sigma}_1(E)\mu_3(3)\mu_3(1). \\
\sigma_3(B,\hat{1}) = \mu_1(1)\sigma_{3[x]}(D,\hat{2})\sigma_{3[x]}(A,\hat{1})\sigma_{3[x]}(A,\hat{2}) = \mu_1(1)\bar{\sigma}_3(E)\bar{\sigma}_3(D)\bar{\sigma}_3(B); \\
\sigma_1(B,\hat{1}) = \mu_3(1). \\
\sigma_3(A,\hat{2}) = \sigma_{3[x]}(A,\hat{2}) = \bar{\sigma}_3(B); \qquad \sigma_1(A,\hat{2}) = \sigma_{1[x]}(A,\hat{2})\mu_3(1) = \bar{\sigma}_1(B)\mu_3(1).
\end{gathered} \tag{A.10}$$

We now show that the local Gauss laws at all the sites are redundant in terms of the new dual variables. Consider the 4 links meeting at a site (x,y).

$$\begin{aligned}
\sigma_1(x,y,\hat{1}) &= \mu_3(x+1,y)\mu_3(x+1,y+1) \\
\sigma_1(x,y,\hat{2}) &= \mu_3(x,y+1)\mu_3(x+1,y+1) \\
\sigma_1(x-1,y,\hat{1}) &= \mu_3(x,y+1)\mu_3(x,y) \\
\sigma_1(x,y-1,\hat{2}) &= \mu_3(x,y)\mu_3(x+1,y)
\end{aligned}$$

Therefore, $\mathcal{G}^a(x,y) = \sigma_1(x,y,\hat{1})\sigma_1(x,y,\hat{2})\sigma_1(x-1,y,\hat{1})\sigma_1(x,y-1,\hat{2}) = 1$.

A.2 SU(N) LATTICE GAUGE THEORY IN 2 + 1 DIMENSIONS

A.2.1 *From links to loops & strings*

In this section, we generalize the three canonical transformations (3.36), (3.39) and (3.40) in the single plaquette case to the entire lattice in two dimension. We define a comb shaped maximal tree with its base along the X axis and make a series of canonical transformations along the maximal tree to construct the string operators $\mathsf{T}_{[xxyy]}(x,y)$ attached to each lattice site (x,y) away from the origin. This is similar to the construction of string operators $\mathsf{T}_{[xy]}(x,y)$ attached to the points $A \equiv (1,0)$, $B \equiv (1,1)$ and $C \equiv (0,1)$ in the simple single plaquette example illustrated in Figure 3.10-a,b,c. The gauge covariant loop operators $\mathcal{W}(x,y)$ are constructed by fusing the string operators with the horizontal link operators $U(x,y;\hat{1})$ again through canonical transformations. As expected, all string operators $\mathsf{T}_{[xxyy]}(x,y)$ decouple as a consequence of SU(N) Gauss laws $\mathcal{G}^a(x,y) = 0$. Thus only the fundamental physical loop operators are left at the end. The iterative canonical transformations are performed in 6 steps. These 6 steps are also illustrated graphically for the sake of clarity.

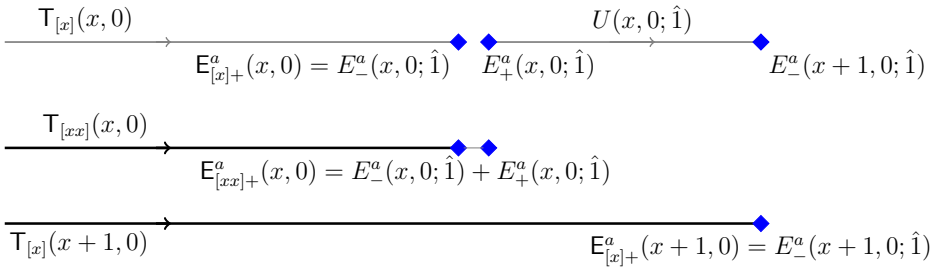

Figure A.2: Graphical representation of the iterative canonical transformations (A.11). The initial $\mathsf{T}_{[x]}(x,0)$ and the final $\mathsf{T}_{[xx]}(x,0)$ string operators at $(x,0)$ are shown. The string operator $\mathsf{T}_{[x]}(x+1,0)$ in the third row replaces $\mathsf{T}_{[x]}(x,0)$ in the first row in the next iterative step. All electric fields involved in (A.11) are also shown along with their locations.

A.2.1.1 *Strings along x axis*

We start by defining iterative canonical transformation along the x axis. They transform the N link operators $U(x,0;\hat{1})$ into N string operators $\mathsf{T}_{[xx]}(x,0)$. These string operators start at the origin and end at $x = 1,2,\cdots \mathsf{N}_s - 1$ along the x axis as shown in the Figure A.2. The canonical transformations are defined iteratively as:

$$\begin{aligned} \mathsf{T}_{[x]}(x+1,y=0) &\equiv \mathsf{T}_{[x]}(x,0)\ U(x,0;\hat{1}), & \mathsf{T}_{[xx]}(x,0) &\equiv \mathsf{T}_{[x]}(x,0), \\ \mathsf{E}^a_{[x]+}(x+1,0) &= E^a_-(x+1,0;\hat{1}), & \mathsf{E}^a_{[xx]+}(x,0) &= E^a_-(x,0;\hat{1}) + E^a_+(x,0;\hat{1}). \end{aligned} \tag{A.11}$$

Above $x = 1,\cdots,\mathsf{N}_s - 1$ and the starting input for the first equation in (A.11) is $T_{[x]}(1,0) \equiv U(1,0;\hat{1})$. The canonical transformations (A.11) iteratively transform the flux operators $\left[\mathsf{T}_{[x]}(x,0),\ U(x,0;\hat{1})\right]$ and their electric fields into $\left[\mathsf{T}_{[xx]}(x,0),\ \mathsf{T}_{[x]}(x+1,0)\right]$ and their electric fields as shown in Figure A.2. At the boundary $x = \mathsf{N}_s - 1$, we define $\mathsf{T}_{[xx]}(\mathsf{N}_s - 1,0) \equiv \mathsf{T}_{[x]}(\mathsf{N},0)$ for later convenience. As is also clear from Figure A.2, the subscript $[xx]$ on the string flux operator $\mathsf{T}_{[xx]}(x,0)$ encodes the structure of its right electric field $\mathsf{E}^a_{[xx]+}(x,0)$ in (A.11). More explicitly, the last equation in (A.11) states that $\mathsf{E}_{[xx]+}(x,0)$ is the sum of two adjacent Kogut-Susskind electric fields in x direction. Note that if we were in one dimension with open boundary conditions, the Gauss law (2.18) would imply $\mathcal{G}^a(x) \equiv \mathsf{T}^a_{[xx]+}(x,0) = 0;\ \forall x$ making all string operators $\mathsf{T}_{[xx]}(x,0)$ unphysical and irrelevant as expected.

A.2.1.2 *Strings along y axis*

We now iterate the above canonical transformations to extend $\mathsf{T}_{[xx]}(x,0)$ in the y direction to get $\mathsf{T}_{[y]}(x,y=1)$ and the final unphysical and ignorable string operators $\mathsf{T}_{[xxy]}(x,0)$ along the x axis as illustrated in Figure A.3-a:

$$\begin{aligned} \mathsf{T}_{[y]}(x,1) &\equiv \mathsf{T}_{[xx]}(x,0)\ U(x,0;\hat{2}), & \mathsf{T}_{[xxy]}(x,0) &\equiv \mathsf{T}_{[xx]}(x,0) \\ \mathsf{E}^a_{[y]+}(x,1) &= E^a_-(x,1;\hat{2}), & \mathsf{E}^a_{[xxy]+}(x,0) &= \mathsf{E}^a_{[xx]+}(x,0) + E^a_+(x,0;\hat{2}). \end{aligned} \tag{A.12}$$

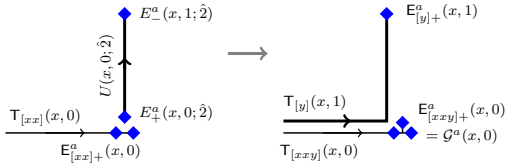

Figure A.3: Graphical representation of the canonical transformations: (a) vertical string constructions at $y = 0$ in (A.12) and the Gauss law (A.13) at $y = 0$, (b) iterative vertical string constructions in (A.14) and the string electric field in (A.15).

In (A.12) we have defined $\mathsf{T}_{[xx]}(0,0) \equiv 1$ and $\mathsf{T}_{[xx]}(\mathsf{N}_s - 1, 0) \equiv \mathsf{T}_{[x]}(\mathsf{N}_s - 1, 0)$ as mentioned above. Substituting $\mathsf{E}^a_{[xx]+}(x,0)$ from (A.11), we get:

$$\mathsf{E}^a_{[xxy]+}(x,0) = \Big(E^a_-(x,0;\hat{1}) + E^a_+(x,0;\hat{1}) + E^a_+(x,0;\hat{2})\Big) \equiv \mathcal{G}^a(x,0) = 0. \tag{A.13}$$

Again the subscript $[xxy]$ on the string operator $\mathsf{T}^a_{[xxy]}(x,0)$ denotes that its electric field at $(x,0)$ is sum of three Kogut-Susskind electric fields, two in x direction and one in y direction as in (A.13) and represented by three squares in Figure A.3-a. We ignore $\mathsf{T}_{[xxy]}(x,0)$ from now onwards and repeat the canonical transformations (A.11) to fuse the links in y direction along the maximal tree at fixed $x(= 0, 1, \cdots \mathsf{N}_s - 1)$. For this purpose, we replace $\mathsf{T}_{[x]}(x,0)$ and $U(x,0;\hat{1})$ in (A.11) by $\mathsf{T}_{[y]}(x,y)$ and $U(x,y;\hat{2})$ respectively with $y = 1, 2, \cdots, (\mathsf{N}_s - 1 - 1)$ and define:

$$\begin{aligned} \mathsf{T}_{[y]}(x,y+1) &\equiv \mathsf{T}_{[y]}(x,y)\ U(x,y;\hat{2}), & \mathsf{T}_{[yy]}(x,y) &\equiv \mathsf{T}_{[y]}(x,y), \\ \mathsf{E}^a_{[y]+}(x,y+1) &= E^a_-(x,y+1;\hat{2}), & \mathsf{E}^a_{[yy]+}(x,y) &= \mathsf{E}^a_{[y]+}(x,y) + E^a_+(x,y;\hat{2}). \end{aligned} \tag{A.14}$$

In (A.14), the initial string operator $\mathsf{T}_{[y]}(x, y = 1)$ is given in (A.12). The transformations (A.14) are illustrated in Figure A.3-b. Again the subscript $[yy]$ on $\mathsf{T}_{[yy]}(x,y)$ is to emphasize that its electric field is sum of two adjacent Kogut-Susskind electric fields in the y direction:

$$\mathsf{E}^a_{[yy]+}(x,y) = \mathsf{E}^a_{[y]+}(x,y) + E^a_+(x,y;\hat{2}) = E^a_-(x,y;\hat{2}) + E^a_+(x,y;\hat{2}). \tag{A.15}$$

In (A.15) we have used (A.14) to replace $\mathsf{E}^a_{[y]+}(x,y)$ in terms of Kogut-Susskind electric fields $E^a_-(x,y;\hat{2})$. We again define $\mathsf{T}_{[yy]}(x, \mathsf{N}_s - 1) = \mathsf{T}_{[y]}(x, \mathsf{N}_s - 1)$ at the boundary for notational convenience.

A.2.1.3 *Plaquette loop operators*

In order to remove all local SU(N) gauge or string degrees of freedom and simultaneously obtain SU(N) covariant loop flux operators, we now fuse the horizontal link operator $U(x, y \neq 0; \hat{1})$ with $\mathsf{T}_{[yy]}(x, y \neq 0)$ through the canonical transformations:

$$\begin{aligned} \mathsf{T}_{[x]}(x+1, y) &\equiv \mathsf{T}_{[yy]}(x, y)\; U(x, y; \hat{1}), \qquad & \mathsf{T}_{[yyx]}(x, y) &= \mathsf{T}_{[yy]}(x, y) \\ \mathsf{E}^a_{[x]+}(x+1, y) &= E^a_-(x+1, y; \hat{1}), \qquad & \mathsf{E}^a_{[yyx]+}(x, y) &= \mathsf{E}^a_{[yy]+}(x, y) + E^a_+(x, y; \hat{1}) \end{aligned} \tag{A.16}$$

at $x = 0, 1, 2, \cdots, (\mathsf{N}_s - 1)$ and $y = 1, 2, \cdots, \mathsf{N}_s - 1$. The above transformations are illustrated in Figure A.4. Using (A.14), the right electric field of the string flux operator $\mathsf{T}_{[yyx]}(x, y)$ is:

$$\mathsf{E}^a_{[yyx]+} = \mathsf{E}^a_{[yy]+}(x, y) + E^a_+(x, y; \hat{1}) = E^a_-(x, y; \hat{2}) + E^a_+(x, y; \hat{2}) + E^a_+(x, y; \hat{1}). \tag{A.17}$$

The initial loop operators $(W(x, y), \mathbb{E}^a(x, y))$ shown in Figure-A.5 are defined as:

$$\begin{aligned} W(x, y) &\equiv \mathsf{T}_{[x]}(x, y \neq 0)\; \mathsf{T}^\dagger_{[yyx]}(x, y), \qquad & \mathsf{T}_{[yyxx]}(x, y) &\equiv \mathsf{T}_{[yyx]}(x, y), \\ \mathbb{E}^a_-(x, y) &= \mathsf{E}^a_{[x]-}(x, y \neq 0), \qquad & \mathsf{E}^a_{[yyxx]+}(x, y) &= \mathsf{E}^a_{[x]+}(x, y \neq 0) + \mathsf{E}^a_{[yyx]+}(x, y). \end{aligned} \tag{A.18}$$

Above $(W(x, y), \mathbb{E}^a_\mp(x, y))$ are canonically conjugate pairs. We note that the conjugate electric fields of the string operators $\mathsf{T}_{[yyxx]}$ vanishes in $\mathcal{H}^p$ as:

$$\begin{aligned} &\mathsf{E}^a_{[yyxx]+}(x, y) = \mathsf{E}^a_{[yyx]+}(x, y) + \mathsf{E}^a_{[x]+}(x, y \neq 0) \\ &= \Big(E^a_-(x, y; \hat{2}) + E^a_+(x, y; \hat{2}) + E^a_+(x, y; \hat{1}) + E^a_-(x, y; \hat{1}) \Big) = \mathcal{G}^a(x, y) = 0. \end{aligned} \tag{A.19}$$

In (A.19), we have used (A.16) and (A.17) to replace $\mathsf{E}^a_{[x]+}(x, y \neq 0)$ and $\mathsf{E}^a_{[yyx]+}(x, y)$ respectively in terms of Kogut-Susskind electric fields. The relationship (A.19) solving the SU(N) Gauss law at (x, y) is graphically illustrated in Figure A.5 and also earlier in Figure 3.12-a.

At this stage all the local gauge degrees of freedom, contained in the string operators $T_{[yyxx]}(x, y)$, have been removed. We now relabel $\mathsf{T}_{[yyxx]}(x, y)$ as $\mathsf{T}(x, y)$ and $\mathsf{E}^a_{[yyxx]\pm}(x, y)$ as $\mathsf{E}^a_\pm(x, y)$ for notational simplicity. To simplify the magnetic field terms in the Kogut-Susskind

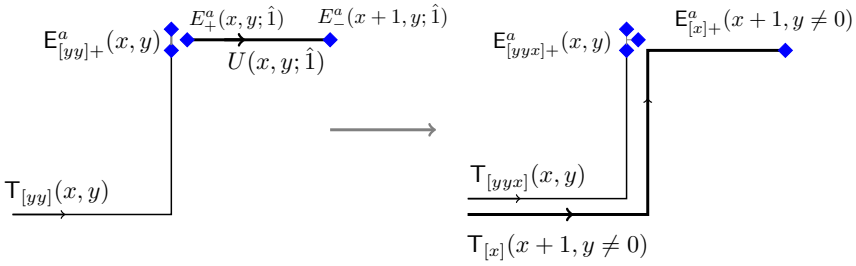

Figure A.4: Graphical representation of the canonical transformation in (A.16).

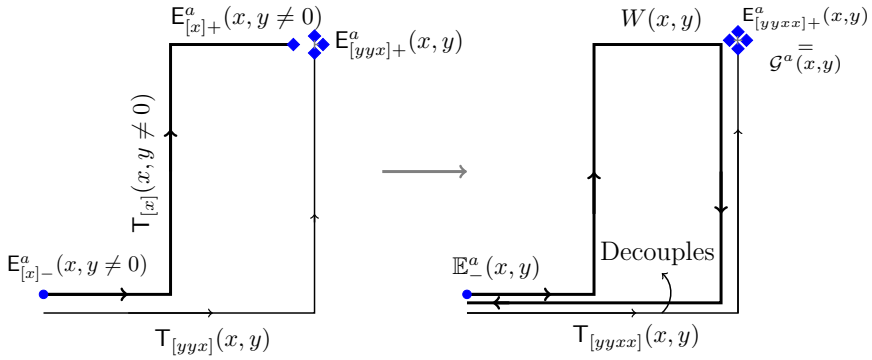

Figure A.5: Graphical representation of the canonical transformation in (A.18).

Hamiltonian (3.59), we further make the last set of canonical transformations (A.20) which transform the loop operators $(W(x,y), \mathbb{E}^a_\pm(x,y))$ in (A.18) into the final plaquette loop operators $(\mathcal{W}(x,y), \mathcal{E}^a_\mp(x,y))$ as shown in Figure A.6. We define:

$$\begin{aligned} \mathcal{W}(x,y) &\equiv W(x,y-1)\ \bar{W}^\dagger(x,y), & \bar{W}(x,y-1) &\equiv W(x,y-1); \\ \mathcal{E}^a_+(x,y) &= \bar{\mathbb{E}}^a_-(x,y), & \bar{\mathbb{E}}^a_+(x,y-1) &= \mathbb{E}^a_+(x,y-1) + \bar{\mathbb{E}}^a_+(x,y) \end{aligned} \tag{A.20}$$

Above $\left[\mathcal{W}(x,y), \mathcal{E}^a_+(x,y)\right]$, $\left[\bar{W}^\dagger(x,y), \bar{\mathbb{E}}^a_+(x,y)\right]$ are canonically conjugate loop operators and $y = \mathsf{N}_s - 1,\ (\mathsf{N}_s - 1), \cdots, 1$. The canonical transformation is initiated with the boundary operator $\bar{W}(x, y = \mathsf{N}_s - 1) \equiv W(x, y = \mathsf{N}_s - 1)$ and at the lower boundary $\mathcal{W}(x,1) \equiv \bar{W}^\dagger(x,1)$.

Having constructed plaquette loop operators and conjugate electric fields using the canonical transformations (A.16)-(A.20), we now use these relations to write the plaquette loop electric fields directly in terms of the Kogut-Susskind link electric fields. Using (A.20),

$$\mathcal{E}^a_+(x,y) \;=\; \bar{\mathbb{E}}^a_-(x,y) = \;-R_{ab}(\bar{W}(x,y))\bar{\mathbb{E}}^a_+(x,y) = \;-R_{ab}(\bar{W}(x,y))\left\{\mathbb{E}^b_+(x,y) + \bar{\mathbb{E}}^b_+(x,y+1)\right\} \tag{A.21}$$

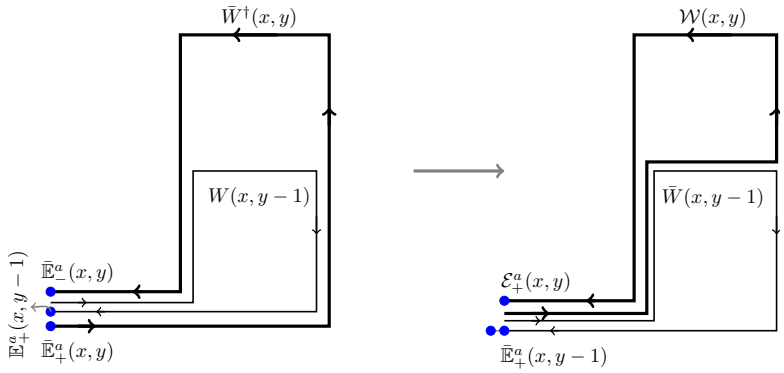

Figure A.6: Graphical representation of the canonical transformation in (A.20).

Iterating this relation and using the relation $\mathbb{E}^b_+(x,y') = -R_{bc}(W^\dagger(x,y'))\mathbb{E}^c_-(x,y')$, we get

$$\mathcal{E}^a_+(x,y) \;=\; -R_{ab}(\bar{W}(x,y)) \sum_{y'=y}^{N_s-1} \mathbb{E}^b_+(x,y') = -R_{ab}(W(x,y)) \sum_{y'=y}^{N_s-1} -R_{bc}(W^\dagger(x,y'))\mathbb{E}^c_-(x,y') \tag{A.22}$$

From eqn. (A.18) we have $\mathbb{E}^c_-(x,y') = \mathsf{E}^c_{[x]_-}(x,y') = -R_{cd}(\mathsf{T}_{[x]}(x,y'))\ \mathsf{E}^d_{[x]_+}(x,y')$ and from (A.16), $\mathsf{E}^d_{[x]_+}(x,y') = E^d_-(x,y')$. Therefore,

$$\mathcal{E}^a_+(x,y) = -\sum_{y'=y}^{N_s-1} R_{ab}\left(W(x,y)W^\dagger(x,y')\mathsf{T}_{[x]}(x,y')\right) E^b_-(x,y',\hat{1}) \tag{A.23}$$

$$= -\sum_{y'=y}^{N_s-1} R_{ab}\Big(\underbrace{\mathsf{T}(x-1,y)\ U(x-1,y;\hat{1}) \prod_{y''=y}^{y'} U(x,y'';\hat{2})}_{S(x,y,y')}\Big) E^b_-(x,y',\hat{1}) \equiv -\sum_{y'=y}^{N_s-1} R_{ab}\left(S(x,y,y')\right) E^b_-(x,y';\hat{1}).$$

This is the relation (3.68) in the text which was further graphically illustrated in Figure 3.12-b.

A.2.2 *From loops & strings to links (Inverse transformations)*

In this part, we systematically write down all Kogut-Susskind link electric fields in terms of loop flux operators and loop electric fields. We calculate the link electric fields in three separate cases: *a)* $E^a(x, y = 0; \hat{1})$ shown in Figure 3.13-a, *b)* $E^a(x, y \neq 0; \hat{1})$ shown in Figure 3.13-b and c) $E^a(x, y; \hat{2})$ shown in Figure 3.13-c.

A.2.2.1 *Case (a): $E^a_+(x, 0; \hat{1})$*

Consider the left electric field of a Kogut-Susskind link operator along the x axis, $E_+(x, 0; \hat{1})$. From canonical transformation A.11(figure. A.2), we have $\mathsf{E}^b_{[xx]_+}(x, 0) = E^b_-(x, 0, \hat{1}) + E^b_+(x, 0; \hat{1})$. Therefore,

$$\begin{aligned} E^a_+(x,0;\hat{1}) &= -R_{ab}(U(x,0,\hat{1}))E^b_-(x+1,0,\hat{1}) \\ &= -R_{ab}(U(x,0,\hat{1}))\left\{\mathsf{E}^b_{[xx]_+}(x+1,0) - E^b_+(x+1,0;\hat{1})\right\} \end{aligned} \tag{A.24}$$

Iterating this expression, we obtain

$$E^a_+(x,0;\hat{1}) = R_{ab}\big(\mathsf{T}^\dagger(x,0)\big) \sum_{\bar{x}=x+1}^{N_s-1} -R_{bc}\left(\mathsf{T}(\bar{x},0)\right) \mathsf{E}^c_{[xx]_+}(\bar{x},0) \tag{A.25}$$

Above, we have made use of the fact that $\mathsf{T}^\dagger(x,0)\mathsf{T}(\bar{x},0) = U(x,0;\hat{1})U(x+1,0;\hat{1})\cdots U(\bar{x}-1,0;\hat{1})$ if $\bar{x} > x$. From this expression it is clear that all the $\vec{\mathsf{E}}_{[xx]_+}(\bar{x},0); \bar{x} > x$ are parallel transported back to the point $(x,0)$ to give $\vec{E}_+(x,0,\hat{1})$ so that the gauge transformations of

link and string operators are consistent with (A.25). This is a general trend which will be seen at each step of canonical transformations.

- $\vec{\mathsf{E}}_{[xx]+} \to \vec{\mathsf{E}}_{[y]+} \to \vec{\mathsf{E}}_{[\mathbf{yy}]+}$

  Writing down $\vec{\mathsf{E}}_{[xx]+}(\bar{x},0)$ in terms of $\vec{\mathsf{E}}_{[xxy]+}(\bar{x},0)$ and $\vec{\mathsf{E}}_{[y]+}(\bar{x},1)$ using canonical transformation A.12 shown in Figure A.3-a:

$$\mathsf{E}^a_{[xx]+}(\bar{x},0) = \mathsf{E}^a_{[xxy]+}(\bar{x},0) - E^a_+(\bar{x},0;\hat{2}) = R_{ab}\left(U(\bar{x},0;\hat{2})\right) \underbrace{E^b_-(\bar{x},1;\hat{2})}_{\mathsf{E}^b_{[y]+}(\bar{x},1)} \tag{A.26}$$

  We have used the fact that $\mathsf{E}_{[xxy]+}(\bar{x},0) = 0$ by Gauss law A.13 at $(\bar{x},0)$. But from (A.14) and Figure A.3-b:

$$\begin{aligned}\mathsf{E}^a_{[y]+}(\bar{x},1) &= \mathsf{E}^a_{[yy]+}(\bar{x},1) - E^a_+(\bar{x},1;\hat{2}) = \mathsf{E}^a_{[yy]+}(\bar{x},1) + R_{ab}\left(U(\bar{x},1;\hat{2})\right) \underbrace{E^b_-(\bar{x},2;\hat{2})}_{\mathsf{E}^b_{[y]+}(\bar{x},2)} \\ &= R_{ab}\left(\mathsf{T}^\dagger(\bar{x},1)\right) \sum_{\bar{y}=1}^{\mathsf{N}_s-1} R_{bc}\left(\mathsf{T}(\bar{x},\bar{y})\right) \mathsf{E}^c_{[yy]+}(\bar{x},\bar{y}). \end{aligned} \tag{A.27}$$

  Substituting it back into eqn. A.26 for $\mathsf{E}^a_{[xx]+}(\bar{x},0)$ and using $U(\bar{x},0;\hat{2})\mathsf{T}^\dagger(\bar{x},1) = \mathsf{T}^\dagger(\bar{x},0)$, we get

$$\mathsf{E}^a_{[xx]+}(\bar{x},0) = R_{ab}\left(\mathsf{T}^\dagger(\bar{x},0)\right) \sum_{\bar{y}=1}^{\mathsf{N}_s-1} R_{bc}\left(\mathsf{T}(\bar{x},\bar{y})\right) \mathsf{E}^c_{[yy]+}(\bar{x},\bar{y}). \tag{A.28}$$

  Putting this into eqn. A.25 we get

$$E^a_+(x,0;\hat{1}) = -R_{ab}\big(\mathsf{T}^\dagger(x,0)\big) \sum_{\bar{x}=x+1}^{\mathsf{N}_s-1} \sum_{\bar{y}=1}^{\mathsf{N}_s-1} R_{bc}\left(\mathsf{T}(\bar{x},\bar{y})\right) \mathsf{E}^c_{[yy]+}(\bar{x},\bar{y}) \tag{A.29}$$

- $\vec{\mathsf{E}}_{[yy]+} \to \vec{\mathsf{E}}_{[x]+} \to \vec{\mathbb{E}}_{\pm}$

  From canonical transformation (A.16) (Figure A.4) we have $\mathsf{E}^c_{[yyx]+}(\bar{x},\bar{y}) = \mathsf{E}^c_{[yy]+}(\bar{x},\bar{y}) + E^c_+(\bar{x},\bar{y},\hat{1})$ and $\mathsf{E}^d_{[x]+}(\bar{x}+1,\bar{y}) = E^d_-(\bar{x}+1,\bar{y},\hat{1})$. Therefore,

$$\mathsf{E}^c_{[yy]+}(\bar{x},\bar{y}) = \mathsf{E}^c_{[yyx]+}(\bar{x},\bar{y}) - E^c_+(\bar{x},\bar{y},\hat{1}) = \mathsf{E}^c_{[yyx]+}(\bar{x},\bar{y}) + R_{cd}\left(U(\bar{x},\bar{y},\hat{1})\right) \underbrace{E^d_-(\bar{x}+1,\bar{y},\hat{1})}_{\mathsf{E}^d_{[x]+}(\bar{x}+1,\bar{y})} \tag{A.30}$$

  Further, the canonical transformations A.18 (Figure A.5) imply:

$$\mathsf{E}^c_{[yyx]+}(\bar{x},\bar{y}) = \mathsf{E}^c_{[yyxx]+}(\bar{x},\bar{y}) - \mathsf{E}^c_{[x]+}(\bar{x},\bar{y}) = -\mathsf{E}^c_{[x]+}(\bar{x},\bar{y})$$

Here, we have used the fact that $\mathsf{E}^c_{[xxyy]+}(\bar{x},\bar{y}) = 0$ by Gauss law at $(\bar{x},\bar{y})$(eqn. A.19). Also, from eqn. (A.18), $\mathsf{E}^d_{[x]-}(\bar{x},\bar{y}) = \mathbb{E}^d_-(\bar{x},\bar{y})$. Therefore,

$$\mathsf{E}^c_{[x]+}(\bar{x},\bar{y}) = -R_{cd}(\mathsf{T}^\dagger_{[x]}(\bar{x},\bar{y}))\mathsf{E}^d_{[x]-}(\bar{x},\bar{y}) = -R_{cd}(\mathsf{T}^\dagger_{[x]}(\bar{x},\bar{y}))\mathbb{E}^d_-(\bar{x},\bar{y}) \tag{A.31}$$

Substituting for $\vec{\mathsf{E}}_{[yyx]+}, \vec{\mathsf{E}}_{[x]+}$ in eqn. A.30 and using the relation $U(\bar{x},\bar{y};\hat{1})\mathsf{T}^\dagger_{[x]}(\bar{x}+1,\bar{y}) = \mathsf{T}^\dagger(\bar{x},\bar{y})$,

$$\mathsf{E}^c_{[yy]+}(\bar{x},\bar{y}) = R_{cd}\left(\mathsf{T}^\dagger_{[x]}(\bar{x},\bar{y})\right)\mathbb{E}^d_-(\bar{x},\bar{y}) - R_{cd}\left(\mathsf{T}^\dagger(\bar{x},\bar{y})\right)\mathbb{E}^d_-(\bar{x}+1,\bar{y}) \tag{A.32}$$

Putting (A.32) in (A.29) and using the defining relations

$$\mathsf{T}(\bar{x},\bar{y})\mathsf{T}^\dagger_{[x]}(\bar{x},\bar{y}) \equiv W^\dagger(\bar{x},\bar{y}); \quad \mathbb{E}^b_+(\bar{x},\bar{y}) \equiv -R_{bd}\left(W^\dagger(\bar{x},\bar{y})\right)\mathbb{E}^d_-(\bar{x},\bar{y}); \quad \mathsf{T}(\bar{x},\bar{y})\mathsf{T}^\dagger(\bar{x},\bar{y}) = \mathsf{I},$$

we get a simple relation:

$$E^a_+(x,0;\hat{1}) = R_{ab}(\mathsf{T}^\dagger(x,0))\sum_{\bar{x}=x+1}^{\mathsf{N_s}-1}\sum_{\bar{y}=1}^{\mathsf{N_s}-1}\left[\mathbb{E}^b_+(\bar{x},\bar{y}) + \mathbb{E}^b_-(\bar{x}+1,\bar{y})\right]. \tag{A.33}$$

- $\vec{\mathbb{E}}_\pm \to \vec{\mathcal{E}}_\pm$

To write $E^a_+(x,0;\hat{1})$ in terms of the final plaquette loop electric fields $\mathcal{E}^b_\pm$, we first use the canonical transformation eqn. A.20 (Figure. A.6), $\mathbb{E}^b_+(\bar{x},\bar{y}) = \bar{\mathbb{E}}^b_+(\bar{x},\bar{y}) - \bar{\mathbb{E}}^b_+(\bar{x},\bar{y}+1)$, to write down the first term in the eqn. (A.33)in terms of $\vec{\mathcal{E}}_-$ as follows:

$$\begin{aligned}\sum_{\bar{y}=1}^{\mathsf{N_s}-1}\mathbb{E}^b_+(\bar{x},\bar{y}) &= \sum_{\bar{y}=1}^{\mathsf{N_s}-1}\left[\bar{\mathbb{E}}^b_+(\bar{x},\bar{y}) - \bar{\mathbb{E}}^b_+(\bar{x},\bar{y}+1)\right] = \bar{\mathbb{E}}^b_+(\bar{x},1)\\ &= -R_{bc}\left(\bar{W}^\dagger(\bar{x},1)\right)\bar{\mathbb{E}}^c_-(\bar{x},1) = -R_{bc}\left(\mathcal{W}(\bar{x},1)\right)\mathcal{E}^c_+(\bar{x},1) = \mathcal{E}^b_-(\bar{x},1).\end{aligned} \tag{A.34}$$

Here, we have used the fact that at the lower boundary, $\bar{W}^\dagger(\bar{x},1) = \mathcal{W}(\bar{x},1)$. We now write down the second term in eqn.(A.33) in terms of $\vec{\mathcal{E}}_\pm$. Again using canonical transformation eqn.(A.20)(Figure. A.6) as follows:

$$\begin{aligned}\mathbb{E}^b_-(\bar{x}+1,\bar{y}) &= -R_{bc}(\bar{W}(\bar{x}+1,\bar{y}))\mathbb{E}^c_+(\bar{x}+1,\bar{y}) = -R_{bc}(\bar{W}(\bar{x}+1,\bar{y}))\left[\bar{\mathbb{E}}^c_+(\bar{x}+1,\bar{y}) - \bar{\mathbb{E}}^c_+(\bar{x}+1,\bar{y}+1)\right]\\ &= \bar{\mathbb{E}}^b_-(\bar{x}+1,\bar{y}) - R_{bc}(\bar{W}(\bar{x}+1,\bar{y})\bar{W}^\dagger(\bar{x}+1,\bar{y}+1))\bar{\mathbb{E}}^c_-(\bar{x}+1,\bar{y}+1)\\ &= \bar{\mathbb{E}}^b_-(\bar{x}+1,\bar{y}) - R_{bc}(\mathcal{W}(\bar{x}+1,\bar{y}+1))\bar{\mathbb{E}}^c_-(\bar{x}+1,\bar{y}+1)\\ &= \mathcal{E}^b_+(\bar{x}+1,\bar{y}) + \mathcal{E}^b_-(\bar{x}+1,\bar{y}+1)\end{aligned} \tag{A.35}$$

Putting both the terms back into eqn. A.33 for $E^a_+(x,0;\hat{1})$, we get

$$E^a_+(x,0;\hat{1}) = R_{ab}\big(\mathsf{T}^\dagger(x,0)\big)\sum_{\bar{x}=x+1}^{N_s-1}\left\{\mathcal{E}^b_-(\bar{x},1)+\sum_{\bar{y}=1}^{N_s-1}\Big[\mathcal{E}^b_+(\bar{x}+1,\bar{y})+\mathcal{E}^b_-(\bar{x}+1,\bar{y}+1)\Big]\right\}$$
$$= R_{ab}\big(\mathsf{T}^\dagger(x,0)\big)\left\{\mathcal{E}^b_-(x+1,1)+\sum_{\bar{x}=x+2}^{N_s-1}\sum_{\bar{y}=1}^{N_s-1}\mathsf{L}^b(\bar{x},\bar{y})\right\} \tag{A.36}$$

Above, $\mathsf{L}^a(\bar{x},\bar{y}) \equiv \mathcal{E}^a_-(\bar{x},\bar{y}) + \mathcal{E}^a_+(\bar{x},\bar{y})$.

A.2.2.2 *Case (b):* $E^a_+(x, y \neq 0; \hat{1})$

The canonical transformation (A.16) and Figure A.4 state $\mathsf{E}^b_{[x]+}(x,y) = E^b_-(x,y;\hat{1})$. Therefore,

$$E^a_+(x,y,\hat{1}) = -R_{ab}(U(x,y,\hat{1}))\; E^b_-(x+1,y;\hat{1}) = -R_{ab}(U(x,y,\hat{1}))\;\mathsf{E}^b_{[x]+}(x+1,y)$$

Using the relations (A.31) and (A.35)

$$\mathsf{E}^b_{[x]+}(x+1,y) = -R_{bc}(\mathsf{T}^\dagger_{[x]}(x+1,y)\;\mathbb{E}^c_-(x+1,y);\quad \mathbb{E}^c_-(x+1,y) = \mathcal{E}^c_+(x+1,y)+\mathcal{E}^c_-(x+1,y+1)$$

and relation $\mathsf{T}^\dagger(x,y) = U(x,y,\hat{1})\mathsf{T}^\dagger_{[x]}(x+1,y)$, we get

$$E^a_+(x,y,\hat{1}) = \Big[R_{ab}(U(x,y,\hat{1}))R_{bc}(\mathsf{T}^\dagger_{[x]}(x+1,y))\Big]\,\mathbb{E}^c_-(x+1,y) \;=\; R_{ac}\Big(\mathsf{T}^\dagger(x,y)\Big)\,\mathbb{E}^c_-(x+1,y)$$
$$= R_{ac}\Big(\mathsf{T}^\dagger(x,y)\Big)\Big\{\mathcal{E}^c_+(x+1,y)+\mathcal{E}^c_-(x+1,y+1)\Big\} \tag{A.37}$$

Clubbing case (a) and case (b) together,

$$E^a_+(x,y;\hat{1}) = R_{ab}(\mathsf{T}^\dagger(x,y))\Big(\mathcal{E}^b_-(x+1,y+1)+\mathcal{E}^b_+(x+1,y)+\delta_{y,0}\sum_{\bar{x}=x+2}^{N_s-1}\sum_{\bar{y}=1}^{N_s-1}\mathsf{L}^b(\bar{x},\bar{y})\Big). \tag{A.38}$$

We have defined $\mathcal{E}_\pm(x,0) \equiv 0;\ \mathcal{E}_\pm(0,y) \equiv 0$ for notational convenience. The relations (A.36) were used in (3.72) and (3.83), (3.84) to write down the Kogut-Susskind Hamiltonian in terms of loop operators.

A.2.2.3 *Case (c):* $E_+(x,y;\hat{2})$

The canonical transformations (A.14) (Figure A.3(b)) state $\mathsf{E}^c_{[y]+}(x,y) = E^c_-(x,y,\hat{2})$. Therefore,

$$E^a_+(x,y;\hat{2}) = -R_{ac}\left(U(x,y;\hat{2})\right)E^c_-(x,y+1,\hat{2}) = -R_{ac}\left(U(x,y;\hat{2})\right)\mathsf{E}^c_{[y]+}(x,y+1)$$

Using the relation $\mathsf{E}^c_{[y]+}(x,y) = \mathsf{E}^c_{[yy]+}(x,y) - E^c_+(x,y,\hat{2})$ from the canonical transformation eqn.A.14 (Figure.A.3(b)),

$$\begin{aligned} E^a_+(x,y;\hat{2}) &= -R_{ac}(U(x,y,\hat{2}))\left\{\mathsf{E}^c_{[yy]+}(x,y+1) - E^c_+(x,y+1,\hat{2})\right\} \\ &= -R_{ac}(U(x,y,\hat{2}))\mathsf{E}^c_{[yy]+}(x,y+1) - R_{ac}\left(U(x,y,\hat{2})U(x,y+1,\hat{2})\right)\mathsf{E}^c_{[yy]+}(x,y+2) - \cdots \\ &= -R_{ab}(\mathsf{T}^\dagger(x,y))\sum_{\bar{y}=y+1}^{\mathsf{N}_s-1} R_{bc}\left(\mathsf{T}(x,\bar{y})\right)\ \mathsf{E}^c_{[yy]+}(x,\bar{y}) \end{aligned} \tag{A.39}$$

Using eqn.A.32, $\mathsf{E}^c_{[yy]+}(x,\bar{y}) = R_{cd}\left(\mathsf{T}^\dagger_{[x]}(x,\bar{y})\right)\ \mathbb{E}^d_-(x,\bar{y}) - R_{cd}\left(\mathsf{T}^\dagger(x,\bar{y})\right)\ \mathbb{E}^d_-(x+1,\bar{y})$ and the expression $W^\dagger(x,\bar{y}) = \mathsf{T}(x,\bar{y})\mathsf{T}^\dagger_{[x]}(x,\bar{y})$ from eqn. A.18,

$$E^a_+(x,y;\hat{2}) = R_{ab}\left(\mathsf{T}^\dagger(x,y)\right)\sum_{\bar{y}=y+1}^{\mathsf{N}_s-1}\left[-R_{bc}\left(W^\dagger(x,\bar{y})\right)\mathbb{E}^c_-(x,\bar{y}) + \mathbb{E}^b_-(x+1,\bar{y})\right]. \tag{A.40}$$

From eqn. A.35, we have $\mathbb{E}^c_-(x,\bar{y}) = \mathcal{E}^c_+(x,\bar{y}) + \mathcal{E}^c_-(x,\bar{y}+1)$. Therefore, $\mathbb{E}^b_-(x+1,\bar{y}) = \mathcal{E}^b_+(x+1,\bar{y}) + \mathcal{E}^b_-(x+1,\bar{y}+1)$ and

$$\begin{aligned} \sum_{\bar{y}=y+1}^{\mathsf{N}_s-1} -R_{bc}\left(W^\dagger(x,\bar{y})\right)\ \mathbb{E}^c_-(x,\bar{y}) &= \sum_{\bar{y}=y+1}^{\mathsf{N}_s-1} -R_{bc}\left(W^\dagger(x,\bar{y})\right)\left[\mathcal{E}^c_+(x,\bar{y}) + \mathcal{E}^c_-(x,\bar{y}+1)\right] \\ &= \sum_{\bar{y}=y+1}^{\mathsf{N}_s-1} R_{bc}\left(W^\dagger(x,\bar{y}-1)\right)\mathcal{E}^c_-(x,\bar{y}) - \sum_{\bar{y}=y+1}^{\mathsf{N}_s-1} R_{bc}\left(W^\dagger(x,\bar{y})\right)\mathcal{E}^c_-(x,\bar{y}+1) \\ &= R_{bc}\left(W^\dagger(x,y)\right)\mathcal{E}^c_-(x,y+1) \end{aligned} \tag{A.41}$$

Above, we have used the relations: $W^\dagger(x,\bar{y}) = W^\dagger(x,\bar{y}-1)\,\mathcal{W}(x,\bar{y})$ and $R_{cd}\left(\mathcal{W}(x,\bar{y})\right)\mathcal{E}^d_+(x,\bar{y}) = \mathcal{E}^c_-(x,\bar{y})$. Putting these two terms back into eqn. (A.40),

$$E^a_+(x,y;\hat{2}) = R_{ab}\left(\mathsf{T}^\dagger(x,y)\right)\left\{R_{bc}\left(W^\dagger(x,y)\right)\mathcal{E}^c_-(x,y+1) + \sum_{\bar{y}=y+1}^{\mathsf{N}_s-1}\left[\mathcal{E}^b_+(x+1,\bar{y}) + \mathcal{E}^b_-(x+1,\bar{y}+1)\right]\right\} \tag{A.42}$$

Therefore,

$$E^a_+(x,y;\hat{2}) = R_{ab}(\mathsf{T}^\dagger(x,y))\left(\mathcal{E}^b_+(x+1,y+1) + R_{bc}(\mathcal{W}_{xy}(x,y))\mathcal{E}^c_-(x,y+1) + \sum_{\bar{y}=y+2}^{\mathsf{N}_s-1}\mathsf{L}^b(x+1,\bar{y})\right) \tag{A.43}$$

Above, $\mathcal{W}_{xy}(x,y)) \equiv \mathcal{W}(x,1)\mathcal{W}(x,2)\cdots\mathcal{W}(x,y)$ as defined in (3.73). The relation (A.43) was stated in (3.72) and used later in (3.83) to get the SU(N) loop Hamiltonian.

Consider the links meeting at a site (x,y). We now show that the local Gauss law at (x,y) are redundant in terms of the new dual loop operators except when $(x,y) = (0,0)$ where it leads to a global Gauss law. We only show explicit calculations for the case when $(x \neq 0, y \neq 0)$ and $(x = 0, y = 0)$. The cases $(x \neq 0, y = 0)$ and $(x = 0, y \neq 0)$ can be similarly shown.

- $x \neq 0, y \neq 0$. The electric fields when written in terms of the physical loop operators are given by:

$$
\begin{aligned}
E^a_+(x,y,\hat{1}) &= \underbrace{R_{ab}(\mathsf{T}^\dagger(x,y))\Big[\mathcal{E}^b_+(x+1,y)+\mathcal{E}^b_-(x+1,y+1)\Big]}_{T_1} \\
E^a_+(x,y,\hat{2}) &= \underbrace{R_{ab}(\mathsf{T}^\dagger(x,y))\Big[\sum_{\bar{y}=y+2}^{\mathsf{N}_s-1}\{\mathcal{E}^b_+(x+1,\bar{y})+\mathcal{E}^b_-(x+1,\bar{y})\}+\mathcal{E}^b_+(x+1,y+1)\Big]}_{T_2}+ \\
&\qquad \underbrace{R_{ab}(U^\dagger(x-1,y;\hat{1}))\mathsf{T}^\dagger(x-1,y)\mathcal{E}^b_-(x,y+1)}_{T_3} \\
E^a_-(x,y,\hat{1}) &= \underbrace{-R_{ab}(U^\dagger(x-1,y;\hat{1})\mathsf{T}^\dagger(x-1,y)\mathcal{E}^b_-(x,y+1)}_{-T_3}+\underbrace{-R_{ab}(U^\dagger(x-1,y;\hat{1})\mathsf{T}^\dagger(x-1,y)\mathcal{E}^b_+(x,y)}_{-T_4} \\
E^a_-(x,y,\hat{2}) &= \underbrace{-R_{ab}(\mathsf{T}^\dagger(x,y))\Big\{\mathcal{E}^b_+(x+1,y)+\mathcal{E}^b_-(x+1,y+1)\Big\}}_{-T_1}+ \\
&\quad \underbrace{-R_{ab}(\mathsf{T}^\dagger(x,y))\Big\{\mathcal{E}^b_+(x+1,y+1)+\sum_{\bar{y}=y+2}^{\mathsf{N}_s-1}\Big[\mathcal{E}^b_+(x+1,\bar{y})+\mathcal{E}^b_-(x+1,\bar{y})\Big]\Big\}}_{-T_2}+ \\
&\quad \underbrace{R_{ab}(U^\dagger(x-1,y,\hat{1})\mathsf{T}^\dagger(x-1,y))\mathcal{E}^b_+(x,y)}_{T_4}
\end{aligned}
\tag{A.44}
$$

  Therefore, $\mathcal{G}^a(x,y) = E^a_+(x,y,\hat{1}) + E^a_+(x,y,\hat{2}) + E^a_-(x,y,\hat{1}) + E^a_+(x,y,\hat{2}) = 0$.

- $x = 0, y = 0$ The electric fields $E^a_+(0,0,\hat{1})$ and $E^a_+(0,0,\hat{2})$ are given by equations (A.38) and (A.43) respectively.

$$
\begin{aligned}
E^a_+(0,0,\hat{1}) &= \mathcal{E}^a_-(1,1)+\sum_{\bar{x}=2}^{\mathsf{N}_s-1}\sum_{\bar{y}=1}^{\mathsf{N}_s-1}\mathsf{L}^a(\bar{x},\bar{y}) \\
E^a_+(0,0,\hat{2}) &= \mathcal{E}^a_+(1,1)+\sum_{\bar{y}=2}^{\mathsf{N}_s-1}\mathsf{L}^a(1,\bar{y})
\end{aligned}
\tag{A.45}
$$

  Therefore,

$$
\mathcal{G}^a(0,0) = E^a_+(0,0,\hat{1}) + E^a_+(0,0,\hat{2}) = \sum_{\bar{x}=1}^{\mathsf{N}_s-1}\sum_{\bar{y}=1}^{\mathsf{N}_s-1}\mathsf{L}^a(\bar{x},\bar{y}). \tag{A.46}
$$

Therefore, the Gauss law at the origin is not redundant in terms of the loop variables. This leads to a residual global Gauss law in the loop picture :

$$
\mathcal{G}^a|phys\rangle = \sum_{\bar{x}=1}^{\mathsf{N}_s-1}\sum_{\bar{y}=1}^{\mathsf{N}_s-1}\mathsf{L}^a(\bar{x},\bar{y})|phys\rangle = 0 \tag{A.47}
$$

Above, $\mathcal{G}^a = \mathcal{G}^a(0,0)$ and $|phys\rangle$ is any state in the physical Hilbert space $\mathcal{H}^p$.

A.3 CANONICAL TRANSFORMATIONS IN 3 + 1 DIMENSIONS

In this section we illustrate Z_2 and $SU(N)$ canonical transformations involved in the construction of a loop formulation on a $3+1$ D lattice. For simplicity, construction is done explicitly for a single cube which contains all the features of the finite lattice case.

A.3.1 *Z_2 lattice gauge theory*

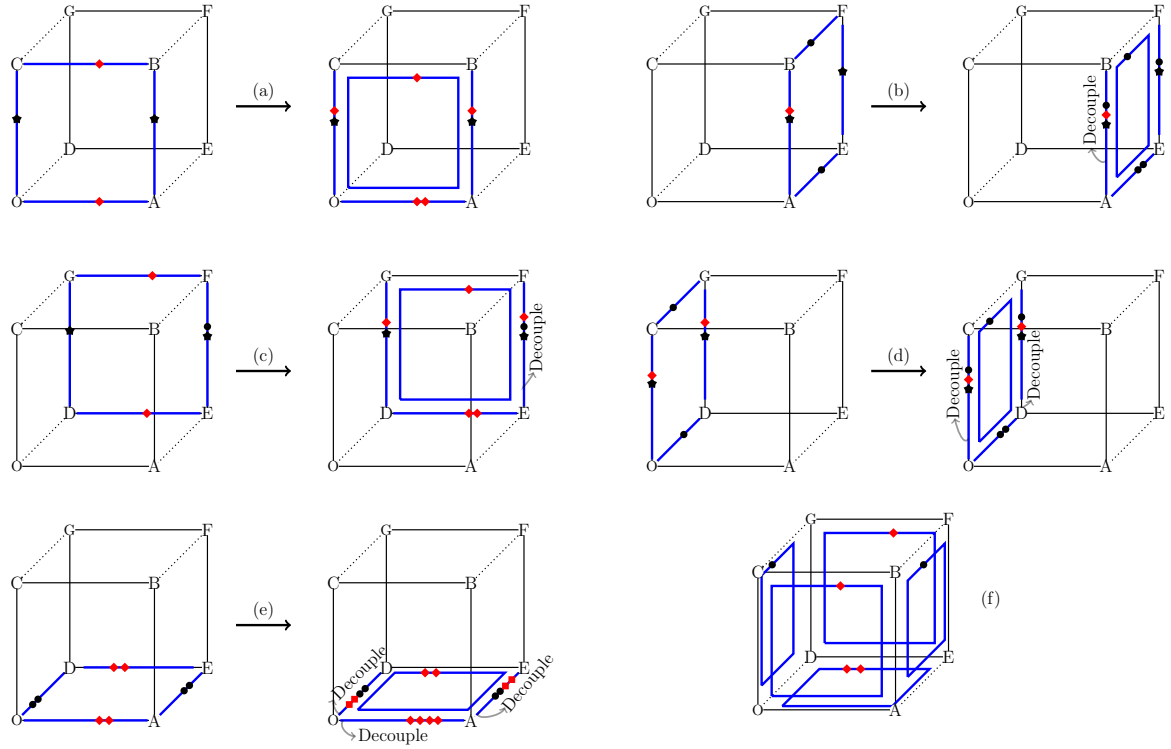

Figure A.7: (a)-(e) shows the plaquette canonical transformation steps involved in the construction of a loop formulation of Z_2 gauge theory on a cube. Just like in the 2D case, the string variables decouple. (f) shows the final plaquette loop variables that results. The plaquette loop operator corresponding to the 'roof' is missing. This solves Bianchi identity constraints automatically.

In this section, we will describe the canonical transformations involved in the construction of a loop formulation of Z_2 gauge theory on a unit 3 dimensional cube. Without any loss of generality, we will describe the construction by iterating plaquette canonical transformations defined in 3.1.2 instead of the fundamental Z_2 canonical transformation. For simplicity, sites of the 3D cube are labelled as : $O \equiv (0,0,0)$; $A \equiv (1,0,0)$; $B \equiv (1,0,1)$; $C \equiv (0,0,1)$; $D \equiv (0,1,0)$; $E \equiv (1,1,0)$; $F \equiv (1,1,1)$; $G \equiv (0,1,1)$. We start with the 12 link operators on the cube as shown in figure A.7. Our notation is such that $\sigma_3(O,\hat{1})$ denotes the σ_3 variable of the link which starts at site O and is in the $\hat{1}$ direction. These 12 link conjugate pairs are then systematically transformed into plaquette operators on the 4 'vertical walls' and the

'floor' of the cube and 7 string variables along OA, AE, OD, OC, AB, EF, DG in 5 plaquette canonical transformations defined in (3.20) and (3.21). This is illustrated in the figure A.7. Just as in $2+1$ dimensions, these string variables decouple from the physical Hilbert space $\mathcal{H}^p$ due to local Gauss laws at the sites A, E, D, C, B, F, G. The Gauss law at the origin O is not independent of Gauss laws at these sites and hence is automatically solved.

1. We begin by performing a plaquette canonical transformation on the plaquette OABC. The plaquette loop conjugate pairs $\{\mu_1(B,\hat{3});\ \mu_3(B,\hat{3})\}$ around the plaquette OABC is given by

$$\mu_1(B,\hat{3}) = \sigma_3(O,\hat{1})\sigma_3(A,\hat{3})\sigma_3(C,\hat{1})\sigma_3(O,\hat{3}) \qquad \mu_3(B,\hat{3}) = \sigma_1(C,\hat{1}) \tag{A.48}$$

Our notation is such that the plaquette operators $\{\mu_1(B,\hat{3});\mu_3(B,\hat{3})\}$ corresponds to a plaquette in the plane perpendicular to the $\hat{3}$ direction (xy plane) with the top right corner site B.[1] The string and redefined link operators around plaquette OABC is given by:

$$\begin{aligned}
\sigma_{3[xz]}(O,\hat{3}) &= \sigma_3(O,\hat{3}) & \sigma_{1[xz]}(O,\hat{3}) &= \sigma_1(O,\hat{3})\sigma_1(C,\hat{1}) \\
\sigma_{3[xz]}(A,\hat{3}) &= \sigma_3(A,\hat{3}) & \sigma_{1[xz]}(A,\hat{3}) &= \sigma_1(A,\hat{3})\sigma_1(C,\hat{1}) \\
\sigma_{3[xx]}(O,\hat{1}) &= \sigma_3(O,\hat{1}) & \sigma_{1[xx]}(O,\hat{1}) &= \sigma_1(O,\hat{1})\sigma_1(C,\hat{1})
\end{aligned} \tag{A.49}$$

The subscript $[xz]$ on $\sigma_{3[xz]}$ denotes that the corresponding conjugate operator $\sigma_{1[xx]}$ is the product of link operator σ_1 along the x and z direction.

2. The second step involves a plaquette canonical transformation on the plaquette AEFB. The plaquette loop conjugate operators $\{\mu_1(F,\hat{1});\mu_3(F,\hat{1})\}$ are given by :

$$\mu_1(F,\hat{1}) = \sigma_3(A,\hat{2})\sigma_3(E,\hat{3})\sigma_3(B,\hat{2})\sigma_3(A,\hat{3}) \qquad \mu_3(F,\hat{1}) = \sigma_1(B,\hat{2}) \tag{A.50}$$

The string and redefined link operators around plaquette AEFB is given by:

$$\begin{aligned}
\sigma_{3[xzy]}(A,\hat{3}) &= \sigma_3(A,\hat{3}) & \sigma_{1[xzy]}(A,\hat{3}) &= \sigma_{1[xz]}(A,\hat{3})\sigma_1(B,\hat{2}) = \mathcal{G}(B) \\
\sigma_{3[yy]}\ (A,\hat{2}) &= \sigma_3(A,\hat{2}) & \sigma_{1[yy]}\ (A,\hat{2}) &= \sigma_1(A,\hat{2})\sigma_1(B,\hat{2}) \\
\sigma_{3[yz]}\ (E,\hat{3}) &= \sigma_3(E,\hat{3}) & \sigma_{1[yz]}\ (E,\hat{3}) &= \sigma_1(E,\hat{3})\sigma_1(B,\hat{2})
\end{aligned} \tag{A.51}$$

As a result of the Gauss law at B, the string operators $\{\sigma_{1[xzy]}(A,\hat{3});\sigma_{3[xzy]}(A,\hat{3})\} \equiv \{\bar{\sigma}_1(B,\hat{3});\bar{\sigma}_3(B,\hat{3})\}$ decouples from the physical Hilbert space. Our notation is such that

1 Top right corner is the point (x,y,z) with the maximum value of (x+y+z) on the plaquette.

the string operators $\{\bar{\sigma}_1(B,\hat{3});\bar{\sigma}_3(B,\hat{3})\}$ are denoted by the end point B of the string and the direction $\hat{3}$ of the string.

3. The third step involves a plaquette canonical transformation along the plaquette DEFG. The resulting plaquette loop conjugate pairs $\{\mu_1(F,\hat{2});\mu_3(F,\hat{2})\}$ are given by :

$$\mu_1(F,\hat{2}) = \sigma_3(D,\hat{1})\sigma_{3[yz]}(E,\hat{3})\sigma_3(G,\hat{1})\sigma_3(D,\hat{3}) \qquad \mu_3(F,\hat{2}) = \sigma_1(G,\hat{1}) \tag{A.52}$$

The redefined link operators and string operators around DEFG are given by :

$$\begin{aligned}
\sigma_{3[xx]}(D,\hat{1}) &= \sigma_3(D,\hat{1}) & \sigma_{1[xx]}(D,\hat{1}) &= \sigma_1(D,\hat{1})\sigma_1(G,\hat{1}) \\
\sigma_{3[xyz]}(E,\hat{3}) &= \sigma_{3[yz]}(E,\hat{3}) & \sigma_{1[xyz]}(E,\hat{3}) &= \sigma_{1[yz]}(E,\hat{3})\sigma_1(G,\hat{1}) = \mathcal{G}(F) \\
\sigma_{3[xz]}(D,\hat{3}) &= \sigma_3(D,\hat{3}) & \sigma_{1[xz]}(D,\hat{3}) &= \sigma_1(D,\hat{3})\sigma_1(G,\hat{1})
\end{aligned}$$

As a result of the Gauss law at F, The string operators $\{\sigma_{1[xyz]}(E,\hat{3});\sigma_{3[xyz]}(E,\hat{3})\} \equiv \{\bar{\sigma}_1(F,\hat{3});\bar{\sigma}_3(F,\hat{3})\}$ decouples from the physical Hilbert space

4. The fourth step involves a plaquette canonical transformation along the plaquette ODGC. The resulting plaquette loop conjugate pairs $\{\mu_1(G,\hat{1});\mu_3(G,\hat{1})\}$ are given by :

$$\mu_1(G,\hat{1}) = \sigma_3(O,\hat{2})\sigma_{3[xz]}(D,\hat{3})\sigma_3(C,\hat{2})\sigma_{3[xz]}(O,\hat{3}) \qquad \mu_3(G,\hat{1}) = \sigma_1(C,\hat{2}) \tag{A.53}$$

The redefined link operators and string operators around ODGC are given by :

$$\begin{aligned}
\sigma_{3[yxz]}(O,\hat{3}) &= \sigma_{3[xz]}(O,\hat{3}) & \sigma_{1[yxz]}(O,\hat{3}) &= \sigma_{1[xz]}(O,\hat{3})\sigma_1(C,\hat{2}) = \mathcal{G}(C) \\
\sigma_{3[yxz]}(D,\hat{3}) &= \sigma_{3[xz]}(D,\hat{3}) & \sigma_{1[yxz]}(D,\hat{3}) &= \sigma_{1[xz]}(D,\hat{3})\sigma_1(C,\hat{2}) = \mathcal{G}(G) \\
\sigma_{3[yy]}(O,\hat{2}) &= \sigma_3(O,\hat{2}) & \sigma_{1[yy]}(O,\hat{2}) &= \sigma_1(O,\hat{2})\sigma_1(C,\hat{2})
\end{aligned} \tag{A.54}$$

As a result of the Gauss law at C and G, The string operators $\{\sigma_{1[xyz]}(O,\hat{3});\sigma_{3[xyz]}(O,\hat{3})\} \equiv \{\bar{\sigma}_1(C,\hat{3});\bar{\sigma}_3(C,\hat{3})\}$ and $\{\sigma_{1[xyz]}(D,\hat{3});\sigma_{3[xyz]}(D,\hat{3})\} \equiv \{\bar{\sigma}_1(G,\hat{3});\bar{\sigma}_3(G,\hat{3})\}$ decouples from the physical Hilbert space. This completes the construction of the plaquettes along the 'vertical walls'.

5. The final step involves a plaquette canonical transformation along the plaquette OAED. The resulting plaquette loop conjugate pairs $\{\mu_1(E,\hat{3});\mu_3(E,\hat{3})\}$ are given by :

$$\begin{aligned}
\mu_1(E,\hat{3}) &= \sigma_{3[xx]}(O,\hat{1})\sigma_{3[yy]}(A,\hat{2})\sigma_{3[xx]}(D,\hat{1})\sigma_{3[yy]}(O,\hat{2}) \\
\mu_3(E,\hat{3}) &= \sigma_{1[yy]}(D,\hat{1}) = \sigma_1(D,\hat{1})\sigma_1(G,\hat{1})
\end{aligned} \tag{A.55}$$

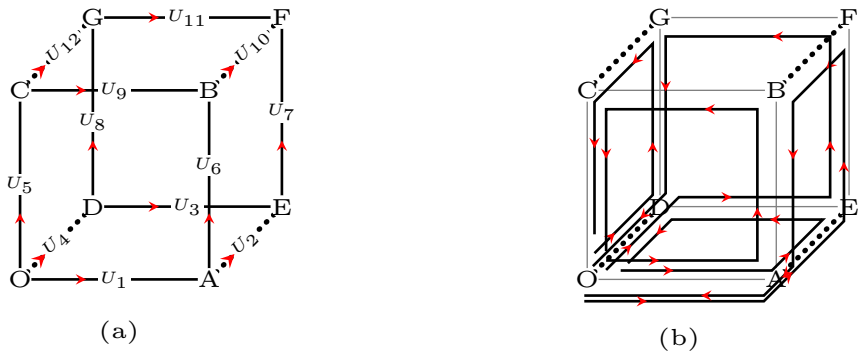

Figure A.8: (a) SU(N) link operators on a cube and (b) SU(N) plaquette loop operators constructed after canonical transformations. Strings to each site is not shown for clarity.

The resulting string operators around OAED are given by:

$$\sigma_{3[xxxx]}(O,\hat{1}) = \sigma_{3[xx]}(O,\hat{1}) \qquad \sigma_{1[xxxx]}(O,\hat{1}) = \sigma_{1[xx]}(O,\hat{1})\sigma_{1[xx]}(D,\hat{1}) = \mathcal{G}(O)\mathcal{G}(D)\mathcal{G}(G)\mathcal{G}(C)$$

$$\sigma_{3[xyy]}(A,\hat{2}) = \sigma_{3[yy]}(A,\hat{2}) \qquad \sigma_{1[xyy]}(A,\hat{2}) = \sigma_{1[yy]}(A,\hat{2})\sigma_{1[xx]}(D,\hat{1}) = \mathcal{G}(E)\mathcal{G}(F)$$

$$\sigma_{3[xyy]}(O,\hat{2}) = \sigma_{3[yy]}(O,\hat{2}) \qquad \sigma_{1[xyy]}(O,\hat{2}) = \sigma_{1[yy]}(O,\hat{2})\sigma_{1[xx]}(D,\hat{1}) = \mathcal{G}(D)\mathcal{G}(G)$$

The string operators $\{\sigma_{1[xxxx]}(O,\hat{1});\ \sigma_{3[xxxx]}(O,\hat{1})\} \equiv \{\bar{\sigma}_1(A,\hat{1});\bar{\sigma}_3(A,\hat{1})\}$, $\{\sigma_{1[xyy]}(A,\hat{2})\ ;\ \sigma_{3[xyy]}(A,\hat{2})\} \equiv \{\bar{\sigma}_1(E,\hat{2});\bar{\sigma}_3(E,\hat{2})\}$ and $\{\sigma_{1[xyy]}(O,\hat{2});\sigma_{3[xyy]}(O,\hat{2})\} \equiv \{\bar{\sigma}_1(D,\hat{2});\bar{\sigma}_3(D,\hat{2})\}$ decouples from the physical Hilbert space, due Gauss laws at O,D,G,C,E,F.

As a result of local Gauss laws at the sites , all the 7 string operators $\{\bar{\sigma}_1(B,\hat{3});\ \bar{\sigma}_3(B,\hat{3})\}$, $\{\bar{\sigma}_1(F,\hat{3});\ \bar{\sigma}_3(F,\hat{3})\}$, $\{\bar{\sigma}_1(C,\hat{3}),\ \{\bar{\sigma}_1(G,\hat{3});\ \bar{\sigma}_3(G,\hat{3})\}$, $\{\bar{\sigma}_1(A,\hat{1});\ \bar{\sigma}_3(A,\hat{1})\}$, $\{\bar{\sigma}_1(E,\hat{2});\bar{\sigma}_3(E,\hat{2})\}$, $\{\bar{\sigma}_1(D,\hat{2});\ \bar{\sigma}_3(D,\hat{2})\}$ decouple from the physical Hilbert space, leaving behind the physical plaquette loop operators $\{\mu_1(B,\hat{3});\mu_3(B,\hat{3})\}$, $\{\mu_1(F,\hat{1});\mu_3(F,\hat{1})\}$, $\{\mu_1(F,\hat{2});\ \mu_3(F,\hat{2})\}$, $\{\mu_1(G,\hat{1});\ \mu_3(G,\hat{1})\}$, $\{\mu_1(E,\hat{3});\ \mu_3(E,\hat{3})\}$.

A.3.2 *SU(N) lattice gauge theory.*

In this section, we iterate the fundamental SU(N) canonical transformation to reformulate SU(N) lattice gauge theory on a single cube in terms of plaquette loop operators. Canonical transformations transforms the link operators on the unit cube to the following operators:

1. Physical plaquette loop conjugate operators on the plaquettes corresponding to the 4 'walls' and the 'floor' of the cube

2. String operators to each site on the cube except the origin.

These string operators decouple, leaving behind the plaquette loop operators. As before, no new constraints are introduced. Just like in the Z_2 case,the sites of the 3D cube are labelled as : $O \equiv (0,0,0)$; $A \equiv (1,0,0)$; $B \equiv (1,0,1)$; $C \equiv (0,0,1)$; $D \equiv (0,1,0)$; $E \equiv (1,1,0)$; $F \equiv (1,1,1)$; $G \equiv (0,1,1)$. This is illustrated in figure A.8. The loop formulation of SU(N) lattice gauge theory on a single cube is achieved in 6 set of canonical transformations as follows.

1. The first set of canonical transformations involves the construction of the plaquette loop operators on the XY plaquette OAEDO.

$$
\begin{aligned}
U(12) &\equiv U_1 U_2 & E^a_+(12) &= E^a_-(E,\hat{2}) \\
U_{[xy]}(1) &= U_1 & E^a_{+[xy]}(1) &= E^a_-(A,\hat{1}) + E^a_+(A,\hat{2}) \\
U(43) &= U_4 U_3 & E^a_+(43) &= E^a_-(E,\hat{1}) \\
U_{[xy]}(4) &= U_4 & E^a_{+[xy]}(4) &= E^a_-(D,\hat{2}) + E^a_+(D,\hat{1}) \\
U(1234) &= U_{12} U^\dagger_{43} & E^a_+(1234) &= E^a_-(43) \\
U_{[xy]}(12) &= U_{12} & E^a_{+[xy]}(12) &= E^a_+(12) + E^a_+(43) = E^a_-(E,\hat{2}) + E^a_-(E,\hat{1})
\end{aligned}
$$

2. Second set of canonical transformation involves construction of string operators to each site.

$$
\begin{aligned}
U(16) &= U_{[xy]}(1) U_6 & E^a_+(16) &= E^a_+(6) \\
U_{[xyz]}(1) &= U_{[xy]}(1) = U_1 & E^a_{+[xyz]}(1) &= E^a_{+[xy]}(1) + E^a_+(A,\hat{3}) = \mathcal{G}(A) \\
U((12)7) &= U_{[xy]}(12) U_7 & E^a_+((12)7) &= E^a_-(F,\hat{3}) \\
U_{[xyz]}(12) &= U_{[xy]}((12)) & E^a_{+[xyz]}((12)) &= E^a_{+[xy]}((12)) + E^a_+(E,\hat{3}) = \mathcal{G}(E) \\
U(48) &= U_{[xy]}(4) U_8 & E^a_+(48) &= E^a_-(G,\hat{3}) \\
U_{[xyz]}(4) &= U_{[xy]}(4) & E^a_{+[xyz]}(4) &= E^a_{+[xy]}(4) + E^a_+(D,\hat{3}) = \mathcal{G}(D)
\end{aligned}
$$

3. The third set involves the construction of vertical plaquette ODGCO.

$$U(5(12)) = U_5 U_{12} \qquad E^a_+(5(12)) = E^a_+((12))$$
$$U_{[zy]}(5) = U_5 \qquad E^a_{+[zy]}(5) = E^a_-(C,\hat{3}) + E^a_+(C,\hat{2})$$
$$U(485(12)) = U(48)U^\dagger(5(12)) \qquad E^a_+(485(12)) = E^a_+(O,\hat{3})$$
$$U_{[yz]}(48) = U(48) \qquad E^a_{+[yz]}(48) = E^a_+(48) + E^a_+(5(12))$$

4. The fourth set involves the construction of vertical plaquette ODGFEDO.

$$U_{48(11)} = U_{[yz]}(48)U_{11} \qquad E^a_+(48(11)) = E^a_-(F,\hat{1})$$
$$U_{[xyz]}(48) = U_{[yz]}(48) \qquad E^a_{+[xyz]}(48) = E^a_{+[yz]}(48) + E^a_+(G,\hat{1})$$
$$U_{127(11)84} = U(127)U^\dagger(48(11)) \qquad E^a_+(127(11)84) = E^a_-(48(11))$$
$$U_{[xz]}(127) = U(127) \qquad E^a_{+[xz]}(127) = E^a_+((12)7) + E^a_+(48(11))$$
$$U_{437(11)84} = U^\dagger(1234)U(127(11)84) \qquad E^a_+(437(11)84) = E^a_+(127(11)84)$$
$$U_{[z]}(1234) = U(1234) \qquad E^a_{-[z]}(1234) = E^a_-(1234) + E^a_-(127(11)84)$$

5. The fifth set involves the construction of vertical plaquette OAEFBAO

$$U_{127(10)} = U_{[xz]}(127)U_{10} \qquad E^a_+(127(10)) = E^a_-(F,\hat{2})$$
$$U_{[xyz]}(127) = U_{[xz]}(127) \qquad E^a_{R[xyz]}(127) = E^a_{+[xz]}(127) + E^a_-(F,\hat{2}) = \mathcal{G}(F)$$
$$U_{127(10)16} = U(127(10))U(16) \qquad E^a_-(127(10)16) = E^a_-(127(10))$$
$$U_{[yz]}(16) = U(16) \qquad E^a_{+[yz]}(16) = E^a_+(16) + E^a_+(127(10))$$

6. The sixth set involves the construction of vertical plaquette OABCO.

$$U_{58} = U_{[yz]}(5)U_8 \qquad E^a_+(58) = E^a_-(G,\hat{3})$$
$$U_{[xyz]}(5) = U_{[yz]}(5) \qquad E^a_{+[xyz]}(5) = E^a_{+[yz]}(5) + E^a_+(D,\hat{3})) = \mathcal{G}(C)$$
$$U_{1685} = U_{[xy]}(16)U^\dagger(58) \qquad E^a_+(1685) = E^a_-(58)$$
$$U_{[xyz]}(16) = U_{[zy]}(16) \qquad E^a_{+[xyz]}(16) = E^a_{+[zy]}(16) + E^a_+(58) = \mathcal{G}(B)$$

Just like before, all the string operators decouple due to the Gauss laws at A, E, D, B, F, G, C leaving behind the plaquette loop operators corresponding to the plaquettes OAEDO, ODGCO, ODGFEDO, OAEFBAO, OABCO. Note that the 'roof' plaquette OCGFBCO is not constructed.

B

MAGNETIC BASIS OF SU(2) LATTICE GAUGE THEORY

In this appendix, we show that all Wilson loops are diagonal in the magnetic basis of $SU(2)$ lattice gauge theory defined in 3.56. We repeat the defining equation [1] for convenience.

$$|\omega,\hat{w}\rangle = \sum_{jm_-m_+} \sqrt{\frac{2j+1}{2\pi^2}} D^j_{m_-m_+}(\omega,\hat{w})\,|j\ m_-\ m_+\rangle = \sum_{j,m,\bar{m},l,\mu} \sqrt{\frac{2j+1}{2\pi^2}} D^j_{m\bar{m}}(\omega,\hat{w})\,\langle nl\mu|jm\bar{m}\rangle\,|nl\mu\rangle$$
$$= \sum_{n,l,m} Y_{nlm}(\omega,\hat{w})\,|nlm\rangle \tag{B.1}$$

Here, $(\omega,\hat{w})$ is the angle axis characterisation of a point on $S^3(SU(2))$ and $Y_{nlm}(\omega,\hat{w})$ are the hyperspherical harmonics on S^3. We have also used the relation [153]:

$$Y_{nlm}(\omega,\hat{w}) = \sqrt{\frac{2j+1}{2\pi^2}} C^{lm}_{jm_-,jm_+} D^j_{m_-m_+}(\omega,\hat{w})$$

The states $|\omega,\hat{w}\rangle$ forms a complete, orthonormal basis. The plaquette loop operators are diagonal in this basis.

$$\mathcal{W}_{\alpha\beta}\,|\omega,\hat{w}\rangle = z_{\alpha\beta}\,|\omega,\hat{w}\rangle \tag{B.2}$$

where

$$z_{\alpha\beta} = \begin{bmatrix} \left(\cos\frac{\omega}{2} - i\sin\frac{\omega}{2}\cos\theta\right) & i\sin\frac{\omega}{2}\sin\theta e^{-i\phi} \\ -i\sin\frac{\omega}{2}\sin\theta e^{-i\phi} & \left(\cos\frac{\omega}{2} + i\sin\frac{\omega}{2}\cos\theta\right) \end{bmatrix}_{\alpha\beta} \tag{B.3}$$

Above, we have suppressed the plaquette index of $\mathcal{W}_{\alpha\beta}$ for simplicity. (B.2) follows from the properties of Wigner matrices $D^j_{m_-m_+}$ as shown below.

$$\mathcal{W}_{11}\,|\omega,\hat{w}\rangle = (F_N)\left[a_1c_1 + a_2^\dagger c_2^\dagger\right](F_N)\sum_{j,m_-,m_+}[j]D^j_{m_-m_+}(\omega,\hat{w})\,|j,m_-,m_+\rangle$$
$$= \sum_{j,m_-,m_+}[j]D^j_{m_-m_+}(\omega,\hat{w})\left[\frac{1}{\sqrt{2j}}\sqrt{(j+m_-)(j+m_+)}\frac{1}{\sqrt{2j+1}}\left|j-\frac{1}{2},m_--\frac{1}{2},m_+-\frac{1}{2}\right\rangle\right.$$
$$\left. + \frac{1}{\sqrt{2j+2}}\sqrt{(j-m_-+1)(j-m_++1)}\frac{1}{\sqrt{2j+1}}\left|j+\frac{1}{2},m_--\frac{1}{2},m_+-\frac{1}{2}\right\rangle\right] \tag{B.4}$$

1 For simplicity, the states $|\Omega(\omega,\hat{w})\rangle$ in 3.56 is denoted here as $|\omega,\hat{w}\rangle$

Above, $F_N = \frac{1}{\sqrt{N+1}}$ and $[j] = \sqrt{\frac{2j+1}{2\pi^2}}$. Putting $J \equiv j - \frac{1}{2}$ in the first term and $J \equiv j + \frac{1}{2}$ in the second term and using the following [115] recursion relation for Wigner D matrices

$$\frac{\sqrt{(J-m_-+\frac{1}{2})(J-m_++\frac{1}{2})}}{2J+1} D^{(J-\frac{1}{2})}_{m_-m_+}(\hat{w},\omega) + \frac{\sqrt{(J+m_-+\frac{1}{2})(J+m_++\frac{1}{2})}}{2J+1} D^{(J+\frac{1}{2})}_{m_-m_+}(\hat{w},\omega)$$
$$= \left(\cos\frac{\omega}{2} - i\sin\frac{\omega}{2}\cos\theta\right) D^{J}_{m_-\,-\frac{1}{2}\;\;m_+-\frac{1}{2}}(\omega,\hat{w})$$

Therefore,

$$\mathcal{W}_{11}\,|\omega,\hat{w}\rangle = \left(\cos\frac{\omega}{2} - i\sin\frac{\omega}{2}\cos\theta\right)|\omega,\hat{w}\rangle = z_{11}\,|\omega,\hat{w}\rangle \tag{B.5}$$

similarly, we get

$$\begin{aligned}
\mathcal{W}_{12}\,|\omega,\hat{w}\rangle &= i\sin\frac{\omega}{2}\sin\theta e^{-i\phi}\,|\omega,\hat{w}\rangle = z_{12}\,|\omega,\hat{w}\rangle \\
\mathcal{W}_{21}\,|\omega,\hat{w}\rangle &= -i\sin\frac{\omega}{2}\sin\theta e^{i\phi}\,|\omega,\hat{w}\rangle = z_{21}\,|\omega,\hat{w}\rangle \\
\mathcal{W}_{22}\,|\omega,\hat{w}\rangle &= \left(\cos\frac{\omega}{2} + i\sin\frac{\omega}{2}\cos\theta\right)|\omega,\hat{w}\rangle = z_{22}\,|\omega,\hat{w}\rangle
\end{aligned} \tag{B.6}$$

Even though $|\omega,\hat{w}\rangle$ forms a complete, orthonormal basis, they are not invariant under global gauge transformations. Under a global gauge transformation Λ, $|\omega,\hat{w}\rangle$ transforms as follows

$$\begin{aligned}
|\omega,\hat{w}\rangle^{\Lambda} &= \sum_{n,l,m} Y_{nlm}(\omega,\hat{w}) D^{l}_{m\bar{m}}(\Lambda)\,|nl\bar{m}\rangle = \sum_{n,l,m} \chi^{j}_{l}(\omega) Y_{lm}(\hat{w}) D^{l}_{m\bar{m}}(\Lambda)\,|nl\bar{m}\rangle \\
&= \sum_{n,l,m} \chi^{j}_{l}(\omega) Y_{lm}(\hat{w}^{\Lambda})|nlm\rangle = |\omega,\hat{w}^{\Lambda}\rangle\,; \qquad j = \frac{(n-1)}{2}.
\end{aligned} \tag{B.7}$$

Here, $\chi^{j}_{l}(\omega)$ are generalized $SU(2)$ characters [115] , $Y_{lm}(\omega,\hat{w})$ are the spherical harmonics on S^2 and $\hat{w}^{\Lambda}$ denotes rotated $\hat{w}$. Thus, under a global gauge transformation Λ, ω is an invariant angle and $\hat{w}$ transforms like a vector :

$$\omega \to \omega; \qquad\qquad \hat{n^a} \to R_{ab}(\Lambda)\hat{w}^b$$

A completely gauge invariant angular basis on a single plaquette can be constructed by integrating out gauge transformations as follows:

$$\begin{aligned}
|\omega\rangle \;\equiv\; \int |\omega,\hat{w}^{\Lambda}\rangle\, d\mu(\Lambda) \;&=\; \sum_{n,l,m}\int d\mu(\Lambda) Y_{nlm}(\omega,\hat{w}) D^{l}_{m\bar{m}}(\Lambda)\,|nl\bar{m}\rangle \\
&=\; \sum_{n} Y_{n00}(\omega,\hat{w})\,|n00\rangle \;=\; \sum_{j}\chi^{j}(\omega)\,|j\rangle
\end{aligned} \tag{B.8}$$

Here we have used the identity [115] $\int d\mu(\Lambda) D^{l}_{m\bar{m}}(\Lambda) = \delta_{l0}\delta_{m0}\delta_{\bar{m}0}$ where

$$\int d\mu(\Lambda) = \frac{1}{4\pi^2}\int_0^{2\pi} \sin^2(\frac{\omega}{2}) d\omega \int_0^{\pi} \sin\theta d\theta \int_0^{2\pi} d\phi$$

is the Haar measure of SU(2) where the SU(2) group element Λ is characterized by ω, θ, ϕ. Also, $j = (n-1)/2$ and $\chi_j(\omega) = \frac{sin(2j+1)\frac{\omega}{2}}{sin\left(\frac{\omega}{2}\right)}$ are the SU(2) characters. Therefore, for a single plaquette lattice the gauge invariant states are characterized by the gauge invariant angle ω as expected.

For a finite lattice, a complete, orthonormal basis is given by the direct product of $|\hat{w}, \omega\rangle$ corresponding to each plaquette. All Wilson loops are diagonal in this basis. A completely gauge invariant magnetic/angular basis can then be constructed by integrating out the gauge transformations :

$$|\Omega\rangle = |\omega_{P_i}, [\Theta_j]\rangle = \int d\mu(\Lambda) \prod_{\otimes p} |\omega_p, \hat{w}_p\rangle^{\Lambda} = \int d\mu(\Lambda) \prod_{\otimes p} |\omega_p, \hat{w}_p^{\Lambda}\rangle \tag{B.9}$$

where $[\Theta_j]$ denotes the set of $2p-3$ independent relative angles between the axes $\hat{w}_{P_i}$, where p is the no of plaquettes in the lattice. These angles are invariant with respect to gauge rotations.

- **2 plaquette lattice** On a 2 plaquette lattice the gauge invariant basis states are :

$$\int |\omega_1, \hat{w}_1^{\Lambda}\rangle\, |\omega_2, \hat{w}_2^{\Lambda}\rangle\, d\mu(\Lambda) = \sum_{\substack{n_1,l_1,m_1\\ n_2,l_2,m_2\\ \bar{m}_1,\bar{m}_2}} \int d\mu(\Lambda) \begin{array}{l} \chi^{j_1}_{l_1}(\omega_1)\; Y_{l_1 m_1}(\hat{w}_1)\; D^{l_1}_{m_1\bar{m}_1}(\Lambda) \\ \chi^{j_2}_{l_2}\omega_2\; Y_{l_2 m_2}(\hat{w}_2)\; D^{l_2}_{m_2\bar{m}_2}(\Lambda) \end{array} \left| \begin{array}{l} n_1\; l_1\; \bar{m}_1 \\ n_2\; l_2\; \bar{m}_2 \end{array} \right\rangle$$

$$= \sum_{\substack{n_1,l_1,m_1\\ n_2,\bar{m}_1}} (-1)^{l_1-m_1}(-1)^{l_1-\bar{m}_1} \frac{16\pi^2}{2l_1+1} \begin{array}{l} \chi^{j_1}_{l_1}(\omega_1)\; Y_{l_1 m_1}(\hat{w}_1) \\ \chi^{j_2}_{l_2}(\omega_2)\; Y_{l_1\; -m_1}(\hat{w}_2) \end{array} \left| \begin{array}{l} n_1\; l_1\; \bar{m}_1 \\ n_2\; l_1\; -\bar{m}_1 \end{array} \right\rangle$$

$$= 16\pi^2 \sum_{\substack{n_1,l_1\\ n_2,m_1}} \underbrace{C^{00}_{l\bar{m}_1\; l-\bar{m}_1} Y_{l_1 m_1}(\hat{w}_1) Y_{l_1\; -m_1}(\hat{w}_2)}_{\text{Bipolar scalar harmonics}} \chi^{j_1}_{l_1}(\omega_1)\; \chi^{j_2}_{l_2}(\omega_2) |n_1\; l_1\; n_2\; l_1\; 0\rangle \tag{B.10}$$

$$= 4\pi \sum_{\substack{n_1,l_1,\\ n_2}} (2l_1+1)\; P_l(cos\Theta_{12})\; \chi^{j_1}_{l_1}(\omega_1)\; \chi^{j_2}_{l_2}(\omega_2)\; |n_1\; l_1\; n_2\; l_1\; 0\rangle \equiv |\omega_1\; \omega_2\; \Theta_{12}\rangle$$

Here, we have used the relations :

$$\int d\mu(\Lambda) D^{l_1}_{m_1\;\bar{m}_1}(\Lambda)\; D^{l_2}_{m_2\;\bar{m}_2}(\Lambda) = (-1)^{\bar{m}_1-m_1} \frac{16\pi^2}{2l_1+1} \delta_{l_1 l_2}\delta_{-m_1\; m_2}\delta_{-\bar{m}_1\bar{m}_2};$$

$$\frac{(-1)^{l-m}}{\sqrt{2l+1}} = C^{00}_{lm\; l-m}; \qquad \sum_{m_1} C^{00}_{l\bar{m}_1\; l-\bar{m}_1} Y_{l_1 m_1}(\hat{w}_1) Y_{l_1\; -m_1}(\hat{w}_2) = \frac{2l_1+1}{4\pi} P_l(cos\Theta_{12})$$

where Θ_{12} is the angle between $\hat{w}_1$ and $\hat{w}_2$.

- **N plaquette** The above process can be generalized to N plaquettes which leads to the following gauge invariant basis on an N plaquette lattice.

$$|\omega_{P_i}, [\Theta_{ij}]\rangle = k \sum_{[n],[l],[ll]} Y_{[n][l][ll]}(\omega_1, \cdots \omega_p, [\Theta_{ij}]) \, |[n], [l], [ll]\rangle \tag{B.11}$$

Here, $Y_{[n][l][ll]}$ is the scalar multipolar spherical harmonics [115]. In general, the procedure of integrating out the gauge transformation projects out the gauge invariant subspace and is equivalent to finding the subspace with 0 total angular momentum.

C

CALCULATIONAL METHODS IN THE LOOP FORMULATION

In this appendix, we discuss some calculational methods in the new loop formulation. Since, the degrees of freedom now lie on the plaquettes instead of the links and the magnetic part of the Hamiltonian involve a single plaquette holonomy, calculations are much more simpler in the present loop formulation.

Variational method

In this section, we study the ground state of SU(2) loop Hamiltonian using a 'single' plaquette variational ansatz. We then compare the results with those obtained from the variational analysis of the standard Kogut-Susskind formulation [70–72, 74]. Note that after canonical transformations each plaquette loop is a fundamental degree of freedom. Therefore, gauge invariant computations in the dual spin model become much simpler. For the ground state of SU(2) gauge theory, the magnetic fluctuations in a spatial region are almost independent of fluctuations in another spatial region which is sufficiently far away [17, 62, 63]. So, the largest contributions to the vacuum state comes from states with little magnetic correlations. Therefore, we use the following separable state without any spin-spin correlations as our variational ansatz:

$$|\psi_0\rangle = e^{S/2}|0\rangle; \qquad S = \alpha \sum_p Tr\mathcal{W}(p).$$
$$= \prod_p |\psi_0\rangle_p. \tag{C.1}$$

Above, $|0\rangle$ is the strong coupling vacuum state defined by $\mathcal{E}^a_{\pm}(m,n)|0\rangle = 0$ and α is the variational parameter. This state (C.1) satisfies Wilson's area law criterion. We consider a Wilson loop $Tr\ (W_C)$ along a large space loop C on the lattice and compute its ground state expectation value: $\frac{<\psi_0|TrW_C|\psi_0>}{\langle\psi_0|\psi_0\rangle}$. In the dual spin model any Wilson loop W_C can be written in terms of the $\mathcal{P}$ fundamental loops $\mathcal{W}_{\alpha\beta}$ as shown in Figure C.1:

$$W_C = \mathcal{W}(p_1)\ \mathcal{W}(p_2)\ \mathcal{W}(p_3)\cdot\cdot\cdot\cdot\cdot\mathcal{W}(p_{n_c}). \tag{C.2}$$

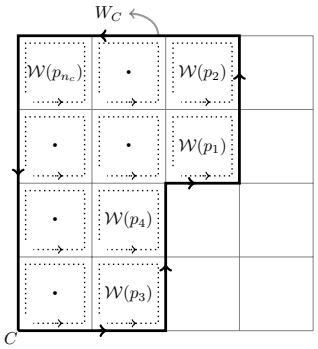

Figure C.1: A Wilson loop W_C can be written as the product of fundamental plaquette loop operators $\mathcal{W}(p)$. $W_C = \mathcal{W}(p_1)\ \mathcal{W}(p_2)\ \mathcal{W}(p_3) \cdots\cdots \mathcal{W}(p_{n_c})$. The tails of the fundamental plaquette loop operators connecting them to the origin (see Figure 3.11-a) are not shown for clarity.

Here p_1 is the plaquette operator in the bottom right corner of C and p_{n_c} is the plaquette operator at the left top corner of C. We now show that this state satisfies Wilson's area law. The expectation value of TrW_C in $|\psi_0\rangle$ is given by

$$\begin{aligned}\langle TrW_C\rangle \ &\equiv\ \frac{\langle\psi_0|TrW_C|\psi_0\rangle}{\langle\psi_0|\psi_0\rangle} = \frac{1}{\langle\psi_0|\psi_0\rangle}\prod_{p\in p_i}\int d\mu(\omega_p,\hat{w}_p)\langle 0|e^S Trz(C)|\omega_p,\hat{w}_p\rangle\langle\omega_p,\hat{w}_p|0\rangle \\ &= \frac{\prod_p\int d\mu(\omega_p,\hat{w}_p)\ e^{2\alpha\cos\omega_p/2}\ 2\cos\left(\omega(C)/2\right)}{\prod_p\int d\mu(\omega_p,\hat{w}_p)\ e^{2\alpha\cos(\frac{\omega_p}{2})}}\end{aligned} \tag{C.3}$$

In (C.3), $\int d\mu(\omega_p,\hat{\omega}_p) \equiv \int_0^{2\pi} 4\sin^2\frac{\omega}{2}d\omega \int_0^{\pi}\sin\theta d\theta \int_0^{2\pi} d\phi$. We have also used the completeness relation of the $|\omega,\hat{w}\rangle$ basis. $z(C)$ is the eigenvalue of W_C corresponding to the eigenstate $\prod_p|\omega_p,\hat{w}_p\rangle$. Since $W_C = \prod_{p_i}\mathcal{W}(p_i)$, $z(C) = \prod_{p_i} z(p_i)$ and $Trz(C) = 2\cos\left(\omega(C)/2\right)$. Here, $\omega(C)$ is the gauge invariant angle characterizing the $SU(2)$ matrix $z(C)$ in its angle axis representation. Using the expression for the product of 2 SU(2) matrices [1] repeatedly, it is easy to show that $\cos(\omega(C)/2) = \prod_i\cos(\omega_{p_i}/2)$ + terms which vanish on θ integration[2] Therefore,

$$\langle TrW_C\rangle = 2\left(\frac{I_2(2\alpha)}{I_1(2\alpha)}\right)^{n_c} = 2e^{-n_c\ \ln\left(\frac{I_1(2\alpha)}{I_2(2\alpha)}\right)} \tag{C.5}$$

1 Product of 2 SU(2) matrices characterized by $(\omega_1,\hat{w}_1)$ and $(\omega_2,\hat{w}_2)$ gives an SU(2) matrix characterized by $(\omega,\hat{w})$ with

$$\begin{aligned}\cos\frac{\omega}{2} &= \cos\frac{\omega_1}{2}\cos\frac{\omega_2}{2} - (\hat{w}_1\cdot\hat{w}_2)\sin\frac{\omega_1}{2}\sin\frac{\omega_2}{2}; \\ \hat{w}\sin\frac{\omega}{2} &= \hat{w}_1\sin\frac{\omega_1}{2}\cos\frac{\omega_2}{2} + \hat{w}_2\sin\frac{\omega_2}{2}\cos\frac{\omega_1}{2} - [\hat{w}_1\times\hat{w}_2]\sin\frac{\omega_1}{2}\sin\frac{\omega_2}{2}.\end{aligned} \tag{C.4}$$

2 The integrand under θ integration contains either $\sin 2\theta$ or a $\cos\theta$, both vanish on θ integration from 0 to π.

In (C.5), n_c is the number of plaquettes in the loop C and $I_l(2\alpha)$ is the l-th order modified Bessel function of the first kind. We have used the relation

$$I_l(2\alpha) = \frac{1}{\pi}\int_0^\pi e^{2\alpha\cos\omega}\cos l\omega\, d\omega. \tag{C.6}$$

and the recurrence relation [166]

$$I_{l-1}(2\alpha) - I_{l+1}(2\alpha) = \frac{2l}{2\alpha} I_l(2\alpha) \tag{C.7}$$

to arrive at (C.5). The string tension is given by $\sigma_T(\alpha) = \ln\left(\frac{I_1(2\alpha)}{I_2(2\alpha)}\right)$.

The local effective SU(2) spin model Hamiltonian is

$$H_{spin} = \sum_{p=1}^{\mathcal{P}}\left\{4g^2\vec{\mathcal{E}}^{\,2}(p) + \frac{1}{g^2}\left[2 - (Tr\mathcal{W}(p))\right]\right\} + g^2\sum_{\langle p,p'\rangle}\left\{\vec{\mathcal{E}}_-(p)\cdot\vec{\mathcal{E}}_+(p')\right\}. \tag{C.8}$$

We now calculate α by minimizing

$$\langle H_{spin}\rangle = \frac{\langle\psi_0|H_{spin}|\psi_0\rangle}{\langle\psi_0|\psi_0\rangle}.$$

In order to calculate $\langle H_{spin}\rangle$, we first find the expectation value of $\mathcal{E}_-(p)\cdot\mathcal{E}_+(p')$ and $\mathcal{E}(p)\cdot\mathcal{E}(p) \equiv \mathcal{E}_+(p)\cdot\mathcal{E}_+(p) \equiv \mathcal{E}_-(p)\cdot\mathcal{E}_-(p)$ in (C.8). First, lets calculate $\langle\psi_0|\mathcal{E}^a_-(p)\mathcal{E}^a_+(P)|\psi_0\rangle$. Here, P is any plaquette.

$$\begin{aligned}\langle\psi_0|\mathcal{E}^a_-(p)\mathcal{E}^a_+(P)|\psi_0\rangle &= \left\langle 0\right|\left(e^{S/2}\mathcal{E}^a_-(p)e^{-S/2}\right)e^S\left(e^{-S/2}\mathcal{E}^a_+(P)e^{S/2}\right)\left|0\right\rangle \\ &= \frac{-1}{4}\langle\psi_0|\left[\mathcal{E}^a_-(p),S\right]\left[\mathcal{E}^a_+(P),S\right]|\psi_0\rangle\end{aligned} \tag{C.9}$$

In (C.9), we have used the fact that $\mathcal{E}_\pm|0\rangle = 0$. Evaluating $\langle\psi_0|\mathcal{E}^a_-(p)\mathcal{E}^a_+(P)|\psi_0\rangle$ in a different way,

$$\begin{aligned}\langle\psi_0|\mathcal{E}^a_-(p)\mathcal{E}^a_+(P)|\psi_0\rangle &= \left\langle 0\right|e^{S/2}\mathcal{E}^a_-(p)e^{S/2}\left(e^{-S/2}\mathcal{E}^a_+(P)e^{S/2}\right)\left|0\right\rangle \\ &= \frac{1}{2}\langle\psi_0|\Big[\mathcal{E}^a_-(p),\left[\mathcal{E}^a_+(P),S\right]\Big]|\psi_0\rangle + \frac{1}{4}\langle\psi_0|\left[\mathcal{E}^a_+(P),S\right]\left[\mathcal{E}^a_-(p),S\right]|\psi_0\rangle\end{aligned} \tag{C.10}$$

The equations (C.9) and (C.10) implies:

$$\langle\psi_0|\mathcal{E}_-(p)\cdot\mathcal{E}_+(P)|\psi_0\rangle = \frac{1}{4}\langle\psi_0|\Big[\mathcal{E}^a_-(p),\left[\mathcal{E}^a_+(P),S\right]\Big]|\psi_0\rangle \tag{C.11}$$

The expression in (C.11) vanishes when $P \neq p$. In particular,

$$\langle\psi_0|\mathcal{E}_-(p)\cdot\mathcal{E}_+(p')|\psi_0\rangle = 0, \tag{C.12}$$
$$\langle\psi_0|\mathcal{E}_-(p)\cdot\mathcal{E}_-(p)|\psi_0\rangle = \tfrac{3\alpha}{16}\langle\psi_0|Tr\mathcal{W}(p)|\psi_0\rangle.$$

Above p, p' are nearest neighbours. Putting $n_c = 1$ in equation (C.5), $\langle Tr\mathcal{W}(p)\rangle = \frac{2I_2(2\alpha)}{I_1(2\alpha)}$. Using the above relations, the expectation value of the effective Hamiltonian H_{spin} is

$$\frac{\langle\psi_0|H_{spin}|\psi_0\rangle}{\langle\psi_0|\psi_0\rangle} = 2\mathcal{P}\left\{\left(\frac{3\alpha}{4}g^2 - \frac{1}{g^2}\right)\frac{I_2(2\alpha)}{I_1(2\alpha)} + \frac{1}{g^2}\right\}. \tag{C.13}$$

Above, $\mathcal{P}$ is the number of plaquettes in the lattice. $\frac{I_2(2\alpha)}{I_1(2\alpha)}$ is a monotonously increasing bounded function of α. It takes values between $+1$ and -1 with $+1$ at $\alpha \to \infty$ and -1 at $\alpha \to -\infty$. In the weak coupling limit, $g^2 \to 0$, $\frac{I_2(2\alpha)}{I_1(2\alpha)}$ should be maximum for the expectation value of H_{spin} to be minimum and therefore, $\alpha \to \infty$. But, using the asymptotic form of the modified Bessel function of the first kind $I_l(2\alpha)$,

$$I_l(2\alpha) \xrightarrow{\alpha\to\infty} \frac{e^{2\alpha}}{\sqrt{2\pi(2\alpha)}}\left(1 + \frac{(1-2l)(1+2l)}{16\alpha} + \cdots\right)$$

In the weak coupling limit , $\frac{I_2(2\alpha)}{I_1(2\alpha)} \approx 1 - \frac{3}{4\alpha}$. Hence,

$$\frac{\langle\psi_0|H_{spin}|\psi_0\rangle}{\langle\psi_0|\psi_0\rangle} = \sum_p 2\left\{\left(\frac{3\alpha}{4}g^2 - \frac{1}{g^2}\right)\left(1 - \frac{3}{4\alpha}\right) + \frac{1}{g^2}\right\} \tag{C.14}$$

Minimizing the expectation value in the weak coupling limit, $\alpha = \frac{1}{g^2}$. The string tension is given by $\sigma_T(\frac{1}{g^2}) = ln\left(I_1(\frac{1}{g^2})/I_2(\frac{1}{g^2})\right)$. This is exactly the result obtained in [70–72] using variational calculation with the fully disordered ground state and Kogut-Susskind Hamiltonian (3.59) which is dual to the full non-local spin Hamiltonian. The general non-local Hamiltonian H differs from the above effective local spin Hamiltonian H_{spin} by terms of the form $R_{ab}(W)\ \mathcal{E}^a_-(p)\mathcal{E}^b_+(\bar{p})$, where p and $\bar{p}$ are any 2 plaquettes on the lattice which are at least 2 lattice spacing away from each other. Above, W is in general the product of many plaquette loop operators. The expectation value of the full Hamiltonian in the variational ground state $|\psi_0\rangle$ reduces to $\langle\psi_0|H_{spin}|\psi_0\rangle$ as the expectation value of the non-local terms in $|\psi_0\rangle$ vanishes. So, the simplified Hamiltonian with nearest neighbour interactions gives the same variational ground state to the lowest order as the full Hamiltonian.

C.0.2.1 *A tensor networks ansatz*

The present loop formulation is tailor-made for tensor network [155–158] and matrix product state (MPS) [159] ansatzes to explore the interesting and physically relevant part of $\mathcal{H}^p$ for low energy states. This is due to the following two reasons:

- The absence of local non-abelian Gauss laws at every lattice site.
- The presence of (spin type) local hydrogen atom orthonormal basis at every plaquette.

We first briefly discuss matrix product state approach in a simple example of spin chain with spin $s = 1$ before directly generalizing it to pure SU(2) lattice gauge theory on a one dimensional chain of plaquettes. In the case of spin chain with $s_x = -1, 0, +1$ at every lattice site $x = 0, 1, \cdots, N$, any state can be written as:

$$|\Psi\rangle = \sum_{s_1, s_2 \cdots s_N = 0, \pm 1} \Psi(s_1, s_2, \cdots s_N) \ |s_1, s_2, \cdots s_N\rangle \, . \tag{C.15}$$

The matrix product state method consists of replacing the wave functional by

$$\Psi(s_1, s_2, \cdots s_N) = Tr\left(T_1^{(s_1)} T_2^{(s_2)} \cdots T_N^{(s_N)}\right). \tag{C.16}$$

In (C.16) T^s are $D \times D$ matrices where D is the bond length. The matrix elements of T^s are fixed by minimizing the spin Hamiltonian. In the hydrogen atoms loop basis we have a similar structure where the three dimensional spin states are replaced by infinite dimensional quantum states of hydrogen atoms: $|s\rangle \rightarrow |n \ l \ m\rangle$. The most general state in the hydrogen atom loop basis can be written as:

$$|\Psi\rangle = \sum_{\{n\}\{l\}\{m\}} \Psi \begin{bmatrix} n_1 & n_2 & \cdots & n_p \\ l_1 & l_2 & \cdots & l_p \\ m_1 & m_2 & & \cdots m_{\mathcal{P}} \end{bmatrix} \left| \begin{matrix} n_1 & n_2 & \cdots & n_p \\ l_1 & l_2 & \cdots & l_p \\ m_1 & m_2 & & \cdots m_{\mathcal{P}} \end{matrix} \right\rangle . \tag{C.17}$$

We now consider SU(2) lattice gauge theory on a chain of $\mathcal{P}$ plaquettes as shown in Figure 3.14. A simple tensor network ansatz, like (C.16 for spins, for the ground state wave function in (C.17) is

$$\Psi_0 \begin{bmatrix} n_1 & n_2 & \cdots & n_p \\ l_1 & l_2 & \cdots & l_p \\ m_1 & m_2 & & \cdots m_{\mathcal{P}} \end{bmatrix} \equiv Tr\left[T_1^{(n_1 l_1 m_1)} \ T_2^{(n_2 l_2 m_2)} \cdots T_{\mathcal{P}}^{(n_{\mathcal{P}} \ l_{\mathcal{P}} \ m_{\mathcal{P}})}\right]. \tag{C.18}$$

In (C.18) $T_x^{(n_x l_x m_x)}$; $x = 1, 2 \cdots, \mathcal{P}$ are $\mathcal{P}$ matrices of dimension $D \times D$ where D is the bond length describing correlations between hydrogen atoms. Assuming a bound on the principal quantum number (e.g., $\mathsf{n} = 1, 2$) and minimizing the energy of the spin model Hamiltonian

within spherically symmetric s-sector should give a good idea of ground state at least in the strong coupling region. The method can then be extrapolated systematically towards weak coupling by extending the range of hydrogen atom principal quantum number on each plaquette. The global SU(2) Gauss law can also be explicitly implemented through the following ansatz:

$$|\Psi\rangle = \sum_{\{n\}\{l\}\{ll\}} \Psi \begin{bmatrix} n_1 & n_2 & \cdots & n_p \\ l_1 & l_2 & \cdots & l_p \\ l_{12} & l_{123} & \cdots & l_{12\cdots\mathcal{P}-2} \end{bmatrix} \left| \begin{matrix} n_1 & n_2 & \cdots & n_p \\ l_1 & l_2 & \cdots & l_p \\ l_1 & l_{12} & \cdots & l_{12\cdots\mathcal{P}-2} \end{matrix} \right\rangle . \tag{C.19}$$

We can now make an explicitly gauge invariant MPS ansatz for the ground state:

$$\Psi_0 \begin{bmatrix} n_1 & n_2 & \cdots & n_p \\ l_1 & l_2 & \cdots & l_p \\ l_{12} & l_{123} & \cdots & l_{12\cdots\mathcal{P}-2} \end{bmatrix} \equiv Tr\left[T^{n_1}_{0,l_1,l_1}(1)\; T^{n_2}_{l_1 l_2 l_{12}}(2)\; T^{n_3}_{l_{12} l_3 l_{123}}(3) \cdots T^{n_{\mathcal{P}}}_{l_{\mathcal{P}} l_{\mathcal{P}} 0}(\mathcal{P}) \right]. \tag{C.20}$$

This ansatz is illustrated in Figure 3.14-b. Much more work is required to implement these ideas on a computer. This will be done in the future.

BIBLIOGRAPHY

[1]S. Mandelstam, "Feynman rules for electromagnetic and yang-mills fields from the gauge-independent field-theoretic formalism," Phys. Rev. **175**, 1580–1603 (1968) (cit. on pp. 1, 2, 7).

[2]S. Mandelstam, "II. vortices and quark confinement in non-abelian gauge theories," Physics Reports **23**, 245 –249 (1976) (cit. on pp. 1, 2).

[3]S. Mandelstam, "Charge-monopole duality and the phases of non-abelian gauge theories," Phys. Rev. D **19**, 2391–2409 (1979) (cit. on pp. 1, 2, 6–8, 12, 18, 73).

[4]T. T. Wu and C. N. Yang, "Concept of nonintegrable phase factors and global formulation of gauge fields," Phys. Rev. D **12**, 3845–3857 (1975) (cit. on pp. 1, 2, 6–8, 12, 18).

[5]K. G. Wilson, "Confinement of quarks," Phys. Rev. D **10**, 2445–2459 (1974) (cit. on pp. 1, 2, 6–8, 12, 18).

[6]J. Kogut and L. Susskind, "Hamiltonian formulation of wilson's lattice gauge theories," Phys. Rev. D **11**, 395–408 (1975) (cit. on pp. 1, 2, 4–8, 12, 17, 18, 45, 52, 62).

[7]J. B. Kogut, "An introduction to lattice gauge theory and spin systems," Rev. Mod. Phys. **51**, 659–713 (1979) (cit. on pp. 1, 2, 5, 9, 12, 17, 30, 45, 73, 74, 77, 78, 81).

[8]J. B. Kogut, "The lattice gauge theory approach to quantum chromodynamics," Rev. Mod. Phys. **55**, 775–836 (1983) (cit. on pp. 1–5, 12, 14, 17, 30, 45, 52, 62).

[9]A Hasenfratz and P Hasenfratz, "Lattice gauge theories," Annual Review of Nuclear and Particle Science **35**, 559–604 (1985), eprint: http://dx.doi.org/10.1146/annurev.ns.35.120185.003015 (cit. on pp. 1, 3, 4).

[10]Y. Nambu, "Strings, monopoles, and gauge fields," Phys. Rev. D **10**, 4262–4268 (1974) (cit. on p. 1).

[11]A. Polyakov, "Compact gauge fields and the infrared catastrophe," Physics Letters B **59**, 82 –84 (1975) (cit. on p. 1).

[12]A. Polyakov, "Quark confinement and topology of gauge theories," Nuclear Physics B **120**, 429 –458 (1977) (cit. on p. 1).

[13]A. Polyakov, "Thermal properties of gauge fields and quark liberation," Physics Letters B **72**, 477 –480 (1978) (cit. on p. 1).

[14]G. 't Hooft, "On the phase transition towards permanent quark confinement," Nuclear Physics B **138**, 1 –25 (1978) (cit. on pp. 1, 73, 85, 86).

[15]G. 't Hooft, "A property of electric and magnetic flux in non-abelian gauge theories," Nuclear Physics B **153**, 141 –160 (1979) (cit. on p. 1).

[16]G. 't Hooft, ed., *Recent developments in gauge theories* (Springer US, 1980) (cit. on p. 1).

[17]R. P. Feynman, "The qualitative behavior of yang-mills theory in 2 + 1 dimensions," Nuclear Physics B **188**, 479 –512 (1981) (cit. on pp. 1, 131).

[18]Y. Nambu, "Qcd and the string model," Physics Letters B **80**, 372–376 (1979) (cit. on p. 1).

[19]J. Greensite, *An introduction to the confinement problem* (Springer Berlin Heidelberg, 2011) (cit. on p. 1).

[20]M. Creutz, *Quarks,gluons and lattices* (Cambridge University Press, 1985) (cit. on pp. 1–3).

[21]H. J. Roethe, *Lattice gauge theories: an introduction* (World Scientific, 2005) (cit. on pp. 1, 2).

[22]M. Istvan and M. Gernot, *Quantum fields on a lattice* (Cambridge University Press, 1994) (cit. on pp. 1, 2).

[23]J. B. Kogut and M. A. Stephanov, *The phases of quantum chromodynamics: from confinement to extreme environments* (Cambridge University Press, 2003) (cit. on pp. 1, 2).

[24]D. J. Gross and F. Wilczek, "Ultraviolet behavior of non-abelian gauge theories," Phys. Rev. Lett. **30**, 1343–1346 (1973) (cit. on p. 1).

[25]H. D. Politzer, "Reliable perturbative results for strong interactions?" Phys. Rev. Lett. **30**, 1346–1349 (1973) (cit. on p. 1).

[26]R. Gambini and J. Pullin, *Loops, knots, gauge theories and quantum gravity* (Cambridge Univ Press, 2000) (cit. on pp. 2, 6–8, 12, 18).

[27]A. Polyakov, "Gauge fields as rings of glue," Nuclear Physics B **164**, 171–188 (1980) (cit. on pp. 2, 6–8, 12, 18).

[28]Y. Makeenko and A. Migdal, "Quantum chromodynamics as dynamics of loops," Nuclear Physics B **188**, 269 –316 (1981) (cit. on pp. 2, 6–8, 12, 18).

[29]A. Jevicki and B. Sakita, "Loop-space representation and the large-n behavior of the one-plaquette kogut-susskind hamiltonian," Phys. Rev. D **22**, 467–471 (1980) (cit. on pp. 2, 6–8, 12, 18).

[30]B. Brügmann, "Method of loops applied to lattice gauge theory," Phys. Rev. D **43**, 566–579 (1991) (cit. on pp. 2, 6–8, 12, 18).

[31]R. Gambini, L. Leal, and A. Trias, "Loop calculus for lattice gauge theories," Phys. Rev. D **39**, 3127–3135 (1989) (cit. on pp. 2, 6–8, 12, 18).

[32]C. Di Bartolo, R. Gambini, and L. Leal, "Hamiltonian lattice gauge theories in a loop-dependent magnetic representation," Phys. Rev. D **39**, 1756–1760 (1989) (cit. on pp. 2, 6–8, 12, 18).

[33]R. Loll, "Independent su(2) loop variables and the reduced configuration space of su(2) lattice gauge theory," Nuclear Physics B **368**, 121 –142 (1992) (cit. on pp. 2, 6–8, 12, 18, 19).

[34]R. Loll, "Yang-mills theory without mandelstam constraints," Nuclear Physics B **400**, 126 –144 (1993) (cit. on pp. 2, 6–8, 12, 18, 19).

[35]N. Watson, "Solution of the su(2) mandelstam constraints," Physics Letters B **323**, 385 –392 (1994) (cit. on pp. 2, 6–8, 12, 18, 19).

[36]N. Watson, "Gauge-invariant variables and mandelstam constraints in su(2) gauge theory," Nuclear Physics B - Proceedings Supplements **39**, 224 –227 (1995) (cit. on pp. 2, 6–8, 12, 18, 19).

[37]Y. Makeenko and A. Migdal, "Exact equation for the loop average in multicolor {qcd}," Physics Letters B **88**, 135 –137 (1979) (cit. on pp. 2, 6–8, 12, 18).

[38]A. Migdal, "Loop equations and 1/n expansion," Physics Reports **102**, 199 –290 (1983) (cit. on pp. 2, 6–8, 12, 18).

[39]N. Ligterink, N. Walet, and R. Bishop, "A many-body treatment of hamiltonian lattice gauge theory," Nuclear Physics A **663**, 983c –986c (2000) (cit. on pp. 2, 6–8, 12, 18).

[40]N. Ligterink, N. Walet, and R. Bishop, "Toward a many-body treatment of hamiltonian lattice su(n) gauge theory," Annals of Physics **284**, 215 –262 (2000) (cit. on pp. 2, 6–8, 12, 14, 18).

[41]D. Robson and D. M. Webber, "Gauge covariance in lattice field theories," Zeitschrift fur Physik C Particles and Fields **15**, 199–226 (1982) (cit. on pp. 2, 6–8, 12, 18, 25, 53).

[42]D. Robson and D. M. Webber, "Gauge theories on a small lattice," Zeitschrift fur Physik C Particles and Fields **7**, 53–60 (1980) (cit. on pp. 2, 6, 53).

[43]W. Furmanski and A. Kolawa, "Yang-mills vacuum: an attempt at lattice loop calculus," Nuclear Physics B **291**, 594 –628 (1987) (cit. on pp. 2, 6–8, 12, 18).

[44]G. Burgio, R. D. Pietri, H. Morales-Tecotl, L. Urrutia, and J. Vergara, "The basis of the physical hilbert space of lattice gauge theories," Nuclear Physics B **566**, 547 –561 (2000) (cit. on pp. 2, 6–8, 12, 18).

[45]R. Giles, "Reconstruction of gauge potentials from wilson loops," Phys. Rev. D **24**, 2160–2168 (1981) (cit. on pp. 2, 6–8, 12, 18).

[46]V. Muller and W. Ruhl, "The energy gap of su(2) lattice gauge theory in 2+1 dimensions," Nuclear Physics B **230**, 49 –61 (1984) (cit. on pp. 2, 6–8, 12, 18).

[47]R. Anishetty, "Local dynamics on a gauge-invariant basis of non-abelian gauge theories," Phys. Rev. D **44**, 1895–1896 (1991) (cit. on pp. 2, 6–8, 12, 18).

[48]M. Mathur, "Loop states in lattice gauge theory," Physics Letters B **640**, 292 –296 (2006) (cit. on pp. 2, 6–8, 12, 18–23, 25, 26, 91).

[49]M. Mathur, "Loop approach to lattice gauge theories," Nuclear Physics B **779**, 32 –62 (2007) (cit. on pp. 2, 6–8, 12, 18–23, 25, 26, 64, 91).

[50]M. Mathur, "Harmonic oscillator pre-potentials in su(2) lattice gauge theory," Journal of Physics A: Mathematical and General **38**, 10015 (2005) (cit. on pp. 2, 6–8, 12, 20, 21).

[51]H. Sharatchandra, "Local observables in non-abelian gauge theories," Nuclear Physics B **196**, 62 –82 (1982) (cit. on pp. 2, 6–8, 20, 21).

[52]M. Mathur and T. P. Sreeraj, "Canonical transformations and loop formulation of su(n) lattice gauge theories," Phys. Rev. D **92**, 125018 (2015) (cit. on pp. 2, 8, 9, 29).

[53]M. Mathur and T. P. Sreeraj, "Lattice Gauge Theories and Spin Models," (2016), arXiv:1604.00315 [hep-lat] (cit. on pp. 2, 8, 9, 29).

[54]M. Mathur and T. P. Sreeraj, "From lattice gauge theories to hydrogen atoms," Physics Letters B **749**, 137 –143 (2015) (cit. on pp. 2, 8, 9, 29, 88).

[55]F. J. Wegner, "Duality in generalized ising models and phase transitions without local order parameters," Journal of Mathematical Physics **12**, 2259–2272 (1971) (cit. on pp. 2, 9, 30, 73, 77, 78).

[56]E. Fradkin and L. Susskind, "Order and disorder in gauge systems and magnets," Phys. Rev. D **17**, 2637–2658 (1978) (cit. on pp. 2, 9, 30, 73, 74, 77, 78, 81, 102).

[57]K. G. Wilson and J. Kogut, "The renormalization group and the epsilon expansion," Physics Reports **12**, 75 –199 (1974) (cit. on pp. 3, 14).

[58]T. Banks, S. Raby, L. Susskind, J. Kogut, D. R. T. Jones, P. N. Scharbach, and D. K. Sinclair, "Strong-coupling calculations of the hadron spectrum of quantum chromodynamics," Phys. Rev. D **15**, 1111–1127 (1977) (cit. on pp. 4, 5, 17).

[59]G. Munster, "Strong coupling expansions for the mass gap in lattice gauge theories," Nuclear Physics B **190**, 439 –453 (1981) (cit. on pp. 4, 5, 17).

[60]J. Kogut, D. Sinclair, and L. Susskind, "A quantitative approach to low-energy quantum chromodynamics," Nuclear Physics B **114**, 199 –236 (1976) (cit. on pp. 4, 5, 17).

[61]J. Smith, "Estimate of glueball masses from their strong coupling series in lattice qcd," Nuclear Physics B **206**, 309 –320 (1982) (cit. on pp. 4, 5, 17).

[62]J. Greensite, "Calculation of the yang-mills vacuum wave functional," Nuclear Physics B **158**, 469 –496 (1979) (cit. on pp. 5, 17, 131).

[63]J. Greensite, "Large-scale vacuum structure and new calculational techniques in lattice su(n) gauge theory," Nuclear Physics B **166**, 113 –124 (1980) (cit. on pp. 5, 17, 131).

[64]J.-M. Drouffe and J.-B. Zuber, "Strong coupling and mean field methods in lattice gauge theories," Physics Reports **102**, 1 –119 (1983) (cit. on pp. 5, 17, 85, 86).

[65] A. Carroll and J. B. Kogut, "Improved strong-coupling expansions and matrix pade approximants for lattice theories," Phys. Rev. D **19**, 2429–2439 (1979) (cit. on pp. 5, 17).

[66] A. Carroll, J. Kogut, D. K. Sinclair, and L. Susskind, "Lattice gauge theory calculations in $1+1$ dimensions and the approach to the continuum limit," Phys. Rev. D **13**, 2270–2277 (1976) (cit. on pp. 5, 17).

[67] T. Banks, L. Susskind, and J. Kogut, "Strong-coupling calculations of lattice gauge theories: $(1+1)$ dimensional exercises," Phys. Rev. D **13**, 1043–1053 (1976) (cit. on pp. 5, 17).

[68] R. Balian, J. M. Drouffe, and C. Itzykson, "Gauge fields on a lattice. III. strong-coupling expansions and transition points," Phys. Rev. D **11**, 2104–2119 (1975) (cit. on pp. 5, 17).

[69] N.D. Haridass, P. Lauwers, and A. Patkos, "An analytical variational study of the phase structure of compact qed on the lattice," Physics Letters B **124**, 387 –393 (1983) (cit. on p. 5).

[70] P. Suranyi, "Variational method in hamiltonian lattice gauge theories," Nuclear Physics B **210**, 519 –528 (1982) (cit. on pp. 5, 131, 134).

[71] H. Arisue, M. Kato, and T. Fujiwara, "Variational study of vacuum wave function for lattice gauge theory in 2+1 dimension," Progress of Theoretical Physics **70**, 229–248 (1983), eprint: http://ptp.oxfordjournals.org/content/70/1/229.full.pdf+html (cit. on pp. 5, 131, 134).

[72] H. Arisue, "Variational investigation of the mass spectrum in 2+1 dimensional su(2) lattice gauge theory," Progress of Theoretical Physics **84**, 951–960 (1990), eprint: http://ptp.oxfordjournals.org/content/84/5/951.full.pdf+html (cit. on pp. 5, 131, 134).

[73] D. R. Campagnari and H. Reinhardt, "Variational approach to yang-mills theory with non-gaussian wave functionals," Progress in Particle and Nuclear Physics **67**, From Quarks and Gluons to Hadrons and Nuclei International Workshop on Nuclear Physics, 33rd Course, 180 –184 (2012) (cit. on p. 5).

[74] D. W. Heys and D. R. Stump, "Variational estimate of the vacuum state of the su(2) lattice gauge theory with a disordered trial wave function," Phys. Rev. D **29**, 1791–1794 (1984) (cit. on pp. 5, 131).

[75] D. Horn and M. Weinstein, "The t expansion: a nonperturbative analytic tool for hamiltonian systems," Phys. Rev. D **30**, 1256–1270 (1984) (cit. on p. 5).

[76] D. Horn, M. Karliner, and M. Weinstein, "The t expansion and su(2) lattice gauge theory," Phys. Rev. D **31**, 2589–2599 (1985) (cit. on p. 5).

[77] Hollenberg and C. Lloyd, "First order analytic diagonalization of lattice qcd," Phys. Rev. D **50**, 6917–6920 (1994) (cit. on p. 5).

[78]C. L. Smith and N. Watson, "The shifted coupled cluster method. a new approach to hamiltonian lattice gauge theories," Physics Letters B **302**, 463 –471 (1993) (cit. on p. 5).

[79]D. Schütte, Z. Weihong, and C. J. Hamer, "Coupled cluster method in hamiltonian lattice field theory," Phys. Rev. D **55**, 2974–2986 (1997) (cit. on p. 5).

[80]R. F. Bishop, N. Ligterink, and N. R. Walet, "Towards a coupled-cluster treatment of su(n) lattice gauge theory," International Journal of Modern Physics B **20**, 4992–5007 (2006), eprint: http://www.worldscientific.com/doi/pdf/10.1142/S021797920603603X (cit. on pp. 5, 53).

[81]D. W. Heys and D. R. Stump, "Green's-function monte carlo calculations on the $su(2)$ and $u(1)$ lattice gauge theories," Phys. Rev. D **30**, 1315–1325 (1984) (cit. on p. 5).

[82]T. M. R. Byrnes, M. Loan, C. J. Hamer, F. D. R. Bonnet, D. B. Leinweber, A. G. Williams, and J. M. Zanotti, "Hamiltonian limit of $(3+1)$-dimensional su(3) lattice gauge theory on anisotropic lattices," Phys. Rev. D **69**, 074509 (2004) (cit. on p. 5).

[83]S. A. Chin, O. S. van Roosmalen, E. A. Umland, and S. E. Koonin, "Exact ground-state properties of the su(2) hamiltonian lattice gauge theory," Phys. Rev. D **31**, 3201–3212 (1985) (cit. on p. 5).

[84]J. Carlsson, "Improvement and analytic techniques in hamiltonian lattice gauge theory," PhD thesis (PhD Thesis, 2003) (cit. on p. 5).

[85]J. Goldstone and R. Jackiw, "Unconstrained temporal gauge for yang-mills theory," Physics Letters B **74**, 81 –84 (1978) (cit. on p. 6).

[86]P. Majumdar and H. Sharatchandra, "$(3+1)$ dimensional yang-mills theory as a local theory of evolution of metrics on 3-manifolds," Physics Letters B **491**, 199 –202 (2000) (cit. on p. 6).

[87]I. Mitra and H. Sharatchandra, "Dreibein (and metric) as prepotential for yang mills theory," (2013), arXiv:1307.0989 [hep-th] (cit. on p. 6).

[88]F. Lunev, "Three dimensional yang-mills theory in gauge invariant variables," Physics Letters B **295**, 99–103 (1992) (cit. on p. 6).

[89]M. Bauer, D. Z. Freedman, and P. E. Haagensen, "Spatial geometry of the electric field representation of non-abelian gauge theories," Nuclear Physics B **428**, 147 –168 (1994) (cit. on p. 6).

[90]P. E. Haagensen and K. Johnson, "Yang-mills fields and riemannian geometry," Nuclear Physics B **439**, 597 –616 (1995) (cit. on p. 6).

[91]P. E. Haagensen, K. Johnson, and C. Lam, "Gauge invariant geometric variables for yang-mills theory," Nuclear Physics B **477**, 273 –292 (1996) (cit. on p. 6).

[92]R. Anishetty, P. Majumdar, and H. Sharatchandra, "Dual gluons and monopoles in 2+1 dimensional yang mills theory," Physics Letters B **478**, 373–378 (2000) (cit. on p. 6).

[93]D. Karabali and V. Nair, "A gauge-invariant hamiltonian analysis for non-abelian gauge theoreies in (2+1) dimensions," Nuclear Physics B **464**, 135 –152 (1996) (cit. on p. 6).

[94]V. Nair and A. Yelnikov, "On the invariant measure for the yang-mills configuration space in $(3+1)$ dimensions," Nuclear Physics B **691**, 182 –194 (2004) (cit. on p. 6).

[95]L. Freidel, R. G. Leigh, and D. Minic, "Towards a solution of pure yang-mills theory in 3+1 dimensions," Physics Letters B **641**, 105 –111 (2006) (cit. on p. 6).

[96]A. Ashtekar, "New variables for classical and quantum gravity," Phys. Rev. Lett. **57**, 2244–2247 (1986) (cit. on p. 7).

[97]C. Rovelli, *Quantum gravity* (Cambridge University Press, 2004) (cit. on p. 7).

[98]C. Rovelli and L. Smolin, "Spin networks and quantum gravity," Phys. Rev. D **52**, 5743–5759 (1995) (cit. on p. 7).

[99]N D Hari Dass and Manu Mathur, "On loop states in loop-quantum gravity," Classical and Quantum Gravity **24**, 2179 (2007) (cit. on p. 7).

[100]K. Liegener and T. Thiemann, "Towards the fundamental spectrum of the quantum yang-mills theory," Phys. Rev. D **94**, 024042 (2016) (cit. on p. 7).

[101]R. Anishetty, M. Mathur, and I. Raychowdhury, "Irreducible SU(3) Schhwinger Bosons," J. Math. Phys. **50**, 053503 (2009), arXiv:0901.0644 [math-ph] (cit. on pp. 7, 8, 20, 21).

[102]R. Anishetty, M. Mathur, and I. Raychowdhury, "Prepotential formulation of su (3) lattice gauge theory," Journal of Physics A: Mathematical and Theoretical **43**, 035403 (2010) (cit. on pp. 7, 8, 20, 21, 26, 27, 53, 99).

[103]M. Mathur, I. Raychowdhury, and R. Anishetty, "Su(n) irreducible schwinger bosons," Journal of Mathematical Physics **51**, 093504 (2010) http://dx.doi.org/10.1063/1.3464267 (cit. on pp. 7, 8, 20, 21, 26, 27, 53, 99).

[104]M. Mathur and I. Raychowdhury, "SU(N) Coherent States and Irreducible Schwinger Bosons," J. Phys. **A44**, 035203 (2011), arXiv:1007.1510 [math-ph] (cit. on pp. 7, 8, 20, 21).

[105]M. Mathur, I. Raychowdhury, and T. P. Sreeraj, "Invariants, Projection Operators and $SU(N) \times SU(N)$ Irreducible Schwinger Bosons," J. Math. Phys. **52**, 113505 (2011), arXiv:1108.5246 [math-ph] (cit. on pp. 7, 8, 20, 21).

[106]R. Anishetty and I. Raychowdhury, "Su(2) lattice gauge theory: local dynamics on nonintersecting electric flux loops," Phys. Rev. D **90**, 114503 (2014) (cit. on pp. 7, 8, 20, 21).

[107]A. Hasenfratz, E. Hasenfratz, and P. Hasenfratz, "Generalized roughening transition and its effect on the string tension," Nuclear Physics B **180**, 353 –367 (1981) (cit. on p. 17).

[108]G. Munster and P. Weisz, "On the roughening transition in abelian lattice gauge theories," Nuclear Physics B **180**, 13 –22 (1981) (cit. on p. 17).

[109]G. Munster and P. Weisz, "On the roughening transition in non-abelian lattice gauge theories," Nuclear Physics B **180**, 330 –340 (1981) (cit. on p. 17).

[110]C. Itzykson, M. Peskin, and J. Zuber, "Roughening of wilson's surface," Physics Letters B **95**, 259 –264 (1980) (cit. on p. 17).

[111]J. Schwinger, *Quantum theory of angular momentum*, edited by L. Biedenharn and E. V. Dam (Academic press,New york, 1965) (cit. on p. 20).

[112]R. Anishetty and H. S. Sharatchandra, "Duality transformation for non-abelian lattice gauge theories," Phys. Rev. Lett. **65**, 813–815 (1990) (cit. on p. 25).

[113]S. Chaturvedi and N. Mukunda, "The schwinger $su(3)$ construction. i. multiplicity problem and relation to induced representations," Journal of Mathematical Physics **43**, 5262–5277 (2002) (cit. on p. 26).

[114]R. Anishetty, G. Gadiyar, M. Mathur, and H. Sharatchandra, "Color invariant additive fluxes for $su(3)$ gauge theory," Physics Letters B **271**, 391 –394 (1991) (cit. on p. 26).

[115]D. Varshalovich, A. Moskalev, and V. Khersonskii, *Quantum theory of angular momentum* (World Scientific, Singapore, 1988) (cit. on pp. 53, 63, 128–130).

[116]G. G. Batrouni, "Plaquette formulation and the bianchi identity for lattice gauge theories," Nuclear Physics B **208**, 467 –483 (1982) (cit. on pp. 67, 69, 71).

[117]J. Kiskis, "Bianchi identity for non-abelian lattice gauge fields," Phys. Rev. D **26**, 429–434 (1982) (cit. on pp. 67, 69, 71).

[118]H. A. Kramers and G. H. Wannier, "Statistics of the two-dimensional ferromagnet. part i," Phys. Rev. **60**, 252–262 (1941) (cit. on pp. 73, 74, 81).

[119]T. Banks, R. Myerson, and J. Kogut, "Phase transitions in abelian lattice gauge theories," Nuclear Physics B **129**, 493 –510 (1977) (cit. on p. 73).

[120]R. Savit, "Duality in field theory and statistical systems," Rev. Mod. Phys. **52**, 453–487 (1980) (cit. on pp. 73, 74).

[121]S. Elitzur, "Impossibility of spontaneously breaking local symmetries," Phys. Rev. D **12**, 3978–3982 (1975) (cit. on p. 73).

[122]D. Horn, M. Weinstein, and S. Yankielowicz, "Hamiltonian approach to $z(n)$ lattice gauge theories," Phys. Rev. D **19**, 3715–3731 (1979) (cit. on pp. 73, 74, 78, 81, 102).

[123]G. H. Wannier, "The statistical problem in cooperative phenomena," Rev. Mod. Phys. **17**, 50–60 (1945) (cit. on pp. 73, 81).

[124]L. P. Kadanoff and H. Ceva, "Determination of an operator algebra for the two-dimensional ising model," Phys. Rev. B **3**, 3918–3939 (1971) (cit. on pp. 73, 77, 81).

[125]M. E. Peskin, "Mandelstam-'t hooft duality in abelian lattice models," Annals of Physics **113**, 122 –152 (1978) (cit. on pp. 73, 81).

[126]E. Fradkin and S. Raby, "Real-space renormalization-group scheme for spin and gauge systems," Phys. Rev. D **20**, 2566–2582 (1979) (cit. on pp. 73, 81).

[127]T. Yoneya, "Z(n) topological excitations in yang-mills theories: duality and confinement," Nuclear Physics B **144**, 195 –218 (1978) (cit. on pp. 73, 81).

[128]A. Ukawa, P. Windey, and A. H. Guth, "Dual variables for lattice gauge theories and the phase structure of $z(n)$ systems," Phys. Rev. D **21**, 1013–1036 (1980) (cit. on pp. 73, 81, 85, 86).

[129]C.P Korthals Altes, "Duality for z(n) gauge theories," Nuclear Physics B **142**, 315 –326 (1978) (cit. on pp. 73, 81).

[130]R. Savit, "Duality transformations for general abelian systems," Nuclear Physics B **200**, 233 –248 (1982) (cit. on p. 73).

[131]T. D. Schultz, D. C. Mattis, and E. H. Lieb, "Two-dimensional ising model as a soluble problem of many fermions," Rev. Mod. Phys. **36**, 856–871 (1964) (cit. on p. 73).

[132]J. V. José, L. P. Kadanoff, S. Kirkpatrick, and D. R. Nelson, "Renormalization, vortices, and symmetry-breaking perturbations in the two-dimensional planar model," Phys. Rev. B **16**, 1217–1241 (1977) (cit. on p. 73).

[133]R. B. Israel and C. R. Nappi, "Quark confinement in the two-dimensional lattice higgs-villain model," Communications in Mathematical Physics **64**, 177–189 (1979) (cit. on p. 73).

[134]D. R. T. Jones, J. Kogut, and D. K. Sinclair, "Electrodynamics of the planar model: its phase diagram, continuum limit, and mass spectrum," Phys. Rev. D **19**, 1882–1905 (1979) (cit. on p. 73).

[135]M. Green, "Discrete and abelian lattice gauge theories," Nuclear Physics B **144**, 473–512 (1978) (cit. on p. 73).

[136]L. P. Kadanoff, "Lattice coulomb gas representations of two dimensional problems," Journal of Physics A: Mathematical and General **11**, 1399 (1978) (cit. on p. 73).

[137]L. Mittag and M. J. Stephen, "Dual transformations in many component ising models," Journal of Mathematical Physics **12**, 441–450 (1971) (cit. on p. 73).

[138]J. Drouffe, C. Itzykson, and J. Zuber, "Lattice models with a solvable symmetry group," Nuclear Physics B **147**, 132–134 (1979) (cit. on p. 73).

[139]P. Goddard, J. Nuyts, and D. Olive, "Gauge theories and magnetic charge," Nuclear Physics B **125**, 1 –28 (1977) (cit. on p. 73).

[140]M. B. Halpern, "Field strength and dual variable formulations of gauge theory," Phys. Rev. D **19**, 517–530 (1979) (cit. on p. 73).

[141]P. Majumdar and H. Sharatchandra, "Gauge field copies, non-abelian gauss law, non-abelian hodge decomposition and duality transformation for $3+1$ dimensional yang-mills theory.," Nuclear Physics B-Proceedings Supplements **73**, 620 –622 (1999) (cit. on p. 73).

[142]P. Majumdar and H. S. Sharatchandra, "Duality transformation for (3+1) dimensional yang-mills theory," International Journal of Modern Physics A **17**, 175–186 (2002), eprint: http://www.worldscientific.com/doi/pdf/10.1142/S0217751X02005785 (cit. on p. 73).

[143]P. Majumdar and H. Sharatchandra, "General solution of the non abelian gauss law and non abelian analogues of the hodge decomposition," Phys. Rev. D **58**, 067702 (1998) (cit. on p. 73).

[144]G Mack and V. Petkova, "Comparison of lattice gauge theories with gauge groups z2 and su(2)," Annals of Physics **123**, 442 –467 (1979) (cit. on pp. 73, 81, 85, 86).

[145]R. Oeckl and H. Pfeiffer, "The dual of pure non-abelian lattice gauge theory as a spin foam model," Nuclear Physics B **598**, 400 –426 (2001) (cit. on p. 73).

[146]E. Tomboulis, "'t hooft loop in su(2) lattice gauge theories," Phys. Rev. D **23**, 2371–2383 (1981) (cit. on pp. 85, 86).

[147]H. Reinhardt, "On 't hooft's loop operator," Physics Letters B **557**, 317 –323 (2003) (cit. on pp. 85, 86).

[148]W. Pauli, "Über das wasserstoffspektrum vom standpunkt der neuen quantenmechanik," Zeitschrift für Physik **36**, 336–363 (1926) (cit. on pp. 88, 94).

[149]V. Fock, "Zur theorie des wasserstoffatoms," Zeitschrift für Physik **98**, 145–154 (1935) (cit. on pp. 88, 94).

[150]S. F. Singer, *Linearity, symmetry, and prediction in the hydrogen atom* (Springer-Verlag New York, 2005) (cit. on pp. 88, 94).

[151]B. G. Wybourne, *Classical group for physicists* (John Wiley and sons, 1974) (cit. on pp. 88–90, 95, 97).

[152]R. Gilmore, *Lie groups, physics and geometry* (Cambridge University Press, 2008) (cit. on pp. 88–90, 95).

[153]M. Bander and C. Itzykson, "Group theory and the hydrogen atom (i)," Rev. Mod. Phys. **38**, 330–345 (1966) (cit. on pp. 88, 127).

[154]V. Bargmann, "Zur theorie des wasserstoffatoms," Zeitschrift für Physik **99**, 576–582 (1936) (cit. on p. 94).

[155]S. Östlund and S. Rommer, "Thermodynamic limit of density matrix renormalization," Phys. Rev. Lett. **75**, 3537–3540 (1995) (cit. on pp. 102, 135).

[156]I. P. McCulloch, "From density-matrix renormalization group to matrix product states," Journal of Statistical Mechanics: Theory and Experiment **2007**, P10014 (2007) (cit. on pp. 102, 135).

[157]F. Verstraete, V. Murg, and J. Cirac, "Matrix product states, projected entangled pair states, and variational renormalization group methods for quantum spin systems," Advances in Physics **57**, 143–224 (2008), eprint: http://dx.doi.org/10.1080/14789940801912366 (cit. on pp. 102, 135).

[158]S. Singh and G. Vidal, "Tensor network states and algorithms in the presence of a global su(2) symmetry," Phys. Rev. B **86**, 195114 (2012) (cit. on pp. 102, 135).

[159]A. Milsted, "Matrix product states and the non-abelian rotor model," Phys. Rev. D **93**, 085012 (2016) (cit. on pp. 102, 135).

[160]H. Casini, M. Huerta, and J. A. Rosabal, "Remarks on entanglement entropy for gauge fields," Phys. Rev. D **89**, 085012 (2014) (cit. on p. 103).

[161]S. Aoki, T. Iritani, M. Nozaki, T. Numasawa, N. Shiba, and H. Tasaki, "On the definition of entanglement entropy in lattice gauge theories," Journal of High Energy Physics **2015**, 1–29 (2015) (cit. on p. 103).

[162]E. Zohar, J. I. Cirac, and B. Reznik, "Quantum simulations of gauge theories with ultracold atoms: local gauge invariance from angular-momentum conservation," Phys. Rev. A **88**, 023617 (2013) (cit. on p. 103).

[163]E. Zohar, J. I. Cirac, and B. Reznik, "Quantum simulations of lattice gauge theories using ultracold atoms in optical lattices," Reports on Progress in Physics **79**, 014401 (2016) (cit. on p. 103).

[164]K. Stannigel, P. Hauke, D. Marcos, M. Hafezi, S. Diehl, M. Dalmonte, and P. Zoller, "Constrained dynamics via the zeno effect in quantum simulation: implementing non-abelian lattice gauge theories with cold atoms," Phys. Rev. Lett. **112**, 120406 (2014) (cit. on p. 103).

[165]L. Tagliacozzo, A. Celi, P. Orland, M. Mitchell, and M. Lewenstein, "Simulation of non-abelian lattice gauge theories with optical lattices," Nature comm. **4**, 2615 (2013) (cit. on p. 103).

[166]M. Abramowitz and I. A. Stegun, *Handbook of mathematical functions* (National Bureau of standards, Applied mathematical series 55, 1964) (cit. on p. 133).